Univerzita Karlova

2. lékařská fakulta

Studijní program: Imunologie

Mgr. Iva Truxová

Imunogenní buněčná smrt a její význam pro biologii a terapii nádorových onemocnění

Immunogenic cell death and it's relevance for biology and therapy of malignant diseases

Dizertační práce

Vedoucí závěrečné práce: prof. MUDr. Radek Špíšek, Ph.D.

Praha, 2018

Prohlášení:

Prohlašuji, že jsem závěrečnou práci zpracovala samostatně a že jsem řádně uvedla a citovala všechny použité prameny a literaturu. Současně prohlašuji, že práce nebyla využita k získání jiného nebo stejného titulu

Souhlasím s trvalým uložením elektronické verze mé práce v databázi systému meziuniverzitního projektu Theses.cz za účelem soustavné kontroly podobnosti kvalifikačních prací.

V Praze, 25.4.2018

IVA TRUXOVÁ

Podpis

Identifikační záznam:

Truxová, Iva. *Imunogenní buněčná smrt a její význam pro biologii a terapii nádorových onemocnění [Immunogenic cell death and it's relevance for biology and therapy of malignant diseases]*. Praha, 2018, 168s, 6 příl., Dizertační práce (Ph.D.). Univerzita Karlova, 2. lékařská fakulta, Ústav imunologie. Vedoucí závěrečné práce: Špíšek, Radek.

Poděkování

Děkuji svému školiteli prof. MUDr. Radku Špíškovi, Ph.D. za odborné vedení během celého doktorského studia a cenné připomínky, které přispěly k vypracování této dizertační práce. Dále bych chtěla poděkovat PharmDr. Jitce Palich Fučíkové, Ph.D. za neustálou podporu, cenné rady jak při samotné experimentální práci, tak při psaní manuskriptů a za přátelské jednání. Děkuji také všem kolegům z Ústavu imunologie 2. LF UK a FN Motol a z výzkumného oddělení firmy Sotio za velmi přátelské a podnětné prostředí a za pomoc při řešení projektů, které jsou součástí této práce.

Speciální poděkování patří celé mé rodině a příteli za trpělivost, toleranci a neustálou snahu mě motivovat a podporovat.

ABSTRAKT

Potenciál nádorových buněk stimulovat imunitní reakci závisí na řadě faktorů, z nichž nejdůležitější je především antigenní repertoár nádorových buněk a schopnost sekretovat, uvolňovat nebo vystavovat na buněčném povrchu molekuly asociované se stresem či poškozením, tzv. DAMPs v průběhu imunogenních forem buněčné smrti. Tyto molekuly souhrnně aktivují buňky imunitního systému, zejména dendritické buňky (DCs), které následně stimulují protinádorovou imunitní reakci. V uplynulých letech bylo popsáno několik induktorů imunogenní buněčné smrti (ICD). Příspěvkem mé dizertační práce do této problematiky byla charakterizace apoptotických drah aktivovaných vysokým hydrostatickým tlakem (HHP), který byl dříve identifikován naší skupinou jako induktor ICD. HHP indukuje rychlou buněčnou smrt nádorových buněk spojenou s uvolněním klíčových DAMPs (zejména kalretikulinu (CRT), HSP70, HSP90, HMGB1 a ATP), dále charakterizovanou nadprodukcí kyslíkových radikálů (ROS) zahajující rozvoj integrovaného buněčného stresu. Aktivace signalizační dráhy zahrnující osu ROS-PERK-eIF2α-kaspáza 2-kaspáza 8 je důležitá pro vystavení CRT na povrch nádorových buněk v průběhu buněčné smrti indukované HHP, a zásadně tedy ovlivňuje imunogenní potenciál těchto buněk. Význam konceptu ICD byl potvrzen také *in vivo*. V naší práci jsme prokázali, že přítomnost CRT na povrchu blastů pacientů s AML koreluje s aktivací specifické protinádorové imunitní odpovědi a signifikantně lepší prognózou onemocnění. Dalším mým příspěvkem byla optimalizace protokolu na výrobu DC v GMP podmínkách. Získané výsledky ukazují, že DC vyrobené pomocí zkráceného (3 denního) protokolu mají porovnatelnou schopnost indukovat antigen-specifické $CD8^+$ T lymfocyty jako DCs připravené standardně během 5 dní. Přiložené výsledky také poukazují na možnost zvýšení účinnosti imunoterapie na bázi DCs pulzovaných nádorovými buňkami inaktivovanými HHP u slabě imunogenních typů nádorů kombinací s vhodnou chemoterapií.

Klíčová slova: imunogenní buněčná smrt, DAMPs, stres endoplazmatického retikula, vysoký hydrostatický tlak, dendritické buňky, imunoterapie

ABSTRACT

Immunostimulatory potential of tumor cells depends on various factors, including primarily tumor antigen repertoire and the capacity to emit molecules associated with cellular stress or injury, so called DAMPs, during immunogenic forms of cell death. These molecules mainly act on dendritic cells (DCs), thus activating the antitumor immune response. Several immunogenic cell death (ICD) inducers have been described in the past years. The contribution of my PhD thesis into this topic was the characterization of the apoptotic pathways activated by high hydrostatic pressure (HHP). HHP induces rapid tumor cell death accompanied by DAMP release (mainly calreticulin (CRT), HSP70, HSP90, HMGB1 and ATP) that is characterized by the overproduction of reactive oxygen species (ROS) causing the establishment of integrated stress response. ROS-PERK-eIF2α-caspase-2-caspase-8 signaling pathway plays an essential role in CRT translocation to the tumor cell surface upon HHP treatment, thus influencing the immunogenic potential of these cells. Moreover, the importance of ICD concept was also confirmed *in vivo*. The results point out that the presence of CRT on the surface of malignant blasts from AML patients correlates with the activation of specific antitumor immune response and improved clinical outcome. Another study focuses on the optimalization of DC manufacuring protocol in GMP conditions. Data obtained in this project shows that DCs differentiated during 3 days are similarly potent in inducing antigen-specific $CD8^+$ T cells as DCs produced by the standard 5 day protocol. The data included in this thesis also show that the efficacy of immunotherapy based on DCs pulsed with HHP-inactivated tumor cells for the treatment of poorly immunogenic tumors can be potentiated by combination with suitable chemotherapy.

Key words: immunogenic cell death, DAMPs, endoplasmic reticulum stress, high hydrostatic pressure, dendritic cells, immunotherapy

OBSAH

SEZNAM ZKRATEK

AIF	apoptosis-inducing factor
AML	acute myeloid leukemia
AMPK	AMP-activated protein kinase
ANXA1	annexin A1
AP1	activator protein 1
APC	antigen-presenting cell
Apaf-1	apoptotic protease-activating factor-1
ASK1	apoptosis signal-regulating kinase 1
ATF	activating transcription factor
ATG	autophagy-related protein
ATP	adenosine triphosphate
Bcl-2	B-cell lymphoma-2
BDCA	blood dendritic cell antigen
BH3	Bcl-2 homology domain 3
BiP	binding immunoglobulin protein
CCL2	chemokine (C-C motif) ligand 2
CCR7	C-C chemokine receptor type 7
cFLIP	cellular FLICE-like inhibitory protein
CRT	calreticulin
CVB3	Coxsackievirus B3
CXCL10	chemokine (C-X-C motif) ligand 10
DAMP	danger-associated molecular pattern
DC	dendritic cell
DISC	death-inducing signaling complex

DR	death receptor
eIF2α	eukaryotic translation initiation factor 2α
EMAPII	endothelial monocyte-activating polypeptide II
ER	endoplasmic reticulum
ERAD	ER-associated degradation
FADD	Fas-associated death domain
FasL	Fas ligand
FDA	Food and Drug Administration
FPR-1	formyl peptide receptor-1
GM-CSF	granulocyte-macrophage colony-stimulating factor
GMP	Good Manufacturing Practice
GSH	reduced L-glutathione
HHP	high hydrostatic pressure
HLA	human leukocyte antigen
HMGB1	high mobility group box 1
HSP	heat shock protein
HSV	herpes simplex virus
Hyp-PDT	hypericin-based photodynamic therapy
GRP78	glucose-regulated protein 78kDa
CHOP	C/EBP homologous protein
ICAM	intercellular adhesion molecule
ICD	immunogenic cell death
IFN	interferon
ILT7	immunoglobulin-like transcript 7
IRE1α	inositol-requiring enzyme 1α

IRF	interferon regulatory factors
JNK	c-Jun N-terminal kinase
LDL	low-density lipoprotein
LOX-1	lectin-type oxidized LDL receptor-1
LPC	lysophosphatidylcholine
LPS	lipopolysacharide
LRP-1	low-density lipoprotein receptor-related protein-1
MAPK	mitogen-activated protein kinase
MCP-1	monocyte chemoattractant protein-1
MDSC	myeloid-derived suppressor cell
MHC	major histocompatibility complex
MLKL	mixed lineage kinase domain-like
MPLA	monofosforyl lipid A
mTORC1	mammalian target of rapamycin complex 1
NAC	N-acetyl-L-cystein
NF-κB	nuclear factor-κB
NK	natural killer
NOD	nucleotide-binding oligomerization domain
NTPD1	nucleoside triphosphate diphosphohydrolase 1
PAMP	pathogen-associated molecular pattern
PBMC	peripheral blood mononuclear cell
PERK	protein kinase R (PKR)-like endoplasmic reticulum kinase
PGE2	prostaglandin E2
PI3K	phosphatidylinositol-3-kinase
PI3P	phosphatidylinositol-3-phosphate

PP1	protein phosphatase 1
PRR	pattern recognition receptor
PS	phosphatidylserine
Puma	p53 upregulated modulator of apoptosis
RAGE	receptor for advanced glycation end-products
RIPK	receptor-interacting protein kinase
ROS	reactive oxygen species
siRNA	small interfering RNA
Smac	second mitochondria-derived activator of caspase
SNARE	SNAP (soluble NSF (N-ethylmaleimide-sensitive factor) attachment protein
SREC-1	scavenger receptor associated with endothelial cells
TAA	tumor-associated antigen
TGF-β1	transforming growth factor-β1
TLR	Toll-like receptor
TNF	tumor necrosis factor
TRAF2	tumor necrosis factor receptor-associated factor 2
TRAIL	tumor necrosis factor-related apoptosis-inducing ligand
TRB3	tribbles homolog 3
Treg	regulatory T cell
TRIF	TIR domain-containing adapter-inducing interferon-β
ULK1	Unc-51-like kinase 1
UPR	unfolded protein response
VAMP1	vesicle-associated membrane protein 1
XBP1	X box-binding protein 1
XIAP	X-linked inhibitor of apoptosis

1. ÚVOD

Ke klasickým onkologickým léčebným postupům – chirurgii, chemoterapii a radioterapii, se v posledních letech přidala také imunoterapie. Klasické přístupy sice vedou k redukci většiny nádorové masy, ale nejsou schopny zničit kmenové nádorové buňky a mikrometastázy, které často způsobují relaps onemocnění a snižují tak účinnost léčby. Úspěšnost protinádorové terapie je kriticky závislá na výběru vhodné kombinace a aplikace látek a modalit, které by kromě efektivní destrukce většiny nádorových buněk, byly také schopny stimulovat imunitní reakci proti reziduálním nádorovým buňkám. Různé protinádorové látky a postupy se liší cytotoxickými mechanismy a schopností modulovat imunitní odpověď. V současnosti je již známo, že určité chemoterapeutické látky, fyzikální modality a onkolytické viry indukují specifický typ buněčné smrti, který zvyšuje imunogenní potenciál nádorových buněk. Tato forma buněčné smrti je označována jako imunogenní buněčná smrt (ICD, immunogenic cell death) a je charakterizována vystavením signálů nebezpečí tzv. DAMPs (damage-associated molecular patterns) na buněčném povrchu, popřípadě jejich sekrecí nebo uvolněním do extracelulárního prostředí. Tyto molekuly mají potenciál stimulovat především buňky vrozené imunity, což následně vede k posílení adaptivní protinádorové imunitní reakce spojené s eliminací reziduálních nádorových buněk rezistentních na léčbu a vytvořením imunologické paměti (Krysko et al., 2012). Tyto poznatky jsou velice důležité pro vývoj protinádorových strategií založených na kombinaci standardních typů léčby jako chemoterapie nebo radioterapie s imunoterapeutickými přístupy.

V první části práce budou shrnuty současné poznatky o roli buněčné smrti v aktivaci imunitní reakce proti nádorovým buňkám. Pozornost bude věnována především charakterizaci imunogenní buněčné smrti a mechanismům vedoucím k sekreci/uvolnění/vystavení DAMPs. Také bude diskutován význam těchto molekul *in vivo* u pacientů s nádorovým onemocněním

a vliv jednotlivých DAMPs na dendritické buňky (DCs) a jejich využití v protinádorové terapii. Druhou část tvoří soubor publikovaných prací, které přímo souvisí s touto tématikou.

2. BUNĚČNÁ SMRT NÁDOROVÝCH BUNĚK A JEJÍ VLIV NA PROTINÁDOROVOU IMUNITNÍ REAKCI

2.1. Hlavní typy buněčné smrti

2.1.1. Apoptóza

Apoptóza běžně probíhá za fyziologických podmínek *in vivo* a hraje důležitou roli při odstraňování starých, poškozených nebo infikovaných buněk buňkami imunitního systému. Ve většině případů se jedná o imunologicky tichý typ programované buněčné smrti, která je charakterizována typickými morfologickými změnami jako kondenzace chromatinu (pyknóza), štěpení chromozomální DNA na internukleozomální fragmenty, smrštění buněčného obsahu a tvorba apoptotických tělísek bez rozpadu plazmatické membrány (Garrido and Kroemer, 2004). Apoptotické buňky jsou rychle rozpoznávány fagocyty prostřednitvím různých tzv. „find-me“ signálů uvolňovaných z umírajících buněk, které zahrnují např. apoptotická tělíska, EMAPII (endothelial monocyte-activating polypeptide II), dimer ribozomálního proteinu S19, lysofosfatidylcholin (LPC), fragmenty tyrosyl tRNA syntetázy, trombospondin 1 a další (Peter et al., 2010). Po rozpoznání profesionálními fagocyty jsou pohlceny a odstraněny fagocytózou, což je umožněno přítomností tzv. „eat-me“ signálů na povrchu apoptotických buněk jako např. fosfatidylserinu (PS), opsoninů, modifikovaného ICAM-3 (intercellular adhesion molecule-3), modifikovaných LDL (low-density lipoproteins) proteinů, doménou trombospondinu 1 vázající heparin, fosfatidyletanolaminem, fosfatidylinositolem, laktoferinem, atd. (Krysko et al., 2006) a současnou supresí tzv. „don’t eat me“ signálů jako např. CD47 (Gardai et al., 2005). Proces

odstranění apoptotických buněk probíhá bez větších známek aktivace imunitní odpovědi v důsledku uvolnění protizánětlivých signálů (např. TGF-β1 (transforming growth factor-β1), prostaglandinu E2 (PGE2) a faktorů aktivujících destičky) (Garg et al., 2010).

Apoptotická buněčná smrt je indukována dvěma hlavními signalizačními dráhami – vnitřní a vnější. Vnější dráha je aktivována interakcí membránově vázaných receptorů smrti z rodiny TNF (tumor necrosis factor) s jejich ligandy. Konkrétně se jedná o vazby Fas (CD95)-Fas ligand (FasL), DR (death receptor) 5-TRAIL (tumor necrosis factor-related apoptosis-inducing ligand) a TNFR1-TNFα (Locksley et al., 2001). Interakce FasL a TRAILu s jejich receptory vede k navázání adaptorové molekuly FADD (Fas-associated death domain) na doménu smrti v intracelulární části receptorů. FADD dále váže pro-kaspázu 8 a cFLIP (cellular FLICE-like inhibitory protein), což vede k formaci makromolekulárního komplexu zvaného DISC (death-inducing signaling complex), který je nutný pro autokatalytické štěpení a aktivaci pro-kaspázy 8 a zahájení apoptotické signalizace. Signalizační dráhy spouštěné vazbou ligandů na TNFR1 jsou komplexnější a mohou vést nejen k apoptóze, ale také nekróze nebo přežívání buňky (Dickens et al., 2012). Aktivní kaspáza 8 může přímo aktivovat efektorové kaspázy 3, 6 a 7 zahajující exekuční fázi apoptózy a také štěpit proapoptotický protein Bid, čímž celá signalizace směřuje k porušení integrity vnější mitochondriální membrány. V tomto bodě se signalizace vnější a vnitřní apoptotické dráhy sbíhají (Green and Llambi, 2015). K aktivaci vnitřní (mitochondriální) dráhy nedochází jen ligací receptorů smrti, ale také v důsledku buněčného stresu různého charakteru - např. poškozením DNA genotoxickými látkami a modalitami nebo defekty v opravných mechanismech DNA, oxidativním stresem nebo stresem endoplazmatického retikula (ER) indukovaným nahromaděním nesbalených nebo špatně sbalených proteinů, infekcí patogeny, hypoxií, nedostatkem živin nebo deprivací růstových faktorů (Green and Llambi, 2015). Endogenní apoptotická signalizace je pod kontrolou proteinů z rodiny Bcl-2 (B-cell lymphoma-2), které

regulují uvolnění specifických faktorů aktivujících kaspázy z mitochondrií. Tato rodina zahrnuje proteiny jak proapoptotické (např. Bid, Bad, Bax, Bak, Puma (p53 upregulated modulator of apoptosis), Noxa, atd.), tak antiapoptotické (např. Bcl-2, Bcl-x_L). Výsledná aktivace členů těchto podskupin je rozhodující pro zahájení apoptózy (Birkinshaw and Czabotar, 2017).

Úvodní událostí v mitochondriální apoptotické dráze je štěpení proteinu Bid kaspázou 8. Aktivní tBid je poté transportován z cytoplazmy do mitochondrií, kde aktivuje proteiny Bax a Bak. Tyto proteiny po aktivaci oligomerizují, což vede k vytvoření pórů ve vnější mitochondriální membráně a uvolnění cytochromu c do cytoplazmy (Green and Reed, 1998). V cytoplazmě tvoří cytochrom c společně s Apaf-1 (apoptotic protease-activating factor-1) a dATP multimerní komplex zvaný apoptosom, jehož hlavní funkcí je štěpení pro-kaspázy 9 na její aktivní formu (Kim et al., 2005). Kromě cytochromu c jsou z poškozených mitochondrií uvolňovány do cytosolu další proapoptotické faktory jako Smac (second mitochondria-derived activator of caspase) a Omi, které posilují aktivitu apoptosomu díky jejich antagonistickým účinkům na inhibitory apoptózy XIAP (X-linked inhibitor of apoptosis) blokujících aktivitu kaspázy 9 a efektorových kaspáz 3 a 7 (Eckelman et al., 2006). Aktivací efektorových kaspáz přechází buňka do terminální fáze apoptózy, během které efektorové kaspázy štěpí proteiny podílející se na udržení integrity DNA, inhibitory endonukleáz a různé cytoskeletální proteiny. Tyto procesy mají za následek rozpad jaderného obalu, fragmentaci DNA a další morfologické změny typické pro apoptózu (Ashkenazi and Salvesen, 2014).

Současné poznatky ukazují, že apoptóza může za určitých okolností stimulovat imunitní odpověď. Tato forma imunogenní apoptózy je závislá především na aktivaci oxidativního stresu a stresu ER. Správná funkce ER je nezbytná pro většinu buněčných funkcí, včetně přežívání. Různé typy stresu vedou k akumulaci špatně sbalených nebo nesbalených proteinů v ER a k narušení jeho fyziologických funkcí. Obnova normální funkce

ER je závislá na indukci adaptivní odpovědi známé jako odpověď na nesbalené nebo špatně sbalené proteiny (UPR, unfolded protein response), která je v savčích buňkách aktivována třemi hlavními senzory sídlícími v membráně ER: IRE1α (inositol-requiring enzyme 1α), ATF6 (activating transcription factor 6) a PERK kinázou (protein kinase R (PKR)-like endoplasmic reticulum kinase). Za fyziologických podmínek jsou tyto receptory udržovány v inaktivním stavu vazbou na chaperonový protein GRP78 (glucose-regulated protein 78kDa, jinak také BiP (binding immunoglobulin protein)). Nahromadění nesbalených proteinů nebo narušení homeostázy Ca^{2+} iontů v ER ale vede k aktivaci těchto transmembránových receptorů (Ma and Hendershot, 2002). Aktivovaná PERK kináza fosforyluje eukaryotický translační iniciační faktor 2α (eIF2α), čímž dochází k zastavení syntézy proteinů zprostředkované eIF2α. To ale naopak umožní translaci transkripčního faktoru ATF4 nezávislou na eIF2α. ATF4 je poté transportován do jádra, kde indukuje transkripci genů nutných pro obnovení homeostázy ER (Harding et al., 2000). ATF6, další ze senzorů stresu ER, je aktivován štěpením po translokaci z ER do Golgiho aparátu. Štěpený ATF6 reguluje v jádře expresi chaperonů a transkripčního faktoru XBP1 (X box-binding protein 1). Aktivní forma XBP1 vzniká po sestřihu mRNA IRE1α, který umožňuje jeho translokaci do jádra, kde indukuje transkripci genů kódujících chaperony a faktory účastnící se degradace proteinů (Ma and Hendershot, 2002). UPR signalizace je znázorněna na Obr.1..

UPR má za normálních okolností podpořit přežití buňky, ale v případě dlouhotrvajícího intenzivního stresu dochází k aktivaci proapoptotické signalizace, která může, i nemusí, vyžadovat mechanismy závislé na mitochondriích. Aktivace PERK/eIF2α/ATF4 dráhy vede k indukci exprese genů kódujících proapoptotické proteiny jako např. CHOP (C/EBP homologous protein). CHOP je transkripční faktor, který spouští transkripci některých genů kódujících proteiny s proapoptotickými funkcemi – např. GADD34, DR5, TRB3 (tribbles homolog 3), atd. a naopak inhibuje expresi antiapoptotického proteinu Bcl-2 (Ma et al., 2002).

Kromě toho fosforylace IRE1α indukovaná stresem ER má za následek vazbu adaptorové molekuly TRAF2 (tumor necrosis factor receptor-associated factor 2) a kinázy ASK1 (apoptosis signal-regulating kinase 1) do cytosolické části membrány ER. Poté dochází k aktivaci JNK kinázy (c-Jun N-terminal kinase), která následně fosforyluje a blokuje antiapoptickou funkci Bcl-2. JNK kináza také fosforyluje proteiny z rodiny Bcl-2 obsahující BH3 (Bcl-2 homology domain 3) doménu (např. Bim), což zvyšuje jejich proapoptotický potenciál (Urano et al., 2000). Dalším mechanismem vedoucím k zahájení apoptotické signalizace v ER je aktivace Bax a Bak na membráně ER. Interakce těchto proteinů s aktivovaným IRE1α má za následek jejich aktivaci a regulované uvolnění Ca^{2+} z ER. Ca^{2+} ionty poté vstupují do mitochondrií a způsobují depolarizaci vnitřní mitochondriální membrány, uvolnění cytochromu c, tvorbu apoptosomu a aktivaci kaspázy 9 s následným zahájením exekuční fáze apoptózy (Malhotra and Kaufman, 2011). Během stresu ER také dochází k aktivaci některých kaspáz – např. kaspázy 12 přímo na membráně ER. Tato signalizace poté může aktivovat efektorové kaspázy (Szegezdi et al., 2003).

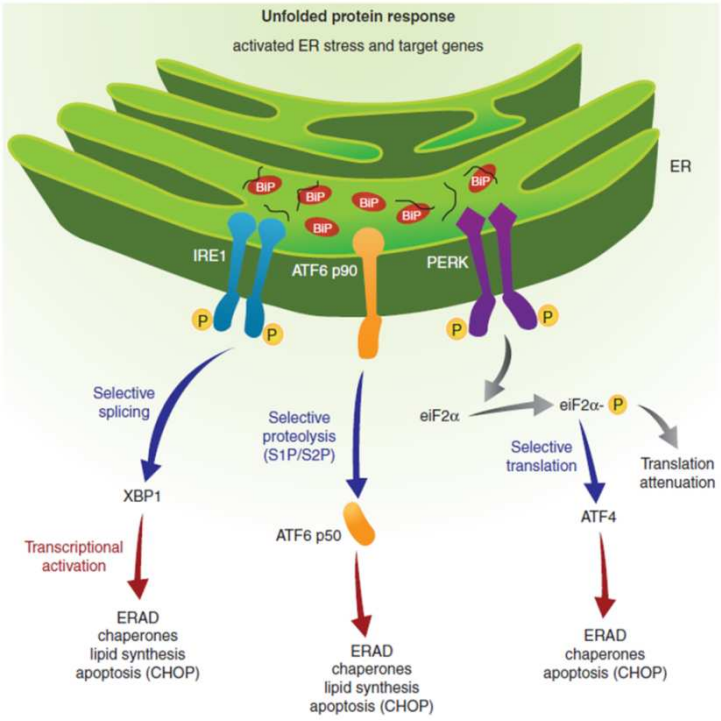

Obr.1. UPR signalizace. *UPR je regulována signalizačními dráhami aktivovanými třemi senzory stresu ER - IRE1α, PERK a ATF6. Za normálních okolností jsou tyto receptory udržovány v inaktivním stavu vazbou BiP na jejich luminální domény. Během akumulace nesbalených proteinů v ER dochází k uvolnění této vazby. IRE1α dimerizuje a po aktivaci iniciuje štěpení mRNA kódující XBP1, který funguje jako transkripční aktivátor. IRE1α/XBP1 dráha indukuje expresi genů kódujících proteiny účastnící se v degradaci proteinů v ER (ERAD, ER-associated degradation). ATF6 je translokován do Golgiho aparátu, kde je S1P a S2P proteázami odštěpen jeho cytoplazmatický konec, který je dále transportován do jádra. V jádře tento fragment aktivuje transkripci genů kódujících proteiny spojené s UPR. PERK po uvolnění BiP dimerizuje a fosforyluje eIF2α, což vede k zastavení iniciace translace. Fosforylace eIF2α ale paradoxně indukuje translaci mRNA pro ATF4. Aktivace PERK/eIF2α/ATF4 dráhy má také za následek indukci exprese genů kódujících proteiny s antioxidativním účinkem a proapoptotickými funkcemi jako např. CHOP. Převzato z (Malhotra and Kaufman, 2011).*

2.1.2. Nekróza/nekroptóza

Nekróza zahrnuje různé formy buněčné smrti, jejichž společným znakem je ztráta integrity plazmatické membrány následovaná uvolněním cytoplazmatického obsahu včetně prozánětlivých molekul jako např. HMGB1 (high mobility group box 1), proteinů teplotního šoku HSP (heat shock protein) 70, 90, 60, 72 a GP96, monosodium urátu, adenosintrifosfátu (ATP), IL-6, ribonukleoproteinů, mRNA, genomické DNA, IL-1β, atd.. Tyto molekuly atrahují a aktivují různé fagocytující buňky, které následně stimulují imunitní odpověď (Krysko et al., 2006).

Nekróza může probíhat následkem intenzivního poškození narušujícího integritu buňky jako je vysoká teplota, opakované zamražení/rozmražení nebo mechanický stres. V těchto

případech se jedná o pasivní proces, který nevyžaduje aktivaci určitých signalizačních drah. Nekrotická morfologie je také pozorována v pozdní fázi apoptózy nebo autofágie. Tento proces je označován jako sekundární nekróza a je závislý pouze na počáteční proapoptotické signalizaci, resp. mechanismech vedoucích k autofágii.

Nicméně nekrotická buněčná smrt není vždy náhodným pasivním procesem, ale může být také výsledkem specificky řízené signalizační kaskády. Nejlépe charakterizovanou formou programované nekrózy je nekróza závislá na kinázách skupiny RIP (receptor-interacting protein), označovaná také jako nekroptóza. Mezi signály indukující tento typ buněčné smrti patří proapoptotické ligandy smrti (TNFα, FasL a TRAIL) a patogenní komponenty (PAMPs, pathogen-associated molecular patterns) - např. lipopolysacharid (LPS), virové nukleové kyseliny, atd., které interagují s Toll-like receptory (TLR), NOD (nucleotide-binding oligomerization domain)-like receptory a virovými DNA receptory (Vanlangenakker et al., 2012). Nejlépe definovanou dráhou zahajující nekroptotickou signalizaci je dráha aktivovaná ligací TNFR1-TNFα. Je potřeba zmínit, že odpověď buněk na přítomnost TNFα je velmi komplexní a může vést jak k indukci nekroptózy, tak apoptózy nebo MAP (mitogen-activated protein) kinázové signalizaci a aktivaci NF-κB (nuclear factor-κB). Indukce nekroptózy přes TNFR1 vyžaduje tvorbu cytoplazmatického multiproteinového komplexu zvaného komplex II, který se skládá z FADD, kaspázy 8, cFLIP a RIPK1. Primární funkcí tohoto komplexu je aktivace kaspázy 8, suprese nekroptózy štěpením RIPK1 a indukce apoptózy (Ashkenazi and Salvesen, 2014). Nicméně za podmínek, kdy dochází k inhibici aktivity kaspázy 8, je umožněna aktivace RIPK1 kinázy a její interakce s RIPK3, což vede k tvorbě signalizačního komplexu zvaného nekrosom. V rámci tohoto komplexu RIPK1 fosforyluje RIPK3 (Ashkenazi and Salvesen, 2014, He et al., 2009), což umožní vazbu MLKL (mixed lineage kinase domain-like). Fosforylace MLKL RIPK3 má za následek jeho oligomerizaci a translokaci do plazmatické membrány a intracelulárních membrán vazbou na specifické

lipidy. Oligomerizace MLKL způsobuje vznik pórů, což narušuje integritu membrán a konečnou fázi nekroptotického procesu (Sun et al., 2012). I když nejsou biochemické události, které zprostředkovávají exekuční fázi nekroptotické smrti dosud zcela známy, existují poznatky, že v tomto procesu hraje roli produkce reaktivních kyslíkových radikálů (ROS, reactive oxygen species) mitochondriemi, uvolnění lysosomálního obsahu a peroxidace lipidů (Vanden Berghe et al., 2010).

2.1.3. Autofágie

Autofágie (někdy také nazývána jako makroautofágie) je buněčný katabolický proces indukovaný metabolickým stresem v důsledku nedostatku živin a růstových faktorů, hypoxie, infekce patogeny, atd.. Jeho cílem je zajistit dostupnost důležitých metabolitů a také zprostředkovat odstranění infikovaných buněk, poškozených organel a proteinových agregátů v cytoplazmě. V případě letálního stresu, kdy tyto mechanismy nestačí k obnovení buněčných funkcí, dochází k indukci autofagické buněčné smrti (Levine and Kroemer, 2008).

Autofágie je charakterizovaná masivní vakuolizací cytoplazmy. Degradace cytoplazmatického obsahu vyžaduje tvorbu útvarů s dvojitou membránou, zvaných autofagosomy. Tyto struktury obklopují intracelulární materiál a fúzují s lysosomy, kde jsou cytoplazmatické komponenty štěpeny lysosomálními hydrolázami. Tvorba a dozrávání autofagosomu je kaskádovitě regulováno proteiny asociovanými s autofágií (ATG, autophagy-related proteins). Signalizační dráha je zahájena aktivací tzv. preiniciačního komplexu tvořeného kinázou ULK1 (Unc-51-like kinase 1), FIP200 a ATG13. Preiniciační komplex dále váže a aktivuje iniciační komplex skládající se z beclinu 1, fosfatidylinositol-3-kinázy (PI3K) III. třídy (Vps34) a protein kinázy Vps15 za vzniku fosfatidylinositol-3-fosfátu (PI3P) (He and Levine, 2010). Tento proces zahajuje tvorbu fagoforu vazbou ATG7, který

indukuje dvě konjugační dráhy nezbytné pro elongaci membrány a uzavření autofagosomu (Green and Llambi, 2015, Hanada et al., 2007).

Autofágie hraje významnou roli v eliminaci buněk napadených patogenními mikroorganismy imunitním systémem a prezentaci antigenů na MHC (major histocompatibility complex) molekulách II. třídy. To je umožněno především interakcí tzv. „pattern recognition“ receptorů (PRRs) (např. TLR a NOD-like receptorů) s patogenními komponentami. Aktivace TLR4 a TLR7 LPS nebo ssRNA vede k tvorbě autofagosomů, indukci Myd88- a TRIF (TIR domain-containing adapter-inducing interferon-β)-dependentní signalizace zprostředkovávající aktivaci NF-κB a AP1 (activator protein 1) a následné stimulaci produkce prozánětlivých cytokinů (Delgado et al., 2008). Během autofágie dochází také k uvolňování HMGB1 a sekreci ATP. Tyto molekuly mají potenciál stimulovat imunitní odpověď a budou podrobněji probrány v následujících kapitolách.

2.2. Koncept imunogenní buněčné smrti

V minulosti byla apoptóza vnímána jako imunologicky neutrální děj. Naopak na nekrózu bylo pohlíženo jako na děj, který vede k indukci imunitní odpovědi. Dnes je již obecně přijímáno, že nejen nekrotické, ale také apoptotické buňky mají potenciál stimulovat imunitní odpověď. Morfologické charakteristiky tedy nepredikují dopad buněčné smrti na aktivaci imunitního systému. Buněčná smrt nádorových buněk může být imunogenní v případě, že je indukována určitými chemoterapeutiky, fyzikálními modalitami a některými viry, které budou dále popsány v této práci. Tato specifická forma regulované buněčné smrti nazvaná jako „imunogenní buněčná smrt“ (ICD, immunogenic cell death) je v imunokompetentních myších schopna aktivovat paměťovou antigen-specifickou adaptivní imunitní odpověď, která je schopna oddálit růst nádoru (Bezu et al., 2015, Krysko et al., 2012). Imunogenní buněčná smrt je většinou (ale ne vždy) doprovázena morfologickými znaky typickými pro klasickou

apoptózu a některé její charakteristiky jsou závislé na složkách apoptotického aparátu (Panaretakis et al., 2009). Imunostimulační kapacita ICD závisí na aktivaci drah buněčného stresu, které se účastní translokace endogenních signálů nebezpečí na plazmatickou membránu umírajících buněk, popřípadě jejich sekrece/uvolnění do extracelulárního prostředí (Zitvogel et al., 2010a). Tyto signály jsou souhrnně označovány jako damage-associated molecular patterns (DAMPs) a mohou být rozděleny do 3 kategorií: 1. DAMPs translokované na buněčnou membránu (kalretikulin (CRT), proteiny teplotního šoku (heat shock) HSP70 a HSP90) (Garg et al., 2010), 2. DAMPs sekretované nebo pasivně uvolňované do extracelulárního prostředí (high mobility group box 1 (HMGB1), ATP, interferony (IFN) I. typu (Sistigu et al., 2014), annexin A1 (ANXA1) (Vacchelli et al., 2015), kyselina močová a prozánětlivé cytokiny zahrnující např. IL-1β a 3. DAMPs uvolňované z umírajících nádorových buněk v pozdní fázi apoptózy jako degradační produkty (DNA a RNA) (Garg et al., 2010). V souladu s dostupnou literaturou jsou za nejdůležitější DAMPs asociované s ICD považovány především CRT, proteiny teplotního šoku HSP70 a HSP90, HMGB1, ATP, IFN I. typu a ANXA1, které budou popsány v následující kapitole.

2.2.1. Hlavní DAMPs asociované s imunogenní buněčnou smrtí a jejich význam pro aktivaci imunitního systému

2.2.1.1. Kalretikulin

Kalretikulin (CRT) je vysoce konzervovaný protein s molekulovou hmotností 46 kDa lokalizovaný převážně v lumen ER. V ER plní zásadní funkci chaperonového proteinu, reguluje Ca^{2+} homeostázu a signalizaci, napomáhá správnému složení MHC molekul I. třídy, vazbě antigenu a stabilizaci komplexu MHC/antigen na buněčném povrchu (Krysko et al., 2012). Kalretikulin se kromě ER nachází také v jádře (konkrétně v lumen jaderného obalu) a

cytoplazmě. Zatímco funkce CRT v cytoplazmě jsou prozatím neznámé, hlavní funkcí jaderného CRT je regulace transportu proteinů v jádře (jak importu, tak exportu) (Mesaeli and Phillipson, 2004). Frakce CRT byla také nalezena na plazmatické membráně živých buněk. Za fyziologických podmínek se povrchový CRT váže na transmembránové receptory (jako např. CD49, CD69, CD91), integriny, složky bazálních membrán (glykosylovaný laminin) a solubilní faktory (thrombospondin 1, komplementová složka C1q) a reguluje fokální adhezi, interakci buněk s extracelulární matrix a migraci (Garg et al., 2010, Truxova et al., 2017, Krysko et al., 2012).

Důležitým zjištěním byl fakt, že CRT může být vystaven na buněčný povrch v časné fázi imunogenní apoptózy. K tomuto procesu dochází v důsledku specifických stimulů schopných indukovat ICD. V roce 2007 Obeid a kolegové definovali antracykliny, oxaliplatinu, UV-C a γ záření jako první induktory ICD. Nádorové buňky ošetřené těmito látkami a modalitami byly lépe rozpoznávány a pohlcovány DCs a jejich aplikace vedla u imunokompetentních myší ke stimulaci protektivní imunitní odpovědi a redukci masy nádoru (Obeid et al., 2007a, Obeid et al., 2007b, Panaretakis et al., 2009, Tesniere et al., 2010). Deplece CRT, např. pomocí siRNA (small interfering RNA) vedla ke snížení imunogenního potenciálu nádorových buněk ošetřených antracykliny a naopak exogenní aplikace rekombinantního CRT nebo použití farmakologických látek usnadňujících translokaci CRT na buněčný povrch (např. inhibitory protein fosfatázy 1 (PP1, protein phosphatase 1)) vedlo k obnovení imunogenicity (Obeid et al., 2007b). Kalretikulin je proto považován za klíčovou determinantu imunogenní formy buněčné smrti. V kontextu imunitního systému je CRT dobře znám především jako klíčový tzv. „eat-me“ signál, který umožňuje rozpoznání a pohlcení umírajících buněk $CD91^+$ buňkami jako jsou makrofágy a DCs. To následně vede k prezentaci nádorových antigenů cytotoxickým $CD8^+$ T lymfocytům a stimulaci protinádorové imunitní odpovědi (Gardai et al., 2005). Hong a kolegové ukázali, že

imunomodulační schopnost CRT leží v jeho N-terminální lektinové doméně, která s vysokou afinitou váže různé glykosylované proteiny. Zajímavým zjištěním bylo, že rekombinantní N-terminální fragment CRT (39-272) je silným induktorem aktivace a maturace B buněk a makrofágů a může *in vitro* a *in vivo* spouštět izotypový přesmyk B buněk bez pomoci T lymfocytů (Hong et al., 2010).

2.2.1.2. Proteiny teplotního šoku HSP70 a HSP90

Transkripční a translační aktivace molekulárních chaperonů patřících do třídy inducibilních HSPs představuje typickou odpověď na různé druhy buněčného stresu zahrnujících oxidativní stres, záření, chemoterapii, atd.. Tyto vysoce konzervované proteiny hrají důležitou roli při skládání nově syntetizovaných proteinů a chrání buňku před smrtí tím, že pomáhají znovu skládat proteiny poškozené v důsledku stresu, které jsou v případě opětovného sbalení do špatné konformace určeny k degradaci v proteasomu (Lanneau et al., 2008). Zatímco většina HSPs zůstává během stresových podmínek v cytoplazmě nebo organelách jako ER a mitochondrie, některé inducibilní HSPs, mezi něž patří např. HSP70 a HSP90, jsou translokovány na plazmatickou membránu v důsledku probíhající ICD aktivované např. antracykliny, bortezomibem, atd. (Fucikova et al., 2011a, Spisek et al., 2007). Základním rozdílem mezi intra a extracelulárními HSPs jsou jejich pronádorové respektive protinádorové funkce. Intracelulární HSPs se vyznačují spíše cytoprotektivními vlastnostmi a schopností inhibovat apoptózu. Naopak extracelulární nebo membránově vázané HSPs působí na nádor supresivně díky silným imunostimulačním vlastnostem (Tesniere et al., 2008). Povrchový HSP70 a HSP90 fungují pro imunitní systém jako signály nebezpečí a za určitých podmínek zvyšují imunonogenní potenciál nádorových buněk. HSP90, translokovaný na plazmatickou membránu myelomových buněk během ICD indukované bortezomibem, se váže na DCs, což vede k jejich aktivaci a sekreci prozánětlivých cytokinů (Spisek et al., 2007). Podobně také

HSP70 působí jako maturační signál pro DCs (Singh-Jasuja et al., 2000). HSPs nevážou pouze proteiny, které potřebují zaujmout správnou konformaci, ale mohou také vázat peptidy, včetně nádorově-specifických antigenů a antigenů asociovaných s nádorem (TAAs, tumor-associated antigens). Komplexy HSPs s peptidy slouží jako zdroj antigenů, které tak mohou být účinně cross-prezentovány cytotoxickým $CD8^+$ T lymfocytům (Binder and Srivastava, 2005). I když jsou imunostimulační účinky HSPs převážně zprostředkovány DCs, mohou tyto molekuly interagovat také s NK (natural killer) buňkami a aktivovat je. HSP70 na povrchu nádorových buněk je schopen selektivně indukovat nárůst cytotoxické aktivity NK buněk *in vitro* (Multhoff et al., 1997). NK buňky mohou přímo rozpoznávat oligomer o velikosti 14-ti aminokyselin (TKD) lokalizovaný v C-terminální doméně HSP70 vazbou na CD94 receptor (Gastpar et al., 2004, Gross et al., 2003). HSP70 asociovaný s nádorovými buňkami, ať už prezentovaný na buněčném povrchu nebo sekretovaný prostřednictvím exosomů, může zvyšovat aktivitu NK buněk proti různým typům nádorů *in vivo* (Elsner et al., 2007, Gastpar et al., 2005). Dále bylo prokázáno, že aktivita jaterních NK buněk proti neoplastickým buňkám zprostředkovaná TRAILem může být také zvýšena upregulací HSP70 (Dang et al., 2014). V porovnání s HSP70 je toho o vztahu NK buněk a HSP90 známo méně. Současné studie ale naznačují, že HSP90 hraje potenciálně také roli v aktivaci NK buněk. Inhibitory HSP90 totiž negativně regulují cytotoxicitu NK buněk tím, že indukují jejich apoptózu, snižují produkci cytokinů a expresi aktivačních NK receptorů (Huyan et al., 2016). Tato data souhrnně ukazují, že přítomnost HSPs na povrchu nádorových buněk je důležitým faktorem pro zahájení efektivní protinádorové imunitní odpovědi jak na úrovni antigen-prezentujících buněk (APCs, antigen-presenting cells), tak NK buněk.

2.2.1.3. HMGB1

HMGB1 představuje protein vázající chromatin, který se za fyziologických podmínek vyskytuje v buněčném jádře. Jeho hlavní rolí v jádře je stabilizace nukleosomů, oprava a rekombinace DNA a regulace transkripce (Tang et al., 2010). Kromě toho také plní funkce v cytosolu a v extracelulárním prostředí. Extracelulární HMGB1 má silné prozánětlivé účinky (Andersson and Tracey, 2011, Scaffidi et al., 2002) a je pasivně uvolňován z poškozených buněk během různých forem buněčné smrti zahrnujících pozdní apoptózu, primární/sekundární nekrózu, nekroptózu a autofágii (Malhotra and Kaufman, 2011, Fucikova et al., 2011a, Garg et al., 2010, Guo et al., 2014, Thorburn et al., 2009). I když uvolnění HMGB1 z buněk nepředstavuje specifický proces doprovázející pouze ICD, bylo experimentálně dokázáno, že HMGB1 je další klíčovou molekulou rozhodující o tom, zda je buněčná smrt vnímána imunitním systémem jako imunogenní. Experimentální studie na myších prokázaly, že imunizace pomocí CT26 buněk ošetřených antracykliny s depletovaným HMGB1 nebo s paralelní injekcí blokační protilátky proti HMGB1 vedla ke snížení imunogenního potenciálu těchto buněk a schopnosti myší odolávat růstu nádoru. Eradikace nádoru indukovaná imunogenní chemoterapií (antracykliny) byla závislá na vazbě HMGB1 na TLR4 na povrchu APCs (Apetoh et al., 2007b).

Z pohledu imunitního systému, je důležitou funkcí HMGB1 zajištění optimální prezentace antigenů z umírající buňky DCs (Krysko et al., 2012). Za zmínku stojí fakt, že imunomodulační vlastnosti HMGB1 závisí na redoxních modifikacích indukovaných buňkou samotnou nebo extracelulárním prostředím. Zatímco plně redukovaný HMGB1 funguje jako chemoatraktant a HMGB1 nesoucí disulfidovou vazbu indukuje produkci prozánětlivých cytokinů, oxidace vede k inaktivaci těchto imunostimulačních účinků (Venereau et al., 2012, Yang et al., 2012). Nádorové mikroprostředí je vysoce variabilní, proto zůstává otázkou, zda

jsou imunostimulační vlastnosti HMGB1 uvolňovaného během ICD relevantní v nádorové tkáni *in vivo*.

2.2.1.4. ATP

ATP představuje hojně zastoupený intracelulární metabolit, který také hraje důležitou roli v autokrinní/parakrinní signalizaci regulací různých buněčných funkcí jako např. purinergní neurotransmise, přežívání, buněčné smrti, adheze, proliferace a diferenciace buněk (Burnstock, 2007, Krysko et al., 2012). K uvolnění nebo aktivní sekreci ATP dochází také během buněčné smrti indukované různými stimuly jako např. mechanickým poškozením, poškozením plazmatické membrány, hypoxií, ošetřením cytotoxickými látkami a fyzikálními modalitami. ATP je také sekretován v důsledku probíhající ICD, ale podobně jako HMGB1 není výlučně charakteristickým znakem pouze pro tento typ buněčné smrti (Ayna et al., 2012, Elliott et al., 2009, Garg et al., 2012b, Martins et al., 2014). Sekrece/uvolnění ATP silně závisí na typu a fázi buněčné smrti a mechanismus tohoto procesu bude detailně popsán v kapitole 2.2.3.2.. Aplikace fotodynamické terapie (induktor ICD) vede u buněk k aktivní sekreci ATP během pre-apoptotické fáze a tato sekrece je závislá na kinázách PERK a PI3K (Garg et al., 2012b). Nádorové buňky, umírající ICD indukovanou antracykliny, mitoxantronem a oxaliplatinou, sekretují ATP mechanismem závislým na autofágii (Martins et al., 2009, Michaud et al., 2011). Z imunologického hlediska působí extracelulární ATP především jako tzv. „find-me“ signál usnadňující rychlé přilákání makrofágů a prekurzorů DCs do míst s intenzivní buněčnou smrtí (Elliott et al., 2009) a může také regulovat fenotyp myeloidních buněk a maturaci DCs (Kroemer et al., 2013). Je potřeba zmínit, že extracelulární ATP může být velmi rychle hydrolyzováno membránově vázanými ektonukleotidázami CD39 (známá také jako NTPD1 (nucleoside triphosphate diphosphohydrolase 1)) a CD73 (ekto-5´-nukleotidáza) na imunosupresivní adenosin. To

znamená, že vysoká koncentrace imunostimulačního ATP v nádorové tkáni může zároveň vést k vyššímu množství adenosinu v těchto místech. Na rozdíl od ATP, adenosin podporuje imunosupresivní prostředí v nádoru a inhibuje tak efektivní protinádorovou imunitní odpověď (Beavis et al., 2012, Robson et al., 2006).

2.2.1.5. Interferony I. typu

Interferony (IFN) I. typu jsou produkovány různými buněčnými populacemi během aktivace PRRs převážně virovými komponentami, ale i složkami bakteriálního původu a také endogenními molekulami jako cytosolickou DNA nebo extracelulární DNA a RNA (Kawai and Akira, 2010). Současné poznatky ukazují, že IFN I. typu jsou sekretovány také nádorovými buňkami v souvislosti s probíhající ICD indukovanou některými imunogenními chemoterapeutiky a onkolytickými viry. Schopnost těchto induktorů vyvolat produkci IFN I. typu je nutná pro aktivaci buněk vrozené imunity a zahájení adaptivní protinádorové imunitní reakce (Donnelly et al., 2013, Sistigu et al., 2014). IFN. I typu se vážou na homodimerické a heterodimerické receptory exprimované řadou imunitních buněk a mají tak velice širokou imunostimulační aktivitu. Působí na myeloidní buňky, např. makrofágy, a indukují jejich aktivaci (Novikov et al., 2011), zvyšují funkční potenciál cytotoxických $CD8^+$ T lymfocytů stimulací cross-prezentace nádorových antigenů DCs a upregulací exprese perforinu a granzymu B, podporují migraci $CD8^+$ T lymfocytů do lymfatických uzlin a přežívání paměťových buněk (Zitvogel et al., 2015) a chrání $CD8^+$ T lymfocyty aktivované antigenem před eliminací NK buňkami (Crouse et al., 2014). Interferony I. typu dále také zvyšují cytotoxicitu NK buněk (Guillot et al., 2005) a inhibují supresivní funkce regulačních T buněk (Treg) (Bacher et al., 2013). Kromě těchto imunostimulačních efektů mohou IFN I. typu regulovat různé signalizační dráhy uvnitř nádorových buněk vedoucích např. k syntéze

chemotaktického faktoru CXCL10 (chemokine (C-X-C motif) ligand 10), který zvyšuje atrakci efektorových $CXCR3^+$ T lymfocytů do nádoru (Sistigu et al., 2014).

2.2.1.6. Annexin A1

Význam ANXA1 pro imunostimulační potenciál ICD byl objeven teprve nedávno. ANXA1 je za fyziologických podmínek cytosolický protein, který je po ošetření nádorových buněk *in vitro* imunogenní chemoterapií (antracykliny) uvolňován do supernatantu. Současná data ukazují, že ANXA1 je důležitým faktorem pro migraci DCs do míst, kde dochází ke smrti nádorových buněk a pro navození stabilních interakcí s umírajícími buňkami. Knockout genu kódujícího ANXA1 nebo jeho receptor na DCs (FPR-1, formyl peptide receptor-1) vede k potlačení imunitní odpovědi proti nádorovým buňkám ošetřeným antracykliny (Vacchelli et al., 2015, Vacchelli et al., 2016).

2.2.2. Induktory imunogenní buněčné smrti

V současnosti existuje celá řada látek a modalit, u kterých bylo prokázáno, že indukují ICD. Induktory ICD jsou značně heterogenní a liší se jak biologickými, tak chemickými/fyzikálními vlastnostmi. Tato diverzita vedla k vytvoření klasifikace, která především odráží mechanismy působení těchto látek a modalit. Klasifikační systém dělí induktory ICD do dvou skupin podle toho, zda spouští apoptózu jako důsledek přímého působení na ER (induktory II. typu) nebo indukují apoptózu a stres ER nezávislými mechanismy (induktory I. typu) (Krysko et al., 2012). Většina z dosud popsaných induktorů ICD způsobuje stres ER nepřímo přes nejrůznější cytosolické proteiny, proteiny plazmatické membrány, DNA a DNA replikační proteiny a řadíme je tedy do induktorů I. typu. Do této skupiny patří zejména antracykliny (Fucikova et al., 2011a, Obeid et al., 2007b), mitoxantron (Obeid et al., 2007b), cyklofosfamid (Schiavoni et al., 2011), oxaliplatina (Tesniere et al.,

2010), bortezomib (Spisek et al., 2007), bleomycin (Bugaut et al., 2013), UVC a γ-záření (Obeid et al., 2007a) a vysoký hydrostatický tlak (HHP, high hydrostatic pressure) (Fucikova et al., 2014). Jako induktory II. typu jsou označovány fotodynamická terapie založená na hypericinu (hyp-PDT, hypericin-based photodynamic therapy) (Garg et al., 2012b) a některé onkolytické viry (Miyamoto et al., 2012). Mechanismus působení jednotlivých induktorů ICD je znázorněn na Obr.2..

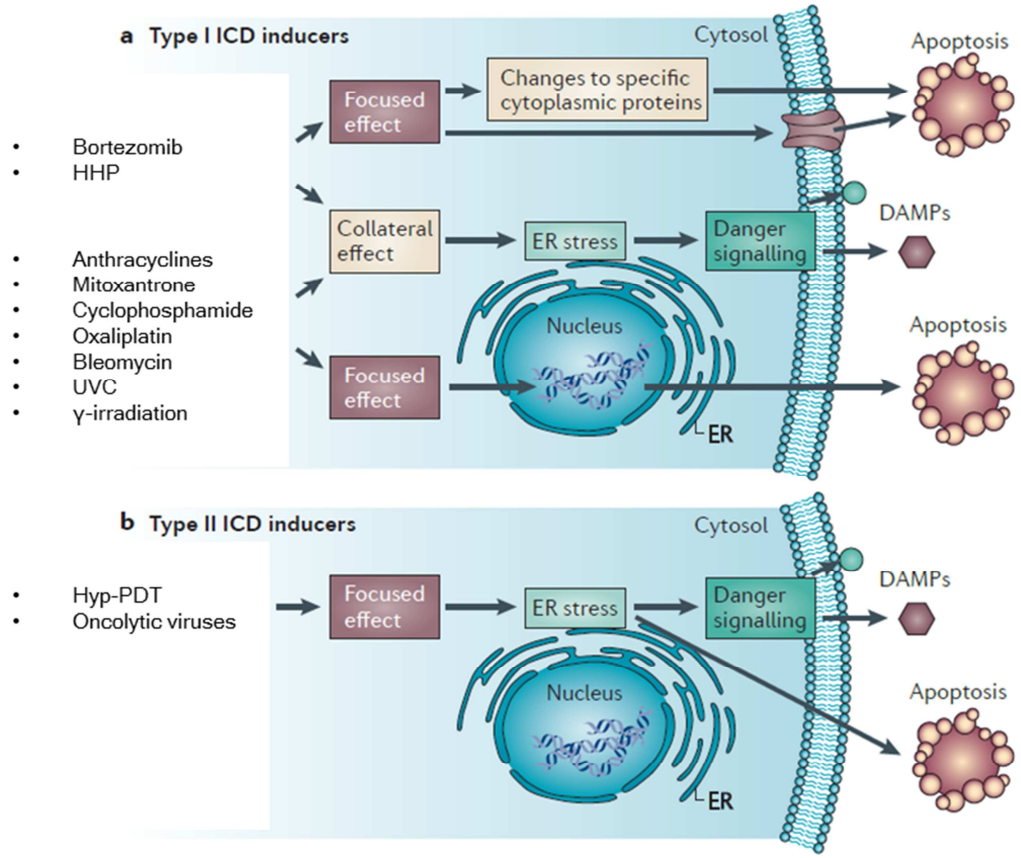

Obr.2. Mechanismy vedoucí k ICD indukované induktory I. a II. typu. *a. Primárními cíly většiny induktorů ICD I. typu jsou jádro (DNA a proteiny účastnící se replikace a opravy DNA), cytoplazmatické proteiny a proteiny plazmatické membrány. Jejich schopnost vyvolávat buněčnou smrt nebo apoptózu je dána především těmito cílenými efekty. Tyto látky a modality mají ale také řadu vedlejších efektů, které mohou sekundárně indukovat stres ER a sekreci/uvolnění/vystavení DAMPs. b. Induktory ICD II. typu naproti tomu cíleně poškozují ER, což vede k intenzivnímu stresu ER. Jak jejich schopnost indukovat apoptózu, tak*

sekreci/uvolnění/vystavení DAMPs, je závislá na efektech cílených přímo na ER. Převzato a upraveno podle (Krysko et al., 2012).

2.2.2.1. Induktory I. typu

2.2.2.1.1. Antracykliny a mitoxantron

Antracykliny (doxorubicin, idarubicin a epirubicin) byly poprvé popsány v roce 1963 jako antibiotika. Díky jejich vysoké účinnosti v protinádorové terapii jsou nadále používány pro léčbu řady solidních a hematologických nádorových onemocnění, např. lymfomů, karcinomu prsu, ovárií, atd.. Cytotoxický účinek antracyklinů a derivátů antrachinonů (mitoxantron) je zprostředkován jejich vazbou mezi páry bazí v DNA nebo RNA řetězci a inhibicí topoizomerázy II. Dochází k zastavení syntézy nukleových kyselin a replikace rychle proliferujících nádorových buněk s následnou indukcí buněčné smrti (Rabbani et al., 2005). Tento typ smrti vykazuje klíčové charakteristiky ICD jako pre-apoptotickou translokaci CRT na buněčný povrch, vystavení HSPs, produkci IFN I. typu, sekreci ATP a pasivní uvolnění HMGB1 během pozdní fáze apoptózy (Fucikova et al., 2011a, Obeid et al., 2007b, Sistigu et al., 2014).

2.2.2.1.2. Cyklofosfamid

Cyklofosfamid je alkylační oxazafosforinové cytostatikum, které je široce používáno v léčbě solidních nádorů a autoimunitních onemocnění. Jeho cytostatická aktivita je závislá na poškození DNA alkylací. Kromě toho má také antiangiogenní a imunomodulační vlastnosti (Sistigu et al., 2011). Schopnost stimulovat imunitní systém je částečně dána tím, že indukuje ICD, během které dochází k vystavení CRT na buněčný povrch a uvolnění HMGB1 z nádorových buněk (Bezu et al., 2015).

2.2.2.1.3. Oxaliplatina

Oxaliplatina patří do skupiny platinových derivátů s cytostatickými účinky. Její protinádorové působení bylo prokázáno v řadě myších a lidských preklinických modelů a kombinace oxaliplatiny s 5-fluorouracilem a kyselinou folinovou byla schválena pro terapii pokročilého karcinomu tlustého střeva (Tesniere et al., 2010). Platinové deriváty (oxaliplatina, cisplatina, karboplatina) interkalují do DNA a způsobují její denaturaci a vznik DNA zlomů, což vede k inhibici syntézy DNA/RNA a replikace a k aktivaci apoptotických signalizačních drah (Stojanovska et al., 2015). Oxaliplatina je, na rozdíl od cisplatiny a karboplatiny, považována za efektivní induktor ICD, vedoucí k sekreci/uvolnění/vystavení DAMPs z umírajících buněk. Buňky ošetřené oxaliplatinou na svém povrchu vystavují CRT a HSP70, sekretují ATP a uvolňují HMGB1 do extracelulárního prostředí (Tesniere et al., 2010). Oxaliplatina také zvyšuje expresi MHC molekul I. třídy na nádorových buňkách, což napomáhá jejich efektivnímu rozpoznávání a odstraňování imunitními buňkami (Liu et al., 2010).

2.2.2.1.4. Bortezomib

Bortezomib (Velcade) byl v roce 2003 schválen pro klinické použití americkým Úřadem pro kontrolu potravin a léčiv (FDA, Food and Drug Administration) a je používán pro léčbu mnohočetného myelomu a lymfomu z plášťových buněk. Bortezomib inhibuje 26S proteasom, klíčový regulátor degradace intracelulárních proteinů, a indukuje zastavení buněčného cyklu a přechod buněk do apoptózy (Chen et al., 2011). Byl také identifikován jako induktor ICD a jeho imunogenní vlastnosti byly prokázány v myších nádorových modelech (Schumacher et al., 2006). Po ošetření nádorových buněk bortezomibem dochází k vystavení HSP90 na plazmatické membráně, což následně vede ke kontaktně-dependentní aktivaci DCs. Navzdory těmto imunostimulačním vlastnostem může bortezomib působit na imunitní systém také negativně, protože snižuje expresi MHC molekul na DCs a ovlivňuje

životnost některých populací imunitních buněk, např. plazmacytoidních DCs nebo aktivovaných T lymfocytů (Schumacher et al., 2006).

2.2.2.1.5. Bleomycin

Bleomycin je antibiotický glykopeptid s protinádorovými vlastnostmi produkovaný bakterií *Streptomyces verticillus*, který je v současnosti indikován pro paliativní léčbu Hodgkinova lymfomu, nádorů penisu a varlat a skvamózního karcinomu hlavy a krku, děložního čípku a vulvy. Nedávno bylo prokázáno, že bleomycin je schopen indukovat ICD a její typické znaky jako translokaci CRT a ERp57 na buněčný povrch, sekreci ATP a uvolnění HMGB1 a dále stimulovat protinádorovou imunitní odpověď, která je závislá na CRT, $CD8^+$ T lymfocytech a IFN-γ (Bugaut et al., 2013).

2.2.2.1.6. Fyzikální modality

Fyzikální modality, spadající do kategorie induktorů ICD I. třídy, zahrnují UVC a γ-záření a vysoký hydrostatický tlak (HHP).

UVC a γ-záření obecně způsobuje poškození DNA, které v závislosti na intenzitě a buněčném typu vede k apoptóze nebo nekróze. Imunostimulační potenciál nádorových buněk ošetřených UVC a γ-zářením byl prokázán *in vivo* v řadě myších imunizačních experimentů (Begovic et al., 1991, Carr-Brendel et al., 1999, Schaue et al., 2012). Z popsaných DAMP molekul klíčových pro koncept ICD, indukují tyto typy záření pre-apoptotickou translokaci CRT a HSP70 na plazmatickou membránu a uvolnění HMGB1. Nádorové buňky inaktivované UVC a γ-zářením zvyšují maturaci DCs a stimulují aktivaci $CD8^+$ T lymfocytů a produkci IFN-γ *in vitro* a *in vivo* (Apetoh et al., 2007b, Obeid et al., 2007a).

Vysoký hydrostatický tlak je běžně používán pro sterilizaci potravin, transplantátů a léčiv. Aplikace HHP v rámci protinádorové terapie byla poprvé popsána v roce 1972 (Helmstein,

1972). Buněčná smrt indukovaná HHP byla více zkoumána Udo Gaiplem a kolegy, kteří navrhli potenciální využití HHP pro výrobu buněčných protinádorových vakcín (Frey et al., 2004, Korn et al., 2004). Průběh buněčné smrti závisí na intenzitě HHP. Zatímco intenzita v rozsahu 1-100 MPa je považována za fyziologickou a působí pouze reverzibilní morfologické změny buňky, hodnoty HHP v rozmezí 150-250 MPa indukují apoptózu. Nekrotická buněčná smrt může být navozena HHP o intenzitě vyšší než 300 MPa, v závislosti na buněčném typu. Ošetření buněk HHP vede k jejich zakulacení, zgelovatění cytoplazmy, inhibici syntézy proteinů a zpomalení enzymatických funkcí (Weiss et al., 2010). V předchozích letech naše skupina identifikovala HHP jako induktor ICD. HHP indukuje translokaci CRT, HSP70 a HSP90 na povrch umírajících nádorových buněk, sekreci ATP a uvolnění HMGB1 v pozdní fázi buněčné smrti (Fucikova et al., 2014). V současné době se tato modalita využívá pro standardizovanou přípravu imunogenních nádorových buněk a je součástí výrobního protokolu vakcíny založené na DCs pro imunoterapii karcinomu prostaty, ovárií a plic, která je testována v rámci několika probíhajících klinických studií (Adkins et al., 2018, Hradilova et al., 2017, Podrazil et al., 2015). Detailní charakteristika ICD indukované HHP a její vliv na aktivaci imunitní odpovědi jsou uvedeny ve dvou přiložených publikacích, které jsou součástí této práce.

2.2.2.2. Induktory II. typu

2.2.2.2.1. Fotodynamická terapie založená na hypericinu

Hyp-PDT představuje modalitu s cytostatickými účinky založenou na akumulaci fotosenzitivní látky hypericinu v ER, která je aktivována excitací světlem o určité vlnové délce. Po aktivaci hypericinu dochází v ER k masivní produkci ROS, což má za následek intenzivní stres ER. Tyto události vedou k indukci buněčné smrti a lokální zánětlivé reakce. Nádorové buňky ošetřené hyp-PDT vykazují znaky ICD a jejich potenciál stimulovat

protinádorovou imunitní odpověď byl potvrzen *in vivo* na myších modelech (Garg et al., 2012a, Garg et al., 2012b). Mezi charakteristiky asociované s ICD indukovanou hyp-PDT patří pre-apoptotické vystavení CRT a HSP70 na buněčný povrch, časná sekrece ATP a pasivní uvolnění CRT, HSP70 a HS90 do extracelulárního prostředí během pozdní fáze apoptózy. Interakce nádorových buněk ošetřených hyp-PDT s DCs vede k fenotypické maturaci a funkční stimulaci DCs (zvýšení produkce IL-1β a oxidu dusného (NO)) (Garg et al., 2012a, Garg et al., 2012b).

2.2.2.2.2. Onkolytické viry

Onkolytické viry byly v posledních letech testovány v řadě preklinických modelů a klinických studií jako potenciální protinádorová terapie (Pol et al., 2016a). Prvním přípravkem na bázi onkolytického viru, schváleného americkou FDA pro terapii nádorů (konkrétně melanomu), se v roce 2015 stal Talimogene laherparepvec (T-VEC) obsahující geneticky modifikovaný herpes simplex virus-1 (HSV-1) (Pol et al., 2016b). Terapeutická účinnost onkolytických virů není závislá pouze na lýze neoplastických buněk, ale také na jejich schopnosti aktivovat adaptivní protinádorovou imunitní odpověď. Onkolytické viry indukují převážně imunogenní typ buněčné smrti, zahrnující imunogenní apoptózu, nekrózu/nekroptózu, pyroptózu nebo autofágii, která je spojena se sekrecí/uvolněním/vystavením DAMPs. Jak DAMPs, tak virově odvozené PAMPs, představují klíčové signály pro aktivaci DCs a jiných APCs, které vedou ke stimulaci T lymfocytů. Mezi doposud identifikované virové induktory ICD patří Coxsackievirus B3 (CVB3) (Korn et al., 2004), herpex simplex viry (Takasu et al., 2016), virus Newcastleské nemoci (Koks et al., 2015), parvovirus H1 (Moehler et al., 2003), virus spalniček (Donnelly et al., 2013), adenoviry (Diaconu et al., 2012), reovirus (Prestwich et al., 2008) a virus vezikulární stomatitidy (Janelle et al., 2014). V průběhu ICD indukované onkolytickými viry dochází k pre-apoptotickému vystavení CRT na povrch umírajících buněk

(CVB3, herpes simplex viry, virus Newcastleské nemoci, adenoviry), uvolnění HSPs (herpes simplex viry, parvovirus H1, virus Newcastleské nemoci) a HMGB1 (CVB3, herpes simplex viry, virus spalniček, adenoviry, virus Newcastleské nemoci) a sekreci ATP (CVB3, herpes simplex viry, adenoviry) (Aurelian, 2016). Současné poznatky ukazují, že kombinace terapie onkolytickými viry a chemoterapie může zvýšit imunogenní potenciál nádorových buněk a schopnost stimulovat imunitní odpověď proti některým typům solidních nádorů (Siurala et al., 2015, Workenhe et al., 2013).

2.2.3. Mechanismy vedoucí k sekreci/uvolnění/vystavení DAMPs v průběhu imunogenní buněčné smrti

2.2.3.1. Mechanismus translokace membránově lokalizovaných DAMPs

Dosud nejlépe prozkoumaným je mechanismus vedoucí k translokaci CRT na buněčný povrch. Tento fenomén probíhá během časné fáze apoptózy, kdy buňky ještě nevystavují PS na plazmatickou membránu a nevykazují změny morfologie typické pro apoptotické buňky. Obecně se dá říci, že translokace CRT na buněčný povrch vyžaduje přítomnost ROS a účast proteinů aktivovaných během stresu ER, proteinů apoptotického aparátu a komplexu proteinů nutných pro anterográdní transport. Kombinace konkrétních proteinů nutných pro vystavení CRT na plazmatickou membránu se liší v závislosti na induktoru, který ji vyvolává (Kepp et al., 2013, Kroemer et al., 2013).

Jak už bylo zmíněno v předchozí kapitole, jednou ze společných vlastností induktorů ICD je schopnost indukovat stres ER. V nádorových buňkách ošetřených antracykliny, oxaliplatinou nebo UVC zářením dochází k rychlé indukci intenzivního stresu ER charakterizovaného nadprodukcí ROS, zvýšením koncentrace Ca^{2+} v cytoplazmě a aktivací PERK kinázy, jedním ze senzorů stresu ER aktivujícím UPR (Panaretakis et al., 2009, Zitvogel et al., 2010b).

Aktivovaná PERK kináza následně fosforyluje eIF2α, což vede k zastavení translace. Antracykliny navíc v buňkách indukují inhibici PP1, která specificky defosforyluje eIF2α, a tím posilují buněčný stres (Kepp et al., 2009). Vystavení CRT na plazmatickou membránu indukované antracykliny nebo oxaliplatinou může být částečně inhibováno antioxidanty N-acetyl-L-cysteinem (NAC) a redukovaným L-glutathionem (GSH), knockoutem/knockdownem PERK kinázy, knock-inem eIF2α vedoucí k jeho neschopnosti se fosforylovat a snížením intracelulární koncentrace Ca^{2+} chelatačními činidly (Panaretakis et al., 2009). Nicméně stres ER není sám o sobě dostačující pro pre-apoptotickou translokaci CRT. Intenzivní stres vede v buňkách ošetřených antracykliny a oxaliplatinou k aktivaci některých proteinů regulujících buněčnou smrt. Dochází k aktivaci kaspázy 8, klíčové iniciátorové kaspázy, proteolytickému štěpení BAP31 nacházejícím se v ER a konformační aktivaci proapoptotických proteinů Bax a Bak, které hrají důležitou roli v permeabilizaci vnější mitochondriální membrány. Bylo dokázáno, že knockout kaspázy 8, Bax a Bak a exprese mutantního BAP31 neschopného se štěpit inhibují translokaci CRT na plazmatickou membránu a snižují imunogenicitu nádorových buněk indukovanou antracykliny a oxaliplatinou (Panaretakis et al., 2009). Po aktivaci apoptotické fáze je CRT translokován z lumen ER na plazmatickou membránu. Tento proces zahrnuje remodelaci aktinového cytoskeletu, anterográdní transport CRT z ER do Golgiho aparátu regulovaný PI3K kinázou a exocytózu váčků obsahujících CRT založenou na vazbě SNARE (SNAP (soluble NSF (N-ethylmaleimide-sensitive factor) attachment protein) receptor) proteinů asociovaných s váčky (např. vesicle-associated membrane protein 1 (VAMP 1)) a SNARE nacházejícími se na plazmatické membráně v lipidových raftech (např. SNAP23/25) (Panaretakis et al., 2009). Během transportu z ER na buněčný povrch zůstává CRT vázaný na disulfid izomerázu ERp57. Tato interakce je nezbytná pro translokaci CRT indukovanou antracykliny a oxaliplatinou, protože delece nebo deplece ERp57 vede k snížení CRT na povrchu umírajících

nádorových buněk (Panaretakis et al., 2008). To, jak je CRT v plazmatické membráně ukotven, prozatím nebylo objasněno.

I když existuje shoda, že transport CRT na buněčný povrch je závislý především na proteinech účastnících se stresu ER, přesné molekulární mechanismy se mohou mezi jednotlivými induktory ICD lišit. To samé platí také pro další fáze tohoto procesu, jako je aktivace proapoptotických proteinů a anterográdního transportu. Zatímco aktivace PERK kinázy je důležitá pro translokaci CRT indukovanou jak antracykliny, tak hyp-PDT, fosforylace eIF2α je nepostradatelná pouze pro první z nich (Garg et al., 2012b, Obeid et al., 2007b). Navíc vystavení CRT na buněčný povrch indukované hyp-PDT je na rozdíl od antracyklinů nezávislé na zvýšení cytosolické koncentrace Ca^{2+}, aktivaci kaspázy 8 a nevyžaduje přítomnost ERp57 a lipidových raftů (Garg et al., 2012b, Obeid et al., 2007b). Rozdíly mezi signalizačními dráhami indukovanými antracykliny a hyp-PDT jsou znázorněny na Obr.3..

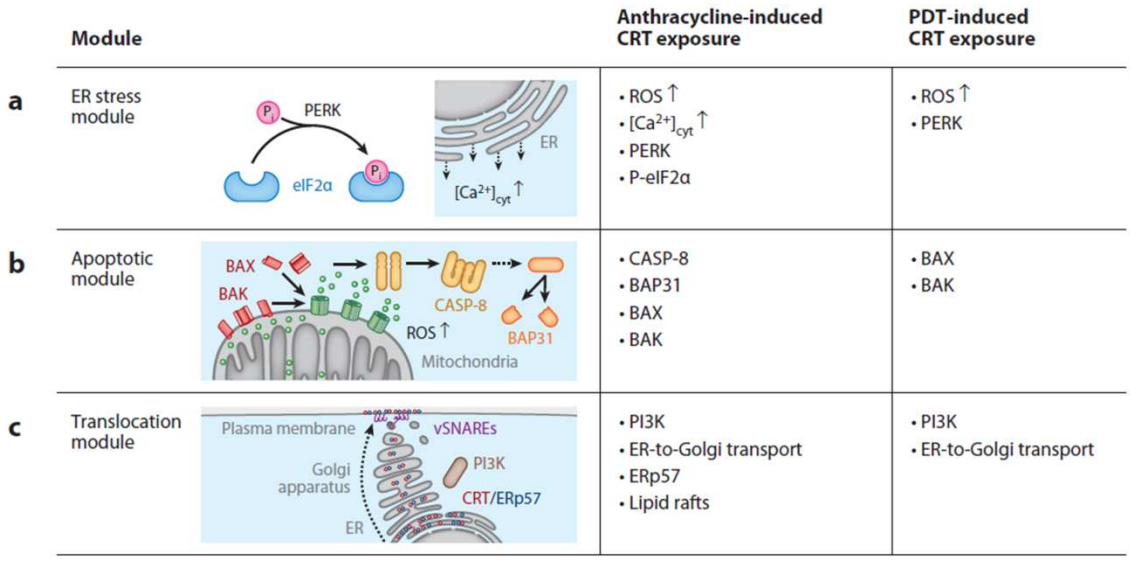

Obr.3. Signalizační dráhy nezbytné pro translokaci CRT na buněčný povrch indukovanou antracykliny vs. Hyp-PDT. *Vystavení CRT indukované antracykliny vyžaduje kotranslokaci chaperonového proteinu ERp57 nacházejícího se v ER a závisí na postupné aktivaci tří*

signalizačních drah: (a) indukce stresu ER doprovázená zvýšenou produkcí ROS, zvýšením koncentrace Ca^{2+} v cytoplazmě, aktivací PERK kinázy a fosforylací eIF2α, (b) účast apoptotického aparátu zahrnující aktivaci kaspázy 8, štěpení BAP31 a aktivaci proteinů z Bcl-2 rodiny Bax a Bak a (c) transport CRT na buněčný povrch zprostředkovaný aktivací PI3K kinázy, aktivací molekulárních komponent anterográdního transportu z ER do Golgiho aparátu a exocytózou závislou na SNARE proteinech a lipidových raftech. Translokace CRT indukovaná jinými induktory ICD je závislá na mechanismech, které se částečně, ale ne kompletně, překrývají s molekulárními kaskádami indukovanými antracykliny. Hyp-PDT indukuje translokaci CRT závislou na PERK, Bax, Bak, PI3K a anterográdním transportu z ER do Golgiho aparátu, ale na rozdíl od antracyklinů je tento proces nezávislý na kotranslokaci ERp57, fosforylaci eIF2α, zvýšení cytoplazmatické koncentrace Ca^{2+} a na přítomnosti lipidových raftů. Tato pozorování naznačují, že vystavení CRT na plazmatickou membránu probíhá díky molekulárním mechanismům, které alespoň částečně závisí na počátečním stimulu. Převzato z (Kroemer et al., 2013).

V tomto roce jsme v rámci naší výzkumné skupiny nově identifikovali kaspázu 2 jako jednu z klíčových molekul důležitých pro vystavení CRT na povrch nádorových buněk v důsledku ošetření HHP (Moserova et al., 2017). Detailní mechanismus je popsán v rámci publikace přiložené v této práci. Tyto poznatky ukazují, že translokace CRT na plazmatickou membránu je důsledkem sítě heterogenních signalizačních drah, z nichž některé jsou společné pro různé induktory ICD, jiné závisí na kontextu a typu vyvolávajícího stimulu.

Co se týká translokace HSPs na buněčný povrch, nejsou mechanismy regulující tento proces dobře známy. Nicméně je pravděpodobné, že se alespoň částečně překrývají se signalizačními dráhami nezbytnými pro vystavení CRT na plazmatickou membránu. Není také známo, zda

frakce HSPs objevující se na povrchu buňky pochází z ER, cytoplazmy nebo z obou kompartmentů (Spisek and Dhodapkar, 2007).

2.2.3.2. Mechanismus sekrece ATP

Mechanismus sekrece nebo uvolnění ATP během ICD silně závisí na stádiu apoptózy a typu stresu, který tuto formu buněčné smrti vyvolává. Během pre-apoptotické nebo časně apoptotické fáze buňky aktivně sekretují ATP. Sekrece ATP probíhá různými mechanismy zahrnujícími exocytózu váčků obsahujících ATP, sekreci cytoplazmatického ATP přes tzv. mezerové spoje (gap junctions), pannexinové kanály a sekreci ATP vazebnými transportéry (ATP-binding cassette proteiny) a purinergními receptory (Lazarowski et al., 2011). V pozdějších fázích apoptózy dochází k pasivnímu uvolňování ATP z buněk poškozených v důsledku sekundární nekrózy. Nádorové buňky, umírající ICD indukovanou antracykliny, mitoxantronem a oxaliplatinou sekretují ATP mechanismem závislým na autofágii a komponentách apoptotického aparátu (např. kaspázy). Autoři této studie ukázali, že knockdown genů kódujících proteiny spojené s autofágií (ATG5/7 a beclin-1) inhibuje časnou apoptotickou sekreci ATP a vede k potlačení protinádorové imunitní odpovědi *in vivo* (Vanden Berghe et al., 2010, Levine and Kroemer, 2008). UVC záření indukuje také aktivní sekreci ATP, ale mechanismem závislým na štěpení a aktivaci pannexinu 1 kaspázou 3 nebo 7 a tvorbě pannexinových kanálů (Chekeni et al., 2010). Aplikace PDT vede u buněk k aktivní sekreci ATP už během pre-apoptotické fáze a tato sekrece je závislá na sekretorické dráze jak klasické, tak regulované PERK kinázou a na exocytóze zprostředkované PI3K kinázou. Tento proces naopak nevyžaduje aktivaci proteinů Bax a Bak (Garg et al., 2012b). Buňky infikované onkolytickými viry mohou sekretovat nebo uvolňovat ATP různými mechanismy. V závislosti na typu viru může docházet k sekreci v časné fázi apoptózy a v průběhu autofágie nebo infikovaná buňka uvolňuje ATP pasivně během nekrózy nebo pyroptózy (Guo et al., 2014).

Různé mechanismy transportu a sekrece/uvolnění ATP z buněk v závislosti na stádiu apoptózy jsou schématicky znázorněny na Obr.4..

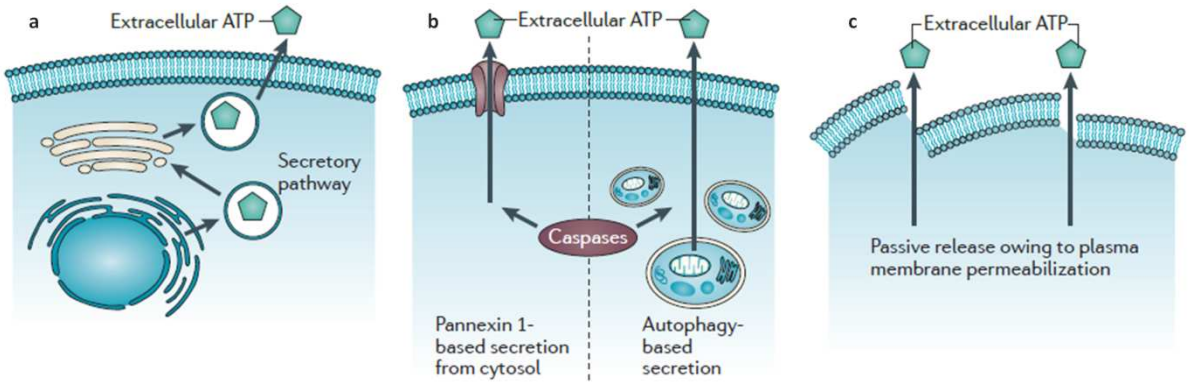

Obr.4. Mechanismy sekrece/uvolnění ATP v závislosti na stádiu apoptózy. *(a) Pre-apoptotická sekrece ATP je podobně jako pre-apoptotická translokace CRT na buněčný povrch převážně závislá na sekretorické dráze zahrnující anterográdní transport z ER do Golgiho aparátu a exocytóze váčků obsahujících ATP. (b) Během časné fáze apoptózy dochází v závislosti na počátečním stimulu k sekreci ATP pannexinovými kanály (UVC záření) nebo je sekrece ATP zprostředkována autofágií (antracykliny, mitoxantron a oxaliplatina). V obou případech je nutná účast kaspáz. (c) Pozdní fáze apoptózy a sekundární nekróza jsou charakterizovány poškozením buněčné membrány, což vede k pasivnímu uvolňování velkého množství ATP z cytoplazmy do extracelulárního prostředí. Převzato a upraveno podle (Krysko et al., 2012).*

2.2.3.3. Mechanismus uvolnění HMGB1

Uvolnění/sekreci HMGB1 doprovází dva různé procesy. V nepřítomnosti buněčné smrti je HMGB1 aktivně sekretován imunitními buňkami jako např. monocyty a makrofágy, aktivovanými patogenními produkty (např. LPS) nebo prozánětlivými cytokiny (např. IL-1β, TNF) (Malhotra and Kaufman, 2011, Garg et al., 2010). Tato aktivní sekrece vyžaduje

sestavení NLRP3 inflamasomu a aktivaci kaspázy 1 (Willingham et al., 2009). Neimunitní buňky uvolňují HMGB1 pasivně v důsledku poškození plazmatické membrány doprovázející pozdní fázi imunogenních forem buněčné smrti. Toto pasivní uvolnění bylo popsáno u pozdní apoptózy přecházející do sekundární nekrózy (Fucikova et al., 2011a), primární nekrózy (Garg et al., 2010, Szegezdi et al., 2003), nekroptózy (Guo et al., 2014, Workenhe et al., 2013) a autofágie (Thorburn et al., 2009).

Molekulární mechanismy umožňující pasivní uvolnění HMGB1 z nádorových buněk umírajících ICD nejsou doposud známy. Tento proces nicméně vyžaduje nejprve transport HMGB1 z jádra do cytoplazmy a až poté jeho uvolnění do extracelulárního prostředí v důsledku ztráty integrity plazmatické membrány. Bylo ukázáno, že k translokaci HMGB1 z jádra do cytoplazmy může docházet ve stresovaných, ale stále ještě živých buňkách. V tomto kontextu může cytoplazmatický HMGB1 aktivovat autofágii, pravděpodobně inhibicí antiautofagických funkcí p53 (Kroemer et al., 2013). Zda tento fenomén ovlivňuje imunogenní potenciál HMGB1 nebylo dosud objasněno. Vzhledem k tomu, že během apoptózy dochází k zesílení vazby HMGB1 na DNA, nebylo dlouhou dobu jasné, zda apoptotické buňky HMGB1 uvolňují. Současné poznatky ale ukázaly, že nádorové buňky uvolňují HMGB1 v průběhu pozdní apoptózy/sekundární nekrózy mechanismem, který může být zablokován pan-kaspázovým inhibitorem z-VAD-fmk, což má za následek zpožděnou indukci sekundární nekrózy (Bell et al., 2006).

Je potřeba zmínit, že HMGB1 aktivně sekretovaný imunitními buňkami je molekulárně odlišný od HMGB1 pasivně uvolňovaného z nekrotických buněk, protože aktivní transport vyžaduje acetylaci na specifických lysinových zbytcích (Palumbo et al., 2004).

2.2.4. Prognostický a prediktivní význam DAMPs u pacientů s nádorovým onemocněním

Jak bylo uvedeno v předcházejících kapitolách, ICD a DAMPs s ní spojené hrají důležitou roli v aktivaci protinádorové imunitní odpovědi. Tato experimentální data byla převážně získána *in vitro* na lidských a myších nádorových buňkách a *in vivo* na myších modelech. I když je většina z dosud popsaných induktorů ICD používána v klinické praxi, důkazy o schopnosti těchto látek navodit ICD *in vivo* u lidí jsou stále omezené. Nejnovější výsledky preklinických studií ale ukazují, že přítomnost procesů vedoucích k sekreci/uvolnění/vystavení DAMPs a míra jejich exprese v nádorových buňkách mají do určité míry dopad na prognózu onkologických pacientů (Fucikova et al., 2015). Je potřeba zmínit, že výsledky studií hodnotících prognostickou a prediktivní roli DAMPs jsou poměrně heterogenní, a obecně tedy nelze konkrétní molekule přisuzovat pozitivní nebo negativní prognostický význam. Tento fakt závisí na řadě faktorů, z nichž stojí za zmínku především typ nádorového onemocnění, stádium, léčba, buněčné a chemické složení nádorového mikroprostředí a v neposlední řadě způsob detekce jednotlivých DAMPs (celková exprese na úrovni mRNA (PCR) nebo proteinu (western blot, imunohistochemie), solubilní DAMPs přítomné v séru detekované metodou ELISA a DAMPs vystavené na povrchu nádorových buněk stanovené pomocí průtokové cytometrie) (Fucikova et al., 2018, Fucikova et al., 2015, Krysko et al., 2012).

Příkladem nejednoznačnosti může být prognostický význam CRT. Množství CRT v nádoru koreluje s protinádorovou imunitní odpovědí u pacientek s ovariálním karcinomem (Garg et al., 2015a), u pacientů s nádorem tlustého střeva (Peng et al., 2010) a nemalobuněčným karcinomem plic (Fucikova et al., 2016a). Vysoká exprese také koreluje s lepší prognózou onemocnění u pacientů s neuroblastomem (Hsu et al., 2005), glioblastomem (Muth et al., 2016), karcinomem tlustého střeva (Peng et al., 2010) a nemalobuněčným karcinomem plic

(Fucikova et al., 2016a). Naopak, u pacientů s karcinomem žaludku a pankreatu je přítomnost CRT korelována se zvýšenou angiogenezí, invazivitou a proliferací nádorových buněk (Chen et al., 2009, Matsukuma et al., 2016). Podobně u pacientů s lymfomem plášťových buněk a karcinomem močového měchýře má přítomnost CRT negativní dopad na prognózu onemocnění (Chao et al., 2010).

Prognostický význam CRT byl hodnocen také u pacientů s hematologickými malignitami (Fucikova et al., 2016c, Wemeau et al., 2010). Jedna z těchto studií byla publikována naší výzkumnou skupinou a ukazuje, že CRT přítomný na povrchu cirkulujících maligních blastů koreluje s vyšším zastoupením nádorově-specifických T lymfocytů a NK buněk v periferní krvi AML pacientů a současně umožňuje identifikovat skupinu pacientů se signifikantně lepší prognózou (Fucikova et al., 2016c). Zajímavým zjištěním bylo, že přítomnost CRT na maligních blastech nezávisí na aplikované terapii antracykliny, ale je spíše důsledkem stresu probíhajícího uvnitř nádorové buňky. Exprese CRT na povrchu blastů totiž koreluje s fosforylací eIF2α a expresí některých genů kódujících proteiny zúčastněné v aktivaci stresových drah asociovaných s ER. Detailní výsledky této studie jsou uvedeny v přiložené publikaci, která je součástí této práce (Fucikova et al., 2016c). Význam CRT pro klinický průběh různých nádorových onemocnění je poté shrnut v přehledovém článku, který souvisí s problematikou popsanou v této práci (Fucikova et al., 2018).

Fosforylovaný protein eIF2α (p-eIF2α) představuje jeden z klíčových ukazatelů probíhajícího ER stresu, který byl podobně jako CRT identifikován jako prognostický faktor u některých nádorových onemocnění. P-eIF2α například koreluje s lepší prognózou pacientů s nemalobuněčným karcinomem plic (Fucikova et al., 2016a, He et al., 2011). U pacientek s karcinomem prsu je naopak fosforylace eIF2α asociována s vyšší infiltrací nádorového mikroprostředí regulačními T lymfocyty a proliferací nádorových buněk a následně s horší prognózou onemocnění po zahájení terapie antracykliny (Senovilla et al., 2012).

Existuje řada studií zabývajících se vlivem dalších DAMPs (HSPs, HMGB1, ATP, IFN I. typu) a proteinů učastnících se signalizace vedoucí k jejich translokaci na buněčnou membránu (popřípadě uvolnění do extracelulárního prostředí) na prognózu onkologických pacientů. Jak již bylo zmíněno, výsledky jsou nejednoznačné a silně závisí na kontextu. Avšak racionální přístup v monitorování těchto parametrů by v budoucnu mohl napomoci stratifikovat pacienty do rizikových skupin a v ideálním případě predikovat průběh onemocnění a odpověď na dostupnou léčbu, popřípadě vést k výběru vhodné léčebné strategie pro skupiny pacientů z různou mírou rizika.

3. DENDRITICKÉ BUŇKY A MODULACE JEJICH FUNKCE DAMPS ASOCIOVANÝMI S IMUNOGENNÍ BUNĚČNOU SMRTÍ

3.1. Detekce signálů nebezpečí dendritickými buňkami

Dendritické buňky představují relativně heterogenní buněčnou populaci tzv. APCs regulujících jak vrozenou, tak adaptivní imunitní odpověď se schopností stimulovat antigen-specifické T lymfocyty. Hrají klíčovou roli v rozpoznávání DAMPs, které jsou uvolňovány nebo vystavovány na povrchu umírajících, stresovaných nebo poškozených buněk včetně buněk nádorových. Tím zaujímají centrální pozici v tzv. „danger modelu“ imunitní odpovědi navrženém v roce 1994 Polly Matzingerovou, který říká, že imunitní systém je schopen rozeznat potenciálně nebezpečné endogenní signály od těch neškodných (Matzinger, 1994). Jak už bylo zmíněno dříve, vystavení DAMPs na povrchu buněk nebo jejich uvolnění do extracelulárního prostředí může být indukováno některými chemoterapeutiky a jinými modalitami, které v buňkách spouští ICD. Společnou vlastností těchto molekul je jejich schopnost se vázat na PRRs na povrchu DCs. Jejich typ, délka interakce s receptorem a načasování regulují funkce DCs jako např. pohlcení a zpracování antigenu, maturace, cross-

prezentace, atd. Tyto signály rozhodují o kvalitě a množství kostimulačních signálů na DCs a tudíž ovlivňují výslednou imunitní odpověď založenou na T lymfocytech (Truxova et al., 2017).

Dendritické buňky rozpoznávají DAMPs asociované s ICD několika různými PRRs: 1. TLRs (konkrétně TLR2 a TLR4) (Garg et al., 2012a, Garg et al., 2012b, Krysko et al., 2012, van Eden et al., 2012), 2. scavenger receptory (scavenger receptor associated with endothelial cells (SREC-1) (Murshid et al., 2014); lectin-type oxidized LDL receptor-1 (LOX-1)), 3. receptory pro IFN I. typu (IFNARs) (Zitvogel et al., 2015), 4. CD14 (Asea et al., 2000), 5. RAGE (receptor for advanced glycation end-products) (Krysko et al., 2012), 6. CD91 (také znám jako low-density lipoprotein receptor-related protein-1 (LRP-1)) (Garg et al., 2012b), 7. purinergními receptory P_2Y_2 a P_2X_7 (Garg et al., 2012b, Ghiringhelli et al., 2009) a 8. FPR-1 (formyl peptide receptor-1) (Vacchelli et al., 2015). Interakce jednotlivých DAMPs s receptory na DCs jsou znázorněny na Obr.6. a dopad jednotlivých DAMPs na funkce DCs je přehledně shrnut v Tab.1..

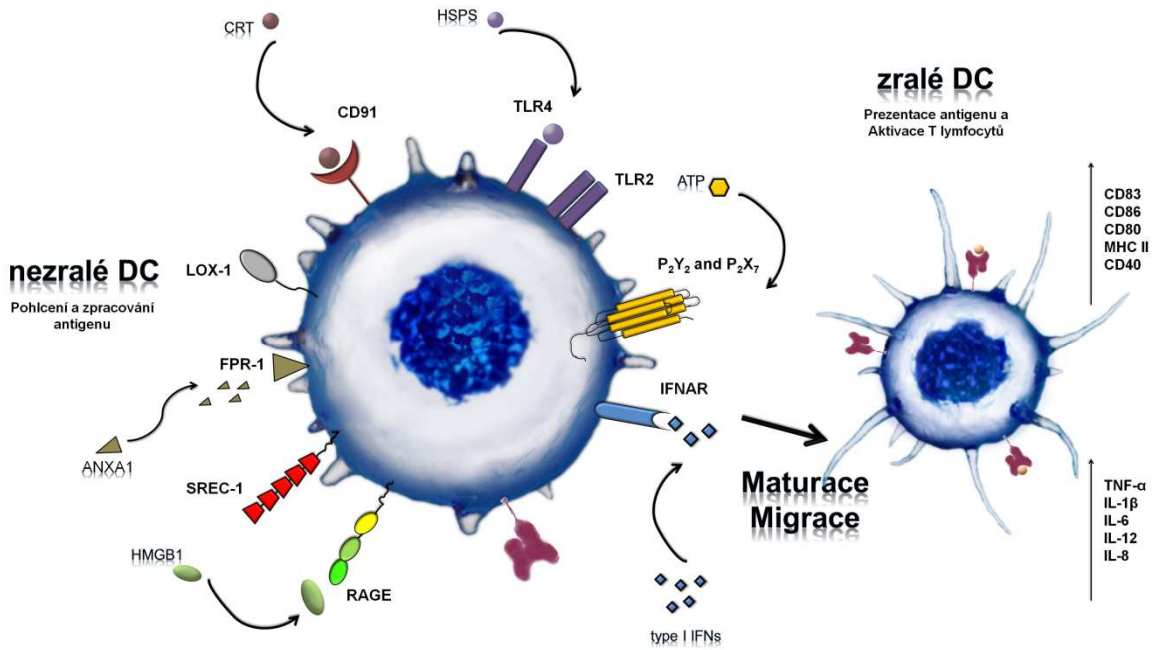

Obr.6. Interakce DAMPs spojených s ICD s receptory na DCs.

DAMPs sekretované, uvolňované nebo vystavované buňkami během ICD zahrnují CRT, HSPs, ATP, HMGB1, IFN I. typu a ANXA1. Tyto molekuly se vážou na příslušné receptory na DCs jako CD91 (CRT a HSPs), TLR2/4 (HSPs a HMGB1), RAGE (HMGB1), P_2Y_2/P_2X_7 (ATP), SREC-1 a LOX-1 (HSPs), IFNAR (IFN I. typu) a FPR-1 (ANXA1). Tyto interakce umožňují pohlcování nádorových buněk a zpracování antigenu DCs, maturaci DCs charakterizované zvýšenou expresí kostimulačních molekul CD80, CD83, CD86, HLA-DR a CD40 a produkci prozánětlivých cytokinů DCs. Maturované DCs tak mohou v kontextu MHC molekul účinně prezentovat antigeny včetně antigenů asociovaných s nádory T lymfocytům a indukovat protinádorovou imunitní odpověď. Obrázek byl převzat a upraven podle (Truxova et al., 2017).

Tab.1. Přehled DAMPs asociovaných s ICD a jejich dopad na funkce DCs.

ICD-associated DAMPs	DC receptors	Effect on DC functions
CRT	CD91	a potent "eat me" signal crucial for anti-tumor immunity; increases susceptibility to phagocytosis by DCs
HSP70, HSP90, HSP60 HSP72, GP96	CD91, TLR2, TLR4, LOX-1, SREC-1, CD14	mediate DC maturation and activation (↑ maturation-associated molecules - CD83, CD80, CD86, CD40, ↑ production of TNF-α, IL-1β, IL-6 and IL-12); form complexes with tumor antigens facilitating antigen processing and presentation by DCs
ATP	P2Y2 and P2X7	act as "find me" signal and enhances the accumulation of DCs in the tumor; causes activation of NLRP3 inflammasome leading to IL-1β release from DCs
HMGB1	TLR2, TLR4, RAGE	"antigen processing" signal crucial for efficient cross-presentation of TAAs by DCs; stimulates the production of TNF-α, IL-1, IL-6 and IL-8 from myeloid cells; can cause DC maturation
type I IFNs	IFNAR	stimulate DC maturation, antigen processing and presentation by DCs; generate DCs with cytotoxic activity
ANXA1	FPR-1	required for DC migration toward anthracycline-treated tumor cells and stable DC-tumor cell interactions

Převzato a upraveno podle (Truxova et al., 2017).

3.2. Rozpoznání a pohlcení nádorových buněk dendritickými buňkami

Je známo, že pohlcení apoptotických buněk nesoucích PS nevede k aktivaci imunitní odpovědi. Naproti tomu uvolnění specifických „find-me“ signálů a vystavení „eat-me“ signálů na povrchu buněk v průběhu ICD vede ke zvýšené migraci DCs, k efektivnějšímu rozpoznávání a pohlcování těchto imunogenních buněk DCs a následné stimulaci antigen-specifické imunitní odpovědi. Migrace myeloidních buněk, včetně DCs, do míst s intenzivním výskytem umírajících buněk může být podpořena ATP, dobře známým „find-me“ signálem. Nádorové buňky ošetřené chemoterapeutiky indukujícími ICD sekretují ATP ve fázi, kdy se na plazmatické membráně objevuje PS. ATP v extracelulárním prostředí je nutné pro navození efektivní protinádorové imunitní odpovědi (Martins et al., 2014). Ma a kolegové navíc ukázali, že antracykliny stimulují akumulaci $CD11c^{+}CD11b^{+}Ly6C^{high}$ DCs v nádoru závislou na ATP a jeho vazbě na purinergní receptor P_2Y_2. Tato populace buněk byla vysoce efektivní v prezentaci nádorových antigenů $CD8^{+}$ T lymfocytům jak *in vitro*, tak *in vivo* (Ma et al., 2013). Současná data ukazují, že také ANXA1 je důležitým faktorem pro migraci DCs a pro navození stabilních interakcí s umírajícími buňkami. Knockout genu kódujícího ANXA1 nebo jeho receptor na DCs (FPR-1) vede k potlačení imunitní reakce proti nádorovým buňkám ošetřeným antracykliny (Vacchelli et al., 2015). Antracykliny také mohou zvyšovat migraci myeloidních buněk včetně DCs do nádoru závislou na produkci urokinázy, IL-8, MCP-1 (monocyte chemoattractant protein-1 a CCL2 (chemokine (C-C motif) ligand 2) nádorovými buňkami (Ma et al., 2014, Niiya et al., 2003).

Přítomnost CRT na plazmatické membráně byla identifikována jako hlavní biochemický rozdíl mezi imunogenní a neimunogenní buněčnou smrtí. Apoptotické buňky postrádající CRT nejsou efektivně odstraňovány fagocyty, což napovídá, že vystavení CRT na povrchu buněk je důležitým molekulárním znakem nutným pro fagocytózu umírajících buněk (Obeid et al., 2007b). Kalretikulin se váže na CD91 receptor na fagocytech, včetně DCs, a indukuje

fagocytózu a makropinocytózu, což stimuluje efektivní odstranění CRT^+ buněk (Gardai et al., 2005). Interakce CD91 s CRT vede v DCs k aktivaci NF-κB a produkci prozánětlivých cytokinů, především TNF-α, IL-6, IL-1β a IL-12. Toto cytokinové prostředí indukované povrchovým CRT umožňuje aktivaci Th17 buněk v imunosupresivním nádorovém mikroprostředí obsahujícím TGF-β (Pawaria and Binder, 2011). V nedávné studii bylo také dokázáno, že vysoká exprese CRT na povrchu nádorových buněk u pacientů s nemalobuněčným karcinomem plic koreluje s vyšším počtem maturovaných DCs infiltrujících do nádoru a s vyšším zastoupením efektorových paměťových T buněk, což nasvědčuje tomu, že CRT je schopen stimulovat protinádorovou imunitní odpověď také *in vivo* (Fucikova et al., 2016b).

3.3. Aktivace dendritických buněk

V přítomnosti různých mikrobiálních a endogenních stimulů (DAMPs) dochází u nezralých DCs k zahájení procesu maturace, který je doprovázen několika událostmi: 1. změna morfologie, 2. ztráta schopnosti fagocytovat, 3. zvýšení exprese kostimulačních molekul CD80, CD86, CD40 a OX40L, 4. upregulace MHC molekul II. třídy, 5. zvýšení produkce cytokinů a chemokinů a 6. zahájení exprese chemokinových receptorů (např. CCR7), což umožňuje DCs migrovat do lymfatických uzlin, kde prezentují antigeny T lymfocytům a aktivují je (Vandenberk et al., 2015).

Maturace DCs může být indukována HSPs, k jejichž translokaci na buněčný povrch nebo uvolnění do extracelulárního prostředí dochází během ICD. Povrchový HSP70 a HSP90 mají silné imunostimulační účinky a v některých myších modelech bylo prokázáno, že schopnost umírajících nádorových buněk stimulovat imunitní systém je závislá právě na těchto molekulách (Tesniere et al., 2008, Udono and Srivastava, 1994). HSP70 a HS90 mohou interagovat s receptory CD91, TLR2 a TLR4 na povrchu DCs, jejichž aktivace spouští

signalizační dráhy vedoucí k fenotypické a funkční maturaci DCs. Bylo popsáno, že kultivace nezralých DCs s nádorovými buňkami ošetřenými bortezomibem nesoucími na povrchu zvýšené množství HSP90 zprostředkovala kontaktně-dependentní upregulaci molekul CD80 a CD86 na povrchu DCs (Spisek et al., 2007). HSP70 také působí jako maturační signál pro DCs a zvyšuje expresi CD86 a CD40 (Singh-Jasuja et al., 2000). Navíc vazba proteinů z HSP70 rodiny na TLR2/4 a CD14 receptory spouští aktivaci NF-κB a proteinů regulujících transkripci genů kódujících interferony (IRF, interferon regulatory factors), což vede k produkci prozánětlivých cytokinů jako např. TNF-α, IL-1β, IL-6 a IL-12 (Asea et al., 2000, Asea et al., 2002).

ATP sekretované z nádorových buněk umírajících ICD nepůsobí jen jako „find-me" signál lákající DCs do nádoru, jak bylo zmíněno v předchozí sekci, ale také umožňuje diferenciaci myeloidních buněk na DCs s prozánětlivými vlastnostmi. ATP se váže na purinergní P_2X_7 receptory na DCs a aktivuje NLRP3 inflamasom obsahující kaspázu 1. Aktivovaná kaspáza 1 štěpí neaktivní prekurzory IL-1β a IL-18 na aktivní formy, které jsou sekretovány DCs. IL-1β je společně s prezentací antigenu nezbytný pro polarizaci $CD8^+$ T lymfocytů produkujících IFN-γ a pro adaptivní protinádorovou imunitní odpověď (Ghiringhelli et al., 2009).

Maturace DCs může být také indukována HMGB1, který stimuluje produkci prozánětlivých cytokinů TNF-α, IL-1, IL-6 a IL-8 myeloidními buňkami (Chen et al., 2004).

Nádorové buňky umírající ICD sekretují IFN I. typu v důsledku aktivace TLR3 antracykliny a tento proces je nutný pro zahájení adaptivní imunitní odpovědi (Sistigu et al., 2014). Bylo také zjištěno, že IFN I. typu mohou vazbou na IFNAR podporovat maturaci DCs a jejich kapacitu zpracovávat a prezentovat antigeny $CD8^+$ T lymfocytům (Zitvogel et al., 2015). Navíc nízké dávky cyklofosfamidu indukují diferenciaci zralých DCs z prekurzorových buněk sídlících v kostní dřeni *in vivo* a *ex vivo* a tyto efekty cyklofosfamidu jsou závislé na endogenních IFN I. typu (Schiavoni et al., 2011). Zajímavé je, že IFN-α má schopnost

indukovat DCs s cytotoxickými vlastnostmi (IFN-DCs). Tyto specifické buňky stimulují nádorově-specifické CD8+ T lymfocyty a vykazují částečnou fenotypickou a funkční podobnost s NK buňkami jako např. expresi CD56, produkci IFN-γ a cytolytické funkce. Cytolytické funkce těchto DCs jsou závislé na TRAILu (Papewalis et al., 2008).

Kyselina močová uvolňovaná z umírajících buněk během pozdní fáze apoptózy může podobně jako ATP v myeloidních buňkách aktivovat NLRP3 inflamasom vedoucí k sekreci IL-1β a IL-18 (Martinon et al., 2006). Dále bylo ukázáno, že krystaly kyseliny močové stimulují maturaci DCs zvýšením exprese kostimulačních molekul CD80 a CD86. Aplikace kyseliny močové jako adjuvans signifikantně zvýšila schopnost DCs pulzovaných nádorovým lyzátem oddálit růst nádoru (Wang et al., 2015).

3.4. Zpracování a prezentace antigenů

Pohlcené exogenní antigeny včetně TAAs jsou v DCs dále zpracovány v endosomech a lysosomech, kde jsou štěpeny na peptidy, které tvoří komplexy s MHC molekulami II. třídy (Lennon-Dumenil et al., 2002). Exogenní antigeny mohou být také alternativně uvolněny do cytosolu, zpracovány proteasomem, hlavní nelysosomální proteázou, a transportovány do ER, kde je zprostředkována jejich vazba na MHC molekuly I. třídy. Tento proces prezentace exogenních antigenů na MHC molekulách I. třídy je označován jako cross-prezentace (Delamarre et al., 2003). Pohlcení, zpracování a prezentace antigenů jsou v DCs přísně regulovány.

Jedním z klíčových proteinů regulujících tyto děje je HMGB1. Tento protein je uvolňován z jádra do extracelulárního prostředí v průběhu imunogenní apoptózy nebo sekundární nekrózy a váže se na PRRs exprimované především APCs jako např. TLR2, TLR4 a RAGE (Apetoh et al., 2007a, Demaria et al., 2005). Pro správný průběh prezentace antigenů DCs se jako klíčová ukázala interakce HMGB1 s TLR4. V případě chybějící TLR4 signalizace

fagosomy fúzují s lysosomy, dochází k degradaci pohlceného materiálu a antigeny nemohou být účinně prezentovány $CD4^+$ a $CD8^+$ T lymfocytům. Myší modely ukázaly, že imunizace myší CT26 buňkami ošetřenými antracykliny s depletovaným HMGB1 snížila schopnost myší eradikovat nádor a tento proces byl závislý na vazbě HMGB1 na TLR4 na povrchu APCs (Apetoh et al., 2007a). Navíc polymorfismus TLR4 genu vedoucí k neschopnosti TLR4 vázat HMGB1 je u pacientek s karcinomem prsu asociován se sníženou kapacitou DCs prezentovat nádorové antigeny, s časným relapsem po terapii antracykliny a horší prognózou (Krysko et al., 2012).

Extracelulární HSPs, uvolňované z buněk v důsledku probíhající ICD, mohou vázat nádorové antigeny a usnadňovat jejich cross-prezentaci interakcí s několika receptory exprimovanými APCs jako např. CD91, CD14 a scavenger receptory SREC-1 a LOX-1 (Calderwood et al., 2007). Komplexy HSPs s nádorovými antigeny jsou endocytovány, rozštěpeny a nádorové peptidy jsou cross-prezentovány $CD8^+$ T lymfocytům prostřednictvím MHC molekul I. třídy (Doody et al., 2004). K aktivaci zpracování a cross-prezentace antigenů z těchto komplexů dochází po vazbě na TLR4 a CD14 (Asea et al., 2000, Asea et al., 2002). V současnosti byl také popsán mechanismus umožňující prezentaci peptidů z komplexů HSPs s antigeny $CD4^+$ T lymfocytům. Tato studie ukázala, že komplexy HSP90-antigen jsou rozpoznány a pohlceny DCs prostřednictvím scavenger receptoru SREC-1 a naštěpené peptidy asociované s HSP90 jsou prezentovány na MHC molekulách II. třídy $CD4^+$ T lymfocytům (Murshid et al., 2014).

3.5. Dendritické buňky a jejich využití v protinádorové terapii

Je známo, že DCs mají významný vliv na onkogenezi, progresi nádorových onemocnění a odpověď na protinádorovou terapii, což bylo dokázáno v řadě preklinických nádorových modelů (Ma et al., 2013, Levine and Kroemer, 2008, Scarlett et al., 2012, Tomihara et al., 2010). Množství a funkce DCs v nádoru byly také korelovány s prognózou pacientů

v klinických studiích (Bloy et al., 2014). V posledním desetiletí proto bylo věnováno značné úsilí vývoji strategií protinádorové terapie využívajících širokého imunomodulačního potenciálu DCs. Toto úsilí bylo ještě více podpořeno výsledky některých klinických studií hodnotících imunologické a terapeutické odpovědi pacientů na imunoterapii založenou na DCs (Bloy et al., 2014). V následující kapitole budou popsány současné přístupy v přípravě a využití DCs v terapii nádorových onemocnění.

3.5.1. Příprava dendritických buněk pro terapii nádorových onemocnění a aspekty ovlivňující účinnost imunoterapie založené na dendritických buňkách

Hlavními strategiemi v protinádorové terapii založené na DCs jsou: 1. příprava DCs *ex vivo*, 2. podání TAAs a jejich cílení na receptory na DCs *in vivo* (např. fúzí TAAs s monoklonálními protilátkami, polypeptidy nebo karbohydráty, které se selektivně vážou na receptory exprimované DCs) a 3. příprava exosomů odvozených z DCs (Galluzzi et al., 2014, Klechevsky et al., 2010, Viaud et al., 2010). Nejrozšířenějším postupem pro klinické využití DCs je příprava myeloidních DCs *ex vivo* z monocytů z periferní krve pacientů. Monocyty jsou izolovány z mononukleárních buněk z periferní krve (PBMCs, peripheral blood mononuclear cells) získaných leukaferézou pomocí adherence na plastik, magnetickou separací $CD14^+$ buněk nebo elutriací využívající separační systém Elutra (Jarnjak-Jankovic et al., 2007). Monocyty jsou poté kultivovány v přítomnosti GM-CSF a IL-4 nejčastěji po dobu 5-7 dní, kdy dochází ke vzniku plně diferencovaných nezralých DCs (Curti et al., 2004). Autologní DCs mohou být dále *ex vivo* kultivovány, pulzovány nádorovými antigeny a maturovány. Pulzace DCs *ex vivo* TAAs může být provedena: 1. kokultivací nezralých DCs s autologními nádorovými lyzáty (Chen et al., 2001, Kandalaft et al., 2013), inaktivovanými nádorovými liniemi (Fucikova et al., 2011b, Podrazil et al., 2015) nebo rekombinantními TAAs (Mayordomo et al., 1997), 2. transfekcí DCs vektory nebo RNA kódujícími TAAs nebo

celkovou RNA izolovanou z nádorových buněk (Garg et al., 2013, Lee et al., 2013) nebo 3. fúzí DCs s inaktivovanými nádorovými buňkami a vznikem tzv. dendritomů (Koido et al., 2013). Velice důležitým faktorem ovlivňujícím účinnost terapie založené na DCs je stupeň zralosti DC, protože jejich maturovaný fenotyp je klíčový pro indukci protinádorové imunitní odpovědi (Czerniecki et al., 2007). Zralé DCs vyrobené za účelem terapeutického podání by měly ideálně exprimovat CCR7 umožňující jejich migraci do lymfatických uzlin, ve vysoké míře exprimovat kostimulační molekuly (např. CD80 a CD86) a produkovat IL-12p70 stimulující $CD8^+$ T lymfocyty a cytokiny polarizující $CD4^+$ T lymfocyty na Th1 typ. Dosud testované protokoly se liší zejména kombinací maturačních signálů vedoucích k diferenciaci nezralých DCs na zralé. Po řadu let byl standardem maturační koktejl obsahující TNF-α, IL-1β, IL-6 a PGE2 (Jonuleit et al., 1997). Takto maturované DCs ale produkovaly velmi malé množství IL-12p70, což bylo dáno přítomností PGE2 v koktejlu (Kalinski et al., 2001). Z tohoto důvodu se začaly používat alternativní kombinace maturačních signálů, z nichž většina obsahuje PAMP nebo DAMP molekuly, které se vážou na PRRs jako TLRs na povrchu DCs. Přidání agonistů TLR3 (Poly (I:C)), TLR4 (LPS) nebo jeho derivát monofosforyl lipid A (MPLA)) nebo TLR7/8 (R848) do maturačních směsí vedlo ke zvýšení produkce IL-12p70 zralými DCs (Lehner et al., 2007, Zobywalski et al., 2007). Bylo také zjištěno, že přidání IFN-γ nebo kombinace více TLR agonistů vedla k dalšímu posílení produkce IL-12p70 DCs. Použití více TLR agonistů také zvýšilo expresi CCR7 (Napolitani et al., 2005).

Autologní DCs byly poprvé využity pro vakcinaci pacientů s maligním melanomem v roce 1995 (Nestle et al., 1998). V následujících letech byla imunoterapie na bázi DCs testována i u dalších solidních a hematologických malignit zahrnujících např. karcinom žaludku, tlustého střeva, prsu, prostaty, ovárií, plic, glioblastom atd. (Truxova et al., 2017). I když některé z těchto studií zaznamenaly pozitivní klinické odpovědi pacientů, vzhledem k celkově

nekonzistentním výsledkům, zůstává klinicky efektivní imunoterapie založená na DCs prozatím nedostiženým cílem. Tyto nejednotné výsledky jsou důsledkem aplikace vakcíny pacientům ve fázi značně pokročilého onemocnění, kdy v nádoru již existuje vysoce imunosupresivní prostředí, které může inhibovat protinádorové funkce DCs. Takové DCs ztrácejí schopnost zprostředkovat nezbytné aktivační signály T lymfocytům (Hargadon, 2013). Současné terapeutické přístupy se proto zaměřují na vývoj vhodných strategií kombinujících imunoterapii založenou na DCs např. s protinádorovými cytotoxickými látkami nebo modalitami, jako je chemoterapie nebo radioterapie. Současné poznatky naznačují, že chemo a radioterapie nedisponují jen přímými cytotoxickými efekty, které primárně vedou k redukci nádorové masy, ale mají také imunomodulační vlastnosti (Menard et al., 2008). Specifické látky a modality mají potenciál selektivně eliminovat imunosupresivní buňky jako regulační T buňky (Tregs, regulatory T cells) nebo myeloidní supresorové buňky (MDSCs, myeloid-derived suppressor cells) (Ghiringhelli et al., 2007), indukovat ICD nádorových buněk (Fucikova et al., 2011a, Obeid et al., 2007b, Panaretakis et al., 2009, Spisek et al., 2007) a v neposlední řadě také mohou indukovat maturaci DCs a zvyšovat cross-prezentaci (Martin et al., 2015, Truxova et al., 2017). Výběr vhodných terapeutických kombinací, které by stimulovaly zvýšení funkční kapacity DCs, by v budoucnu mohl vést k dosažení optimální účinnosti imunoterapie založené na DCs. Součástí této práce jsou dvě studie zabývající se testováním protinádorového efektu imunoterapie založené na DCs pulzovaných nádorovými buňkami inaktivovanými HHP v kombinaci s chemoterapií *in vivo* na myších nádorových modelech (Mikyskova et al., 2017, Mikyskova et al., 2016). Kombinované přístupy léčby nádorových onemocnění založené na spojení imunoterapie na bázi DCs s chemoterapií jsou poté shrnuty v přehledovém článku, který úzce souvisí s problematikou popsanou v této práci (Truxova et al., 2017).

4. CÍLE PRÁCE

Hlavním cílem této práce je popsat hlavní charakteristiky ICD a mechanismy vedoucí k sekreci/uvolnění/vystavení DAMPs v průběhu ICD. Také bude diskutován význam těchto molekul *in vivo* u pacientů s nádorovým onemocněním a vliv jednotlivých DAMPs na dendritické buňky (DCs) a jejich využití v protinádorové terapii. Jednotlivá témata jsou rozdělena do následujích částí:

1. Testování schopnosti HHP indukovat ICD lidských nádorových linií a stanovení potenciálu nádorových buněk ošetřených HHP aktivovat DCs a stimulovat nádorově-specifické T lymfocyty
    - Hypotéza: HHP v nádorových buňkách spouští imunogenní formu buněčné smrti spojenou s uvolněním/vystavením DAMPs s imunostimulačními vlastnostmi.
2. Identifikace klíčových mechanismů vedoucích k vystavení DAMPs, konkrétně CRT, na povrchu nádorových buněk v průběhu ICD indukované HHP
    - Hypotéza: Translokace CRT na povrch nádorových buněk ošetřených HHP vyžaduje podobné děje jako translokace indukovaná antracykliny nebo hyp-PDT, tzn. především aktivaci stresu ER a produkci ROS.
3. Sledování vlivu CRT na povrchu primárních maligních blastů na protinádorovou imunitní odpověď *in vivo* u pacientů s akutní myeloidní leukémií (AML)
    - Hypotéza: CRT přítomný na povrchu maligních blastů koreluje se zvýšenou imunitní odpovědí proti leukemickým antigenům u pacientů s AML.
4. Optimalizace protokolu pro přípravu DCs za účelem imunoterapie nádorových onemocnění

- Hypotéza: Zkrácení protokolu diferenciace DCs signifikantně neovlivňuje jejich fenotyp a schopnost stimulovat antigen-specifické T lymfocyty.

5. Testování protinádorového efektu imunoterapie založené na DCs s chemoterapií *in vivo* na myších nádorových modelech (1. studie)
    - Hypotéza: Kombinace imunoterapie založené na DCs pulzovaných nádorovými buňkami ošetřenými HHP s chemoterapií vede ke zvýšení terapeutického potenciálu DC vakcíny v myších nesoucích slabě imunogenní nádory.
6. Testování protinádorového efektu imunoterapie založené na DCs s chemoterapií *in vivo* na myších nádorových modelech (2. studie)
7. Sumarizace literárních poznatků o významu CRT pro klinický průběh nádorových onemocnění
8. Sumarizace literárních poznatků zabývajících se kombinovaným přístupem léčby nádorových onemocnění založeným na spojení imunoterapie na bázi DCs s chemoterapií

5. VÝSLEDKY

Seznam autorských publikací:

- Publikace *in extenso*, které jsou podkladem dizertační práce:

Fucikova J, Moserova I, **Truxova I**, Hermanova I, Vancurova I, Partlova S, Fialova A, Sojka L, Cartron PF, Houska M, Rob L, Bartunkova J, Spisek R. High hydrostatic pressure induces immunogenic cell death in human tumor cells. Int J Cancer. 2014 Sep 1;135(5):1165-77. doi: 10.1002/ijc.28766. **IF 6.513**

Moserova I***** and **Truxova I***, Garg AD, Tomala J, Agostinis P, Cartron PF, Vosahlikova S, Kovar M, Spisek R, Fucikova J. Caspase-2 and oxidative stress underlie the immunogenic potential of high hydrostatic pressure-induced cancer cell death. Oncoimmunology. 2016 Nov 18;6(1):e1258505. doi: 10.1080/2162402X.2016.1258505. **IF 7.719**
* oba autoři přispěli stejnou měrou

Fucikova J***** and **Truxova I***, Hensler M, Becht E, Kasikova L, Moserova I, Vosahlikova S, Klouckova J, Church SE, Cremer I, Kepp O, Kroemer G, Galluzzi L, Salek C, Spisek R. Calreticulin exposure by malignant blasts correlates with robust anticancer immunity and improved clinical outcome in AML patients. Blood. 2016 Dec 29;128(26):3113-3124. doi: 10.1182/blood-2016-08-731737. **IF 13.164**
* oba autoři přispěli stejnou měrou

Truxova I, Pokorna K, Kloudova K, Partlova S, Spisek R, Fucikova J. Day 3 Poly (I:C)-activated dendritic cells generated in CellGro for use in cancer immunotherapy trials are fully comparable to standard Day 5 DCs. Immunol Lett. 2014 Jul;160(1):39-49. doi: 10.1016/j.imlet.2014.03.010. **IF 2.860**

Mikyšková R, Štěpánek I, Indrová M, Bieblová J, Šímová J, **Truxová I**, Moserová I, Fučíková J, Bartůňková J, Špíšek R, Reiniš M. Dendritic cells pulsed with tumor cells killed by high hydrostatic pressure induce strong immune responses and display therapeutic effects both in murine TC-1 and TRAMP-C2 tumors when combined with docetaxel chemotherapy. Int J Oncol. 2016 Mar;48(3):953-64. doi:10.3892/ijo.2015.3314. **IF 3.079**

Mikyskova R, Indrova M, Stepanek I, Kanchev I, Bieblova J, Vosahlikova S, Moserova I, **Truxova I**, Fucikova J, Bartunkova J, Spisek R, Sedlacek R, Reinis M. Dendritic cells pulsed with tumor cells killed by high hydrostatic pressure inhibit prostate tumor growth in TRAMP mice. Oncoimmunology.2017 Aug24;6(12):e1362528. doi:10.1080/2162402X.2017.1362528. **IF 7.719**

Žadatelka je také (spolu)autorkou 2 přehledových publikací souvisejících s tématem dizertační práce:

Fucikova J, Kasikova L, **Truxova I**, Laco J, Skapa P, Ryska A, Spisek R. Relevance of the chaperone-like protein calreticulin for the biological behavior and clinical outcome of cancer. Immunol Lett. 2017 Nov 23;193:25-34. doi: 10.1016/j.imlet.2017.11.006. **IF 2.860**

Truxova I, Hensler M, Skapa P, Halaska MJ, Laco J, Ryska A, Spisek R, Fucikova J. Rationale for the Combination of Dendritic Cell-Based Vaccination Approaches With Chemotherapy Agents. Int Rev Cell Mol Biol. 2017;330:115-156. doi:10.1016/bs.ircmb.2016.09.003. **IF 3.752**

- Publikace *in extenso* bez vztahu k tématu dizertační práce:

Lövgren T, Sarhan D, **Truxová I**, Choudhary B, Maas R, Melief J, Nyström M, Edbäck U, Vermeij R, Scurti G, Nishimura M, Masucci G, Karlsson-Parra A, Lundqvist A, Adamson L, Kiessling R. Enhanced stimulation of human tumor-specific T cells by dendritic cells matured in the presence of interferon-γ and multiple toll-like receptor agonists. Cancer Immunol Immunother. 2017 Jun 10. doi:10.1007/s00262-017-2029-4. **IF 4.711**

Partlová S, Bouček J, Kloudová K, Lukešová E, Zábrodský M, Grega M, Fučíková J, **Truxová I**, Tachezy R, Špíšek R, Fialová A. Distinct patterns of intratumoral immune cell infiltrates in patients with HPV-associated compared to non-virally induced head and neck squamous cell carcinoma. Oncoimmunology. 2015 Jan 30;4(1):e965570. **IF 7.719**

5.1. Vysoký hydrostatický tlak indukuje imunogenní buněčnou smrt nádorových buněk

Některé cytostatické látky (antracykliny, oxaliplatina, bortezomib, atd.), fyzikální modality (radioterapie a fotodynamická terapie) a onkolytické viry spouští v nádorových buňkách imunogenní formu buněčné smrti, která je charakterizována sekrecí/uvolněním/vystavením DAMPs z umírajících buněk. Společnou vlastností těchto molekul je schopnost aktivovat imunitní buňky, především DCs, což vede k indukci protinádorové imunitní reakce.

V této práci jsme identifikovali HHP jako další fyzikální modalitu, která vyvolává ICD u širokého spektra primárních lidských nádorových buněk a nádorových linií. Ošetření HHP o intenzitě 150 MPa a vyšší vedlo k rychlé buněčné smrti nádorových buněk, translokaci HSP70, HSP90 a CRT na buněčný povrch a uvolnění HMGB1 a ATP do extracelulárního prostředí. Nádorové buňky ošetřené HHP byly rychleji fagocytovány DCs v porovnání s kontrolními buňkami ošetřenými UVB zářením a tato interakce byla spojena s maturací a aktivací DCs (zvýšení exprese CD83, CD86 a HLA-DR a produkce prozánětlivých cytokinů IL-6, IL-12p70 a TNF-α). Takto aktivované DCs byly následně schopné indukovat zvýšenou proliferaci a produkci IFN-γ antigen-specifickými $CD4^+$ a $CD8^+$ T lymfocyty, bez současné expanze regulačních T lymfocytů.

Imunogenní vlastnosti HHP jsou v současnosti testovány v rámci probíhajících klinických studií přípravku DCVAC, imunoterapie na bázi DC, pro terapii pacientů s karcinomem prostaty, ovaria a plic.

K této práci jsem přispěla následovně: příprava nádorových linií ošetřených HHP, měření viability a detekce DAMPs (HSP70, HSP90 a CRT) na povrchu nádorových linií ošetřených HHP pomocí průtokové cytometrie, detekce HMGB1 v supernatantech nádorových buněk ošetřených HHP pomocí metody ELISA, analýza těchto dat.

IJC
International Journal of Cancer

High hydrostatic pressure induces immunogenic cell death in human tumor cells

Jitka Fucikova[1,2], Irena Moserova[2], Iva Truxova[2], Ivana Hermanova[3], Irena Vancurova[2], Simona Partlova[2], Anna Fialova[1,2], Ludek Sojka[1,2], Pierre-Francois Cartron[4], Milan Houska[5], Lukas Rob[6], Jirina Bartunkova[1,2] and Radek Spisek[1,2]

[1] Department of Immunology, 2nd Faculty of Medicine and University Hospital Motol, Charles University, Prague, Czech Republic
[2] Sotio, Prague, Czech Republic
[3] Childhood Leukemia Investigation, 2nd Faculty of Medicine and University Hospital Motol, Charles University, Prague, Czech Republic
[4] Centre de Recherche en Cancérologie Nantes-Angers, INSERM, U892, Apoptose et Progression tumorale, Equipe labellisée Ligue Nationale Contre le Cancer, Nantes, France
[5] Food Research Institute, Prague, Czech Republic
[6] Department of Gynecology and Obstetrics, 2nd Faculty of Medicine and University Hospital Motol, Charles University, Prague, Czech Republic

Recent studies have identified molecular events characteristic of immunogenic cell death (ICD), including surface exposure of calreticulin (CRT), the heat shock proteins HSP70 and HSP90, the release of high-mobility group box protein 1 (HMGB1) and the release of ATP from dying cells. We investigated the potential of high hydrostatic pressure (HHP) to induce ICD in human tumor cells. HHP induced the rapid expression of HSP70, HSP90 and CRT on the cell surface. HHP also induced the release of HMGB1 and ATP. The interaction of dendritic cells (DCs) with HHP-treated tumor cells led to a more rapid rate of DC phagocytosis, upregulation of CD83, CD86 and HLA-DR and the release of interleukin IL-6, IL-12p70 and TNF-α. DCs pulsed with tumor cells killed by HHP induced high numbers of tumor-specific T cells. DCs pulsed with HHP-treated tumor cells also induced the lowest number of regulatory T cells. In addition, we found that the key features of the endoplasmic reticulum stress-mediated apoptotic pathway, such as reactive oxygen species production, phosphorylation of the translation initiation factor eIF2α and activation of caspase-8, were activated by HHP treatment. Therefore, HHP acts as a reliable and potent inducer of ICD in human tumor cells.

Current anticancer treatments, including radiotherapy and chemotherapy, disrupt the activity of tumor cells through the selective killing or growth arrest of these cells. However, in most (but not all) instances, chemotherapy-induced cell death does not lead to enhanced antitumor immunity because apoptosis in cancer cells is mostly a nonimmunogenic, or even tolerogenic, cell death process.[1,2] In addition to the standard treatment of metastatic disease using combinations of chemotherapeutics, it would be beneficial to patients with cancer to elicit tumor-specific immunity that would control or slow the growth of residual tumor cells.[3] Accumulating evidence indicates that cytostatic agents[4] such as anthracyclines,[5] oxaliplatin[6] and bortezomib,[7] radiotherapy and photodynamic cancer therapy (PDT)[8] can stimulate tumor cells to undergo an immunogenic form of apoptosis, which causes these dying tumor cells to induce an effective antitumor immune response.[9]

Immunogenic cell death (ICD) involves changes in the composition of the cell surface as well as the release of soluble mediators, occurring in a defined temporal sequence. Such signals operate on a series of receptors expressed by dendritic cells (DCs) to stimulate the presentation of tumor antigens to T cells. Tumor cells undergoing ICD start to express and secrete a critical immunogenic factors, such as damage-associated molecular patterns (DAMPs).[10] Several DAMPs have recently been identified as hallmark features of immunogenic apoptosis, namely, several members of the heat shock protein family, HSP70[11,12] and HSP90, and calreticulin (CRT).[13–16] Within hours after the initiation of ICD, preapoptotic tumor cells translocate CRT and HSPs from the endoplasmic reticulum (ER) to the cell surface.[17] CRT exposure serves as an engulfment signal that targets dying tumor cells to DCs,[18,19] and disruption of the plasma membrane facilitates the release of the late apoptotic marker high-mobility group box 1 (HMGB1) into the extracellular milieu.[20] HMGB1 can bind to several pattern recognition receptors (PRRs), such as Toll-like receptor (TLR) 2 and 4 and the receptor of advanced glycosylation end products

Key words: immunogenic cell death, high hydrostatic pressure, heat shock proteins, cancer immunotherapy, dendritic cells
Additional Supporting Information may be found in the online version of this article.
Grant sponsor: Ministry of Health, Czech Republic; **Grant number:** IGA NT12402-5, IGA NT1159
DOI: 10.1002/ijc.28766
History: Received 22 Aug 2013; Accepted 14 Jan 2014; Online 5 Feb 2014
Correspondence to: Radek Spisek, Department of Immunology, 2nd Faculty of Medicine and University Hospital Motol, Charles University, V Uvalu 84, Prague 5, Czech Republic, Tel.: +420-224-435-961, Fax: +420-224-435-962,
E-mail: radek.spisek@lfmotol.cuni.cz

What's new?
Some cytotoxic agents used in cancer treatment activate an immunogenic form of apoptosis, which causes the dying tumor cells to induce an effective antitumor immune response. Here, the authors find that exposure to high hydrostatic pressure (HHP) induces *bona fide* immunogenic cell death in a wide range of human tumor cell lines and primary tumor cells. As HHP treatment is relatively easily standardized under good manufacturing practices conditions, the authors initiated multiple clinical trials evaluating the potential of dendritic cells loaded with HHP-treated cancer cells to induce tumor cell-specific immune responses in patients with prostate cancer.

(RAGE).[21] DCs are known to express several types of PRRs essential for anticancer immune responses elicited by chemotherapy; for example, tumors that are controlled by chemotherapy in control mice fail to respond to chemotherapy in mice lacking TLR4.[20] Furthermore, the release of HMGB1 protein seems to be required for the optimal release and presentation of antigens from dying tumor cells, T-cell priming by DCs[22] and subsequent T-cell-mediated elimination of the tumor. Recently, ATP has been shown to be released during the course of ICD.[23] Secreted ATP acts either as a "find me" signal or as an activator of the NLRP3 inflammasome, which leads to the subsequent activation of caspase-1 and processing of prointerleukin-1β; prointerleukin-1β is then released from the cell and plays an important role in the anticancer immune response elicited by dying tumor cells.[24,25]

Here, we report that an additional physical modality, high hydrostatic pressure (HHP), induces the expression on the cell surface and the release of all of the aforementioned immunogenic molecules on the wide spectrum of primary human tumor cells and human cancer cell lines (leukemia, ovarian cancer and prostate cancer). We also compare the effect of HHP to previous studies on anthracyclines, which are known to induce ICD, and nonimmunogenic UV-B irradiation, which is often used in immunotherapeutic protocols. This study identifies HHP as a reliable and potent inducer of ICD in a wide range of human tumor cell lines and primary tumor cells.[26,27]

Material and Methods

Cell lines

Acute lymphoblastic leukemia (ALL) cell lines were kindly provided by Childhood Leukemia Investigation Prague (CLIP; REH, HLA-A2 positive). Ovarian cancer cells (OV90, HLA-A2 positive; ATCC, Manassas, VA) and prostate cancer cells (LNCap, HLA-A2 positive; ATCC) were also used. All cell lines were cultured in RPMI 1640 medium (Gibco) supplemented with 10% heat-inactivated fetal bovine serum (PAA), 100 U/ml penicillin and 2 mmol/l L-glutamine.

Antibodies and reagents

Antibodies recognizing phospho-eIF2α (Ser51), eIF2α, caspase-3, caspase-8, caspase-9 (Cell Signaling Technology, Danvers, MA), cytochrome *c* (BD Bioscience, Franklin Lakes, NJ) and GAPDH (GeneTex, Irvine, CA) were used. Secondary anti-rabbit and anti-mouse antibodies conjugated to horseradish peroxidase (Jackson ImmunoResearch Laboratories, West Grove, PA) were also used.

The following monoclonal antibodies (mAbs) against the indicated molecules were used: CD80-FITC, CD83-PE, CD86-PE-Cy5, CD14-PE-Dy590, CD8-PE-Dy590 (Exbio, Vestec, Czech Republic), CD11c-PE, HLA-DR-Alexa700, IFN-γ-FITC, CD4-PC7 (BD Biosciences, San Diego, CA), FoxP3-Alexa488 (eBioscience), CD25-PerCP-Cy5.5, Ki67-PE, CD28-PC7, CD62L-FITC, CD57-APC (BioLegend), anti-HSP70 (R&D, Basel, Switzerland), anti-HSP90 and anti-CRT (Enzo, Farmingdale, NY).

CellRox orange reagent (Invitrogen, Carlsbad, CA) was used for the detection of reactive oxygen species (ROS) production. The following caspase inhibitors were used: caspase-3 (Z-DEVD-FMK), caspase-8 (Z-IETD-FMK) and caspase-9 (Z-LEHD-FMK; MBL, Wobrun, MA).

Apoptosis induction and detection

Tumor cell death was induced by UV-B light exposure, HHP treatment and idarubicin (Fig. 2). Induction of cell death by UV-B and anthracyclines was previously described.[5] Cells were treated by HHP in the custom-made device (Resato International BV, Netherlands) that is located in the GMP manufacturing facility. This device allows for the reliable treatment of the tumor cells by defined levels of HHP for specified periods of time. Cell death was assessed by annexin V/fluorescein isothiocyanate staining. Briefly, 2×10^5 cells per sample were collected, washed in PBS, pelleted and resuspended in an incubation buffer containing annexin V/fluorescein isothiocyanate antibodies (Exbio). The samples were kept in the dark and incubated for 15 min prior to the addition of DAPI, and subsequent analysis was performed with a FACScan Aria (BD Bioscience) using FlowJo software (Treestar, Ashland, OR).

Flow cytometric analysis of HSP70, HSP90 and CRT on the cell surface

A total of 1×10^6 cells were plated in 12-well plates and then UV-B irradiated or treated with HHP or idarubicin for 6, 12 or 24 hr. The cells were collected and washed twice with PBS. The cells were then incubated for 30 min with primary antibody diluted in cold blocking buffer (2% fetal bovine serum in PBS), followed by washing and incubation with an Alexa 648-conjugated monoclonal secondary antibody in blocking solution. Each sample was then analyzed using a FACScan Aria (BD Bioscience). Cell surface

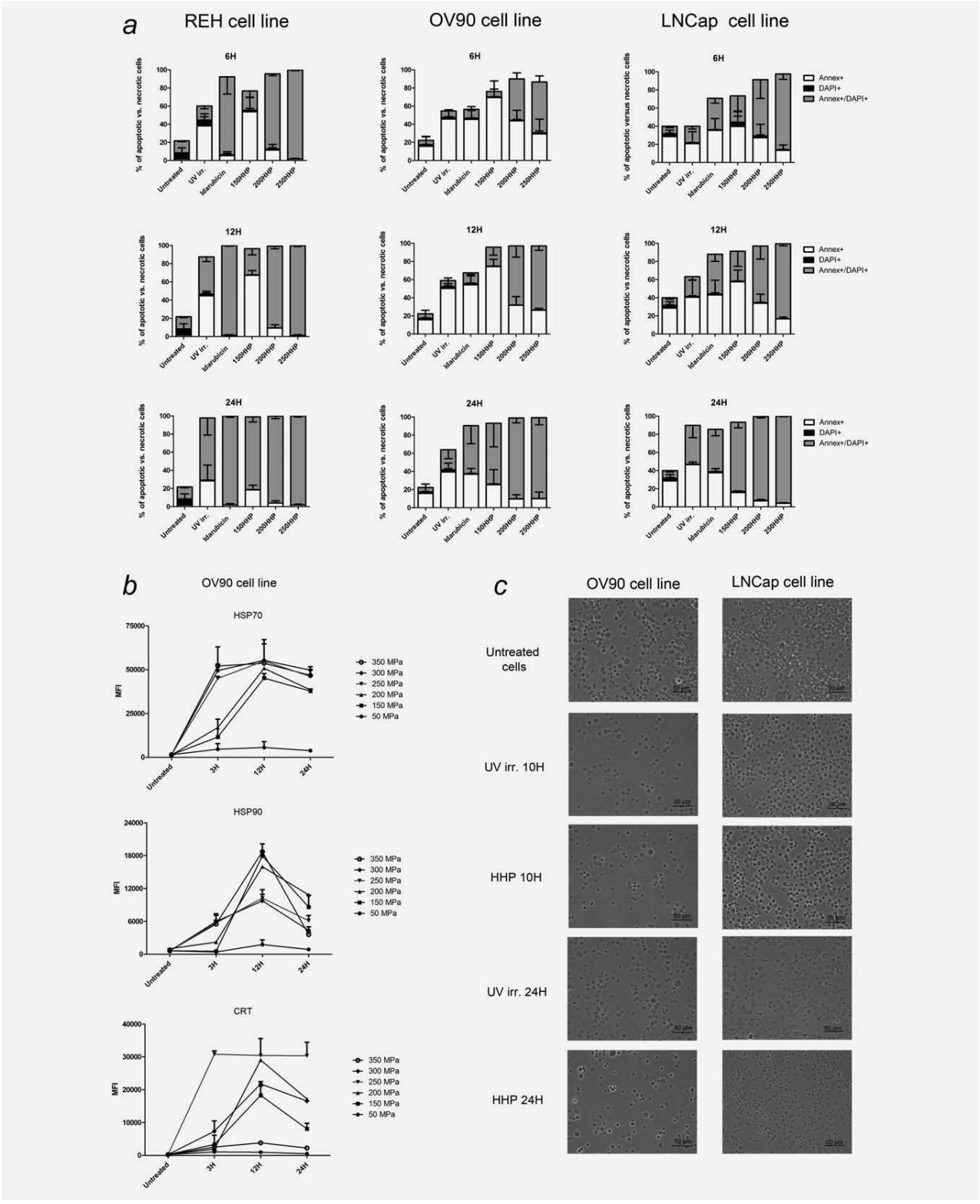

Figure 1. Sensitivity of the T-ALL (REH), OV90 (ovarian cancer) and LNCap (prostate cancer) cell lines to different intensities of HHP. (*a*) The REH, OV90 and LNCap cell lines were treated for 6, 12 or 24 hr with different levels of HHP (150, 200 and 250 MPa) and compared to idarubicin and nonimmunogenic UV-B irradiation. The percentage of early (annexin V+/DAPI−), late (annexin V+/DAPI+) apoptotic cells and necrotic cells (annexin V−/DAPI+) was determined by flow cytometry. (*b*) The kinetics of HSP70, HSP90 and calreticulin expression on the ovarian cancer cell line (OV90) treated with six different levels of HHP (50, 150, 200, 250, 300 and 350 MPa) for 10 min. (*c*) The morphology of the OV90 and LNCap cell lines after UV-B irradiation or HHP treatment for 10 or 24 hr.

expression of HSP70, HSP90 and CRT was analyzed on non-permeabilized annexin V-positive/DAPI-negative cells.

Detection of HMGB1 release

REH cells, OV90 cells, LNCap cells, primary ovarian cells and leukemic blasts were plated at 1×10^6 cells per well in 1 ml of complete medium appropriate for the cell type. After UV-B irradiation or HHP or idarubicin treatment, supernatants were collected at different time points (6, 12, 24 and 48 hr). Dying tumor cells were removed by centrifugation, and the supernatants were isolated and frozen immediately. Quantification of HMGB1 in the supernatants was assessed using an enzyme-linked immunosorbent assay according to the manufacturer's instructions (IBL, Hamburg, Germany).

Immunofluorescence

For the detection of HMGB1, the cells were placed on ice, washed twice with PBS and fixed in 0.25% paraformaldehyde in PBS for 5 min. The cells were then washed twice in PBS, and a primary anti-HMGB1 antibody (Abcam, Cambridge, MA) diluted in cold blocking buffer was added for 30 min. After two washes in cold PBS, the cells were incubated for 30 min with the appropriate DyLight 594-conjugated secondary antibody. The cells were fixed with 4% paraformaldehyde for 20 min, washed in PBS for 20 min and mounted on slides.

For phagocytosis, the DCs were stained with Vybrant® DiD cell labeling solution (Invitrogen). The tumor cells were stained with Vybrant® DiO cell labeling solution (Invitrogen) and treated as indicated. Immature DCs (Day 5) were fed tumor cells at a DC/tumor cell ratio of 5:1. The cells were fixed with 4% paraformaldehyde for 20 min, washed in PBS for 20 min and mounted on slides with ProLong Gold antifade reagent (Invitrogen). For the detection of ROS activity, cells were stained with CellRox orange reagent before HHP treatment. After the treatment, cells were washed twice with culture media and fixed in 0.25% paraformaldehyde in PBS for 5 min and mounted on slides.

Generation of tumor-loaded DCs and induction of tumor cell death

DCs were generated by culturing purified $CD14^+$ cells isolated from buffy coats in the presence of granulocyte–macrophage colony-stimulating factor (Gentaur, Kampenhout, Belgium) and interleukin IL-4 (Gentaur). The tumor cells were treated as indicated by UV-B irradiation and HHP. The extent of apoptosis was monitored by annexin V/DAPI staining. The cells were extensively washed prior to feeding to DCs. Immature DCs (Day 5) were fed tumor cells at a DC/tumor cell ratio of 5:1. In some experiments, pulsed DCs were stimulated with 100 ng/ml of lipopolysaccharide (LPS; Sigma-Aldrich, St. Louis, MO) for 12 hr.

Flow cytometry analysis of DCs after treatment with killed tumor cells

The phenotype of DCs cultured with tumor cells was monitored by flow cytometry. Tumor cells were treated with UV-B irradiation or HHP and then cocultured for 24 hr with immature DCs. For some experiments, the DCs and tumor cells were dye-labeled prior to coculture to monitor phagocytosis. mAbs against the following molecules were used: CD80-A700 (Exbio), CD83-PerCP-Cy5.5 (BioLegend, San Diego, CA), CD86-A647 (BioLegend), CD14-PE (Exbio), CD11c-APC (Exbio) and HLA-DR PC7 (BD Biosciences).

The DCs were stained for 30 min at 4°C, washed twice in PBS and analyzed using a FACScan Aria (BD Biosciences) with FlowJo software. The DCs were gated according to the FSC and SSC properties. The appropriate isotype controls were included, and 50,000 viable DCs were acquired for each experiment.

Cytokine measurements

Cytokines in the supernatants released from immature and mature DCs were measured using a MILLIPLEX Human Cytokine/Chemokine kit (Millipore, Billerica, MA) and analyzed with a Luminex 200 analyzer (Luminex).[28] This kit is designed for the multiplexed quantitative measurement of multiple cytokines in a single well. Six cytokines were detected, including IL-12p70, IL-6, IL-1β, TNF-α, IL-10 and IFN-α.

Evaluation of IFN-γ-producing tumor-specific T cells

Unpulsed or tumor-loaded DCs were added to autologous T cells at a ratio of 1:5 on Days 0 and 7 of culture. IL-2 (25–50 U/ml; PeproTech) was added every second day of culture. The cultures were tested for the presence of tumor-specific T cells two weeks after the last stimulation with DCs. The induction of tumor-reactive, IFN-γ-producing T cells by tumor-loaded DCs was determined by flow cytometry. The T cells were stained with anti-human CD8/IFN-γ.

Preparation of cell extracts and Western immunoblot analysis

Cell extracts were prepared at the indicated time points following UV-B irradiation and HHP treatment. After treatment, the cells were washed with ice-cold PBS and lysed on ice in RIPA buffer (10 mM Tris pH 7.5, 150 mM NaCl, 5 mM EDTA and 1% Triton X-100) with a protease inhibitor cocktail (Roche Diagnostics) and 1 mM phenylmethylsulfonyl fluoride. Proteins were separated by 9–15% SDS-PAGE and transferred to nitrocellulose membranes (Bio-Rad, Hercules, USA).

The membranes were blocked in 5% nonfat dry milk in TBST buffer (50 mM Tris, 150 mM NaCl and 0.05% Tween 20) for 1 hr at room temperature and incubated with primary antibody overnight at 4°C. The membranes were then washed in TBST buffer and incubated for 1 hr at room temperature with horseradish peroxidase-conjugated secondary antibodies. Detection was carried out with the enhanced chemiluminescence detection system. Equal protein loading was ensured with a BCA assay, verified by an analysis of Ponceau-S staining of the membrane and GADPH reprobing.

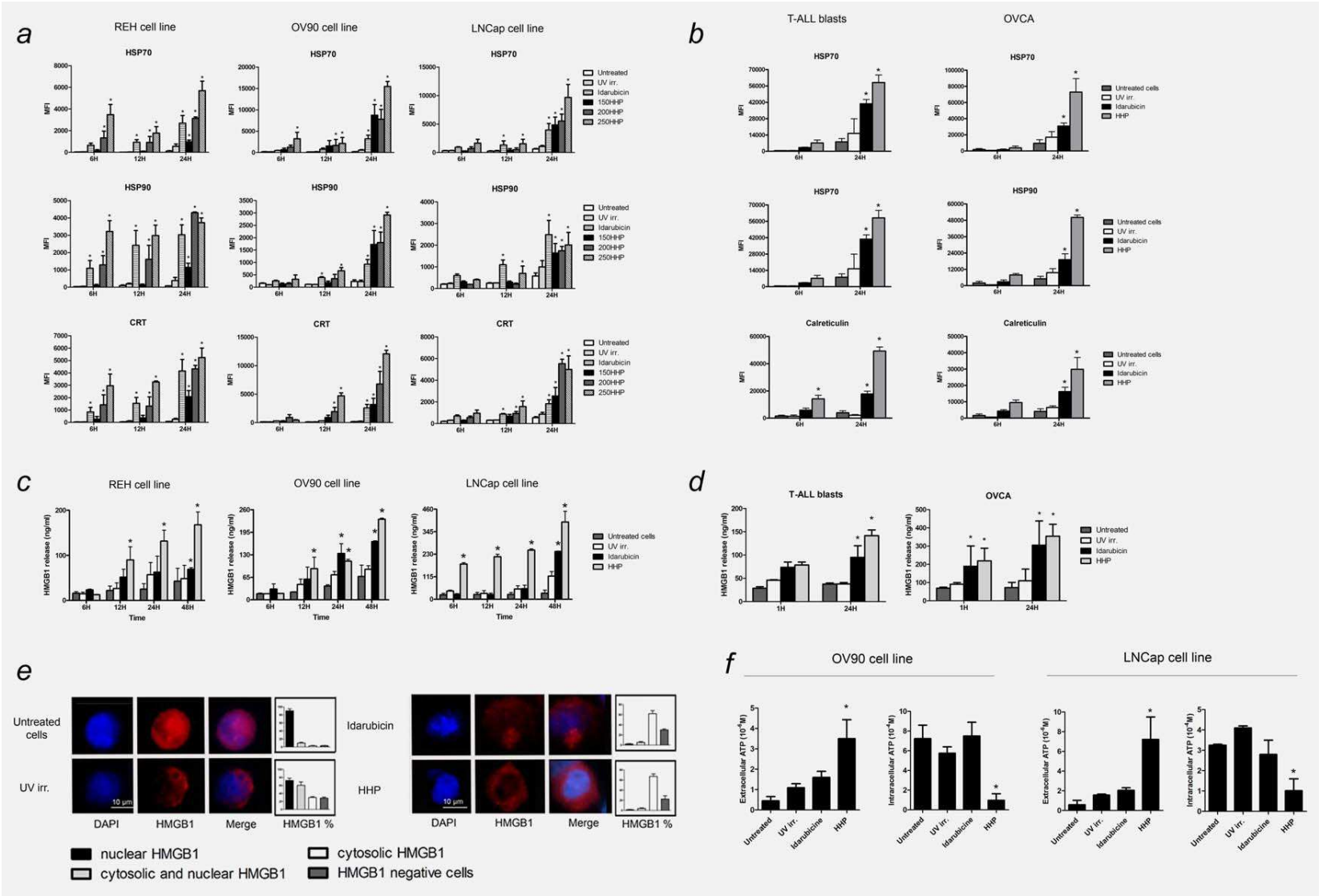

Figure 2. Anthracyclines (idarubicin) and HHP induce the expression of HSPs and CRT and the release of HMGB1 by human tumor cells. The kinetics of HSP70, HSP90 and calreticulin expression in the (*a*) T-ALL cell line (REH), ovarian cancer cell line (OV90) and prostate cancer cell line (LNCap) and (*b*) leukemic blasts isolated from T-ALL patients and primary ovarian cancer cells treated with idarubicin, UV-B or HHP for 6 or 24 hr. The expression of the indicated markers by treated cells is shown as mean fluorescence intensity (MFI). The compiled results of a total of three experiments are shown; $*p < 0.05$. (*c*) The kinetics of the release of HMGB1 into the culture supernatants of tumor cells treated with idarubicin, UV-B or HHP for 6, 12, 24 or 48 hr. The data show the summary (mean ± SD) of three independent experiments for the T-ALL cell line (REH), ovarian cancer cell line (OV90) and prostate cancer cell line (LNCap) and (*d*) for leukemic blasts isolated from T-ALL patients and primary ovarian cancer cells treated with idarubicin and HHP. $*p < 0.05$ compared to untreated cells. (*e*) Fluorescence microscopy images of cells treated for 24 hr with UV-B irradiation, idarubicin or HHP and stained for HMGB1. (*f*) Declining intracellular ATP levels and the accumulation of extracellular ATP concentrations in tumor cells exposed to UV-B irradiation, idarubicin or HHP for 1 hr.

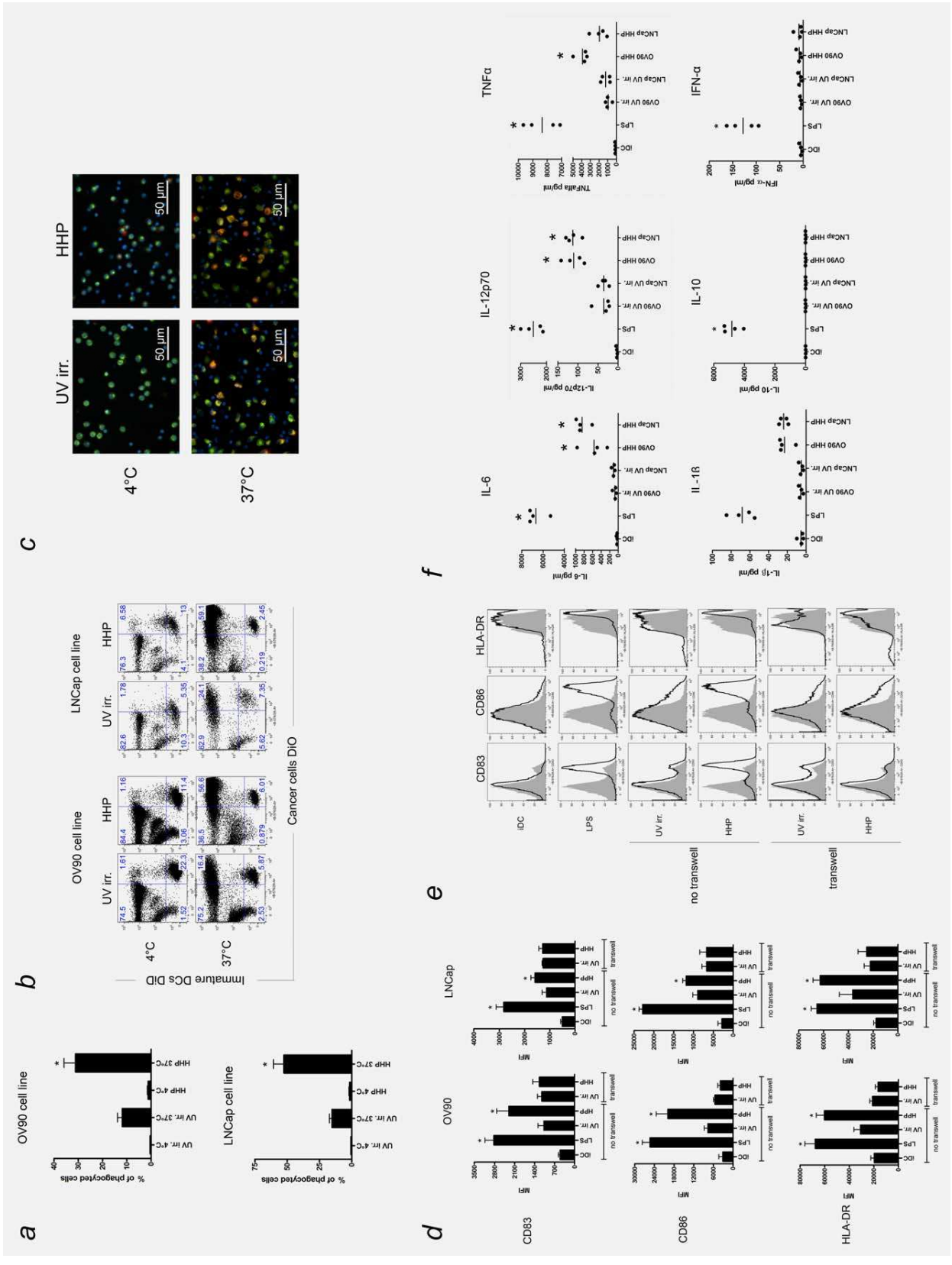
a
OV90 cell line
% of phagocyted cells
UV irr. 4°C
UV irr. 37°C
HHP 4°C
HHP 37°C
LNCap cell line
b
OV90 cell line
LNCap cell line
UV irr.
HHP
4°C
37°C
Immature DCs DiD
Cancer cells DiO
c
UV irr.
HHP
50 µm
4°C
37°C
d
OV90
LNCap
CD83
CD86
HLA-DR
MFI
iDC
LPS
UV irr.
HHP
no transwell
transwell
e
CD83
CD86
HLA-DR
iDC
LPS
UV irr
HHP
no transwell
transwell
f
IL-6
IL-12p70
TNFα
IL-1ß
IL-10
IFN-α
iDC
LPS
OV90 UV irr.
LNCap UV irr.
OV90 HHP
LNCap HHP

Figure 3.

Cytosolic and mitochondrial fractions were prepared using a cell fractionation kit (Abcam) according to the manufacturer's instructions. We used cytosolic GAPDH as internal loading control for the fractionation experiments. Additional information can be found in Supplementary materials.

Results

HHP induces apoptosis and the expression of ICD markers on cancer cells

To initially determine the ability of HHP to induce ICD, tumor cells were treated for 10 min with a broad range of HHP (150, 200 and 250 MPa) and repeatedly analyzed over the course of 24 hr according to DAPI and annexin V staining (Fig. 1*a*). Treatment of tumor cells with HHP greater than 150 MPa led to the apoptosis (% annexin V+ cells) of more than 80% of cells within 12 hr, with the majority of cells demonstrating a staining pattern typical of apoptosis (annexin V+/DAPI−) rather than necrosis (annexin V−/DAPI+; Fig. 1*a*) and morphology typical of apoptotic cells (Fig. 1*c*). We also examined the kinetics of the expression of ICD markers on tumor cells undergoing apoptosis induced by HHP in the ovarian cancer (Fig. 1*b*), prostate cancer and leukemic cell lines (data not shown). Treatment of tumor cells with HHP greater than 150 MPa led to the significant expression of HSP70, HSP90 and CRT. Because HHP values above 350 MPa led to accelerated apoptosis and rapid degradation of apoptotic bodies, we chose a HHP value of 250 MPa for subsequent experiments.

HHP induces the expression of HSPs and CRT on human cancer cell lines and human primary tumor cells

After the initial examination of the presence of ICD markers after HHP treatment, we performed an extensive analysis of the expression of known ICD markers in tumor cell lines (REH, LNCap and OV90) and freshly isolated primary tumor cells (T-ALL and ovarian tumor cells). We directly compared HHP treatment to UV-B irradiation, which does not induce ICD, and idarubicin member of anthracyclines family, which is known to induce immunogenic apoptosis.[5] Expression of ICD markers was analyzed on apoptotic annexin V-positive/DAPI-negative cells. HHP induced significant expression of HSP70, HSP90 and CRT on the cell surface of all tested cell lines and primary tumor cells (Figs. 2*a* and 2*b*). Furthermore, the kinetics of this expression were similar to those induced by idarubicin, with all markers expressed after 6 hr and showing maximum induction between 12 and 24 hr after treatment. HHP, however, induced 1.5-fold to twofold higher expression of HSP70, HSP90 and CRT compared to idarubicin (Figs. 2*a* and 2*b*). We did not observe any significant upregulation of ICD markers on ovarian, prostate or ALL human tumor cells after UV-B light exposure.

HHP induces the release of HMGB1 by human cancer cells

We next analyzed the release of the late-stage marker of ICD HMGB1 in the supernatants of T-ALL, ovarian and prostate cancer cell lines and primary T-ALL and ovarian tumor cells. Of the tested treatments, HHP and idarubicin induced significant release of HMGB1 in all tested human tumor cells (Figs. 2*c* and 2*d*). Maximal release of HMGB1 nuclear protein was detected 48 hr after the induction of tumor cell death. The amount of HMGB1 released from HHP-induced apoptotic cells was even greater than that detected following idarubicin treatment. Furthermore, the quantity of released HMGB1 was tumor cell type-dependent, as a twofold greater release was detected in prostate and ovarian cancer cells in comparison to the other cell types tested. These data were further verified by immunofluorescence microscopy, which documented the release of HMGB1 from the nuclei to the cytosol in ovarian cells (OV90; Fig. 2*e*).

HHP reduces intracellular ATP and increases extracellular ATP levels

The extracellular release of ATP is a hallmark of ICD. Therefore, we measured intracellular and extracellular ATP levels in LNCap and OV90 cell lines at 1 hr (Fig. 2*f*), 6 hr and 12 hr (data not shown) after exposure to specific cell death inducers. For all tested treatments (HHP, idarubicin and UV-B), we found that the induction of cell death was accompanied by a reduction in the intracellular ATP concentration and an accumulation of extracellular ATP in different time points (Fig. 2*f*). HHP (1 hr after treatment) and idarubicin (6 hr after treatment; data not shown) induced the most significant release of ATP into the culture supernatants.

HHP treatment increases the rate of phagocytosis of killed tumor cells by DCs

In view of the established role of CRT as a phagocytosis-promoting signal, we first investigated the rate of phagocytosis of HHP-treated ovarian (OV90) and prostate (LNCap) tumor cells by DCs. HHP-treated tumor cells were phagocytosed at a

Figure 3. HHP treatment of ovarian (OV90) and prostate (LNCap) tumor cells increases the rate of phagocytosis of killed tumor cells by DCs and induces the expression of maturation-associated molecules on DCs. (*a*) Percentage of phagocytosis at 24 hr following HHP treatment compared to the control. (*b*) Dot plots of representative experiments are shown. Killed OV90 and LNCap cells were labeled with DiO and cocultured with DiD-labeled immature DCs. (*c*) Fluorescence microscopy analysis of the phagocytosis experiments. After 24 hr of coculture of killed tumor cells with immature DCs, the engulfment of tumor cells was verified by fluorescence microscopy. (*d*) Immature DCs (Day 5) were cultured for 24 hr with OV90 or LNCap cells killed by UV-B irradiation or HHP. After 24 hr, the expression of CD83, CD86 and HLA-DR by DCs was analyzed by flow cytometry. The MFI and representative histograms are shown (*e*). $*p < 0.05$ compared to immature DCs. (*f*) Determination of cytokine concentrations in culture supernatants of DCs cultured for 24 hr with OV90 or LNCap cells treated with UV-B irradiation or HHP. The data show the compiled results (mean ± SD) of three independent experiments. $*p < 0.05$ compared to untreated cells.

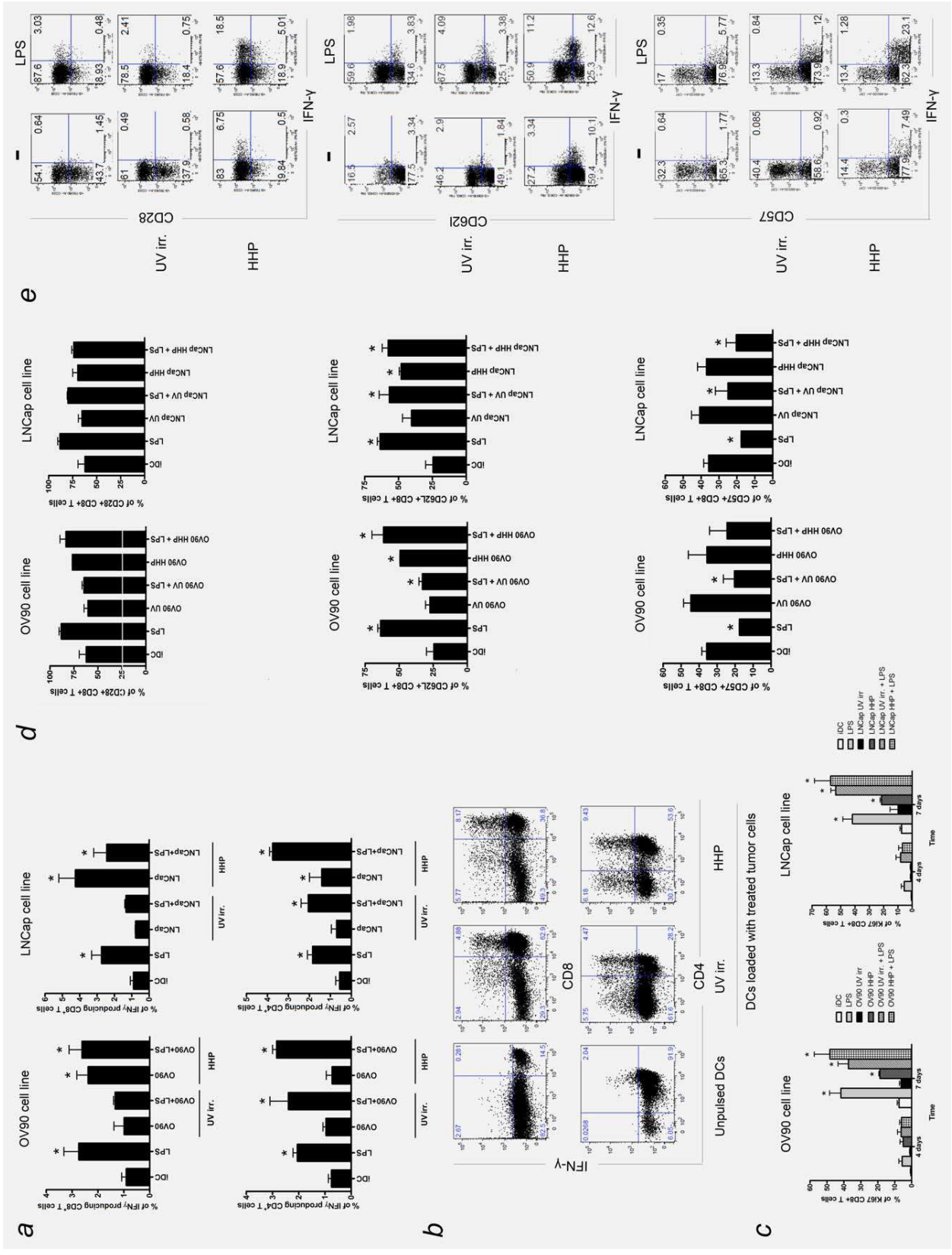
a
OV90 cell line
LNCap cell line
% of IFNγ producing CD8+ T cells
% of IFNγ producing CD4+ T cells
iDC
LPS
OV90
OV90+LPS
LNCap
LNCap+LPS
UV irr.
HHP
b
CD8
CD4
IFN-γ
Unpulsed DCs
DCs loaded with treated tumor cells
c
% of Ki67 CD8+ T cells
4 days
7 days
Time
iDC
LPS
OV90 UV irr
OV90 HHP
OV90 UV irr. + LPS
OV90 HHP + LPS
LNCap UV irr
LNCap HHP
LNCap UV irr. + LPS
LNCap HHP + LPS
d
% of CD28+ CD8+ T cells
% of CD62L+ CD8+ T cells
% of CD57+ CD8+ T cells
OV90 UV
OV90 UV + LPS
OV90 HHP
OV90 HHP + LPS
LNCap UV
LNCap UV + LPS
LNCap HHP
LNCap HHP + LPS
e
-
LPS
IFN-γ
CD28
CD62l
CD57
UV irr.
HHP

Figure 4.

faster rate and to a greater extent than tumor cells killed by UV-B irradiation. After 24 hr, the rate of phagocytosis of tumor cells treated with HHP was threefold higher in comparison to cells killed by UV-B irradiation (Fig. 3).

Phagocytosis of HHP-treated tumor cells induces the expression of maturation-associated molecules on DCs and proinflammatory cytokine production

The ability of DCs to activate the immune response depends on their maturation status and the expression of costimulatory molecules. We analyzed the phenotype of DCs that had phagocytosed ovarian (OV90) or prostate (LNCap) tumor cells killed by HHP or UV-B irradiation and found that the interaction of DCs with HHP-treated tumor cells induced the significant upregulation of CD83, CD86 and HLA-DR, albeit to a lesser extent than treatment with LPS (Fig. 3*d*). Importantly, the ability of HHP-killed tumor cells to promote DC maturation was abrogated when the DCs were separated from the dying tumor cells by a transwell, suggesting the need for cell–cell contact between the tumor cells and DCs. We next evaluated cytokine production by activated DCs. The interaction between DCs and HHP-treated tumor cells induced significant release of IL-6, IL-12p70 and TNF-α compared to immature DCs and DCs pulsed with UV-B-treated tumor cells. There was no increase in the production of IL-10 or IFN-α by DCs pulsed with HHP-treated tumor cells (Fig. 3*f*).

DCs pulsed with HHP-treated tumor cells induce tumor-specific T cells

To investigate whether tumor cells expressing ICD markers induce antitumor immunity, we evaluated the ability of tumor cell-loaded DCs to activate tumor cell-specific T-cell responses. Ovarian (OV90) and prostate (LNCap) tumor cells killed by HHP or UV-B irradiation were cocultured with immature DCs with or without subsequent maturation with LPS. These DCs were then used as stimulators of autologous T cells, and the frequency of IFN-γ-producing T cells was analyzed 2 weeks later, after restimulation with tumor cell-loaded DCs. DCs pulsed with tumor cells killed by HHP induced a greater number of tumor-specific $CD4^+$ and $CD8^+$ IFN-γ-producing T cells compared to DCs pulsed with UV-B light-exposed cells in all experiments ($n = 5$), even in the absence of an additional maturation stimulus (LPS; Fig. 4*a*). We also evaluated the proliferative capacity of the induced antigen-specific T cells by examining Ki67 expression (Fig. 4*c*). Antigen-specific T cells induced by DCs pulsed with HHP-treated tumor cells proliferated more significantly compared to T cells induced by DCs pulsed with UV-B-treated tumor cells. To further investigate the phenotype of the antigen-specific T cells, we evaluated the expression of several T-cell surface markers and found that the interaction of autologous T cells with DCs pulsed with HHP-treated tumor cells induced the significant upregulation of CD28 and CD62L and the downregulation of CD57 (Fig. 4*d*).

In addition, we tested the frequency of regulatory T cells (Tregs) induced in the DC and T-cell cocultures. DCs pulsed with ovarian (OV90) or prostate (LNCap) cells killed by HHP were less able to expand Tregs compared to both immature DCs and LPS-activated DCs (Fig. 5*a*). This finding was further confirmed using a quantitative real-time PCR-based methylation assay, which assessed the percentage of stable Tregs that were demethylated at the *FoxP3* TSDR in autologous T-cell suspensions (Fig. 5*c*).

Characteristics of the apoptotic pathways induced by HHP treatment

We next investigated whether HHP, as an inducer of cell death with immunogenic characteristics, activates analogous apoptotic pathways similar to anthracyclines or photodynamic therapy.[17,25] We therefore characterized key components of the ER stress-mediated apoptotic pathway, such as ROS production, the phosphorylation of the translation initiation factor eIF2α and the activation of caspase-8. In cells treated by HHP, we detected increased production of ROS (Figs. 6*a* and 6*b*) that was suppressed in cells pretreated with *N*-acetyl-L-cysteine or L-glutathione. In addition, we detected an increased activity of catalase, which is preferentially used by cells exposed to ROS, in HHP-treated cells (Fig. 6*c*). Our results indicate the rapid phosphorylation of eIF2α in OV90 and LNCap cells after HHP treatment, in contrast to untreated or UV-B-irradiated cells (Fig. 6*d*). We also observed the rapid activation of caspase-3, -8 and -9 following HHP treatment, and all detected caspases were activated rapidly after HHP treatment (Fig. 6*e*). To evaluate the importance of the individual caspases for the kinetics of HHP-induced cell death, we tested the effect of selective caspase inhibitors. Only a selective inhibitor of caspase-8 (Z-IETD-FMK) significantly decreased the kinetics of apoptosis after HHP treatment, as documented by annexin V/DAPI staining (Fig. 6*f*), and the inhibition of caspase-3 (with Z-DEVD-FMK) or caspase-9 (with Z-LEHD-FMK) did not affect the kinetics of apoptosis. This finding documents the importance of caspase-8 in HHP-induced apoptosis, although caspase-3 and -9 were also shown to be activated. Cells treated with HHP had a decreased mitochondrial potential compared to UV-B-irradiated tumor cells, and this finding also correlates

Figure 4. The induction of tumor-specific T cells by HHP-killed OV90 and LNCap cells without the need for an exogenous DC maturation stimulus. (*a*) Monocyte-derived DCs were pulsed with OV90 or LNCap cells killed by UV-B irradiation or HHP and then used to stimulate autologous T cells for 2 weeks. The number of IFN-γ-producing cells in cultures with unpulsed DCs or DCs pulsed with tumor cells was analyzed by intracellular IFN-γ staining after restimulation. The data show a summary and (*b*) representative staining of five independent experiments. (*c*) Ki67 staining of tumor-specific T cells. (*d*) Evaluation of CD28, CD62L and CD57 expression by tumor-specific T cells to determine the T-cell phenotype. The data show the compiled results of three total experiments. $*p < 0.05$. Representative dot plots are shown (*e*). [Color figure can be viewed in the online issue, which is available at wileyonlinelibrary.com.]

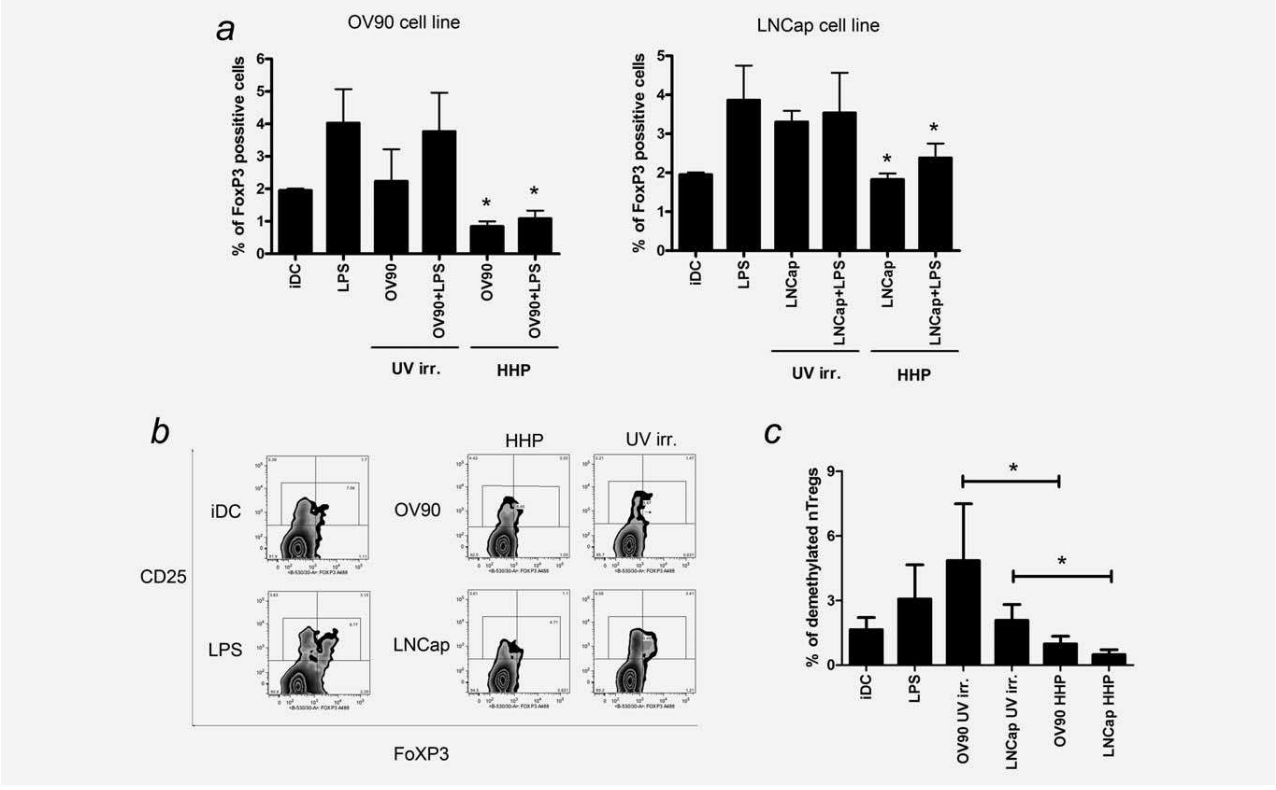

Figure 5. DCs pulsed with ovarian (OV90) or prostate (LNCap) cells killed by HHP have a reduced capacity to expand Tregs. Monocyte-derived DCs were pulsed with tumor cells killed by UV irradiation or HHP and then used to stimulate magnetically isolated $CD4^+$ naive autologous T cells. After 2 weeks, the frequency of $CD4^+CD25^+CD127^-FoxP3^+$ Tregs in the culture was analyzed. The data show the compiled results (*a*) and (*b*) representative staining for three independent experiments. $*p < 0.05$ compared to immature DCs. (*c*) Columns represent the proportions of Tregs demethylated in the FoxP3 TSDR.

with the rapid release of cytochrome *c* into the cytosol within 30 min to 1 hr after the induction of apoptosis by HHP in both ovarian and prostate cancer cell lines (Fig. 6*g*).

Discussion

The textbook view of apoptosis as a nonimmunogenic event has recently been challenged. For instance, under specific circumstances, particularly in response to chemotherapy (anthracyclines,[5,13,17,29] oxaliplatin[6] or bortezomib[7]) or physical treatment modalities (γ-irradiation or hypericin-based photodynamic therapy[30–32]), cancer cells undergo cell death linked to the release of specific molecules that subsequently initiate tumor-specific immune responses.[33,34] This type of cell death program has been termed ICD or immunogenic apoptosis. Immunogenic apoptosis of cancer cells involves the biochemical hallmarks of "classical," tolerogenic apoptosis, including phosphatidylserine exposure, caspase activation and mitochondrial depolarization.[14,35] However, this type of cell death also appears to have two other important properties: (*i*) surface exposure or secretion of critical immunogenic signals known as DAMPs and (*ii*) the ability to elicit a protective immune response against tumor cells.[36] Several DAMPs have recently been identified as common and indispensable features of immunogenic apoptosis, including surface CRT,[13] surface HSP90 and HSP70 and secreted ATP[24] and HMGB1.[37] Rapid translocation of the ER-resident chaperone protein CRT to the cell surface of dying tumor cells was previously identified as a molecular mechanism enhancing the phagocytosis of these cells by DCs, as the depletion of CRT by siRNA knockdown averted the immunogenicity of cancer cell death.[13] Similarly, we published findings showing that the induction of ICD by bortezomib correlated with expression of HSP90 on the surface of myeloma cells, and HSP90 exposure has been shown to be crucial for the activation of DCs, both in human and murine cells.[7] Furthermore, the soluble endogenous danger signal protein HMGB1, a specific ligand of TLR4, is released from dying tumor cells during late apoptosis,[20,21] and depletion of HMGB1 from tumor cells was shown to abolish DC-mediated presentation of tumor antigens. Recently, studies by Martins *et al.*[24] and Garg *et al.*[25] led to the discovery of ATP as a soluble endogenous danger signal, in which ATP is released during immunogenic apoptosis. ATP binds with high affinity to the purinergic receptor P2X7 and is reportedly released from stressed and dying cells, including chemotherapy-treated cancer cells. Secreted ATP acts both as a homing signal and as an activator of the NLRP3 inflammasome. In addition to chemotherapeutic agents, hypericin-based PDT was identified as an additional inducer of ICD; Garg *et al.*[25,38] demonstrated that

hypericin-based PDT initiated ICD *via* signaling pathways that overlap with, but are not identical to, those elicited by anthracyclines.[8]

In our study, we describe HHP as a novel modality capable of inducing ICD in human tumor cells. The first indications that HHP treatment upregulates markers of

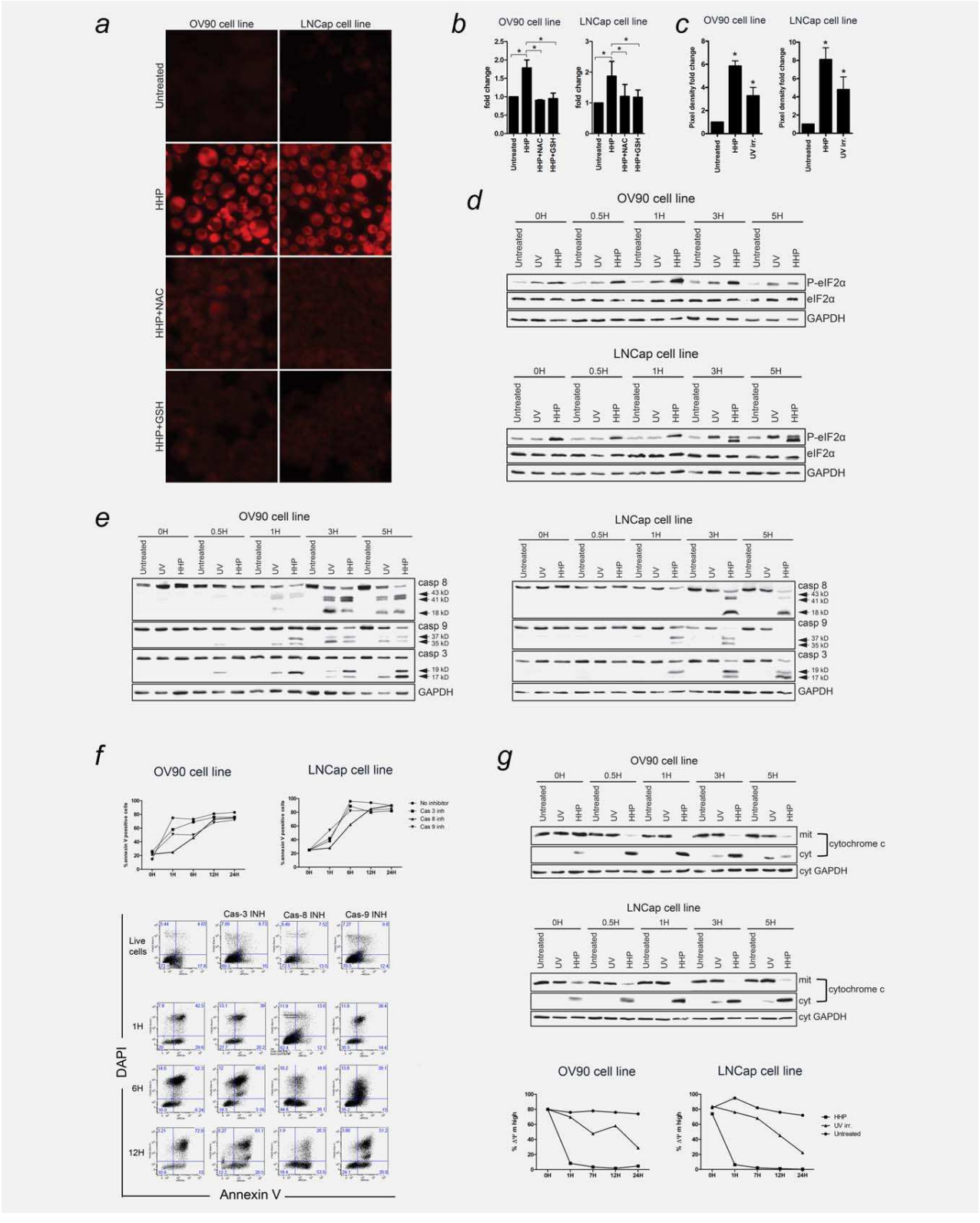

Figure 6.

immunogenic apoptosis were shown by Frey *et al*. in mouse models.[39–41] We therefore chose to extensively analyze the impact of HHP treatment on dying tumor cells. We assessed the expression of known markers of ICD (CRT, HSP70, HSP90, HMGB1 and ATP), the impact of HHP-killed tumor cells on the phenotypic and functional characteristics of DCs and the capacity of HHP-killed tumor cells to activate tumor-specific immunity. We also analyzed the signaling pathways activated by HHP treatment.

Our results showed that HHP treatment at a dose greater than 150 MPa induces rapid apoptosis of cells while preserving apoptotic bodies important for inducing ICD.[39] The rapid induction of apoptosis correlated with the rapid activation of caspase-3, -8 and -9 within 1 hr of treatment.[42] In the initial set of experiments, we showed that, similarly to anthracyclines, HHP induces the rapid translocation of CRT, HSP70 and HSP90 to the cell surface and the release of ATP and HMGB1 within 12 hr in all tested tumor cell systems (in both primary tumor cells and tumor cell lines). The interaction of immature monocyte-derived DCs with immunogenic HHP-killed tumor cells led to the increased uptake of tumor cells by DCs and induced the expression of maturation-associated markers on DCs. The interaction between DCs and HHP-killed tumor cells also induced the production of IL-1, IL-6, TNF-α and IL-12p70, demonstrating that HHP-treated tumor cells provide a potent activation stimulus to DCs. This finding is in accordance with a study showing that extracellular ATP released from immunogenic tumor cells can stimulate NLRP3-dependent IL-1β production by DCs.[43] Furthermore, DCs pulsed with HHP-treated tumor cells efficiently stimulated tumor-specific IFN-γ-producing CD28+CD62+CD57− T cells. However, HHP-treated tumor cell-loaded DCs also induced significantly lower numbers of CD4+CD127−CD25highFoxP3+ Tregs compared to nonimmunogenic tumor cells, which may be relevant for the design of cancer immunotherapy studies.[44] Moreover, a PCR-based methylation assay that assessed the percentage of stable Tregs demethylated at the *FoxP3* TSDR found that these induced Tregs were stable and functional.

In addition to the expression of ICD markers, the release of HMGB1 and ATP and the activation of tumor-specific immunity, ICD is also characterized by the activation of specific apoptotic signaling pathways. The signaling pathways induced by chemotherapeutics and hypericin-based PDT largely overlap; however, these pathways are not identical. The production of ROS and ER stress are essential for the activation of intracellular pathways that govern ICD. Chemotherapy-induced expression of ICD markers is dependent on PERK-mediated eIF2α phosphorylation and caspase-8-mediated activation of the BAX and BAK proteins. In contrast, hypericin-based PDT requires PERK, BAX and BAK for CRT translocation, whereas phosphorylated eIF2α and caspase-8 activation appear to be dispensable.[17,25,45] Our results show that HHP treatment stimulated ROS production, the phosphorylation of eIF2α and the rapid activation of caspase-3, -8 and -9, although only the specific inhibition of caspase-8 decreased the kinetics of HHP-induced cell death. Severe ER stress induced by HHP culminated in intrinsic mitochondrial apoptosis. Further studies are conducted to dissect and characterize the signaling pathways triggered by HHP treatment.

In our study, we identified HHP as a reliable and potent inducer of ICD in a wide range of human tumor cell lines and primary tumor cells. HHP-induced tumor cell death fulfills all currently described criteria of ICD, including the activation of analogous intracellular signaling pathways, which is similar to chemotherapy and hypericin-based PDT.[46] HHP treatment of tumor cells can be easily standardized and performed in GMP conditions to allow its incorporation into manufacturing protocols for cancer immunotherapy products.[26,47–50] We have now initiated multiple clinical trials for prostate cancer evaluating the potential of DCs loaded with HHP-treated cancer cells to induce tumor cell-specific immune responses and to modify the clinical course of patients with prostate cancer.[26]

Acknowledgement

The authors thank Dr. Abhishek D. Garg for his valuable comments and critical review of the manuscript.

Figure 6. HHP induces the activation of key apoptotic markers in the ER stress-mediated apoptotic pathway, similar to anthracyclines and photodynamic stress inducers. (*a*) Fluorescent microscopy analysis of ROS production in HHP-treated ovarian (OV90) and prostate (LNCap) tumor cells and in the presence of ROS inhibitors *N*-acetyl-L-cysteine and L-glutathione by CellRox. (*b*) Detection of ROS production by flow cytometry using CellRox staining of HHP-treated ovarian (OV90) and prostate (LNCap) tumor cells. (*c*) Detection of catalase activity in UV-B- or HHP-treated ovarian (OV90) and prostate (LNCap) tumor cells. The data represent the compiled results (mean ± SD) of three independent experiments. (*d*) The kinetics of eIF2α phosphorylation were detected by Western blot analysis in tumor cells treated with UV-B irradiation or HHP for 30 min or 1, 3 or 5 hr. The activity of eIF2α was determined by a phospho-specific antibody (P-), and then the membranes were reprobed with antibodies against total eIF2α. Equal protein loading was demonstrated by GAPDH reprobing. The data show the compiled results (mean ± SD) of three independent experiments. (*e*) Kinetics of the activation of caspase-3, -8 and -9 in tumor cells treated with UV-B or HHP for 30 min or 1, 3, 5 or 24 hr. The activation of caspases was determined by Western blot analysis. Equal protein loading was demonstrated by GAPDH reprobing. (*f*) The effect of caspase inhibitors on the kinetics of apoptosis. Cells were treated with specific caspase inhibitors and then treated with UV-B or HHP. The kinetics of apoptosis (at 1, 6, 12 and 24 hr) were determined according to annexin V/DAPI staining using flow cytometry. (*g*) Kinetics of cytoplasmic cytochrome *c* release and the loss of mitochondrial membrane potential after UV-B or HHP treatment for 30 min or 1, 3 or 5 hr. The cytosolic and mitochondrial extracts were prepared and analyzed by Western blot analysis with specific antibodies recognizing cytochrome *c* and GAPDH. The data show the compiled results (mean ± SD) of three independent experiments. The decrease in mitochondrial membrane potential after treatment of ovarian and prostate cancer cells with UV-B or HHP for 1, 7, 12 or 24 hr was evaluated by measuring the fluorescence intensity of TMRE by flow cytometry.

References

1. Green DR, Ferguson T, Zitvogel L, et al. Immunogenic and tolerogenic cell death. *Nat Rev Immunol* 2009;9:353–63.
2. Krysko DV, Vandenabeele P. From regulation of dying cell engulfment to development of anticancer therapy. *Cell Death Differ* 2008;15:29–38.
3. Zitvogel L, Tesniere A, Kroemer G. Cancer despite immunosurveillance: immunoselection and immunosubversion. *Nat Rev Immunol* 2006; 6:715–27.
4. Zitvogel L, Apetoh L, Ghiringhelli F, et al. Immunological aspects of cancer chemotherapy. *Nat Rev Immunol* 2008;8:59–73.
5. Fucikova J, Kralikova P, Fialova A, et al. Human tumor cells killed by anthracyclines induce a tumor-specific immune response. *Cancer Res* 2011;71:4821–33.
6. Tesniere A, Schlemmer F, Boige V, et al. Immunogenic death of colon cancer cells treated with oxaliplatin. *Oncogene* 2010;29:482–91.
7. Spisek R, Charalambous A, Mazumder A, et al. Bortezomib enhances dendritic cell (DC) mediated induction of immunity to human myeloma via exposure of cell surface heat shock protein 90 on dying tumor cells: therapeutic implications. *Blood* 2007;109:4839–45.
8. Galluzzi L, Kepp O, Kroemer G. Enlightening the impact of immunogenic cell death in photodynamic cancer therapy. *EMBO J* 2012;31:1055–7.
9. Spisek R, Dhodapkar MV. Towards a better way to die with chemotherapy: role of heat shock protein exposure on dying tumor cells. *Cell Cycle* 2007;6:1962–5.
10. Kroemer G, Galluzzi L, Kepp O, et al. Immunogenic cell death in cancer therapy. *Annu Rev Immunol* 2013;31:51–72.
11. Lehner T, Wang Y, Whittall T, et al. Functional domains of HSP70 stimulate generation of cytokines and chemokines, maturation of dendritic cells and adjuvanticity. *Biochem Soc Trans* 2004; 32:629–32.
12. Masse D, Ebstein F, Bougras G, et al. Increased expression of inducible HSP70 in apoptotic cells is correlated with their efficacy for antitumor vaccine therapy. *Int J Cancer* 2004;111:575–83.
13. Obeid M, Tesniere A, Ghiringhelli F, et al. Calreticulin exposure dictates the immunogenicity of cancer cell death. *Nat Med* 2007;13: 54–61.
14. Krysko DV, Garg AD, Kaczmarek A, et al. Immunogenic cell death and DAMPs in cancer therapy. *Nat Rev Cancer* 2012;12:860–75.
15. Lanneau D, Brunet M, Frisan E, et al. Heat shock proteins: essential proteins for apoptosis regulation. *J Cell Mol Med* 2008;12:743–61.
16. Hickman-Miller HD, Hildebrand WH. The immune response under stress: the role of HSP-derived peptides. *Trends Immunol* 2004;25:427–33.
17. Panaretakis T, Kepp O, Brockmeier U, et al. Mechanisms of pre-apoptotic calreticulin exposure in immunogenic cell death. *EMBO J* 2009;28: 578–90.
18. Kepp O, Tesniere A, Schlemmer F, et al. Immunogenic cell death modalities and their impact on cancer treatment. *Apoptosis* 2009;14:364–75.
19. Martins I, Kepp O, Galluzzi L, et al. Surface-exposed calreticulin in the interaction between dying cells and phagocytes. *Ann NY Acad Sci* 2010;1209:77–82.
20. Apetoh L, Ghiringhelli F, Tesniere A, et al. Toll-like receptor 4-dependent contribution of the immune system to anticancer chemotherapy and radiotherapy. *Nat Med* 2007;13:1050–9.
21. Park JS, Gamboni-Robertson F, He Q, et al. High mobility group box 1 protein interacts with multiple Toll-like receptors. *Am J Physiol* 2006;290: C917–C924.
22. Joffre O, Nolte MA, Sporri R, et al. Inflammatory signals in dendritic cell activation and the induction of adaptive immunity. *Immunol Rev* 2009; 227:234–47.
23. Aymeric L, Apetoh L, Ghiringhelli F, et al. Tumor cell death and ATP release prime dendritic cells and efficient anticancer immunity. *Cancer Res* 2010;70:855–8.
24. Martins I, Tesniere A, Kepp O, et al. Chemotherapy induces ATP release from tumor cells. *Cell Cycle* 2009;8:3723–8.
25. Garg AD, Krysko DV, Verfaillie T, et al. A novel pathway combining calreticulin exposure and ATP secretion in immunogenic cancer cell death. *EMBO J* 2012;31:1062–79.
26. Rozkova D, Tiserova H, Fucikova J, et al. FOCUS on FOCIS: combined chemo-immunotherapy for the treatment of hormone-refractory metastatic prostate cancer. *Clin Immunol* 2009;131:1–10.
27. Nouri-Shirazi M, Banchereau J, Fay J, et al. Dendritic cell based tumor vaccines. *Immunol Lett* 2000;74:5–10.
28. Boura E, Liebl D, Spisek R, et al. Polyomavirus EGFP-pseudocapsids: analysis of model particles for introduction of proteins and peptides into mammalian cells. *FEBS Lett* 2005;579:6549–58.
29. Mattarollo SR, Loi S, Duret H, et al. Pivotal role of innate and adaptive immunity in anthracycline chemotherapy of established tumors. *Cancer Res* 2011;71:4809–20.
30. Garg AD, Krysko DV, Vandenabeele P, et al. Hypericin-based photodynamic therapy induces surface exposure of damage-associated molecular patterns like HSP70 and calreticulin. *Cancer Immunol Immunother* 2012;61:215–21.
31. Moserova I, Kralova J. Role of ER stress response in photodynamic therapy: ROS generated in different subcellular compartments trigger diverse cell death pathways. *PLoS One* 2012;7:e32972.
32. Garg AD, Krysko DV, Vandenabeele P, et al. The emergence of phox-ER stress induced immunogenic apoptosis. *Oncoimmunology* 2012;1:786–88.
33. Garg AD, Krysko DV, Vandenabeele P, et al. DAMPs and PDT-mediated photo-oxidative stress: exploring the unknown. *Photochem Photobiol Sci* 2011;10:670–80.
34. Garg AD, Nowis D, Golab J, et al. Immunogenic cell death, DAMPs and anticancer therapeutics: an emerging amalgamation. *Biochim Biophys Acta* 2010;1805:53–71.
35. Krysko DV, Vandenabeele P. Clearance of dead cells: mechanisms, immune responses and implication in the development of diseases. *Apoptosis* 2010;15:995–7.
36. Tesniere A, Panaretakis T, Kepp O, et al. Molecular characteristics of immunogenic cancer cell death. *Cell Death Differ* 2008;15:3–12.
37. Yang D, Chen Q, Yang H, et al. High mobility group box-1 protein induces the migration and activation of human dendritic cells and acts as an alarmin. *J Leukoc Biol* 2007;81:59–66.
38. Castano AP, Mroz P, Hamblin MR. Photodynamic therapy and anti-tumour immunity. *Nat Rev Cancer* 2006;6:535–45.
39. Frey B, Janko C, Ebel N, et al. Cells under pressure—treatment of eukaryotic cells with high hydrostatic pressure, from physiologic aspects to pressure induced cell death. *Curr Med Chem* 2008;15:2329–36.
40. Weiss EM, Meister S, Janko C, et al. High hydrostatic pressure treatment generates inactivated mammalian tumor cells with immunogeneic features. *J Immunotoxicol* 2010;7:194–204.
41. Aertsen A, Meersman F, Hendrickx ME, et al. Biotechnology under high pressure: applications and implications. *Trends Biotechnol* 2009;27:434–41.
42. Casares N, Pequignot MO, Tesniere A, et al. Caspase-dependent immunogenicity of doxorubicin-induced tumor cell death. *J Exp Med* 2005;202: 1691–701.
43. Ghiringhelli F, Apetoh L, Housseau F, et al. Links between innate and cognate tumor immunity. *Curr Opin Immunol* 2007;19:224–31.
44. Klein O, Ebert LM, Zanker D, et al. Flt3 ligand expands CD4(+) FoxP3(+) regulatory T cells in human subjects. *Eur J Immunol* 2013;43:533–9.
45. Agostinis P, Buytaert E, Breyssens H, et al. Regulatory pathways in photodynamic therapy induced apoptosis. *Photochem Photobiol Sci* 2004; 3:721–9.
46. Gollnick SO, Vaughan L, Henderson BW. Generation of effective antitumor vaccines using photodynamic therapy. *Cancer Res* 2002;62:1604–8.
47. Fucikova J, Rozkova D, Ulcova H, et al. Poly I: C-activated dendritic cells that were generated in CellGro for use in cancer immunotherapy trials. *J Transl Med* 2011;9:223.
48. Tobiasova Z, Pospisilova D, Miller AM, et al. In vitro assessment of dendritic cells pulsed with apoptotic tumor cells as a vaccine for ovarian cancer patients. *Clin Immunol* 2007;122: 18–27.
49. Vacchelli E, Vitale I, Eggermont A, et al. Trial watch: dendritic cell-based interventions for cancer therapy. *Oncoimmunology* 2013;2:e25771.
50. Fialova A, Partlova S, Sojka L, et al. Dynamics of T-cell infiltration during the course of ovarian cancer: the gradual shift from a Th17 effector cell response to a predominant infiltration by regulatory T-cells. *Int J Cancer* 2013;132:1070–9.

5.2. Kaspáza 2 a oxidativní stres určují imunogenní potenciál buněčné smrti indukované vysokým hydrostatickým tlakem

Dosud publikované studie poukazují na jedinečnou roli CRT v konceptu ICD. Translokace CRT z lumen ER na buněčný povrch předchází morfologickým projevům apoptózy. Rychlé pre-apoptotické vystavení CRT na plazmatickou membránu je spouštěno některými chemoterapeutiky a fyzikálními modalitami (např. hyp-PDT), které indukují produkci ROS a aktivují stres ER. Oba tyto procesy hrají klíčovou roli v translokaci DAMPs na buněčný povrch a jejich blokace vede k narušení imunogenního potenciálu umírajících nádorových buněk.

V této práci jsme se zaměřili na identifikaci signalizačních drah indukovaných HHP, které vedou k vystavení DAMPs na plazmatickou membránu a jejich roli pro vlastní imunogenicitu nádorové buňky. Současně jsme tyto mechanismy chtěli porovnat s již známými signalizačními dráhami aktivovanými imunogenní chemoterapií a hyp-PDT.

Z našich výsledků vyplývá, že nádorové buňky ošetřené HHP jsou imunogenní *in vivo* a stimulují imunitní odpověď založenou na $CD4^+$ a $CD8^+$ T lymfocytech, která v imunizovaných myších vede ke zpomalení růstu nádoru a delšímu přežívání myší. Dále jsme zjistili, že buněčná smrt indukovaná HHP je závislá na nadprodukci ROS iniciující rychlý rozvoj integrovaného buněčného stresu, fosforylaci eIF2α PERK kinázou s následnou aktivací kaspázy 2, 8 a 3. Neschopnost eIF2α se fosforylovat, deplece PERK a kaspázy 2 nebo 8 vede u nádorových buněk ošetřených HHP k signifikantní redukci CRT vystaveného na buněčném povrchu, ale neovlivňuje průběh buněčné smrti. Interakce DCs s nádorovými buňkami s knockdownem kaspázy 2 má za následek sníženou schopnost DCs fagocytovat, což naznačuje, že kaspáza 2 hraje důležitou roli při zprostředkování interakcí umírajících nádorových buněk s APCs. Tato data souhrnně ukazují, že imunogenicita buněčné smrti

indukované HHP je závislá na signalizační dráze zahrnující osu ROS-PERK-eIF2α-kaspáza 2-kaspáza 8.

K této práci jsem přispěla následovně: příprava nádorových linií ošetřených HHP, měření viability a detekce CRT na povrchu nádorových linií ošetřených HHP pomocí průtokové cytometrie, transfekce myší nádorové linie CT26 siRNA, knockdown kaspázy 8 a ověření pomocí western blotu, příprava DCs, kokultivace DCs s OV-90 buňkami ošetřenými HHP a stanovení fagocytózy pomocí průtokové cytometrie a fluorescenční mikroskopie, analýza těchto dat a účast na přípravě manuskriptu.

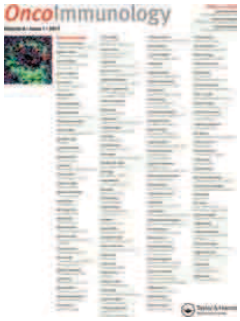

OncoImmunology

ISSN: (Print) 2162-402X (Online) Journal homepage: http://www.tandfonline.com/loi/koni20

Caspase-2 and oxidative stress underlie the immunogenic potential of high hydrostatic pressure-induced cancer cell death

Irena Moserova, Iva Truxova, Abhishek D. Garg, Jakub Tomala, Patrizia Agostinis, Pierre Francois Cartron, Sarka Vosahlikova, Marek Kovar, Radek Spisek & Jitka Fucikova

To cite this article: Irena Moserova, Iva Truxova, Abhishek D. Garg, Jakub Tomala, Patrizia Agostinis, Pierre Francois Cartron, Sarka Vosahlikova, Marek Kovar, Radek Spisek & Jitka Fucikova (2017) Caspase-2 and oxidative stress underlie the immunogenic potential of high hydrostatic pressure-induced cancer cell death, OncoImmunology, 6:1, e1258505, DOI: 10.1080/2162402X.2016.1258505

To link to this article: http://dx.doi.org/10.1080/2162402X.2016.1258505

ONCOIMMUNOLOGY
2017, VOL. 6, NO. 1, e1258505 (12 pages)
http://dx.doi.org/10.1080/2162402X.2016.1258505

Taylor & Francis
Taylor & Francis Group

ORIGINAL RESEARCH

Caspase-2 and oxidative stress underlie the immunogenic potential of high hydrostatic pressure-induced cancer cell death

Irena Moserova[a,b,*], Iva Truxova[a,b,*], Abhishek D. Garg [c], Jakub Tomala [d], Patrizia Agostinis[c], Pierre Francois Cartron[e], Sarka Vosahlikova[a], Marek Kovar [d], Radek Spisek[a,b], and Jitka Fucikova[a,b]

[a]Sotio, Prague, Czech Republic; [b]2nd Medical Faculty and University Hospital Motol, Charles University, Prague, Czech Republic; [c]Cell Death Research and Therapy Unit, Department of Cellular and Molecular Medicine, KU Leuven University of Leuven, Leuven, Belgium; [d]Laboratory of Tumor Immunology, Institute of Microbiology, Academy of Sciences of the Czech Republic, Prague, Czech Republic; [e]Centre de Recherche en Cancérologie Nantes-Angers, INSERM, U892, Nantes, France

ABSTRACT

High hydrostatic pressure (HHP) promotes key characteristics of immunogenic cell death (ICD), in thus far resembling immunogenic chemotherapy and ionizing irradiation. Here, we demonstrate that cancer cells succumbing to HHP induce $CD4^+$ and $CD8^+$ T cell-dependent protective immunity *in vivo*. Moreover, we show that cell death induction by HHP relies on the overproduction of reactive oxygen species (ROS), causing rapid establishment of the integrated stress response, eIF2α phosphorylation by PERK, and sequential caspase-2, −8 and −3 activation. Non-phosphorylatable eIF2α, depletion of PERK, caspase-2 or −8 compromised calreticulin exposure by cancer cells succumbing to HHP but could not inhibit death. Interestingly, the phagocytosis of HHP-treated malignant cells by dendritic cells was suppressed by the knockdown of caspase-2 in the former. Thus, caspase-2 mediates a key function in the interaction between dying cancer cells and antigen presenting cells. Our results indicate that the ROS→PERK→eIF2α→caspase-2 signaling pathway is central for the perception of HHP-driven cell death as immunogenic.

ARTICLE HISTORY
Received 2 September 2016
Revised 2 November 2016
Accepted 2 November 2016

KEYWORDS
Caspases; ecto-CALR; ER stress; high hydrostatic pressure; immunogenic cell death

Introduction

Conventional anticancer treatments including chemotherapy and radiotherapy operate by inducing widespread cancer cell death thereby helping in "debulking" of the tumor. It has been long hypothesized that most anticancer therapies induce poorly immunogenic or even tolerogenic cancer cell death.[1] However, accumulating evidence indicates that in response to certain chemotherapeutics (e.g., anthracyclines, mitoxantrone, oxaliplatin, or bortezomib),[2,3] ionizing irradiation,[4] oncolytic viruses,[5,6] and Hypericin-based photodynamic therapy (Hyp-PDT),[7,8] tumor cells can undergo an immunogenic form of apoptosis called "immunogenic cell death" (ICD) inducing an effective antitumor immune response in immunocompetent mice compared with vaccination of immunodeficient mice.[9,10] These findings demonstrate the important role of the immune system in the efficacy of anticancer therapy.

The ICD is mediated largely by spatiotemporally defined release or exposure of "danger signals" or damage-associated molecular patterns (DAMPs) that can function as either adjuvants or danger signals for the innate immune system[10] leading to the induction of host protective anticancer immunity.[11,12] Several DAMPs have recently been associated with ICD, of which surface exposure (ecto-) of the endoplasmic reticulum (ER)-resident chaperone calreticulin (CALR) constitutes one of the major checkpoints determining the immunogenicity of cell death.[12,13] Ecto-CALR is best characterized for its prominent function as an "eat me" signal for CD91 positive cells (mostly macrophages and dendritic cells) and stimulates antigen-presenting cells, particularly DCs, to efficiently engulf dying cells, process their antigens, and prime a specific immune response.[14]

Ecto-CALR's importance for ICD is outlined by the fact that its blockade (*via* CALR-neutralizing antibodies), depletion of CALR with small interfering RNAs (siRNAs) or depletion/inhibition of danger signaling pathway components mediating ecto-CALR exposure, abolishes the immunogenicity of ICD in multiple tumor models.[4,7,11,13,15] CALR translocates from the ER lumen to the cell surface after treatment with various ICD inducers, before the cell manifests signs of programmed cell death.[16] Rapid, pre-apoptotic ecto-CALR is potently triggered by chemotherapeutics and physicochemical modalities such as Hyp-PDT, which induce the production of reactive oxygen species (ROS) and ER stress response (concomitant or sequential).[17] Of note, both ROS and ER stress "modules" are required for efficient danger signaling and ICD such that the absence of either compromises immunogenicity.[7,15] For instance, scavenging of ROS by antioxidants abolishes ecto-CALR induced by anthracyclines[15] and Hyp-PDT.[18] Similarly, ER stress response also plays an important role in mediating CALR exposure. However depending on the ICD inducer, ecto-CALR mediating signaling components can be subdivided into either "core

CONTACT Jitka Fucikova fucikova@sotio.com SOTIO a.s., Jankovcova 1518/2, Prague 17000, Czech Republic.
Supplemental data for this article can be accessed on the publisher's website.
*These authors contributed equally to this work.

components" (i.e., signaling components shared by all ICD inducers for ecto-CALR exposure) or "private components" (i.e., signaling components specific to certain ICD inducers).[19] Here, in the case of chemotherapy, ER stress response consisting of the ER stress sensor, PERK (protein kinase R (PKR)-like endoplasmic reticulum kinase)-induced phosphorylation of eukaryotic translation initiation factor, eIF2α, both, playing an important role in ecto-CALR exposure.[15] Ecto-CALR exposure in response to chemotherapy requires downstream of ER stress, caspase-8-mediated cleavage of the ER-resident protein, BAP31, and conformational activation of Bax and Bak.[15] However, the Hyp-PDT pathway differs markedly, such that only PERK and Bax/Bak are required for ecto-CALR exposure.[7] Thus, based on these observations, although PERK and Bax/Bak represent the "core signaling components" mediating ecto-CALR for both chemotherapy and Hyp-PDT, eIF2α phosphorylation, caspase-8 and BAP31 represent the "private signaling components" only applicable to chemotherapy-induced ecto-CALR. However, in absence of analysis for other ICD inducers, it is not yet known whether such a subdivision of danger signaling components is consistently applicable to other contexts and whether additional as-yet-undiscovered "private signaling components" mediating ecto-CALR, exist.[10] We previously described a novel physical modality, high hydrostatic pressure (HHP), inducing ICD in a wide spectrum of primary human tumor cells and human cancer cell lines.[20,21] The early danger signaling pathways activated by HHP in cancer cells are completely unknown. Therefore, we decided to investigate the signaling events associated with the ICD induced by HHP treatment and compare them with known pathways triggered by immunogenic chemotherapy or Hyp-PDT.[7,15]

Materials and methods

Mice

Female BALB/c and male C57BL/6 (B6) mice were obtained from the animal facility of the Institute of Physiology (Academy of Sciences of the Czech Republic), v.v.i. Mice were used at 9–15 weeks of age and kept in the conventional animal facility of Institute of Microbiology of ASCR, v.v.i. Mice were regularly screened for MHV and other pathogens according to FELASA. All experiments were approved by the Animal Welfare Committee at the Institute of Microbiology of ASCR, v.v.i.

Treatment of CT26 colon carcinoma and LL2 lung carcinoma in vivo

BALB/c (CT26 carcinoma) or B6 (LL2 carcinoma) mice were s.c. injected into lower left flank with 5×10^6 HHP-treated CT26 or LL2 cells in 200 μL of PBS on days 0 and 21, respectively. Control mice were injected with the same volume of PBS. Mice were then s.c. injected into lower right flank with 10^5 live CT26 cells or LL2 cells in 100 μL of PBS on day 31. 250 μg of depleting anti-CD4$^+$ (clone GK1.5, BioXcell) and/or anti-CD8$^+$ (clone 53-6.72, BioXcell) mAbs were injected i.p. and control mice were injected with the same volume (250 μL) of PBS. Mice surviving day 130 without any signs of tumor were considered as long-term survivors (LTS). Tumor size was measured every 2–4 d by caliper. A total of 10 mice per group were used in the experiments. Every experiment was repeated twice with the similar results.

Cell lines

All cell lines were purchased from American Type Culture Collection (Manassas, VA, USA). Ovarian cancer cell line OV-90 (ATCC) and mouse colon adenocarcinoma CT26 cell lines were cultured in RPMI 1640 (Gibco) supplemented with 10% heat-inactivated FBS (PAA), 2 mM GlutaMAX I CTS (Gibco) and 100 U/mL penicillin + 100 μg/mL streptomycin (Gibco). MEF-wild type (WT) and Bax$^{-/-}$Bak$^{-/-}$, a kind gift of Dr. G. Kroemer (INSERM U848, Institut Gustave Roussy, France). MEF cells expressing normal eIF2α (WT) or a non-phosphorylable mutant heterozygously (S51A knock-in mutation) were kindly provided by Dr. R.L. Rasor, University of Michigan. MEF and LL2 cell lines were cultured in DMEM medium (Sigma Aldrich) supplemented with 10% heat-inactivated FBS (PAA), 2 mM GlutaMAX I CTS (Gibco), and 100 U/mL penicillin + 100 μg/mL streptomycin (Gibco).

Antibodies and reagents

Antibodies against phospho-eIF2α (Ser51), eIF2α, phospho-PERK, PERK, caspase-3, caspase-8, caspase-2, CHOP, Bax, Bak (Cell Signaling Technology, Inc.), and GAPDH (GeneTex) were used. Secondary anti-rabbit and anti-mouse antibodies conjugated to horseradish peroxidase (Jackson ImmunoResearch Laboratories) were also used.

Anti-calreticulin antibodies were purchased from Enzo Life Sciences and Abcam. The chicken polyclonal antibody against calreticulin was purchased from ThermoFisher Scientific. Anti-mouse DyLight 649- and anti-rabbit Alexa Fluor 647-conjugated secondary antibodies were purchased from Jackson ImmunoResearch Laboratories, Molecular Probes, and Cell Signaling, respectively. The chicken IgY isotype control antibody was from GeneTex. Cell death was assessed by Annexin V-PerCP-eFluor 710 (eBioscience) and DAPI (Molecular Probes) staining. For phagocytosis, the dendritic cells and tumor cells were stained with Vybrant® DiO and Vybrant® DiD cell labeling solutions (Molecular Probes), respectively.

CellRox orange reagent (Molecular Probes) was used for the detection of ROS production. N-acetyl-L-cysteine (NAC; 5 mM) and reduced L-glutathione (GSH; 5 mM) from Sigma Aldrich were used as ROS inhibitors. NAC and GSH were prepared at 5 mM concentration in complete media followed by pH adjustment to pH 7.3–7.4. Idarubicin hydrochloride and thapsigargin were from Sigma Aldrich.

Generation of shRNA stable clones of OV-90 cells

For knockdown experiments, cells were stably transfected using Scramble sequences (SHC001V; SHC002V) or shRNA transduction particles expressing siRNA against target genes. Sequences of the shRNAs are provided in Table S1. Transfection was performed according to the manufacturer's instructions (Mission® pLKO.1-puro lentiviral particles, Sigma Aldrich). Cells were seeded at 5×10^3 in 96-well plates, and infected with a

multiplicity of infection of Puromycine (1 μg/mL, Sigma Aldrich) selected infected cells.

siRNA transfection of CT26 cells

A total of 1×10^5 OV-90 or CT26 cells per well were plated in six-well plates and allowed to reach 50% confluence on the day of transfection. siRNA specific for mouse PERK (ON-TARGET plus Mouse Eif2ak3 siRNA SMART pool L-044901-00-0010), human PERK (ON-TARGET plus Human Eif2ak3 siRNA SMART pool L-004883-00-0010), human caspase-2 (ON-TARGET plus Human CASP2 siRNA SMART pool L-003465-00-0010, mouse caspase-8 (ON-TARGET plus Mouse Casp8 siRNA SMART pool L-043044-00-0010) and an unrelated control (ON-TARGET plus Non-targeting pool D-001810-10-05) were purchased from Dharmacon. Cells were transfected with siRNA at a final concentration of 25 nM using Lipofectamine® RNAiMAX Transfection Reagent (Invitrogen) according to the manufacturer's instructions. Knockdown of PERK, caspase-8, and caspase-2 was confirmed by western blotting.

Induction of cell death

Tumor cell death was induced by UV-B (312 nm), idarubicin or HHP. UV-B irradiated and idarubicin treated (37 μM for human OV-90 cells and 18.5 μM for mouse MEF and CT26 cells) tumor cells were used as a negative and positive control, respectively. Cells were treated by value of HHP 250 MPa (OV-90 cells), 175 MPa (CT26 and LL2), and 150 MPa (MEF and CT26 cells) for 10 min in the custom made service (Resato International BV, Netherlands). A total of 1×10^6 UV-B irradiated (7.6 J/cm^2), idarubicin or HHP treated cells per well were plated in 24-well plates, cultured for 1, 2, 6, and 24 h at 37 °C under 5% CO_2, and used for subsequent experiments.

Flow cytometric analysis of apoptosis and cell surface CALR expression

Briefly, 2×10^5 cells per sample were collected and washed in PBS. The cells were then incubated for 30 min with primary anti-CALR antibody diluted in PBS, followed by washing and incubation with DyLight 649- or Alexa Fluor 647-conjugated secondary antibody. For cell death assessment, the cells were washed with PBS and resuspended in an incubation buffer containing Annexin V-PerCP-eFluor 710 (eBioscience). The samples were kept in the dark and incubated for 15 min prior to the addition of DAPI (Molecular Probes) and subsequent analysis on LSRFortessa (BD Biosciences) using FlowJo software (Tree Star). The cell surface expression of CALR was analyzed only on non-permeabilized Annexin$^+$/DAPI$^-$ cells. Annexin$^+$/DAPI$^+$ and Annexin$^-$/DAPI$^+$ cells were excluded from analysis.

Preparation of cell extracts and immunoblotting analysis

Cell extracts were prepared at the indicated time points following UV-B irradiation, idarubicin, or HHP treatment. The cells were washed with ice-cold PBS and lysed on ice in RIPA buffer (10 mM Tris pH 7.5, 150 mM NaCl, 5 mM EDTA, and 1% Triton X-100) with a protease inhibitor cocktail (Roche Diagnostics) and 1 mM PMSF (phenylmethylsulfonyl fluoride) or in sample buffer (300 mM Tris pH 6.8, 5% SDS, 50% Glycerol, 360 mM β-Mercaptoethanol, and 0.05% Bromophenol blue). Proteins were separated by 12% SDS-PAGE and transferred to nitrocellulose membranes (Bio-Rad).

The membranes were blocked in 5% nonfat dry milk in TBST buffer (50 mM Tris, 150 mM NaCl, and 0.05% Tween 20) for 1 h at room temperature and incubated with primary antibody overnight at 4 °C. Then, the membranes were washed in TBST and incubated for 1 h at room temperature with horseradish peroxidase-conjugated secondary antibodies. Detection was performed with the enhanced chemiluminescence (ECL) detection system. Equal protein loading was ensured with a BCA assay, verified by an analysis of Ponceau-S staining of the membrane and GAPDH reprobing.

Generation of immature dendritic cells

Peripheral blood mononuclear cells (PBMCs) were isolated from buffy coats of healthy donors by Ficoll-Paque PLUS gradient centrifugation (GE Healthcare) and CD14$^+$ cells were isolated by EasySep Human CD14 positive selection kit (STEMCELL Technologies). CD14$^+$ cells were subsequently cultured for 5 d in RPMI 1640 (Gibco) supplemented with 10% heat-inactivated FBS (PAA), 2 mM GlutaMAX I CTS (Gibco), and 100 U/mL penicillin + 100 μg/mL streptomycin (Gibco) in the presence of GM-CSF (Gentaur) at a concentration of 500 U/mL and 20 ng/mL of IL-4 (Gentaur).

Uptake of dying tumor cells by dendritic cells

For flow cytometry analysis of phagocytosis, OV-90 cells were harvested and labeled with Vybrant® DiD cell labeling solution (Molecular Probes). A fraction of tumor cells was labeled with Vybrant® DiI cell labeling solution (Molecular Probes) and used for fluorescent microscopy analysis. Stained OV-90 cells were treated by HHP, plated in 24-well plates at a concentration of 1×10^6 cells/mL and cultured for 6 h at 37 °C under 5% CO_2 before use. To prepare UVB-irradiated cells, stained OV-90 cells were seeded in RPMI 1640 (Gibco) supplemented with 10% heat-inactivated FBS (PAA), 2 mM GlutaMAX I CTS (Gibco), and 100 U/mL penicillin + 100 μg/mL streptomycin (Gibco) in 24-well plates at a concentration of 1×10^6 cells/mL and subjected to a 312 nm UV-B-irradiation for 10 min to induce apoptosis. Cells were then incubated for 24 h at 37 °C with 5% CO_2 before use. OV-90 cells treated by idarubicin (37 μM) were also used after 24 h of culture in the presence of chemotherapeutic agent. To determine the uptake of killed tumor cells by dendritic cells, immature dendritic cells were stained with Vybrant® DiO cell labeling solution (Invitrogen) and co-cultured with OV-90 cells at a cell ratio of 5:1 in Nunclon U-bottom 96-well plates (Nunc) for 3 h at 37 °C under 5% CO_2. The cells were extensively washed prior to feeding to dendritic cells. Parallel control cultures were set up on ice to evaluate the passive transfer of dye or labeled tumor fragments to dendritic cells. The phagocytic ability of dendritic cells was evaluated by flow cytometry and fluorescent microscopy.

Immunofluorescence

Phagocytosis detection

A suspension of Vybrant® DiO labeled dendritic cells and Vybrant® DiI labeled UV-B irradiated, idarubicin or HHP treated OV-90 cells was washed in PBS and the cells were fixed with 4% paraformaldehyde (Serva) for 20 min. After washing with PBS, the cells were mounted on slides with ProLong Gold antifade reagent (Molecular Probes) using StatSpin Cytofuge (Iris Sample Processing, Westwood, MA). The slides were analyzed by a fluorescence microscope Leica DMI6000 B.

ROS detection

For the detection of ROS activity, cells were stained with CellRox orange reagent (Molecular Probes) before HHP treatment. After the treatment, cells were washed twice with culture medium and fixed in 4% paraformaldehyde for 5 min and mounted on slides.

Statistical analysis

Results are shown as mean values of at least three independent experiments and standard deviation (± SD) represented by bars. The significance of differences was estimated by Student's unpaired or paired two-tailed t test using GraphPad Prism 6 (GraphPad Software, Inc.). Values $^{*}p < 0.05$, $^{**}p < 0.01$, $^{***}p < 0.001$ represent the level of significance ($p < 0.05$ was considered significant).

Results

HHP-treated cancer cells are immunogenic and induce $CD4^+$ and $CD8^+$ T cell-dependent immunity in mice

To test whether HHP-treated cancer cells are immunogenic *in vivo*, we have exposed CT26 and LL2 cells to 175 MPa and used such treated cells for immunization of BALB/c and B6 mice, respectively. Mice were immunized with two doses of HHP-treated cancer cells 3 weeks apart and immunized mice were challenged with live tumor cells about 10 d after last immunization (Fig. 1A). Both CT26 and LL2 tumor cells treated with HHP elicited protective immunity in experimental mice (Fig. 1B and D) since immunized mice showed slower growth of tumors and shift in the survival curves (Fig. 1C and E). The resistance to the given challenge of tumor cells was recorded only in the CT26 model as 3 out of 10 mice survived more than 150 d without any signs of tumor growth. Further, we decided to investigate if the antitumor immunity induced by HHP-treated cancer cells is T-cell-dependent and address the importance of $CD4^+$ or $CD8^+$ T cells populations in immunization experiments. Antitumor immunity induced by HHP-treated CT26 cancer cells is clearly T-cell-dependent as depletion of both $CD4^+$ and $CD8^+$ T cells almost completely eliminated the immunity elicited by HHP-treated CT26 cells (Fig. 1F and G). Depletion of either $CD4^+$ or $CD8^+$ T cells dampened the antitumor immunity to certain extend; however, $CD8^+$ T cells seems to be more important than $CD4^+$ T cells although both participate in antitumor immunity induced by HHP-treated cancer cells.

ROS generation in response to HHP treatment elicits pro-danger and pro-death signals

ROS production and ER stress have been characterized as major proximal pre-requisites for ecto-CALR induction in anthracyclines and Hyp-PDT-induced immunogenic apoptosis. HHP triggered vast ROS production in human ovarian cancer cell line (OV-90) shortly after the treatment (Fig. 2A and B). Moreover, N-acetyl-L-cysteine (NAC) and reduced L-glutathione (GSH), two well-established ROS scavengers, partly reduced the HHP-induced ROS production (Fig. 2A and B).

HHP-treated cancer cells seemed to undergo rapid cell death (Fig. S1A) which was largely dependent on oxidative stress since suppression of ROS production by NAC/GSH antioxidants significantly reduced cell death in this set-up (Fig. S1A). We then decided to analyze the impact of HHP-mediated ROS on ICD associated danger-signaling events, including the eIF2α phosphorylation and caspase signaling arms, which are known to regulate the surface exposure of the major immunogenic eat-me signal ecto-CALR.[15]

Immunoblotting of OV-90 cell lysates collected immediately after HHP treatment (0 h) showed an early induction of P-eIF2α and of caspase-2 cleavage, followed by caspase-8 and −3 cleavage 2 h post-HHP. Pretreatment of OV-90 cells with the ROS scavengers, and especially with NAC, blunted the fast induction of phosphorylated eIF2α and caspase-2 processing, and later caspase-signaling events as well (Fig. 2C). Moreover, reduction of ROS levels in HHP-treated cells, caused a partial but significant reduction of ecto-CALR (Fig. 2D) (especially 2 h post-treatment). Of note, ecto-CALR was analyzed only on $DAPI^-$ cells (i.e., residual cells that managed to survive the HHP-insult) to exclude intracellular CALR in permeabilized cells ($DAPI^+$) by flow cytometry (Fig. S1B). These findings suggest that HHP-induced ROS production contributes to the early induction of pro-danger signals and the rapid evolution of cell death.

Integrated stress response participates in HHP-induced CALR surface exposure

To further characterize the relevance of the early pro-danger signal activated by HHP treatment, we decided to validate and compare the results obtained in OV-90 cells in the colon carcinoma CT26 cell line. We also compared the ICD signature elicited by HHP to that of the more characterized idarubicin. We initially focused on the role of the apical PERK-P-eIF2α axis, since P-eIF2α pathway was one of the earliest signaling event observed in HHP treated cells and PERK-P-eIF2α is considered an apical danger module during ICD.[15]

Similarly to what found in OV-90 cells, in CT26 cells HHP induced molecular signatures of ER stress and/or integrated stress response (ISR) such as rapid PERK and eIF2α phosphorylation however in absence of CHOP induction (Fig. 3A).

To elucidate the role of PERK phosphorylation evoked by HHP treatment, we performed a set of additional experiments with OV-90 cells with shRNA-based stable knockdown of PERK (OV-90 shPERK—we used clone 1399 in which PERK was near-to-completely depleted (Fig. S1C). These cells had slightly reduced capacity to phosphorylate eIF2α upon UV-B, HHP and idarubicin treatment (1–6 h post-treatment)

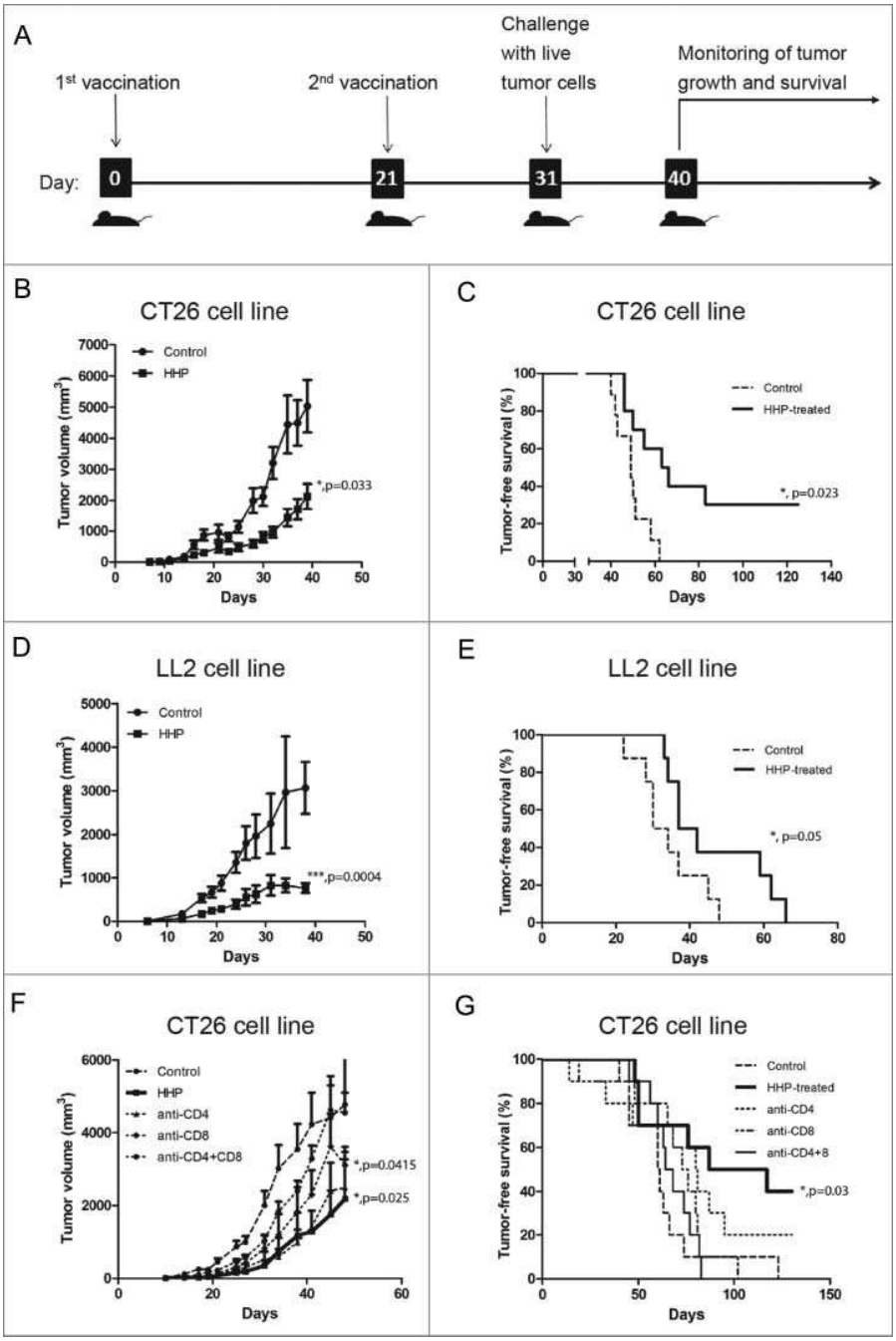

Figure 1. High hydrostatic pressure (HHP)-treated cancer cells elicit T-cell-dependent antitumor immunity. BALB/c mice were s.c. injected into lower left flank with 5×10^6 HHP-treated CT26 cells in 200 μL of PBS on days 0 and 21. Control mice were injected with the same volume of PBS. Mice were than s.c. injected into lower right flank with 10^5 live CT26 cells in 100 μL of PBS on day 31 (A). Growth of the tumors (B) and survival of mice (C) were recorded. The same experiment was performed in LL2 cell line growing in B6 mice (D, E). BALB/c mice s.c. injected with HHP-treated CT26 cells were also i.p. injected with either 250 μg of anti-CD4$^+$ mAb, anti-CD8$^+$ mAb or both in 250 μL of PBS on day 28 (F, G). Significant differences are shown ($^*p \leq 0.05$, $^{***}p < 0.001$).

(Fig. 3B). Moreover, knockdown of PERK reduced the cleavage of pro-caspase-2 (Fig. 3C). On the contrary, we did not observe any effect of caspase-2 knockdown on eIF2α phosphorylation (Fig. 3D). These results were also confirmed in OV-90 in which PERK or caspase-2 was depleted by using siRNAs (Fig. 3E) and suggest that PERK activity could be upstream of pro-caspase-2 cleavage following HHP treatment.

Unlike ROS production, these molecular events (i.e., ER stress/ISR or caspase activation) did not contribute toward HHP-induced cell death *per se* since strategies that ablated PERK or caspases (−2, −3, −8) expression (e.g., via siRNA-mediated knockdown of gene expression or by gene deletion) or the ability of eIF2α to get phosphorylated, did not impede HHP-induced cell death (Figs. S1D–F, S2D–F, and S3A), thereby, establishing these events as bystanders to cell death in the current setting.

It has been previously documented by Panaretakis et al., that following treatment with anthracyclines, ER stress associated events acting as bystanders to cell death (i.e., activation of the PERK-eIF2α arm) mediated ecto-CALR

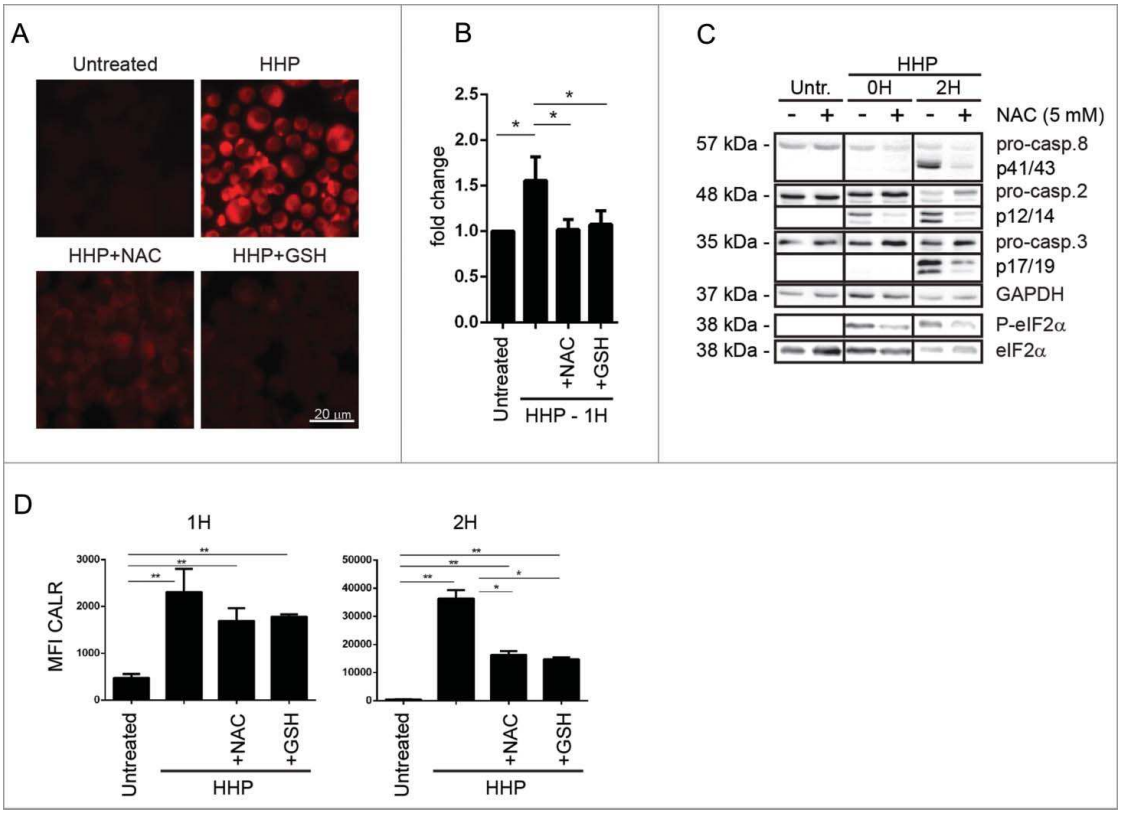

Figure 2. HHP induces the ROS production playing role in CALR surface exposure. Analysis of ROS production using CellRox orange reagent staining in HHP treated OV-90 cells in the presence or absence of N-acetyl-L-cysteine (NAC; 5 mM) and reduced L-glutathione (GSH; 5 mM) 1 h after treatment. Cells were analyzed by immunofluorescence (A) and flow cytometry (B). Scale bar: 20 μm. Data are presented as the mean ± SD for three independent experiments. Significant differences are shown ($^{*}p < 0.05$). (C) Kinetics of the pro-caspase-2, −3, −8 cleavage and eIF2α phosphorylation in OV-90 cells pretreated with ROS scavenger NAC after 0 and 2 h after HHP application was analyzed by western blotting. The activity of eIF2α was determined by a phospho-specific antibody, and then the membranes were reprobed with antibodies against total eIF2α. Equal protein loading was demonstrated by GAPDH reprobing. Experiments were performed in triplicate. (D) CALR surface exposure in HHP treated OV-90 cells pretreated with ROS scavengers (NAC, GSH) using flow cytometry at 1 and 2 h after treatment. Data are presented as the mean ± SD for three independent experiments. Significant differences are shown ($^{*}p \leq 0.05$, $^{**}p < 0.01$).

induction.[15] Therefore, we decided to ascertain the importance of the above events in regulating HHP-induced ecto-CALR. For this, we used three different types of "modified" cancer cells, OV-90 shPERK cells, CT26 in which PERK was depleted by transient transfection with specific siRNA against mouse PERK (CT26 siRNA PERK) and mice embryonic fibroblasts (MEF) cells in which the wild-type (WT) eIF2α was replaced heterozygously with a non-phosphorylatable S51A mutant (MEF eIF2α S51A).

Importantly, PERK knockdown reduced the early ecto-CALR induced by HHP (especially at 1–2 h post-treatment) (Fig. 3F). UV-B irradiation, a non-ICD inducer, did not induce CALR and there was no significant difference between UV-B treated OV-90 control and OV-90 shPERK cells (Fig. 3F). These data were substantiated in CT26 siRNA PERK cells (Fig. 3G).

We also found out that not only ROS and PERK, but also eIF2α plays a role in ecto-CALR exposure, as MEF cells in which WT eIF2α has been replaced by the non-phosphorylable S51A mutant (Fig. S1G) exhibited lower capacity to expose early ecto-CALR in response to HHP (Fig. 3H).

These data together suggest that HHP elicits a high degree of oxidative stress leading to a stress response involving ROS production, PERK and eIF2α phosphorylation which tend to be involved in HHP-induced ecto-CALR.

Caspase-8 contributes to CALR surface exposure induced by HHP

The pathways involved in ER stress-associated molecular mechanisms behind pre-apoptotic ecto-CALR induction are governed by a caspase-module involving an ER-proximal caspase-8 and Bax/Bak activation.[15] In accordance with published results, we next decided to assess the importance of caspase-8 in CALR induced by HHP; for which we conducted a set of experiments on OV-90 cells with caspase-8 knockdown (OV-90 shcaspase-8—we used clone 75 in which caspase-8 was appreciably depleted by using shRNA; Fig. S2A) and on CT26 cells transiently transfected with specific siRNA against mouse caspase-8 (CT26 siRNA caspase-8; Fig. S2B). We observed pro-caspase-8 cleavage 2 h after HHP treatment (Fig. 4A). OV-90 shcaspase-8 expressing cells, upon HHP treatment, exhibited reduced capacity to cleave pro-caspase-3 (at 1, 2, and 6 h, post-treatment) but we observed only slight reduction in cleavage of pro-caspase-2 1 h after HHP treatment (Fig. 4A).

Of note, caspase-8 knockdown led to a small but significant reduction in ecto-CALR after HHP treatment (Fig. 4B) and similar results were obtained for CT26 siRNA caspase-8 (Fig. 4C). On the other hand we did not observe any reduction in ecto-CALR in either of these cells upon idarubicin treatment (Fig. S2E and F).

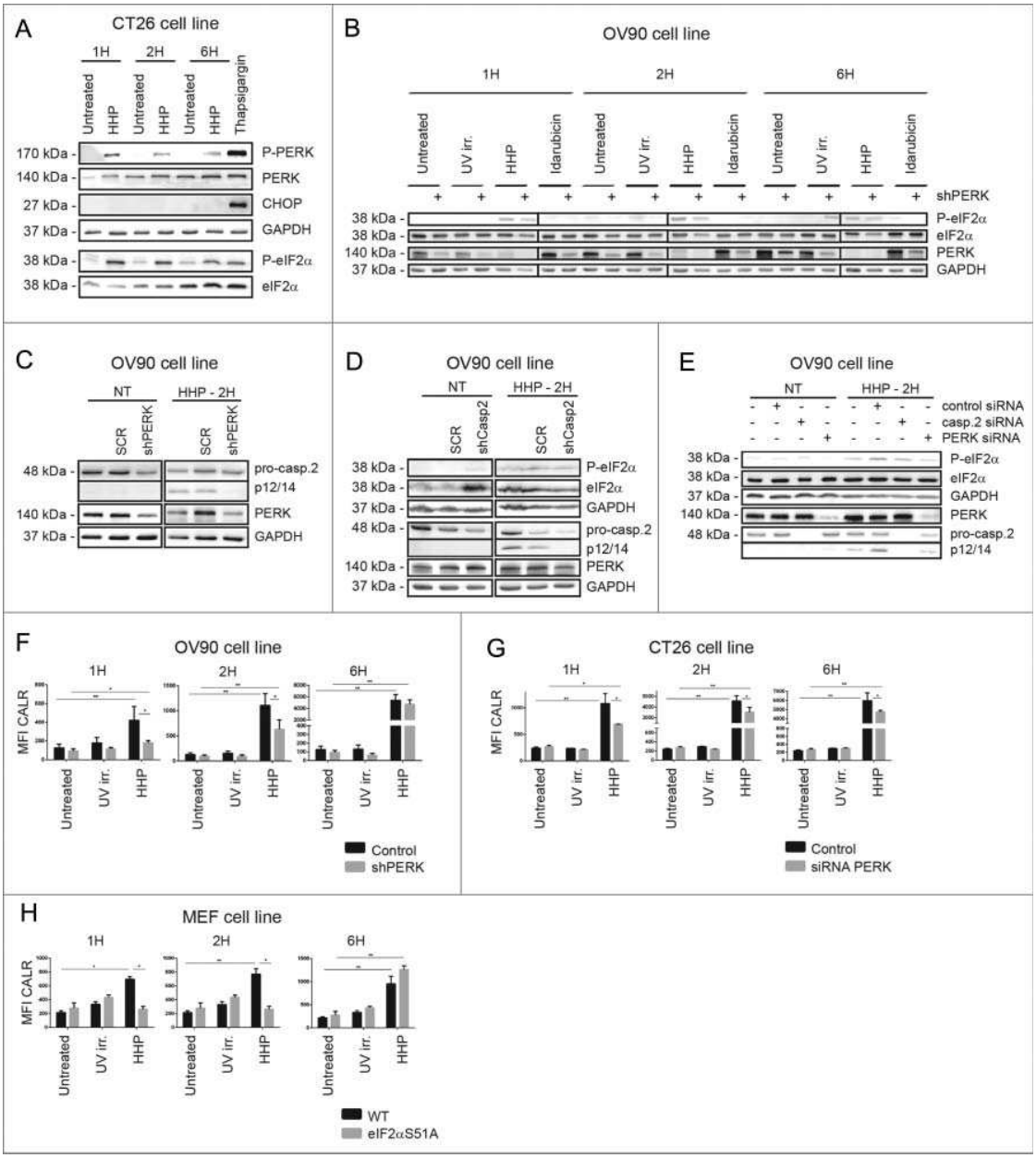

Figure 3. HHP induces ER stress (PERK and eIF2α phosphorylation) involved in CALR surface exposure. (A) Kinetics of the PERK and eIF2α phosphorylation and CHOP activation in CT26 cells 1, 2, and 6 h after HHP treatment. Thapsigargin was used as a positive control. Equal protein loading was demonstrated by GAPDH reprobing. (B) Western blot analysis of eIF2α phosphorylation kinetics in OV-90 control and OV-90 shPERK cells 1, 2, and 6 h after UV-B, HHP, and idarubicin treatment. The activity of eIF2α was determined by a phospho-specific antibody, and then the membranes were reprobed with antibody against total eIF2α. Equal protein loading was demonstrated by using GAPDH as a loading control. Experiments were performed in triplicate. (C) Western blot analysis of pro-caspase-2 cleavage in non-transfected OV-90 cells, SCR, and shPERK cells. PERK knockdown was verified by western blotting. Equal protein loading was demonstrated by using GAPDH as loading control. (D) Western blot analysis of eIF2α phosphorylation and pro-caspase-2 cleavage in non-transfected OV-90 cells, SCR and shcaspase-2 cells 2 h after HHP treatment. Caspase-2 knockdown was verified by western blotting. Equal protein loading was demonstrated by using GAPDH as loading control. (E) OV-90 cells were transfected with siRNA against caspase-2 and PERK. Knockout was verified by western blotting. The activity of eIF2α was determined by a phospho-specific antibody and the membranes were reprobed with antibody against total eIF2α. Equal protein loading was demonstrated by using GAPDH as a loading control. (F) CALR surface exposure was measured in untreated, UV-B and HHP treated OV-90 shPERK and OV-90 control cells after 1, 2, and 6 h by flow cytometry. The data show the compiled results (mean $\pm$ SD) of three independent experiments. Significant differences are shown ($^{*}p < 0.05$, $^{**}p < 0.01$). (G) Detection of surface CALR exposure in untreated, UV-B irradiated and HHP treated CT26 control and CT26 siRNA PERK cells at 1, 2, and 6 h post-treatment using flow cytometry. The data show the compiled results (mean $\pm$ SD) of three independent experiments. Significant differences are shown ($^{*}p < 0.05$, $^{**}p < 0.01$). (H) CALR surface exposure in untreated, UV-B irradiated and HHP treated MEF WT and eIF2α S51A cells at 1, 2, and 6 h after treatment was measured by flow cytometry. Data are presented as the mean $\pm$ SD for three independent experiments. Significant differences are shown ($^{*}p < 0.05$, $^{**}p < 0.01$).

Next, we also decided to ascertain the role of Bax and Bak in ecto-CALR exposure induced by HHP; since downstream of caspase-8, Bax/Bak have been found to be crucial for anthracycline-induced ecto-CALR.[15,16] For addressing this, we used MEF cells with Bax and Bak double knockout phenotype (MEF $Bax^{-/-}/Bak^{-/-}$; Fig. S3B). We found that Bax/Bak deficiency did not affect CALR exposure induced by HHP (Fig. 4D). Similarly, knockdown of caspase-3, an executioner caspase, did not block the translocation of CALR to the cell surface of HHP-treated tumor cells (Fig. S2C).

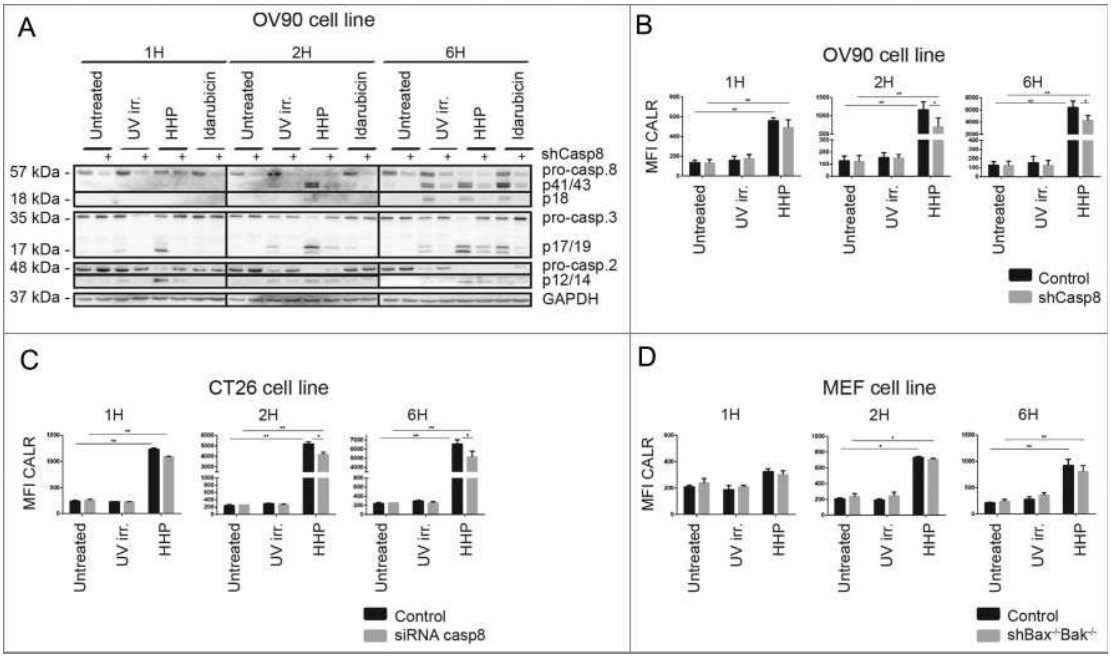

Figure 4. Caspase-8 knockdown reduces CALR exposure induced by HHP. (A) The kinetics of pro-caspase-8, pro-caspase-3 and pro-caspase-2 cleavage in OV-90 control and OV-90 shcaspase-8 cells 1, 2, and 6 h after UV-B, HHP, or idarubicin treatment was analyzed by western blotting. Caspase-8 knockdown was verified by western blotting and equal protein loading was demonstrated by using GAPDH as a loading control. Experiments were performed in triplicate. (B) CALR surface exposure was measured in OV-90 control and OV-90 shcaspase-8 cells 1, 2, and 6 h after UV-B or HHP treatment by flow cytometry. Data are presented as the mean ± SD for three independent experiments. Significant differences are shown ($^{*}p < 0.05$, $^{**}p < 0.01$). (c) CALR surface exposure in UV-B or HHP treated CT26 control and CT26 siRNA caspase-8 cells at 1, 2, and 6 h post-treatment was analyzed by flow cytometry. The data show the compiled results (mean ± SD) of three independent experiments. Significant differences are shown ($^{*}p < 0.05$, $^{**}p < 0.01$). (d) CALR surface detection in UV-B or HHP treated MEF $Bax^{-/-}/Bak^{-/-}$ cells at 1, 2, and 6 h post-treatment using flow cytometry. Relevant control cells (MEF WT) were included in the experiments. Data are presented as the mean ± SD for three independent experiments. Significant differences are shown ($^{*}p < 0.05$, $^{**}p < 0.01$).

In contrast, cells lacking Bax/Bak showed compromised ability to expose CALR on the surface in response to idarubicin 24 h post-treatment (Fig. S3B). In the case of UV-B irradiation, we did not observe differences in CALR expression between relevant controls and MEF $Bax^{-/-}/Bak^{-/-}$ cells (Fig. 4D).

In conclusion, HHP causes pro-caspase-8 cleavage which to a small extent participates in ecto-CALR induction following HHP treatment. On the other hand, surprisingly, Bax and Bak were found to be dispensable for HHP-induced CALR trafficking.

Caspase-2 is involved in CALR surface exposure in HHP treated cancer cells

Recent studies have shown that cellular stress responses can induce caspase-2 activation.[22–24] For this reason, we also investigated a potential role of this caspase in HHP-induced ecto-CALR.

To confirm a role of caspase-2, a stable OV-90 clone expressing a caspase-2 small hairpin (shRNA) in which caspase-2 was significantly depleted (clone 06 in Fig. S3A) was prepared. We observed cleavage of pro-caspase-2 in OV-90 cells 1 h after HHP treatment (Fig. 5A). Our data suggest that caspase-2 processing could be an upstream event that precedes caspase-8 processing.

Caspase-2 was also activated in OV-90 cells upon idarubicin and UV-B treatment. Furthermore, OV-90 shcaspase-2 expressing cells had reduced capacity to cleave caspase-3 (6 h) upon idarubicin treatment and these cells exhibited decreased cleavage of pro-caspase-8 (at 2 and 6 h) after UV-B irradiation (Fig. 5A).

Next, we analyzed the role of caspase-2 in ecto-CALR exposure induced by HHP. The involvement of caspase-2 in this process was demonstrated by relatively lower capacity of OV-90 shcaspase-2 cells to expose CALR in response to HHP treatment (Fig. 5B). On the contrary, caspase-2 knockdown had no effect on CALR induced by idarubicin (Fig. S3A). The kinetics of cell death of OV-90 shcaspase-2 cells was similar to control cells upon HHP, idarubicin and also UV-B treatment (Fig. S3A).

Taken together, our results indicate that caspase-2 plays a role in HHP-mediated ecto-CALR exposure.

CALR on HHP treated cells is important for phagocytosis by dendritic cells

Considering the established role of ecto-CALR as an "eat me" signal,[25] we further investigated the possible effect of ecto-CALR on phagocytosis of HHP treated tumor cells by dendritic cells, an important antigen-presenting cells of the innate immune system.[26] For this purpose, we used specific antibody to block CALR[16] and we also investigated the interaction of dendritic cells with OV-90 shPERK, shcaspase-8 and shcaspase-2 expressing cells which had lower capacity to expose CALR (depending upon the signaling molecule, i.e., caspases-2 shRNA > PERK shRNA > caspases-8 shRNA) after HHP treatment (Figs. 3F, 4B, and 5B). In general, HHP treated cancer cells were phagocytosed faster and to a greater extent than tumor cells killed by UV-B or by idarubicin. After 3 h, the rate of phagocytosis of HHP treated cancer cells was 2.5-fold higher

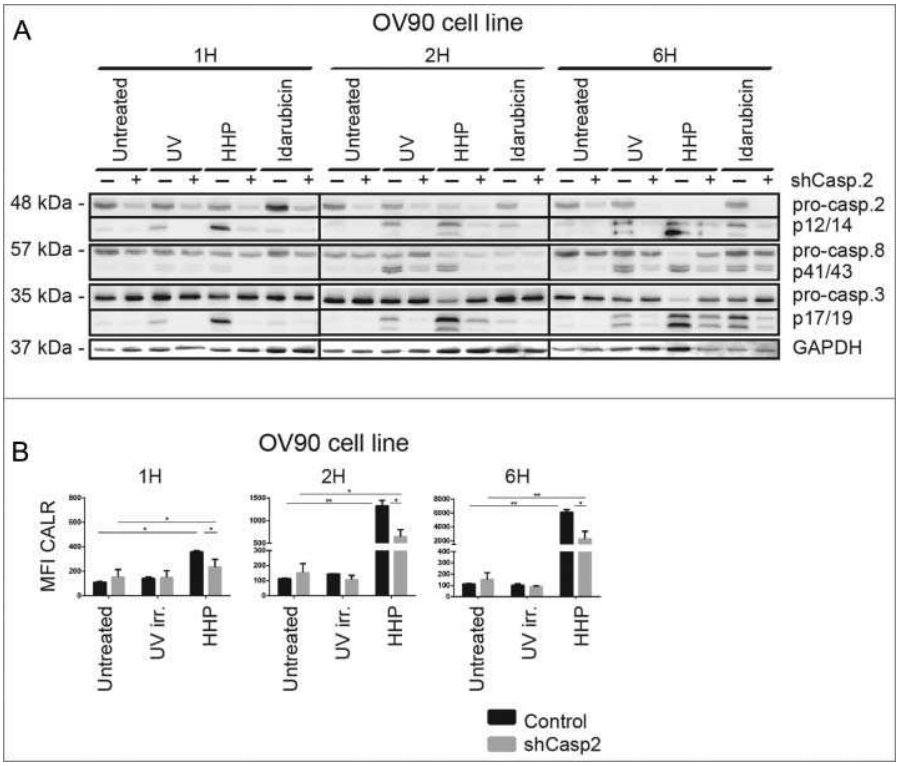

Figure 5. Caspase-2 is involved in the CALR cell surface exposure induced by HHP. (A) The kinetics of pro-caspase-8, pro-caspase-3, and pro-caspase-2 cleavage upon UV-B, HHP, or idarubicin treatment in OV-90 control and OV-90 shcaspase-2 cells at the indicated time points (1, 2, and 6 h). Caspase-2 knockdown was verified by western blotting and equal protein loading was demonstrated by using GAPDH as a loading control. Experiments were performed in triplicate. (B) CALR surface exposure was measured in OV-90 control and OV-90 shcaspase-2 cells 1, 2, and 6 h after UV-B or HHP treatment by flow cytometry. Data are presented as the mean ± SD for three independent experiments. Significant differences are shown ($^{*}p < 0.05$, $^{**}p < 0.01$).

compared with UV-B irradiated cells and 1.8-fold higher in comparison to cells killed by idarubicin (Figs. 6A and B and S4A). The analysis of the interaction of dendritic cells with HHP treated OV-90 shPERK, shcaspase-8 and shcaspase-2 cells revealed strong linear correlation between phagocytosis of HHP treated tumor cells and their CALR levels 6 h after HHP treatment (Fig. 6C). Among the modified OV-90 cells chosen for this experiment, HHP treated OV-90 shcaspase-2 expressing cells were phagocytosed to a significantly lower extent compared with OV-90 control cells (Fig. 6A and B). These results correlated with the finding that, OV-90 shcaspase-2 expressing cells had the most prominent decrease in CALR expression compared with OV-90 control cells (2.7-fold lower MFI values of CALR) relative to shPERK or shcaspase-8 cells (Fig. 5B). Thus, although the depletion of caspase-2 affects ecto-CALR exposure in both a statistically significant and biologically relevant manner (as it limits uptake by DCs), the reduction of CALR caused by PERK or caspase-8 knockdown is not biologically relevant.

When the engulfment of idarubicin treated cells was investigated, we detected significantly lower rate of phagocytosis in the case of OV-90 shPERK expressing cells (Fig. 6A and B). This result is in the line with the fact that these cells treated by idarubicin for 24 h had the greatest reduction of ecto-CALR compared with OV-90 control cells (2.7-fold lower MFI values of CALR) (data not shown). Moreover, blockade of the CALR on HHP and also idarubicin treated tumor cells by a specific antibody inhibited their phagocytosis by dendritic cells (Fig. 6A and B).

Therefore, CALR is required not only for phagocytosis of idarubicin killed tumor cells but also for phagocytosis of HHP treated cells by dendritic cells and for HHP, this process is strongly compromised in absence of caspase-2.

Discussion

HHP was identified as an inducer of anticancer immunity in a wide range of human tumor cell lines and primary tumor cells in our previous study. This physical modality was, due to its immunogenic properties, standardized and validated for incorporation into manufacturing protocols for cancer immunotherapy products.[20] We have initiated multiple clinical trials for prostate, ovarian and lung cancer evaluating the potential of DCs loaded with HHP treated cancer cells to induce tumor cell-specific immune responses.[20,27] Nevertheless, HHP-treated cancer cells were utilized so far solely for pulsing of *ex vivo* cultured DCs but their direct use to induce antitumor immunity has not been validated. Here, we show in two different mouse tumor models that HHP-treated tumor cells evoke protective immune memory response when s.c. injected *per se*, i.e., without any adjuvant. Since we proved that immunization with HHP-treated tumor cells induce $CD4^{+}$ and $CD8^{+}$ T cell-dependent immune memory, it is most likely that HHP-treated tumor cells are immunogenic *in vivo* because they are effectively taken up and processed by DCs. Furthermore, we have shown that HHP-treated cancer cells also induce maturation of DCs due to the release of "danger" signaling molecules like HMGB1 or ATP as shown in *in vitro* studies.[20]

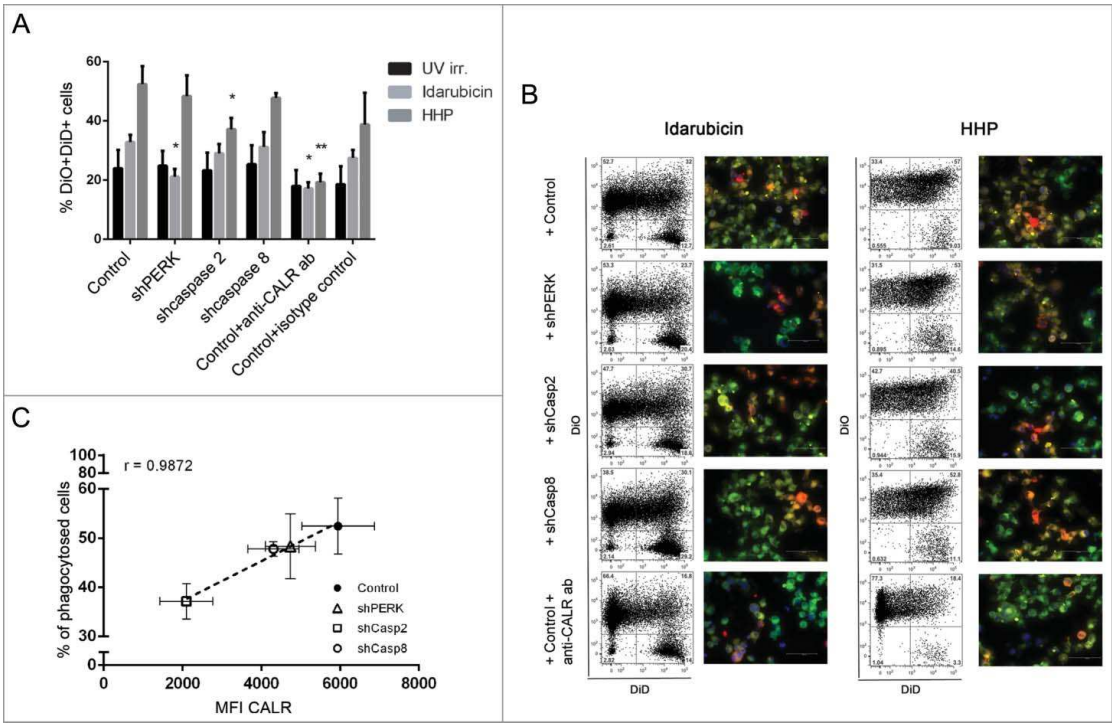

Figure 6. CALR surface expression is important for phagocytosis of HHP treated tumor cells by population of dendritic cells. (A) Flow cytometry analysis of phagocytosis. DiO-labeled immature dendritic cells were co-cultured with DiD-labeled OV-90 control, shPERK, shcaspase-2, or shcaspase-8 cells treated with UV-B and idarubicin for 24 h and with HHP for 6 h at 37 °C for 3 h. A fraction of DiO-labeled dendritic cells was loaded with DiD-labeled OV-90 control cells which were pre-incubated with blocking anti-CALR antibody or relevant isotype control antibody. As a control, dendritic cells and tumor cells were co-cultured on ice for 3 h (Fig. S4B). Dendritic cells that phagocytosed killed tumor cells were identified as $DiO^{+}DiD^{+}$ double-positive cells. Data are presented as the mean ± SD for three independent experiments. Significant differences are shown ($^{*}p < 0.05$, $^{**}p < 0.01$). (B) Representative dot plots of flow cytometry and fluorescence microscopy analysis of the phagocytosis. DiO-labeled immature dendritic cells were co-cultured for 3 h with DiI-labeled HHP and idarubicin treated tumor cells and the engulfment of tumor cells was verified by fluorescence microscopy. (C) Correlation between phagocytosis of HHP treated tumor cells and their CALR levels. The percentage of dendritic cells taking up HHP killed tumor cells was determined and correlated with CALR levels on tumor cells 6 h after HHP treatment.

Considering the importance of ecto-CALR for tumor cells phagocytosis,[25] induction of tumor specific immune response in vaccinated patients[28] and patient prognosis,[13] we aimed to unravel a sequence of key events that are required (but not necessarily sufficient) to transform cellular stress into immunogenic signaling (similar to previously described anthracyclines and Hyp-PDT[7]). Therefore it was not the main aim of the study to characterize in details the cell death mechanisms triggered by HHP but mostly to identify the key components responsible for ecto-CALR exposure. The ecto-CALR inducing capacity of ICD inducers has been shown to depend on the properties of ER stress and ROS production.[16,29,30] We observed that HHP treatment results in ROS production, a proximal event triggering other downstream signaling pathways, such as ISR and cleavage of caspase-2, caspase-8, and caspase-3. The application of various ROS scavengers suggested that for HHP-induced CALR, ROS production is one of the pre-requisites, an observation that is in line with previous studies concerning Hyp-PDT, mitoxantrone, oxaliplatin, UV-C or oncolytic coxsackievirus B3.[7,15,31] However, the suppression of ROS production was not sufficient to completely abolish HHP-induced CALR exposure suggesting that ROS-independent mechanisms may also participate in this process.

The danger signaling pathways causing the translocation of CALR to the cell surface in response to various chemotherapeutic treatments or Hyp-PDT overlap, but are not identical.[7,15] We showed that HHP-induced pathway leading to ecto-CALR exposure also overlaps with those induced by chemotherapy or Hyp-PDT but is not entirely identical to either. More specifically, HHP-mediated ROS production, possibly impinging on ER homeostasis, further triggers early PERK activation, eIF2α phosphorylation, and caspase-2 cleavage (but not Bax/Bak), which are important for HHP-induced danger signaling involving CALR induction.

Recent studies have shown that ROS production as well as ER stress may[22–24,32] or may not[33] induce caspase-2 cleavage, depending on the context. In our context, we found that caspase-2 cleavage following HHP is downstream of ROS-based ISR. Our study also shows that compromising PERK expression mitigates processing of caspase-2—an interesting observation requiring further mechanistic studies. Moreover, in the current study, we report for the first time, a role of caspase-2 in CALR trafficking during ICD. While it is not yet clear how caspase-2 might be regulating CALR exposure, the localization of this caspase in the ER/Golgi system suggests possibility of participation in regulating trafficking mechanisms—a hypothesis that needs verification in near future.[34]

It was shown that caspase-8 activation is not required for the CALR induction by Hyp-PDT, although it is necessary for mitoxantrone/oxaliplatin-induced CALR.[7,15] In our study HHP-induced CALR was found to be at least partially mediated by caspase-8. Unfortunately, we did not observe any reduction of CALR in either of these cells upon idarubicin treatment,

which might be due to differences in mode of action between idarubicin and mitoxantrone which was used in previous studies,[16] showing the context-dependent importance of caspase-8 for proper CALR exposure even for different anthracyclines.[7,15] Moreover, Bax/Bak were previously classified as "core molecular entities" participating in ICD-associated danger signaling because of their role in both Hyp-PDT and chemotherapy-induced CALR. However, in contrast to these results, we observed that Bax/Bak deficiency does not affect CALR trafficking induced by HHP. Thus, our results taken together with previous publications[7,15] clearly show that across HHP, Hyp-PDT and immunogenic chemotherapy, PERK is apparently an important molecular entity involved in danger signaling pathways in an ICD-inducer independent fashion while all the other molecules tend to show an ICD-inducer dependent involvement in CALR induction.

CALR and another "eat me" signals like translocation of phosphatidylserine from inside the cell to the surface, together with the downregulation of "don't eat me" signals such as CD47, elicit the recognition and removal of dying cells by phagocytes, most importantly by professional phagocytes such as dendritic cells.[25,35] We have previously shown that the interaction of immature dendritic cells with HHP killed tumor cells led to the increased uptake of tumor cells by dendritic cells and induced the expression of maturation-associated markers on dendritic cells and the production of IL-12p70 and proinflammatory cytokines, demonstrating that HHP-treated tumor cells provide a potent activation stimulus to dendritic cells.[20] Faster phagocytosis was similarly observed in this study and correlated with the rapid induction of CALR after HHP treatment. Moreover, the blockade of CALR by specific antibody or depletion of caspase-2, an important player in CALR surface exposure, significantly inhibited their engulfment by dendritic cells.

In conclusion, we characterized the molecular mechanism of ecto-CALR exposure pathway induced by HHP which is more analogous to that induced by anthracycline treatment rather than that induced by Hyp-PDT. Moreover, we characterized a novel role of PERK-caspase-2 axis in mediating CALR induction. Altogether, our findings reveal that the PERK–eIF2α phosphorylation–caspase-2 axis plays an important role in the HHP-mediated CALR exposure. This kind of information might help to prepare more efficient cancer vaccine in which the relative expression levels of proteins required for full inactivation of tumor cells and stress-elicited immunogenic signaling can be used with respect to their prognostic and predictive impact in cancer patient's treatment.

Disclosure of potential conflicts of interest

No potential conflicts of interest were disclosed.

Funding

This project was supported by the research grant IGA NT12402-5, student research grant GAUK 682214, the Ministry of Education, Youth and Sports of CR within the LQ1604 National Sustainability Program II (Project BIOCEV-FAR) and by the project "BIOCEV" (CZ.1.05/1.1.00/02.0109).

ORCID

Abhishek D. Garg http://orcid.org/0000-0002-9976-9922
Jakub Tomala http://orcid.org/0000-0002-6315-2832
Marek Kovar http://orcid.org/0000-0002-6602-1678

References

1. Galluzzi L, Vacchelli E, Bravo-San Pedro JM, Buque A, Senovilla L, Baracco EE, Bloy N, Castoldi F, Abastado JP, Agostinis P et al. Classification of current anticancer immunotherapies. Oncotarget 2014; 5 (24):12472-508; PMID:25537519; http://dx.doi.org/10.18632/oncotarget.2998
2. Fucikova J, Kralikova P, Fialova A, Brtnicky T, Rob L, Bartunkova J, Spísek R. Human tumor cells killed by anthracyclines induce a tumor-specific immune response. Cancer Res 2011; 71(14):4821-33; PMID:21602432; http://dx.doi.org/10.1158/0008-5472.CAN-11-0950
3. Tesniere A, Schlemmer F, Boige V, Kepp O, Martins I, Ghiringhelli F, Aymeric L, Michaud M, Apetoh L, Barault L et al. Immunogenic death of colon cancer cells treated with oxaliplatin. Oncogene 2010; 29 (4):482-91; PMID:19881547; http://dx.doi.org/10.1038/onc.2009.356
4. Obeid M, Panaretakis T, Joza N, Tufi R, Tesniere A, van Endert P, Zitvogel L, Kroemer G. Calreticulin exposure is required for the immunogenicity of gamma-irradiation and UVC light-induced apoptosis. Cell Death Differ 2007; 14(10):1848-50; PMID:17657249; http://dx.doi.org/10.1038/sj.cdd.4402201
5. Koks C, Garg AD, Ehrhardt M, Riva M, Vandenberk L, Boon L, De Vleeschouwer S, Agostinis P, Graf N, Van Gool SW. Newcastle disease virotherapy induces long-term survival and tumor-specific immune memory in orthotopic glioma through the induction of immunogenic cell death. Int J Cancer 2014; 136(5):E313-25; PMID:25208916; http://dx.doi.org/10.1002/ijc.29202
6. Vacchelli E, Eggermont A, Sautes-Fridman C, Galon J, Zitvogel L, Kroemer G, Galluzzi L. Trial watch: oncolytic viruses for cancer therapy. Oncoimmunology 2013; 2(6):e24612; PMID:23894720; http://dx.doi.org/10.4161/onci.24612
7. Garg AD, Krysko DV, Verfaillie T, Kaczmarek A, Ferreira GB, Marysael T, Rubio N, Firczuk M, Mathieu C, Roebroek AJ et al. A novel pathway combining calreticulin exposure and ATP secretion in immunogenic cancer cell death. EMBO J 2012; 31(5):1062-79; PMID:22252128; http://dx.doi.org/10.1038/emboj.2011.497
8. Garg AD, Vandenberk L, Koks C, Verschuere T, Boon L, Van Gool SW, Agostinis P. Dendritic cell vaccines based on immunogenic cell death elicit danger signals and T cell-driven rejection of high-grade glioma. Sci Transl Med 2016; 8(328):328ra327; PMID:26936504; http://dx.doi.org/10.1126/scitranslmed.aae0105
9. Kepp O, Senovilla L, Vitale I, Vacchelli E, Adjemian S, Agostinis P, Apetoh L, Aranda F, Barnaba V, Bloy N et al. Consensus guidelines for the detection of immunogenic cell death. Oncoimmunology 2014; 3(9):e955691; PMID:25941621; http://dx.doi.org/10.4161/21624011.2014.955691
10. Garg AD, Galluzzi L, Apetoh L, Baert T, Birge RB, Bravo-San Pedro JM, Breckpot K, Brough D, Chaurio R, Cirone M et al. Molecular and translational classifications of DAMPs in immunogenic cell death. Front Immunol 2015; 6: 588; PMID:26635802; http://dx.doi.org/10.3389/fimmu.2015.00588
11. Cao C, Han Y, Ren Y, Wang Y. Mitoxantrone-mediated apoptotic B16-F1 cells induce specific anti-tumor immune response. Cell Mol Immunol 2009; 6(6):469-75; PMID:20003823; http://dx.doi.org/10.1038/cmi.2009.59
12. Spisek R, Charalambous A, Mazumder A, Vesole DH, Jagannath S, Dhodapkar MV. Bortezomib enhances dendritic cell (DC)-mediated induction of immunity to human myeloma via exposure of cell surface heat shock protein 90 on dying tumor cells: therapeutic implications. Blood 2007; 109(11):4839-45; PMID:17299090; http://dx.doi.org/10.1182/blood-2006-10-054221
13. Garg AD, Elsen S, Krysko DV, Vandenabeele P, de Witte P, Agostinis P. Resistance to anticancer vaccination effect is controlled by a cancer cell-autonomous phenotype that disrupts immunogenic phagocytic

removal. Oncotarget 2015; 6(29):26841-60; PMID:26314964; http://dx.doi.org/10.18632/oncotarget.4754
14. Martins I, Kepp O, Galluzzi L, Senovilla L, Schlemmer F, Adjemian S, Menger L, Michaud M, Zitvogel L, Kroemer G. Surface-exposed calreticulin in the interaction between dying cells and phagocytes. Ann NY Acad Sci 2010; 1209: 77-82; PMID:20958319; http://dx.doi.org/10.1111/j.1749-6632.2010.05740.x
15. Panaretakis T, Kepp O, Brockmeier U, Tesniere A, Bjorklund AC, Chapman DC, Durchschlag M, Joza N, Pierron G, van Endert P et al. Mechanisms of pre-apoptotic calreticulin exposure in immunogenic cell death. EMBO J 2009; 28(5):578-90; PMID:19165151; http://dx.doi.org/10.1038/emboj.2009.1
16. Obeid M, Tesniere A, Ghiringhelli F, Fimia GM, Apetoh L, Perfettini JL, Castedo M, Mignot G, Panaretakis T, Casares N et al. Calreticulin exposure dictates the immunogenicity of cancer cell death. Nat Med 2007; 13(1):54-61; PMID:17187072; http://dx.doi.org/10.1038/nm1523
17. van Vliet AR, Martin S, Garg AD, Agostinis P. The PERKs of damage-associated molecular patterns mediating cancer immunogenicity: from sensor to the plasma membrane and beyond. Semin Cancer Biol 2015; 33: 74-85; PMID:25882379; http://dx.doi.org/10.1016/j.semcancer.2015.03.010
18. Garg AD, Dudek AM, Ferreira GB, Verfaillie T, Vandenabeele P, Krysko DV, Mathieu C, Agostinis P. ROS-induced autophagy in cancer cells assists in evasion from determinants of immunogenic cell death. Autophagy 2013; 9(9):1292-307; PMID:23800749; http://dx.doi.org/10.4161/auto.25399
19. Galluzzi L, Kepp O, Kroemer G. Enlightening the impact of immunogenic cell death in photodynamic cancer therapy. EMBO J 2012; 31(5):1055-7; PMID:22252132; http://dx.doi.org/10.1038/emboj.2012.2
20. Fucikova J, Moserova I, Truxova I, Hermanova I, Vancurova I, Partlova S, Fialova A, Sojka L, Cartron PF, Houska M et al. High hydrostatic pressure induces immunogenic cell death in human tumor cells. Int J Cancer 2014; 135(5):1165-77; PMID:24500981; http://dx.doi.org/10.1002/ijc.28766
21. Adkins I, Fucikova J, Garg AD, Agostinis P, Spisek R. Physical modalities inducing immunogenic tumor cell death for cancer immunotherapy. Oncoimmunology 2014; 3(12):e968434; PMID:25964865; http://dx.doi.org/10.4161/21624011.2014.968434
22. Mishra R, Karande AA. Endoplasmic reticulum stress-mediated activation of p38 MAPK, caspase-2 and caspase-8 leads to abrin-induced apoptosis. PLoS One 2014; 9(3):e92586; PMID:24664279; http://dx.doi.org/10.1371/journal.pone.0092586
23. Uchibayashi R, Tsuruma K, Inokuchi Y, Shimazawa M, Hara H. Involvement of Bid and caspase-2 in endoplasmic reticulum stress- and oxidative stress-induced retinal ganglion cell death. J Neurosci Res 2011; 89(11):1783-94; PMID:21805492; http://dx.doi.org/10.1002/jnr.22691
24. Upton JP, Austgen K, Nishino M, Coakley KM, Hagen A, Han D, Papa FR, Oakes SA. Caspase-2 cleavage of BID is a critical apoptotic signal downstream of endoplasmic reticulum stress. Mol Cellular Biol 2008; 28(12):3943-51; PMID:18426910; http://dx.doi.org/10.1128/MCB.00013-08
25. Gardai SJ, McPhillips KA, Frasch SC, Janssen WJ, Starefeldt A, Murphy-Ullrich JE, Bratton DL, Oldenborg PA, Michalak M, Henson PM. Cell-surface calreticulin initiates clearance of viable or apoptotic cells through trans-activation of LRP on the phagocyte. Cell 2005; 123(2):321-34; PMID:16239148; http://dx.doi.org/10.1016/j.cell.2005.08.032
26. Blachere NE, Darnell RB, Albert ML. Apoptotic cells deliver processed antigen to dendritic cells for cross-presentation. PLoS Biol 2005; 3(6):e185; PMID:15839733; http://dx.doi.org/10.1371/journal.pbio.0030185
27. Podrazil M, Horvath R, Becht E, Rozkova D, Bilkova P, Sochorova K, Hromadkova H, Kayserova J, Vavrova K, Lastovicka J et al. Phase I/II clinical trial of dendritic-cell based immunotherapy (DCVAC/PCa) combined with chemotherapy in patients with metastatic, castration-resistant prostate cancer. Oncotarget 2015; 6(20):18192-205; PMID:26078335; http://dx.doi.org/10.18632/oncotarget.4145
28. Zappasodi R, de Braud F, Di Nicola M. Lymphoma immunotherapy: current status. Front Immunol 2015; 6: 448; PMID:26388871; http://dx.doi.org/10.3389/fimmu.2015.00448
29. Menger L, Vacchelli E, Adjemian S, Martins I, Ma Y, Shen S, Yamazaki T, Sukkurwala AQ, Michaud M, Mignot G et al. Cardiac glycosides exert anticancer effects by inducing immunogenic cell death. Sci Transl Med 2012; 4(143):143ra199; PMID:22814852; http://dx.doi.org/10.1126/scitranslmed.3003807
30. Martins I, Kepp O, Schlemmer F, Adjemian S, Tailler M, Shen S, Michaud M, Menger L, Gdoura A, Tajeddine N et al. Restoration of the immunogenicity of cisplatin-induced cancer cell death by endoplasmic reticulum stress. Oncogene 2011; 30(10):1147-58; PMID:21151176; http://dx.doi.org/10.1038/onc.2010.500
31. Miyamoto S, Inoue H, Nakamura T, Yamada M, Sakamoto C, Urata Y, Okazaki T, Marumoto T, Takahashi A, Takayama K et al. Coxsackievirus B3 is an oncolytic virus with immunostimulatory properties that is active against lung adenocarcinoma. Cancer Res 2012; 72(10):2609-21; PMID:22461509; http://dx.doi.org/10.1158/0008-5472.CAN-11-3185
32. Prasad V, Chandele A, Jagtap JC, Sudheer Kumar P, Shastry P. ROS-triggered caspase 2 activation and feedback amplification loop in beta-carotene-induced apoptosis. Free Radic Biol Med 2006; 41(3):431-42; PMID:16843824; http://dx.doi.org/10.1016/j.freeradbiomed.2006.03.009
33. Sandow JJ, Dorstyn L, O'Reilly LA, Tailler M, Kumar S, Strasser A, Ekert PG. ER stress does not cause upregulation and activation of caspase-2 to initiate apoptosis. Cell Death Differ 2014; 21(3):475-80; PMID:24292555; http://dx.doi.org/10.1038/cdd.2013.168
34. Krumschnabel G, Sohm B, Bock F, Manzl C, Villunger A. The enigma of caspase-2: the laymen's view. Cell Death Differ 2009; 16(2):195-207; PMID:19023332; http://dx.doi.org/10.1038/cdd.2008.170
35. Lauber K, Blumenthal SG, Waibel M, Wesselborg S. Clearance of apoptotic cells: getting rid of the corpses. Mol Cell 2004; 14(3):277-87; PMID:15125832; http://dx.doi.org/10.1016/S1097-2765(04)00237-0

5.3. Kalretikulin přítomný na povrchu maligních blastů koreluje se zvýšenou protinádorovou imunitní odpovědí a lepší prognózou pacientů s akutní myeloidní leukémií

Smrt nádorových buněk může být *in vivo* vnímána jako imunogenní jen pokud umírající nádorové buňky sekretují/uvolňují/vystavují imunostimulační signály (DAMPs) a to v důsledku aktivace buněčného stresu. Výsledky preklinických a klinických studií naznačují, že schopnost ICD reaktivovat protinádorovou imunitní odpověď má zásadní vliv na účinnost nejrůznějších chemoterapeutik a radioterapie. Bylo prokázáno, že míra exprese některých DAMPs a PRRs a také polymorfismy genů kódujících tyto molekuly mohou mít vliv na prognózu pacientů s nádorovým onemocněním. Konkrétně míra exprese CRT nebo množství CRT na povrchu nádorových buněk bylo korelováno s prognózou pacientů u řady solidních nádorů (např. neuroblastom, nemalobuněčný karcinom plic, karcinom ovárií, kolorektální karcinom, atd.). O poznání méně se toho ví o možném vlivu CRT na prognózu pacientů s hematologickými malignitami.

Hlavním cílem této práce bylo zjistit, zda u pacientů s AML dochází k vystavení DAMPs, konkrétně CRT, HSP70 a HSP90, na plazmatickou membránu maligních blastů v závislosti na aplikované imunogenní chemoterapii antracykliny a zda přítomnost těchto molekul koreluje s imunitní odpovědí a prognózou pacientů. Ukázali jsme, že množství chaperonových proteinů CRT, HSP70 a HSP90 na povrchu blastů je nezávislé na aplikované chemoterapii. Povrchový CRT koreluje s vyšším zastoupením efektorových paměťových $CD4^+$ a $CD8^+$ T lymfocytů a NK buněk v periferní krvi. Současně přítomnost CRT na blastech je asociována s vyšším množstvím cirkulujících T lymfocytů specifických pro antigeny asociované s leukémií, což naznačuje, že povrchový CRT napomáhá u AML pacientů iniciaci protinádorové imunitní odpovědi. Přítomnost všech tří stanovovaných DAMPs na maligních blastech je asociována s delší dobou do dosažení relapsu, ale pouze povrchový CRT

signifikantně koreluje s celkovou dobou přežití. Kalretikulin proto představuje nový prognostický znak u AML pacientů, který odráží aktivaci klinicky relevantní imunitní reakce namířené proti blastům.

K této práci jsem přispěla následovně: zpracování periferní krve pacientů s AML, měření viability a detekce DAMPs (HSP70, HSP90 a CRT) na povrchu maligních blastů pomocí průtokové cytometrie, optimalizace detekce HSP70, HSP90 a CRT v sérech AML pacientů metodou ELISA, testování vhodných peptidových mixů odvozených od antigenů asociovaných s leukémií za účelem detekce T lymfocytů specifických pro tyto leukemické antigeny pomocí průtokové cytometrie, účast na přípravě obrázků a psaní manuskriptu.

Regular Article

blood

MYELOID NEOPLASIA

Calreticulin exposure by malignant blasts correlates with robust anticancer immunity and improved clinical outcome in AML patients

Jitka Fucikova,[1,2,*] Iva Truxova,[1,2,*] Michal Hensler,[2] Etienne Becht,[3-5] Lenka Kasikova,[1,2] Irena Moserova,[1,2] Sarka Vosahlikova,[2] Jana Klouckova,[6] Sarah E. Church,[3-5] Isabelle Cremer,[3-5] Oliver Kepp,[3-5,7,8] Guido Kroemer,[3-5,7-10] Lorenzo Galluzzi,[3-5,7,11,12] Cyril Salek,[13,14] and Radek Spisek[1,2]

[1]Department of Immunology, Charles University, 2nd Faculty of Medicine and University Hospital Motol, Prague, Czech Republic; [2]Sotio, Prague, Czech Republic; [3]INSERM, U1138, Centre de Recherche des Cordeliers, Paris, France; [4]Université Pierre et Marie Curie/Paris VI, Paris, France; [5]Université Paris Descartes/Paris 5, Paris, France; [6]Institute of Medical Biochemistry and Laboratory Diagnostics, 1st Faculty of Medicine and General University Hospital, Prague, Czech Republic; [7]Equipe 11 labellisée par la Ligue Nationale contre le Cancer, Centre de Recherche des Cordeliers, Paris, France; [8]Metabolomics and Cell Biology Platforms, Gustave Roussy Cancer Campus, Villejuif, France; [9]Pôle de Biologie, Hôpital Européen Georges Pompidou, AP-HP, Paris, France; [10]Department of Women's and Children's Health, Karolinska University Hospital, Stockholm, Sweden; [11]Gustave Roussy Cancer Campus, Villejuif, France; [12]Department of Radiation Oncology, Weill Cornell Medical College, New York, NY; [13]Institute of Hematology and Blood Transfusion, Prague, Czech Republic; and [14]Institute of Clinical and Experimental Hematology, 1st Faculty of Medicine, Charles University, Prague, Czech Republic

Key Points

- Malignant cells from patients with AML expose danger signals on the plasma membrane regardless of chemotherapy.
- Such danger signals correlate with markers of a clinically relevant tumor-specific immune response and with improved disease outcome.

Cancer cell death can be perceived as immunogenic by the host only when malignant cells emit immunostimulatory signals (so-called "damage-associated molecular patterns," DAMPs), as they die in the context of failing adaptive responses to stress. Accumulating preclinical and clinical evidence indicates that the capacity of immunogenic cell death to (re-)activate an anticancer immune response is key to the success of various chemo- and radiotherapeutic regimens. Malignant blasts from patients with acute myeloid leukemia (AML) exposed multiple DAMPs, including calreticulin (CRT), heat-shock protein 70 (HSP70), and HSP90 on their plasma membrane irrespective of treatment. In these patients, high levels of surface-exposed CRT correlated with an increased proportion of natural killer cells and effector memory $CD4^+$ and $CD8^+$ T cells in the periphery. Moreover, CRT exposure on the plasma membrane of malignant blasts positively correlated with the frequency of circulating T cells specific for leukemia-associated antigens, indicating that ecto-CRT favors the initiation of anticancer immunity in patients with AML. Finally, although the levels of ecto-HSP70, ecto-HSP90, and ecto-CRT were all associated with improved relapse-free survival, only CRT exposure significantly correlated with superior overall survival. Thus, CRT exposure represents a novel powerful prognostic biomarker for patients with AML, reflecting the activation of a clinically relevant AML-specific immune response. (*Blood*. 2016;128(26):3113-3124)

Introduction

For nearly a century, cancer has been viewed as an immunologically silent entity that should be treated with high-dose chemotherapy or radiation therapy, pretty much as a bacterial infection to be eradicated with potent antibiotics.[1,2] The limitations of such a view became clear throughout the past decade, as several laboratories worldwide demonstrated that tumors arise, become clinically manifest, and respond to treatment in the context of a bidirectional crosstalk with the host immune system.[1-4] One of the mechanisms whereby neoplastic cells succumbing to specific treatments can activate the immune system is commonly referred to as "immunogenic cell death" (ICD).[5-7] Thus, malignant cells exposed to some chemotherapeutic agents like anthracyclines, oxaliplatin and bortezomib, as well as to fractionated radiation therapy or high hydrostatic pressures, succumb as they expose (on their surface) or release (in the extracellular milieu) a set of molecules that alert the immune system of incipient danger.[8-11] Importantly, the emission of such danger signals, which altogether are known as damage-associated molecular patterns (DAMPs), mechanistically relies on the activation of adaptive stress responses in dying cells, and hence, can be pharmacologically modulated.[12]

ICD-relevant DAMPs encompass but are not limited to the following[13,14]: (1) the exposure of endoplasmic reticulum (ER) chaperones like calreticulin (*CALR*, best known as CRT), heat shock protein family A (Hsp70) member 1A (HSPA1A, best known as HSP70), and heat shock protein 90 α family class A member 1 (HSP90AA1, best known as HSP90) on the plasma membrane[15,16]; (2) the secretion of adenosine triphosphate (ATP), annexin A1 (ANXA1), and high mobility group box 1 (HMGB1) in the extracellular microenvironment[17,18]; and (3) the activation of autocrine/paracrine

Submitted 3 August 2016; accepted 24 October 2016. Prepublished online as *Blood* First Edition paper, 1 November 2016; DOI 10.1182/blood-2016-08-731737.

*J.F. and I.T. contributed equally to this study.

The online version of this article contains a data supplement.

The publication costs of this article were defrayed in part by page charge payment. Therefore, and solely to indicate this fact, this article is hereby marked "advertisement" in accordance with 18 USC section 1734.

type I interferon (IFN) signaling in malignant cells, eventually resulting in the secretion of C-X-C motif chemokine ligand 10 (CXCL10).[19]

DAMPs mediate robust immunostimulatory effects upon interaction with pattern recognition receptors (PRRs) expressed on myeloid or lymphoid cells,[20] including LDL receptor related protein 1 (LRP1, best known as CD91), which binds CRT, HSP70, and HSP90; purinergic receptor P2X7 (P2RX7) and purginergic receptor P2Y2 (P2RY2), which bind ATP; formyl peptide receptor 1, which binds ANXA1; Toll-like receptor 4, which binds HMGB1; and C-X-C motif chemokine receptor 3 (CXCR3), the T-cell receptor for CXCL10.[13] In particular, surface-exposed (ecto)-CRT, ecto-HSP70, and ecto-HSP90 foster the uptake of dead cancer cells or their corpses; ATP stimulates the recruitment of myeloid cells to the tumor microenvironment (via P2RY2) and their activation (via P2RX7), and ANXA1 guides the homing of myeloid cells toward dying cancer cells. HMGB1 has multipronged proinflammatory functions, and CXCL10 favors T-cell infiltration.[1]

Corroborating the clinical relevance of ICD and its proper perception, several DAMPs and DAMP-associated parameters (eg, DAMP and PRR expression levels, genetic polymorphisms in DAMP- or PRR-coding genes, etc) have been attributed prognostic value in several cohorts of patients with cancer.[21] In particular, CRT levels or exposure has been shown to convey robust prognostic information in subjects with multiple solid tumors, including neuroblastoma, non–small cell lung carcinoma, ovarian cancer, and colorectal carcinoma.[22-25] However, little is known on the prognostic value of CRT in patients with hematological malignancies, irrespective of the fact that these patients often receive ICD inducers, including anthracyclines and bortezomib. In a preliminary study, we reported that malignant blasts from patients with acute myeloid leukemia (AML) may expose CRT on the plasma membrane regardless of chemotherapy,[26] but did not investigate the prognostic relevance of these findings. Driven by these premises, we decided to investigate the immunological and prognostic correlates of DAMP emission in an independent cohort of patients with AML, finding that CRT exposure (and less so HSP70 and HSP90 exposure) on malignant blasts correlates with the activation of tumor-targeting immune responses and improved clinical outcome.

Materials and methods

Patients and samples

Fifty patients with a confirmed diagnosis of AML who were treated at the Institute of Hematology and Blood Transfusion of Prague, Czech Republic between January 2013 and July 2015 were enrolled in this study. Informed consent was obtained according to the Declaration of Helsinki, and the study was approved by the local ethics committee. The main clinical and biological characteristics of the patients are summarized in Table 1. Peripheral blood samples were obtained before chemotherapy, 12 hours after the initiation of chemotherapy, and once blood cell counts were restored after chemotherapy (50-70 days after chemotherapy). Serum was separated and stored at −80°C, and peripheral blood mononuclear cells (PBMCs) were isolated by Ficoll density centrifugation (GE Healthcare). An EasySep kit (StemCell Technologies) was employed to separate normal PBMC from $CD33^+$ malignant blasts.

Cell culture

Patient-derived PBMCs were cultured in RPMI 1640 medium (Life Technologies) supplemented with 10% heat-inactivated pooled human AB serum, 100 U/mL penicillin, 2 mM *L*-glutamine, nonessential amino acids, and sodium pyruvate (Life Technologies). Kasumi-1 and MOLM-13 cells were maintained in RPMI 1640 medium supplemented with 20% (Kasumi-1) and 10% (MOLM-13) fetal bovine serum, 100 U/mL penicillin, and 2 mM *L*-glutamine.

Flow cytometry

For the analysis of CRT, HSP70, or HSP90 exposure, PBMCs were labeled with primary anti-CD45 (PerCP; BD Bioscience), anti-CD33 (PE; BD Bioscience), and either anti-CRT (Enzo Life Sciences), anti-HSP70 (R&D Systems), or anti-HSP90 (R&D Systems) antibodies for 20 minutes at 4°C, followed by 1 wash in phosphate-buffered saline and incubation with an antigen-presenting cell (APC)-conjugated secondary antibody (Jackson Immunoresearch). Kasumi-1 and MOLM-13 cells were stained according to the same protocol in the absence of primary anti-CD45 and anti-CD33 antibodies. In both cases, cell suspensions were eventually costained with fluorescein isothiocyanate–conjugated annexin V (Exbio Antibodies) plus 4',6-diamidino-2-phenylindole (DAPI). For the assessment of dendritic cell (DC) activation, monocyte-derived DCs pulsed with Kasumi-1 cells succumbing to idarubicin or daunorubicin were stained with CD86-PE-Cy5 (Exbio Antibodies) and HLA-DR-PE-Cy7 (BD Biosciences). Flow cytometry data were acquired on an LSRFortessa Analyzer (BD) and analyzed with the FlowJo software package (Tree Star, Inc). Ecto-CRT, ecto-HSP70, and ecto-HSP90 were monitored on $DAPI^-$ (living) cells, as per gold-standard procedures.[27,28]

Phagocytosis

DCs were generated by culturing purified $CD14^+$ cells isolated from buffy coats in the presence of 500 IU/mL granulocyte-macrophage colony-stimulating factor and 248 IU/mL interleukin-4 (IL-4) (both Gentaur). On day 5, immature DCs stained with Vybrant DiD cell labeling solution (Life Technologies) were fed Kasumi-1 cells previously exposed to 20 μM idarubicin or 20 μM daunorubicin for 24 hours (at a 5:1 DC/tumor cell ratio) and stained with VybrantV DiO cell labeling solution (Life Technologies). After 24 hours at either 37°C or 4°C, phagocytosis was analyzed by flow cytometry as the percentage of DiO^+DiD^+ events.

Enzyme-linked immunosorbent assay

Circulating levels of CRT, HSP70, HSP90, and HMGB1 were assessed on frozen sera by enzyme-linked immunosorbent assay with commercial kits (Enzo Life Sciences or IBL), according to the manufacturer's instructions.

Detection of antigen-specific T cells

The frequency of T cells specific for baculoviral IAP repeat containing 5 (BIRC5; best known as survivin), cyclin B1 (CCNB1), preferentially expressed antigen in melanoma (PRAME), and Wilms tumor 1 (WT1) was assessed by flow cytometry according to standard methods. In brief, PBMCs were cultured for 10 days together with mixtures of overlapping peptides (PepMix; JPT Peptide Technologies) spanning the whole sequence of BIRC5, CCNB1, PRAME, or WT1 at a final concentration of 1 μg/mL. On days 4 and 7, 20 UI/mL IL-2 (Gentaur) was added. On day 9, PBMCs were restimulated with peptide mixtures, and 5 μg/mL brefeldin A (BioLegend) was added after 4 hours of incubation. Alternatively, PBMCs were exposed to immature DCs alone or immature DCs pulsed with (1) 25 μg/mL polyinosinic-polycytidylic acid, (2) Kasumi-1 cells succumbing to 20 μM idarubicin, or (3) Kasumi-1 cells succumbing to 20 μM daunorubicin, for a total time of 14 days (restimulated twice). Eventually, PBMCs were costained with CD3-PE-Cy5, CD4-PE-Cy7 (eBioscience), and CD8-PE-Dy590 (Exbio) conjugates plus the Aqua Blue Live/Dead cell viability dye (Life Technologies). Thereafter, cells were fixed with fixation/permeabilization buffer (BD Bioscience), permeabilized with permeabilization buffer (BD Bioscience), and incubated with a fluorescein isothiocyanate–conjugated antibody specific for IFN-γ plus an APC-conjugated antibody specific for IL-2 (both from BD Bioscience), according to the manufacturer's instructions. Flow cytometry was performed on an LSRFortessa Analyzer (BD), and data were analyzed with the FlowJo software package (Tree Star, Inc). Upon exclusion of dead cells, IFN-γ expression was considered to be antigen specific if the frequency of $IFN\text{-}\gamma^+$ T cells detected in response to peptide stimulation was at least twice the frequency of $IFN\text{-}\gamma^+$ cells detected in control conditions.

Table 1. Clinical and biological characteristics of patients with AML

Variable	Value
Sex, n (%)	
Male	26 (52)
Female	24 (48)
Age at diagnosis, y (%)	
<50	15 (30)
≥50	35 (70)
Median, y	56
Range, y	21-69
Peripheral blood white cell count	
<30 000/mm^3, n (%)	29 (58)
≥30 000/mm^3, n (%)	21 (42)
Median (10^9 cells/L)	23.6
Range (10^9 cells/L)	0.4-385
Circulating blasts, %	
Median	32
Range	0-99
Bone marrow blasts, %	
Median	60
Range	23-96
Diagnosis, n (%)	
De novo AML	41 (82)
Secondary AML (MDS-related)	7 (14)
Secondary AML (therapy-related)	2 (4)
FAB classification, n (%)	
M0	1 (2)
M1	14 (28)
M2	15 (30)
M4	11 (22)
M5	5 (10)
M6	2 (4)
MDS RAEB-T	2 (4)
Cytogenetic profile,* n (%)	
Favorable	4 (8)
Intermediate	34 (68)
Unfavorable	8 (16)
Missing data	4 (8)
Molecular features, n (%)	
NPM1 mutation	19 (38)
FLT3/ITD translocation	14 (28)
MLL mutation	4 (8)
RUNX1/RUNX1T1 translocation	3 (6)
CEBPA mutation	2 (4)
CBFB/MYH11 translocation	1 (2)
Induction chemotherapy, n (%)	
Daunorubicine 90 mg/m^2 3 d + Cytarabine 100 mg/m^2 7 d	35 (70)
Idarubicine 10 mg/m^2 3 d + Cytarabine 100 mg/m^2 7 d	14 (28)
Fludarabine 15 mg/m^2 + Cytarabine 500 mg/m^2 twice-daily 4 d	1 (2)
Consolidation therapy, n (%)	
Chemotherapy only	34 (68)
Hematopoietic stem cell transplantation	28 (56)
Treatment response, n (%)	
Complete remission	38 (76)
After 1 induction cycle	29 (58)
After 2 induction cycles	9 (18)
Induction failure	11 (22)
Death in aplasia	1 (2)

CBFB, core binding factor β; CEBPA, CCAAT/enhancer-binding protein alfa; FAB, Franco-Americano-British; FLT3, Fms-like tyrosine kinase 3; ITD, internal tandem duplication; MLL, mixed-lineage leukemia; MDS, myelodysplastic syndrome; MYH11, myosin heavy chain 11; NPM1, nucleophosmin 1; RAEB-T, refractory anemia with excess blasts in transformation; RUNX1, runt-related transcription factor 1; RUNX1T1, RUNX1 translocation partner 1.
*Per Grimwade et al.[40]

Statistical analyses

Survival analyses were performed upon patient stratification into 2 groups based on median levels of ecto-CRT, ecto-HSP70, ecto-HSP90, circulating HMGB1, or *CALR* messenger RNA (mRNA) levels. As an alternative, patients were stratified based on *BIRC5*, *BMI1* proto-oncogene, polycomb ring finger (*BMI1*), *CCNB1*, elastase, neutrophil expressed (*ELANE*), hyaluronan-mediated motility receptor (*HMMR*, also known as *RHAMM*), *MOK* protein kinase (*MOK*, also known as *RAGE1*), membrane palmitoylated protein 1 (*MPP1*), *PRAME*, proteinase 3 (*PRTN3*), or *WT1* expression levels. Univariate and multivariate Cox proportional hazard analysis was performed to assess the association of clinicopathological or immunological parameters with relapse-free (RFS) or overall survival (OS). Fisher's exact test, Student *t* test, Wilcoxon, and Mann-Whitney tests were used to assess statistical significance. *P* values are reported (and were considered not significant when >.05).

Additional Materials and Methods are available as supplemental information, available on the *Blood* Web site.

Results

AML blasts emit DAMPs regardless of chemotherapy

To expand our previous observations,[26] we used flow cytometry to investigate the exposure of CRT, HSP70, and HSP90 on the plasma membrane of CD33$^+$ malignant blasts from 50 patients with AML prior to and after induction anthracycline-based chemotherapy (Table 1; supplemental Figure 1). Forty-one patients with AML (82%) exhibited >5% circulating CD45$^+$CD33$^+$ blasts with surface-exposed CRT prior to the initiation of treatment, whereas PBMCs from 10 healthy donors contained (on average) <5% ecto-CRT$^+$ cells (Figure 1A). Of note, the percentage of living (DAPI$^-$) blasts staining positively for ecto-CRT was highly heterogeneous within the cohort, ranging from 5% to 95% of the CD45$^+$CD33$^+$ cell population (Figure 1A). Along similar lines, the blasts of patients with AML stained positively for ecto-HSP70 and ecto-HSP90 in a rather heterogeneous fashion, contrasting with living (DAPI$^-$) PBMCs from healthy donors that never contained >5% ecto-HSP70$^+$ or ecto-HSP90$^+$ cells (Figure 1B-C). Indeed, CRT, HSP70, and HSP90 exposure on malignant blasts exhibited considerable mutual correlation (Figure 1D). The percentage of living (DAPI$^-$) ecto-CRT$^+$, ecto-HSP70$^+$, and ecto-HSP90$^+$ blasts was not influenced by disease subtype (supplemental Figure 2A-C). Of note, IV anthracycline-based chemotherapy failed to increase the percentage of living (DAPI$^-$) blasts exposing CRT, HSP70, or HSP90 on their surface (Figure 1A-C), suggesting that in this specific setting DAMP emission may reflect a treatment-independent, cancer-cell intrinsic state of stress. No difference in the percentage of living (DAPI$^-$) ecto-CRT$^+$ blasts was observed in patients receiving idarubicin-based vs daunorubicin-based chemotherapy (supplemental Figure 2D). Accordingly, idarubicin and daunorubicin induced comparable degrees of CRT exposure in cultured human Kasumi-1 and MOLM-13 AML cells (supplemental Figure 2E), resulting in comparable phagocytosis of AML cells by cocultured myeloid cells (supplemental Figure 2F), similar expression of activation markers by the latter (supplemental Figure 2G), and comparable ability to drive the accumulation of IFN-γ$^+$ CD4$^+$ or CD8$^+$ T cells (supplemental Figure 2H-I).

Because CRT expression relies on premortem ER stress responses,[6] we checked whether the mRNA levels of 3 distinct genes intimately involved in this process,[29] namely, activating transcription factor 4 (*ATF4*), heat shock protein family A (Hsp70) member 5 (*HSPA5*), and DNA damage inducible transcript 3 (*DDIT3*), would correlate with CRT exposure on malignant blasts. We observed a positive correlation between the percentage of living (DAPI$^-$) ecto-CRT$^+$ blasts and *ATF4*,

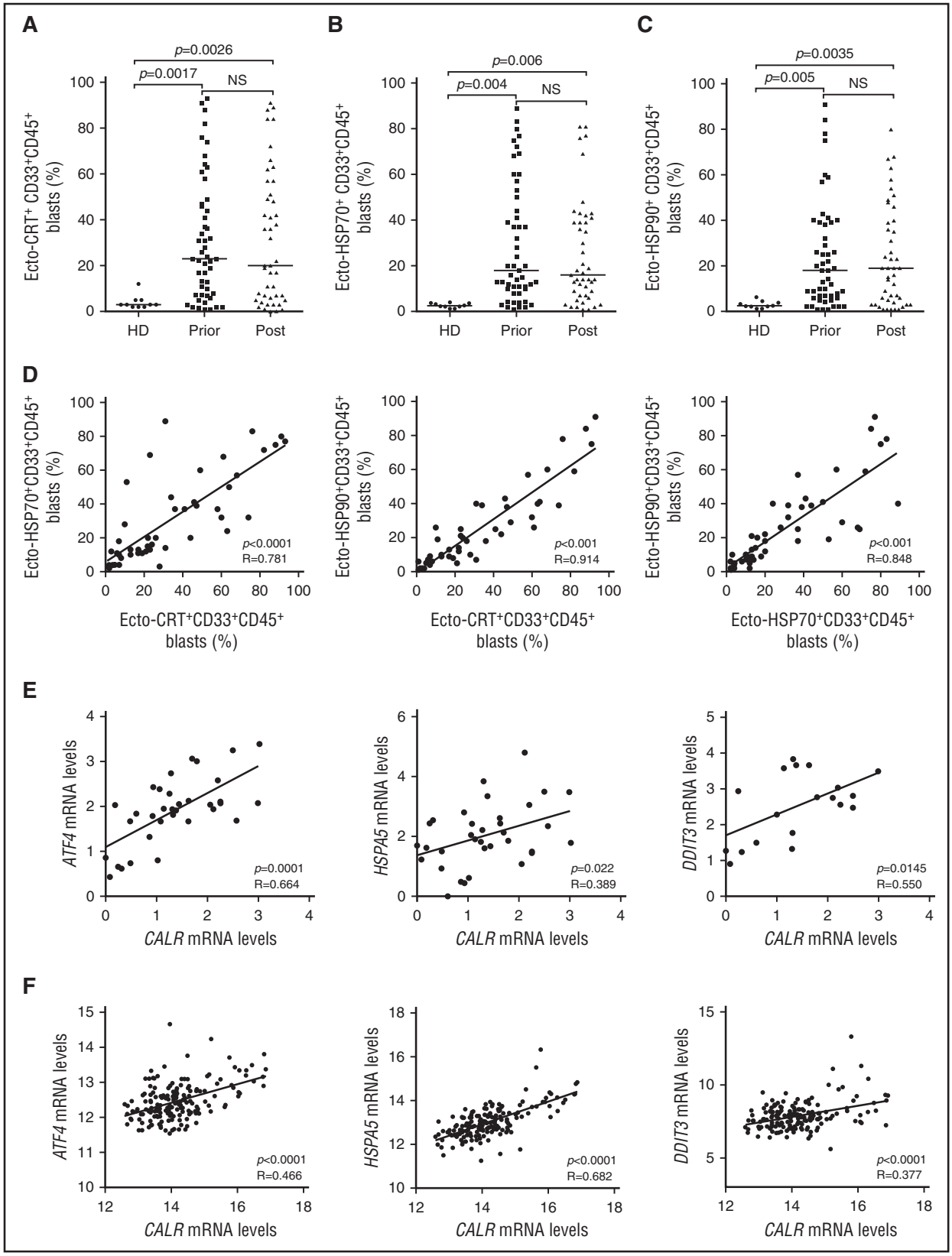

Figure 1. Chemotherapy-independent emission of danger signals by malignant AML blasts. (A-C) Percentage of ecto-CRT$^+$ (A), ecto-HSP70$^+$ (B), or ecto-HSP90$^+$ (C) CD45$^+$CD33$^+$ cells from 10 healthy donors (HD) or 50 patients with AML before (Prior) or after (Post) the initiation of induction chemotherapy. Median values are reported. NS, nonsignificant. (D) Correlation between the percentage of ecto-CRT$^+$, ecto-HSP70$^+$, and ecto-HSP90$^+$ CD45$^+$CD33$^+$ cells measured in 50 patients with AML before induction chemotherapy. R, Pearson correlation coefficient. (E) Correlation between *CALR* mRNA levels and *ATF4*, *HSP5A*, or *DDIT3* mRNA levels in 34 patients with AML before induction chemotherapy. (F) Correlation between *CALR* mRNA levels and *ATF4*, *HSP5A*, or *DDIT3* mRNA levels in 173 patients with AML from the TGCA public database. (G) Circulating HMGB1 levels from 10 HD or 50 patients with AML before the initiation of induction chemotherapy (Prior), 12 hours after induction chemotherapy (Post), or at the reestablishment of normal hematopoiesis (Recovery). Median values are indicated.

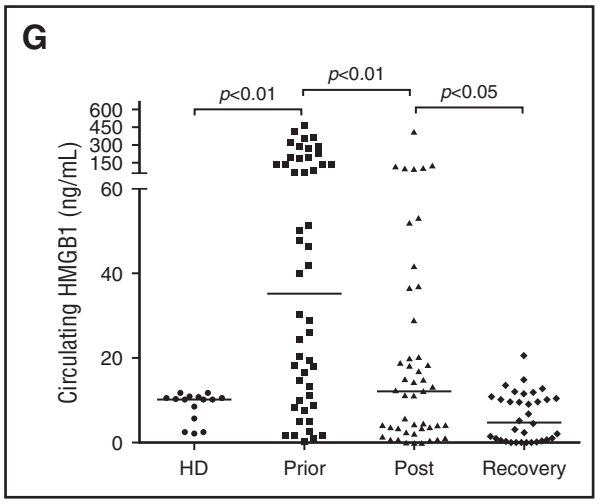

Figure 1. (Continued).

HSPA5, and *DDIT3* mRNA levels (Figure 1E). To corroborate our findings in an independent patient cohort, we retrieved normalized *ATF4*, *HSPA5*, and *DDIT3* expression levels for 173 patients with AML from The Cancer Genome Atlas (TCGA) public database and analyzed their correlation with *CALR* mRNA abundance. Also, in this setting, *ATF4*, *HSPA5*, and *DDIT3* mRNA levels exhibited a highly significant positive correlation with *CALR* expression (Figure 1F), corroborating the notion that AML blasts are subjected to high levels of ER stress irrespective of treatment, resulting in spontaneous CRT exposure in a majority of patients.

Next, we monitored the levels of circulating ICD-related DAMPs (including HMGB1, CRT, HSP70, and HSP90), in the sera of healthy volunteers and patients with AML prior to induction chemotherapy, 12 hours after induction chemotherapy, and at recovery. All these circulating DAMPs were more abundant in patients with AML before treatment than in healthy individuals (Figure 1G; supplemental Figure 3A-C). Although the amount of CRT and HSP70 did not change significantly throughout the study, patients with AML exhibited a reduction in circulating HMGB1 (and HSP90) levels as they recovered normal blood counts (Figure 1G; supplemental Figure 3C). This finding may simply reflect the reduction in circulating blasts spontaneously releasing HMGB1 (and HSP90) imposed by chemotherapy. Of note, we failed to identify a correlation between the percentage of living ($DAPI^-$) ecto-CRT^+, ecto-$HSP70^+$, and ecto-$HSP90^+$ blasts and the serum concentration of CRT, HSP70, and HSP90, respectively (supplemental Figure 3D). Moreover, disease subtype did not influence the circulating levels of HMGB1, CRT, HSP70, and HSP90 (supplemental Figure 4A-D).

CRT exposure is associated with markers of a T_H1 cytotoxic $CD8^+$ T-cell response upon treatment

Because ecto-CRT is best known for its ability to promote the phagocytosis of dying cancer cells by APCs and hence initiate antitumor immunity, we set out to evaluate the expression of immune system–related genes in normal ($CD33^-$) PBMCs from 26 patients with AML. Patients were stratified based on the median percentage of living ($DAPI^-$) ecto-CRT^+ blasts into a CRT^{Hi} (n = 13) and a CRT^{Lo} (n = 13) group. In baseline conditions (prior to induction chemotherapy), we were unable to identify statistically significant differences between the expression of immune cell population-, T_H1 polarization-, T_H2 polarization-, $CD8^+$ T-cell cytotoxicity-, T-cell activation-, immunosuppression-, inflammation-, and angiogenesis-related gene clusters in CRT^{Hi} vs CRT^{Lo} patients (Figure 2A). Conversely, upon complete remission and the recovery of normal, nonmalignant hematopoiesis, the gene clusters related to immune cell populations, T_H1 polarization, $CD8^+$ T-cell cytotoxicity, and T-cell activation were considerably upregulated in CRT^{Hi} vs CRT^{Lo} patients with AML (Figure 2B). The expression of gene clusters related to T_H2 polarization, immunosuppression, inflammation, and angiogenesis did not differ between CRT^{Hi} and CRT^{Lo} patients with AML even at recovery (Figure 2B). A correlation matrix was built to confirm clustering (supplemental Figure 5). Moreover, we validated the majority of these findings by analyzing the expression levels of *CD8A*, *CD28*, *CXCR3*, *IFNG*, T-box 21 (*TBX21*, best known as T-bet), Fas ligand (*FASLG*), granulysin (*GNLY*), granzyme B (*GZMB*), perforin 1 (*PRF1*), C-C motif chemokine ligand 5 (*CCL5*), C-C motif chemokine receptor 4 (*CCR4*), *CCR5*, and CD40 ligand (*CD40LG*) by quantitative reverse transcription polymerase chain reaction (qRT-PCR) (Figure 2C).

To extend these findings to other genes potentially involved in anticancer immunity, we employed the Nanostring technology to assess the relative abundance of 770 cancer and immune system mRNAs in the PBMCs of 6 CRT^{Hi} and 6 CRT^{Lo} patients with AML upon recovery of normal hematopoiesis. We identified a cluster of natural killer (NK) cell-related genes that was significantly overexpressed in CRT^{Hi} vs CRT^{Lo} patients (Figure 3A). We validated these results by qRT-PCR in a larger group of patients (20 CRT^{Hi} and 20 CRT^{Lo} individuals), confirming that several members of the CD158 gene family (namely, *KIR2DL1*, *KIR2DL2*, and *KIR2DL3*), killer cell lectin–like receptor F1 (*KLRF1*), killer cell lectin–like receptor C2 (*KLRC2*), and natural cytotoxicity triggering receptor 1 (*NCR1*, also known as NK-p46) were significantly overexpressed in CRT^{Hi} patients with AML as compared with their CRT^{Lo} counterparts (Figure 3B). In line with this notion, we detected an increased percentage of $CD33^-CD3^-CD56^+$ NK cells in the blood of CRT^{Hi} vs CRT^{Lo} patients recovering normal hematopoiesis after chemotherapy (Figure 3C). Interestingly, the relative abundance of $CD4^+$ and $CD8^+$ T cells virtually did not differ in these 2 patient subgroups, except for a slightly higher proportion of $CD3^+CD8^+$ T lymphocytes in CRT^{Hi} patients with AML at recovery (Figure 3D). Conversely, CRT^{Hi} patients with AML had an increased percentage of $CD4^+$ and $CD8^+$ T cells responding with IFN-γ production to nonspecific stimulation (with phorbol 12-myristate 13-acetate plus ionomycin) as compared with their CRT^{Lo} counterparts, both in baseline conditions (before induction chemotherapy) and at recovery (Figure 3E). Moreover, whereas there was no difference in the proportion of circulating $CD45RA^-CD45RO^+CCR7^-CD62L^-$ effector memory T cells between these patient subgroups, CRT^{Lo} patients exhibited a high frequency of $CD45RA^+CD45RO^-CCR7^-CD62L^-$ terminally differentiated T cells, whereas CRT^{Hi} individuals manifested an increased abundance of $CD45RA^+CD45RO^-CCR7^+CD62L^+$ naive and $CD45RA^-CD45RO^+CCR7^+CD62L^+$ central memory T cells (Figure 3F).

CRT exposure is associated with anticancer immune responses

Leukemia-associated antigens (LAAs) have previously been shown to elicit tumor-specific immune responses in (at least some) patients.[30] We therefore set out to investigate the relationship between CRT exposure and the frequency of leukemia-specific T cells in the peripheral blood of patients with AML prior to chemotherapy and upon the restoration of normal hematopoiesis. To this aim, we evaluated IFN-γ production by

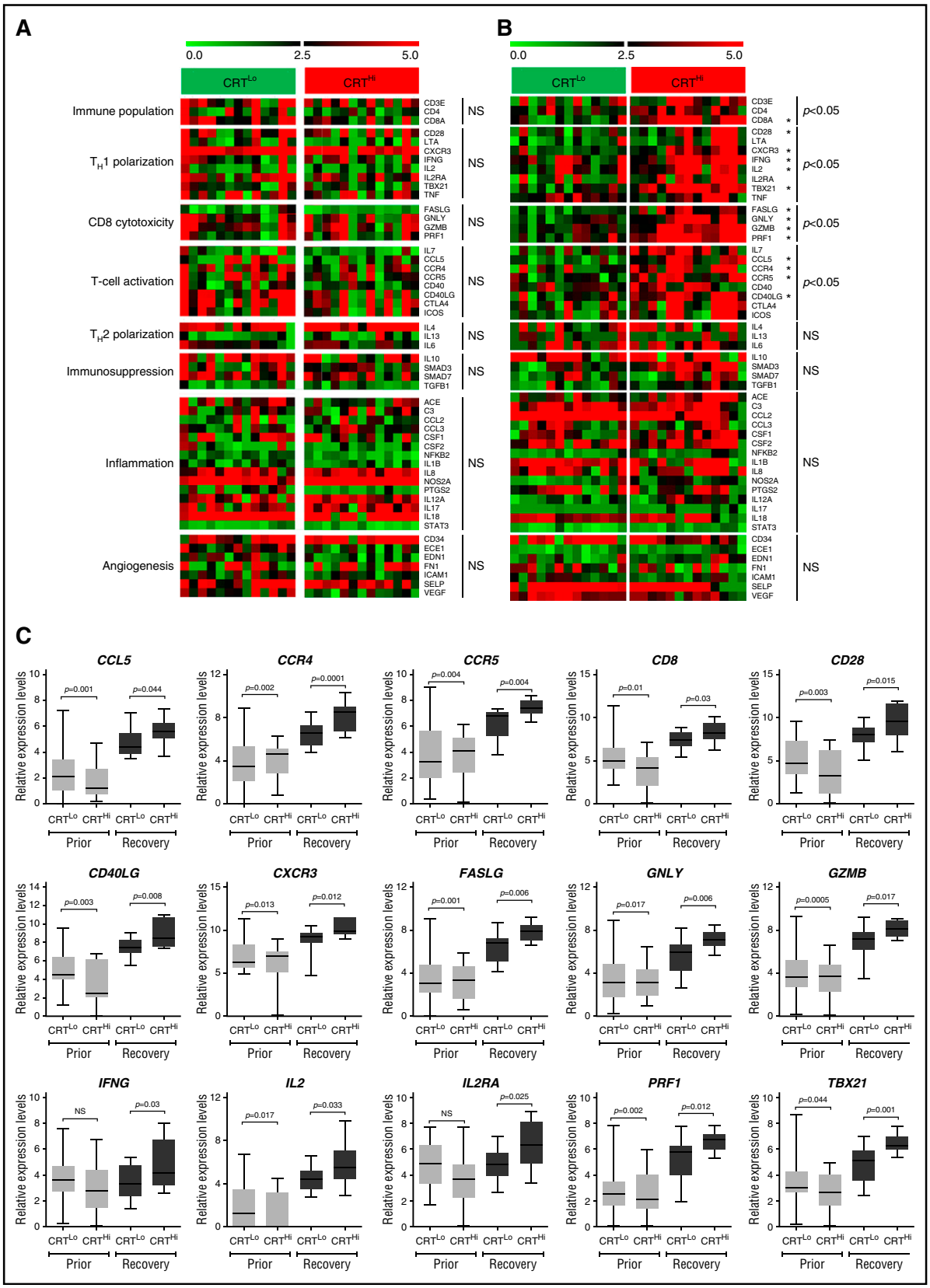

Figure 2. Transcriptional signatures of PBMCs in patients with AML exhibiting robust vs weak CRT exposure on blasts. (A-B) Expression levels of genes from the Human Immune Panel TaqMan low-density array in PBMCs from 13 CRT^{Hi} vs 13 CRT^{Lo} patients with AML prior to the initiation of induction chemotherapy (A), or at recovery of normal hematopoiesis (B). The Mann-Whitney test was employed to assess intergroup variations. (C) qRT-PCR–assisted quantification of *CD8A*, *CD28*, *CXCR3*, *IFNG*, *IL2*, *IL2RA*, *TBX21*, *FASLG*, *GNLY*, *GZMB*, *PRF1*, *CCL5*, *CCR4*, *CCR4*, *CCR5*, *CD40LG* expression levels in PBMCs from 13 CRT^{Hi} vs 13 CRT^{Lo} patients with AML prior to the initiation of induction chemotherapy, or at recovery of normal hematopoiesis. Box plots: lower quartile, median, upper quartile; whiskers, minimum value, maximum value.

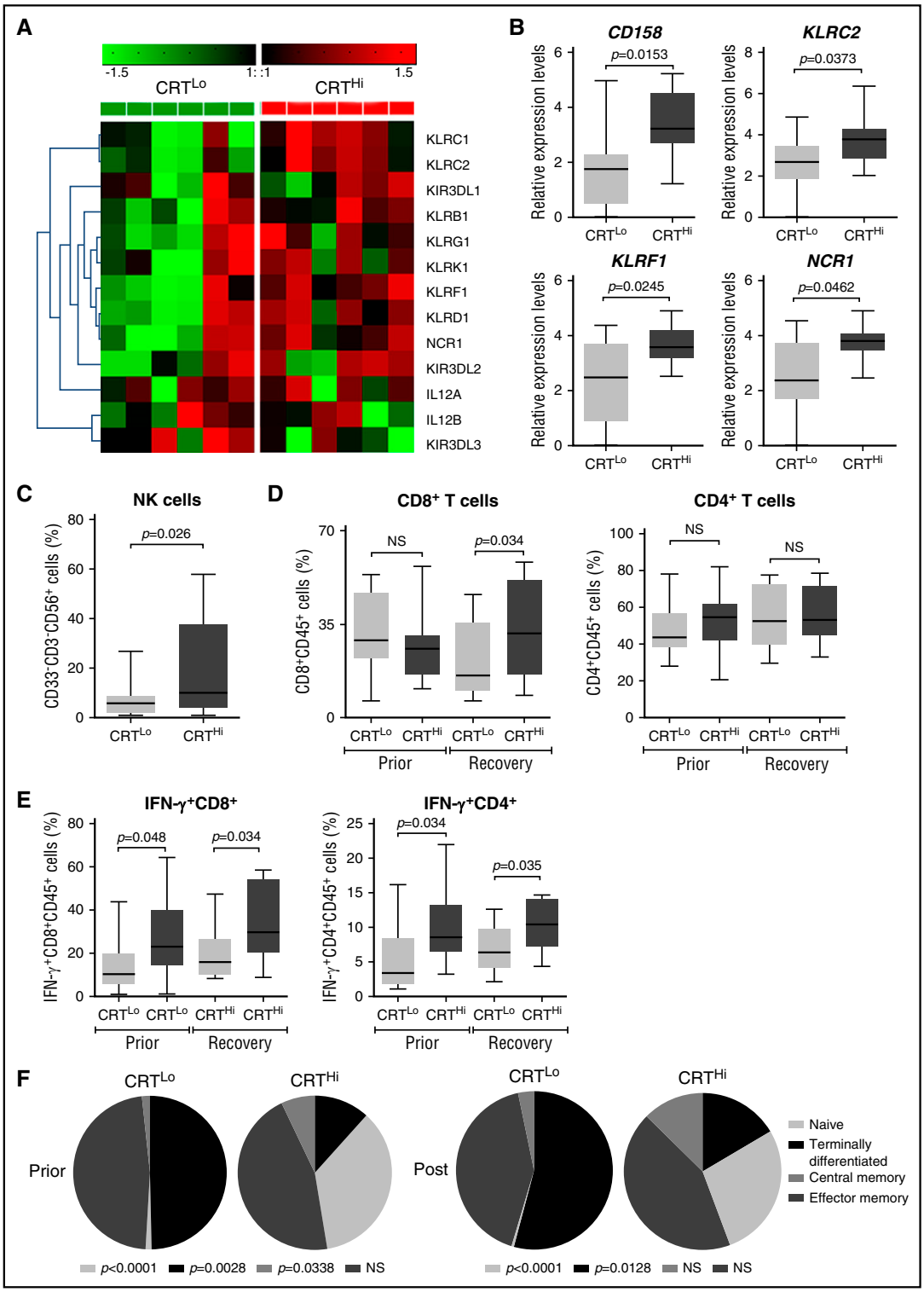

Figure 3. Transcriptional and phenotypic signatures of PBMCs in patients with AML exhibiting robust vs weak CRT exposure on blasts. (A) Nanostring-assisted quantification of NK cell–related mRNAs in PBMCs from 6 CRT^{Hi} vs 6 CRT^{Lo} patients with AML at recovery of normal hematopoiesis. The Mann-Whitney test was employed to assess intergroup variations. (B) qRT-PCR–assisted quantification of *KIR2DL1*, *KIR2DL2*, and *KIR2DL3* (cumulatively as CD158 family members), *KLRF1*, *KLRC2*, and *NCR1* in PBMCs from 20 CRT^{Hi} vs 20 CRT^{Lo} patients with AML at recovery of normal hematopoiesis. Box plots: lower quartile, median, upper quartile; whiskers, minimum value, maximum value. (C-D) Percentage of circulating $CD33^{-}CD3^{-}CD56^{+}$ NK cells (C), $CD45^{+}CD3^{+}CD4^{+}$ T cells, and $CD45^{+}CD3^{+}CD8^{+}$ T cells in 13 CRT^{Hi} vs 13 CRT^{Lo} patients with AML before induction chemotherapy (Prior, D) and at reestablishment of normal hematopoiesis (Recovery, C-D). Box plots: lower quartile, median, upper quartile; whiskers, minimum value, maximum value. (E) Percentage of IFN-γ–producing cells among $CD45^{+}CD3^{+}CD4^{+}$ T cells and $CD45^{+}CD3^{+}CD8^{+}$ T cells from 13 CRT^{Hi} vs 13 CRT^{Lo} patients with AML before induction chemotherapy (Prior) and at reestablishment of normal hematopoiesis (Recovery). Box plots: lower quartile, median, upper quartile; whiskers, minimum value, maximum value. (F) Distribution of circulating $CD45^{+}CD3^{+}CD8^{+}$ T cells and $CD45^{+}CD3^{+}CD4^{+}$ T cells in 20 CRT^{Hi} vs 20 CRT^{Lo} patients with AML before (Prior) and after (Post) induction chemotherapy. Mean percentage values are depicted as pie charts. Central memory: $CD45RA^{-}CD45RO^{+}CCR7^{+}CD62L^{+}$; effector memory: $CD45RA^{-}CD45RO^{+}CCR7^{-}CD62L^{-}$; naive: $CD45RA^{+}CD45RO^{-}CCR7^{+}CD62L^{+}$; terminally differentiated: $CD45RA^{+}CD45RO^{-}CCR7^{-}CD62L^{-}$.

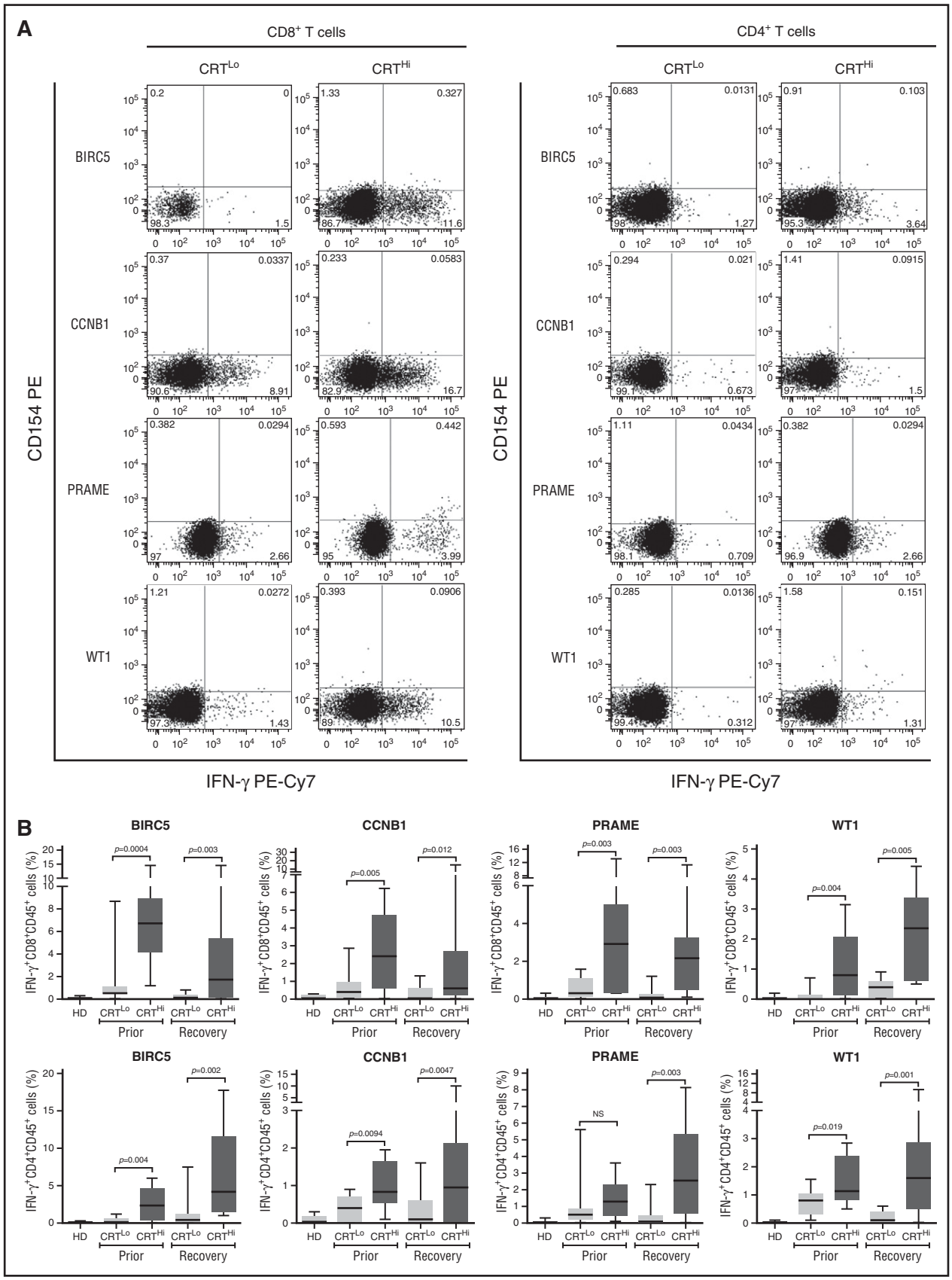

Figure 4. Antigen-specific immune responses in patients with AML exhibiting ecto-CRT^{+} vs ecto-CRT^{-} blasts. (A-B) Representative dot plots (A) and quantitative data (B) of IFN-γ–secreting CD45^{+}CD3^{+}CD4^{+} T cells and CD45^{+}CD3^{+}CD8^{+} T cells from 10 HD or 15 CRT^{Hi} vs 15 CRT^{Lo} patients with AML before induction chemotherapy (Prior, B) and at reestablishment of normal hematopoiesis (Recovery, A-B), upon exposure of the corresponding PBMCs to peptide mixture spanning BIRC5, CCNB1, PRAME, or WT1. Box plots: lower quartile, median, upper quartile; whiskers, minimum value, maximum value.

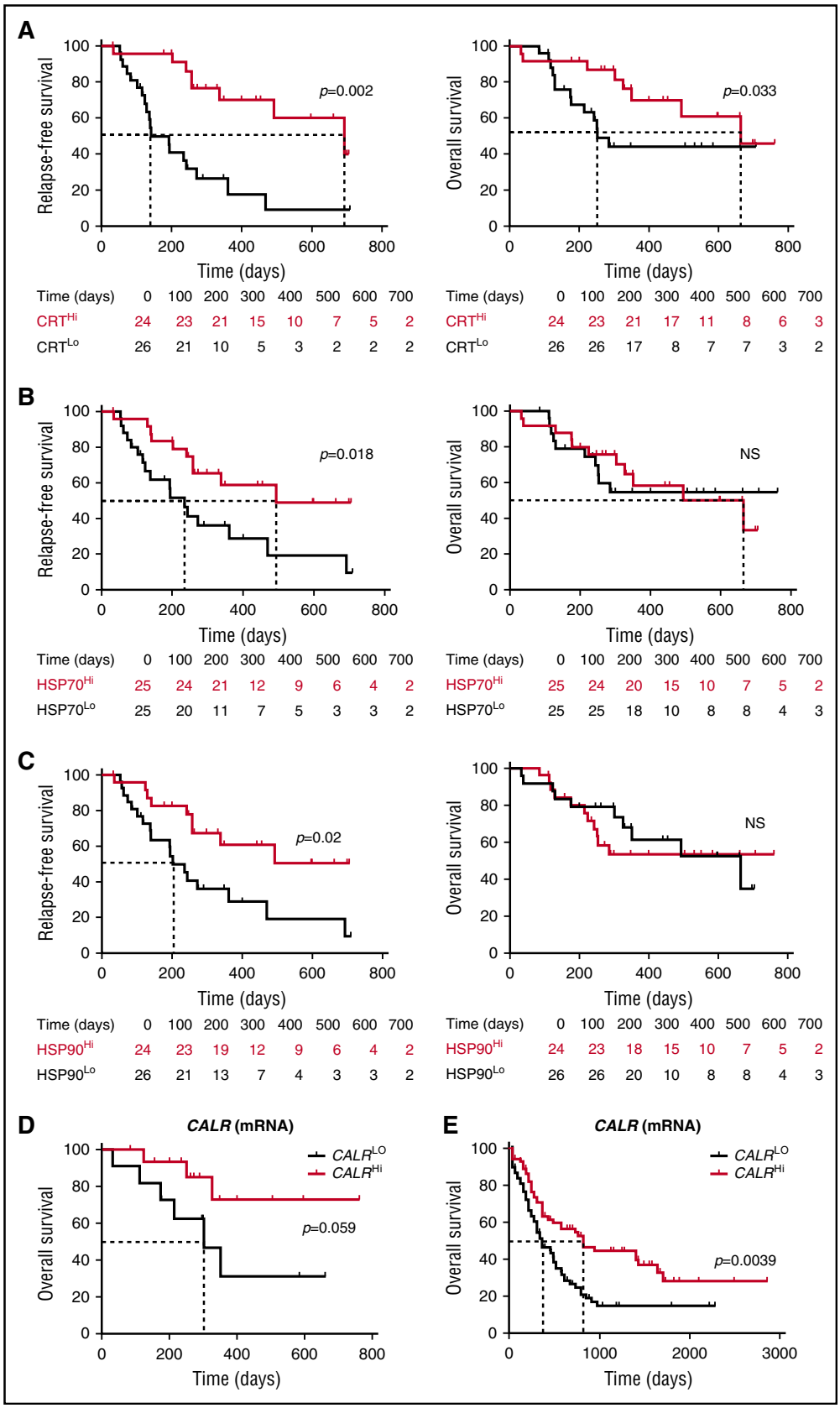

Figure 5. Prognostic value of CRT, HSP70, and HP90 exposure in patients with AML. (A-C) RFS and OS among 50 patients with AML stratified in 2 groups based on median percentage of circulating ecto-CRT^{+} (A), ecto-HSP70^{+} (B), or ecto-HSP90^{+} (C) blasts measured prior to induction chemotherapy. Patients at risk are reported. The Wilcoxon test was employed to assess statistical significance. (D-E) Overall survival of 30 patients with AML from our cohort (D) and 173 patients with AML from the TCGA public database (E) stratified in 2 groups based on median *CALR* mRNA levels. Patients at risk are reported.

Table 2. Univariate Cox proportional hazards analysis

	RFS		OS	
Variable	HR (95% CI)	P	HR (95% CI)	P
Age	1.02 (0.99-1.05)	.12	1.07 (1.02-1.13)	.01*
CRT percentage	0.97 (0.95-0.99)	.006*	1.00 (0.98-1.02)	.75
HSP70 percentage	0.97 (0.95-0.99)	.009*	0.99c (0.97-1.01)	.57
HSP90 percentage	0.97 (0.95-0.99)	.04*	1.00 (0.98-1.02)	.98
HMGB1 levels	1.00 (0.99-1.00)	.50	1.00 (1.00-1.00)	.76
BIRC5	1.06 (0.87-1.28)	.54	1.05 (0.83-1.32)	.68
BMI1	1.21 (0.89-1.64)	.20	0.99 (0.68-1.45)	.98
CCNB1	1.09 (0.84-1.39)	.52	1.00 (0.74-1.35)	1.00
ELANE	1.03 (0.94-1.12)	.53	1.01 (0.92-1.12)	.78
HMMR	1.10 (0.90-1.34)	.32	1.06 (0.84-1.34)	.60
MOK	1.05 (0.88-1.24)	.58	0.96 (0.78-1.18)	.72
MPP11	0.98 (0.66-1.46)	.93	0.82 (0.50-1.36)	.45
PRAME	1.15 (0.99-1.34)	.06	1.14 (0.95-1.36)	.15
PRTN3	1.11 (0.99-1.24)	.07	1.06 (0.93-1.21)	.37
WT1	1.07 (0.94-1.21)	.27	1.02 (0.88-1.19)	.75

HR, hazard ratio.
*$P < .05$.

$CD4^+$ and $CD8^+$ T cells after exposing PBMCs from patients to peptide mixtures spanning several domains of BIRC5, CCNB1, PRAME and WT1 (supplemental Figure 6A). Both prior to the initiation of chemotherapy and at recovery, CRT^{Hi} patients with AML exhibited moderately increased amounts of LAA-specific $CD4^+$ and $CD8^+$ T lymphocytes in the peripheral blood as compared with their CRT^{Lo} counterparts (Figure 4A-B). Conversely, the percentage of circulating $CD4^+$ and $CD8^+$ T lymphocytes responding with IFN-γ secretion to a mixture of influenza-, cytomegalovirus-, and Epstein-Barr virus–derived epitopes did not differ between CRT^{Hi} and CRT^{Lo} patients (supplemental Figure 6B).

ICD-associated DAMPs correlate with improved disease outcome in patients with AML

To evaluate the prognostic impact of ecto-CRT, we investigated RFS and OS upon stratifying the entire patient cohort based on median percentage of living ($DAPI^-$) ecto-CRT^+ blasts into a CRT^{Hi} (n = 24) and a CRT^{Lo} (n = 26) group. Importantly, CRT^{Hi} patients exhibited a significantly improved RFS (median: 692 vs 141 days; $p = .002$) and OS (median: 665 vs 252 days; $P = .033$) as compared with their CRT^{Lo} counterparts (Figure 5A). Using a similar median cutoff approach, we investigated RFS and OS in $HSP70^{Hi}$ (n = 25) vs $HSP70^{Lo}$ (n = 25) patients with AML, as well as in $HSP90^{Hi}$ (n = 24) vs $HSP90^{Lo}$ (n = 26) individuals. We found that both $HSP70^{Hi}$ and $HSP90^{Hi}$ patients exhibited an improved RFS as compared with their $HSP70^{Lo}$ (median: 493 vs 235 days; $P = .018$) and $HSP90^{Lo}$ counterparts (median: >700 vs 202 days; $P = .02$) (Figure 5B-C). However, neither the percentage of living ($DAPI^-$) ecto-$HSP70^+$ blasts nor that of living ($DAPI^-$) ecto-$HSP90^+$ blasts had a significant impact on OS in this cohort, although there was a tendency for improved OS among $HSP70^{Hi}$ patients (Figure 5B-C). Along similar lines, the circulating levels of HMGB1 measured prior to the initiation of chemotherapy did not influence disease outcome for these patients (supplemental Figure 7). Univariate Cox proportional hazards analysis confirmed that reduced percentages of living ($DAPI^-$) ecto-CRT^+, ecto-$HSP70^+$, and ecto-$HSP90^+$ blasts before induction chemotherapy (but not the circulating levels of HMGB1) were all associated with an increased risk for relapse (Table 2). However, this could not be confirmed on multivariate Cox proportional hazards analysis (Table 3), most likely owing to the limited number of patients.

As compared with their CRT^{Lo} counterparts, CRT^{Hi} patients exhibited reduced levels of multiple LAAs, including BIRC5, BMI1 proto-oncogene, polycomb ring finger, CCNB1, ELANE, HMMR; MOK; MPP1, PRAME, PRTN3, and WT1, in either a subsignificant or statistically significant manner (supplemental Figure 8A). Because LAA levels have been previously associated with improved disease outcome in patients with AML,[31,32] we tested whether this would hold true in our cohort using the median cutoff approach. We failed to identify prognostic value (on both RFS and OS) for the expression levels of all the aforementioned LAAs (supplemental Figure 8B; Tables 2 and 3), suggesting that CRT exposure conveys superior prognostic information in this setting. It remains to be determined whether the decrease in LAA expression observed among CRT^{Hi} patients is a consequence of ecto-CRT–driven anticancer immune responses.

Finally, driven by recent results demonstrating that increased levels of the *CALR* mRNA in the tumor predict the response of patients with lung and ovarian cancer to chemotherapy with ICD inducers,[33] we investigated the prognostic value of *CALR* mRNA levels in our patient cohort. We identified a trend for improved OS among patients with AML whose blasts contained higher-than-median (as compared with lower-than-median) *CALR* mRNA levels ($P = .059$) (Figure 5D). When we analyzed 173 patients from the TCGA database with the same median cutoff approach, high intratumoral *CALR* mRNA levels were strongly associated with improved OS ($P = .0039$) (Figure 5E). Unfortunately, ecto-CRT data are not available to investigate the prognostic impact of CRT exposure in this cohort. Taken together, these findings indicate that the spontaneous overexpression and exposure of CRT by malignant blasts conveys robust prognostic information for patients with AML.

Discussion

Throughout the past decade, our understanding of the mechanisms underlying the recognition and elimination of dying cancer cells by the immune system has considerably advanced.[6,7] Nonetheless, little is known on the prognostic value of DAMPs and DAMP-associated processes in hematologic malignancies like AML, irrespective of the fact that these tumors are often treated with ICD inducers like anthracyclines and bortezomib.[21] Here, we assessed the exposure and/or release of various DAMPs by malignant blasts in a prospective cohort of 50 patients with

Table 3. Multivariate Cox proportional hazards analysis

	RFS		OS	
Variable	HR (95% CI)	P	HR (95% CI)	P
Age	1.05 (1.00-1.10)	.03*	1.11 (1.03-1.19)	.006*
CRT percentage	0.96 (0.91-1.01)	.12	1.01 (0.95-1.07)	.74
HSP70 percentage	0.96 (0.90-1.03)	.27	0.98 (0.90-1.06)	.54
HSP90 percentage	1.04 (0.95-1.14)	.40	1.00 (0.90-1.30)	.86
HMGB1 levels	1.00 (0.99-1.00)	.16	1.00 (0.99-1.00)	.71
BIRC5	0.40 (0.11-1.50)	.18	0.66 (0.20-2.20)	.50
BMI1	1.95 (0.92-4.12)	.08	1.44 (0.50-4.14)	.50
CCNB1	1.80 (0.38-8.59)	.46	0.36 (0.04-3.08)	.35
ELANE	0.88 (0.71-1.10)	.28	0.92 (0.67-1.25)	.58
HMMR	1.60 (0.53-4.84)	.40	2.14 (0.61-7.48)	.23
MOK	0.54 (0.24-1.21)	.13	1.04 (0.33-3.25)	.95
MPP11	0.40 (0.13-1.31)	.13	0.38 (0.10-1.40)	.15
PRAME	0.83 (0.58-1.20)	.32	1.32 (0.88-1.98)	.19
PRTN3	1.81 (1.19-2.76)	.005*	1.36 (0.86-2.15)	.19
WT1	1.04 (0.82-1.33)	.075	1.08 (0.78-1.49)	.64

*$P < .05$.

AML, before and after induction chemotherapy as well as upon the restoration of normal hematopoiesis. We found a rather heterogeneous proportion of blasts exposing CRT, HSP70, or HSP90 in patients (but not in healthy volunteers), regardless of chemotherapy (Figure 1). This observation suggests that, in the majority of patients with AML, malignant blasts experience chemotherapy-independent stress leading to the emission of danger signals, most likely as a consequence of malignant transformation itself (which imposes a considerable overload on most cellular processes, including protein synthesis and folding).[34] Accordingly, we identified a robust correlation between *CALR* expression and the expression of 3 distinct genes involved in ER stress responses (ie, *ATF4*, *HSPA5*, and *DDIT3*) among 174 patients with AML from the TCGA database (Figure 1).

By combining transcriptomic studies and flow cytometry, we demonstrated that CRT exposure on malignant blasts correlates with the activation of a tumor-targeting T_H1 immune response culminating in an increase in circulating tumor-specific IFN-γ-producing $CD4^+$ and $CD8^+$ cells (Figures 2-4). These results are in line with previous findings by us and others demonstrating that CRT exposure by neoplastic cells is associated with increased tumor infiltration by myeloid cells and effector memory $CD8^+$ T cells in patients with non–small cell lung carcinoma,[22] a high density of intratumoral T cells in patients with colorectal carcinoma,[24] and signs of a tumor-specific immune response in patients with AML.[26] Intriguingly, CRT exposure on malignant blasts also correlated with elevated amounts of circulating NK cells (Figure 3), perhaps reflecting the coexposure of HSP70 (which has previously been involved in clinically relevant antileukemia NK-cell responses).[35,36]

Importantly, exposure of CRT, HSP70, and HSP90 on malignant blasts (which was not influenced by disease subtype) was associated with improved RFS and decreased odds for relapse on univariate (but not multivariate) Cox proportional hazard analysis (Figure 5; Tables 2-3). These findings were corroborated by the association between high *CALR* mRNA levels and improved OS in 173 patients with AML from the public TCGA database (Figure 5), as well as by previous results linking CRT expression and/or exposure on neoplastic cells with improved disease outcome in patients with neuroblastoma, non–small cell lung carcinoma, colorectal carcinoma, and ovarian carcinoma.[22-24,33] Nonetheless, some studies that did monitor subcellular CRT localization failed to document a positive association between total CRT expression levels and favorable disease outcome.[16,37,38] Intriguingly, we observed improved disease outcome among CRT^{Hi} patients irrespective of the chemotherapy employed for induction or consolidation, which included potentially immunosuppressive purine analogs (ie, cytarabine). These findings suggest that the chemotherapeutic regimens evaluated in this study are compatible with the activation of a tumor-targeting immune response.

Contrary to other studies,[21] circulating HMGB1 levels did not correlate with RFS or OS in our patient cohort (supplemental Figure 7), but (1) were elevated in patients with AML as compared with healthy volunteers, and (2) returned to baseline along with the recovery of normal hematopoiesis (Figure 1). Thus, it is tempting to speculate that, in our patient cohort, serum HMGB1 may simply reflect the amount of circulating blasts (a proportion of which spontaneously releases HMGB1 in response to stress). This hypothesis remains to be formally addressed. Finally, we found that the expression level of multiple LAAs previously linked to disease outcome[31,32] was devoid of prognostic value in our patients (supplemental Figure 8). Interestingly enough, however, all LAAs studied exhibited a (statistically significant or subsignificant) trend toward downregulation in CRT^{Hi} vs CRT^{Lo} patients (supplemental Figure 8). Whether such a decrease is a consequence of LAA-targeting immune responses supported by CRT exposure remains to be elucidated. It will also be interesting to investigate whether CRT^{Hi} patients with AML are more responsive to immunotherapy than their CRT^{Lo} counterparts, reflecting the increased immunogenicity of their blasts. If this were indeed the case, monitoring CRT exposure on malignant blasts could identify a subset of patients with AML that respond to some forms of immunotherapy (knowing that AML is generally refractory to multiple immunotherapeutics).[39]

Irrespective of these incognita, CRT stands out as a robust prognostic biomarker in patients with AML treated with chemotherapy. We surmise that a similar consideration may hold true for other hematological malignancies, and we plan to test this in the near future.

Acknowledgments

The authors thank Anna Fialova for her valuable help with statistical analyses.

I.T. was supported by Student Research grant GAUK 682214 (Charles University, Prague, Czech Republic). The work of the Department of Immunology of Charles University is supported by Ministry of Health, Czech Republic-Conceptual Development of Research Organization (University Hospital Motol, Prague, Czech Republic, 00064203). O.K., L.G., and G.K. are supported by the Ligue contre le Cancer (équipe labelisée) and the European Research Council.

Authorship

Contribution: J.F., L.G., C.S., and R.S. planned the concept and design; J.F. and S.E.C. developed the methodology; J.F., I.T., M.H., L.K., I.M., S.V., J.K., and S.E.C. acquired the data; J.F., I.T., M.H., E.B., I.M., S.V., J.K., S.E.C., and I.C. analyzed and interpreted the data; J.F., I.C., O.K., G.K., L.G., C.S., and R.S. wrote, reviewed, and/or revised the manuscript; J.F. and R.S. were responsible for the study supervision.

Conflict-of-interest disclosure: The authors declare no competing financial interests.

Correspondence: Radek Spisek, Sotio, Jankovcova 1518/2, 170 00 Prague 7, Czech Republic; e-mail: spisek@sotio.com.

References

1. Kroemer G, Senovilla L, Galluzzi L, André F, Zitvogel L. Natural and therapy-induced immunosurveillance in breast cancer. *Nat Med*. 2015;21(10):1128-1138.
2. Schreiber RD, Old LJ, Smyth MJ. Cancer immunoediting: integrating immunity's roles in cancer suppression and promotion. *Science*. 2011;331(6024):1565-1570.
3. Vesely MD, Kershaw MH, Schreiber RD, Smyth MJ. Natural innate and adaptive immunity to cancer. *Annu Rev Immunol*. 2011; 29:235-271.
4. Galluzzi L, Buqué A, Kepp O, Zitvogel L, Kroemer G. Immunological effects of conventional chemotherapy and targeted anticancer agents. *Cancer Cell*. 2015;28(6): 690-714.
5. Garg AD, Dudek-Peric AM, Romano E, Agostinis P. Immunogenic cell death. *Int J Dev Biol*. 2015; 59(1-3):131-140.
6. Kroemer G, Galluzzi L, Kepp O, Zitvogel L. Immunogenic cell death in cancer therapy. *Annu Rev Immunol*. 2013;31:51-72.
7. Krysko DV, Garg AD, Kaczmarek A, Krysko O, Agostinis P, Vandenabeele P. Immunogenic cell death and DAMPs in cancer therapy. *Nat Rev Cancer*. 2012;12(12):860-875.
8. Dudek AM, Garg AD, Krysko DV, De Ruysscher D, Agostinis P. Inducers of immunogenic cancer

cell death. *Cytokine Growth Factor Rev*. 2013; 24(4):319-333.

9. Fucikova J, Kralikova P, Fialova A, et al. Human tumor cells killed by anthracyclines induce a tumor-specific immune response. *Cancer Res*. 2011;71(14):4821-4833.
10. Fucikova J, Moserova I, Truxova I, et al. High hydrostatic pressure induces immunogenic cell death in human tumor cells. *Int J Cancer*. 2014; 135(5):1165-1177.
11. Golden EB, Frances D, Pellicciotta I, Demaria S, Helen Barcellos-Hoff M, Formenti SC. Radiation fosters dose-dependent and chemotherapy-induced immunogenic cell death. *OncoImmunology*. 2014;3:e28518.
12. Bezu L, Gomes-de-Silva LC, Dewitte H, et al. Combinatorial strategies for the induction of immunogenic cell death. *Front Immunol*. 2015;6:187. doi:10.3389/fimmu.2015.00187.
13. Garg AD, Galluzzi L, Apetoh L, et al. Molecular and translational classifications of DAMPs in immunogenic cell death. *Front Immunol*. 2015;6: 588. doi:10.3389/fimmu.2015.00588.
14. Woo SR, Corrales L, Gajewski TF. Innate immune recognition of cancer. *Annu Rev Immunol*. 2015; 33:445-474.
15. Spisek R, Charalambous A, Mazumder A, Vesole DH, Jagannath S, Dhodapkar MV. Bortezomib enhances dendritic cell (DC)-mediated induction of immunity to human myeloma via exposure of cell surface heat shock protein 90 on dying tumor cells: therapeutic implications. *Blood*. 2007; 109(11):4839-4845.
16. Chao MP, Jaiswal S, Weissman-Tsukamoto R, et al. Calreticulin is the dominant pro-phagocytic signal on multiple human cancers and is counterbalanced by CD47. *Sci Transl Med*. 2010; 2(63):63ra94.
17. Michaud M, Martins I, Sukkurwala AQ, et al. Autophagy-dependent anticancer immune responses induced by chemotherapeutic agents in mice. *Science*. 2011;334(6062):1573-1577.
18. Vacchelli E, Ma Y, Baracco EE, et al. Chemotherapy-induced antitumor immunity requires formyl peptide receptor 1. *Science*. 2015; 350(6263):972-978.
19. Sistigu A, Yamazaki T, Vacchelli E, et al. Cancer cell-autonomous contribution of type I interferon signaling to the efficacy of chemotherapy. *Nat Med*. 2014;20(11):1301-1309.
20. Linkermann A, Stockwell BR, Krautwald S, Anders HJ. Regulated cell death and inflammation: an auto-amplification loop causes organ failure. *Nat Rev Immunol*. 2014;14(11):759-767.
21. Fucikova J, Moserova I, Urbanova L, et al. Prognostic and predictive value of DAMPs and DAMP-associated processes in cancer. *Front Immunol*. 2015;6:402. doi:10.3389/fimmu. 2015.00402.
22. Fucikova J, Becht E, Iribarren K, et al. Calreticulin expression in human non-small cell lung cancers correlates with increased accumulation of antitumor immune cells and favorable prognosis. *Cancer Res*. 2016;76(7): 1746-1756.
23. Hsu WM, Hsieh FJ, Jeng YM, et al. Calreticulin expression in neuroblastoma–a novel independent prognostic factor. *Ann Oncol*. 2005; 16(2):314-321.
24. Peng RQ, Chen YB, Ding Y, et al. Expression of calreticulin is associated with infiltration of T-cells in stage IIIB colon cancer. *World J Gastroenterol*. 2010;16(19):2428-2434.
25. Vaksman O, Davidson B, Tropé C, Reich R. Calreticulin expression is reduced in high-grade ovarian serous carcinoma effusions compared with primary tumors and solid metastases. *Hum Pathol*. 2013;44(12):2677-2683.
26. Wemeau M, Kepp O, Tesnière A, et al. Calreticulin exposure on malignant blasts predicts a cellular anticancer immune response in patients with acute myeloid leukemia. *Cell Death Dis*. 2010;1:e104.
27. Kepp O, Senovilla L, Vitale I, et al. Consensus guidelines for the detection of immunogenic cell death. *OncoImmunology*. 2014;3(9):e955691.
28. Kepp O, Galluzzi L, Lipinski M, Yuan J, Kroemer G. Cell death assays for drug discovery. *Nat Rev Drug Discov*. 2011;10(3):221-237.
29. Galluzzi L, Bravo-San Pedro JM, Kroemer G. Organelle-specific initiation of cell death. *Nat Cell Biol*. 2014;16(8):728-736.
30. Greiner J, Schmitt M, Li L, et al. Expression of tumor-associated antigens in acute myeloid leukemia: Implications for specific immunotherapeutic approaches. *Blood*. 2006; 108(13):4109-4117.
31. Zhang L, Greiner J. Leukemia-associated antigens are immunogenic and have prognostic value in acute myeloid leukemia. *Immunotherapy*. 2011;3(6):697-699.
32. Anguille S, Van Tendeloo VF, Berneman ZN. Leukemia-associated antigens and their relevance to the immunotherapy of acute myeloid leukemia. *Leukemia*. 2012;26(10): 2186-2196.
33. Garg AD, Elsen S, Krysko DV, Vandenabeele P, de Witte P, Agostinis P. Resistance to anticancer vaccination effect is controlled by a cancer cell-autonomous phenotype that disrupts immunogenic phagocytic removal. *Oncotarget*. 2015;6(29):26841-26860.
34. Hanahan D, Weinberg RA. Hallmarks of cancer: the next generation. *Cell*. 2011;144(5):646-674.
35. Elsner L, Flügge PF, Lozano J, et al. The endogenous danger signals HSP70 and MICA cooperate in the activation of cytotoxic effector functions of NK cells. *J Cell Mol Med*. 2010;14(4): 992-1002.
36. Stringaris K, Sekine T, Khoder A, et al. Leukemia-induced phenotypic and functional defects in natural killer cells predict failure to achieve remission in acute myeloid leukemia. *Haematologica*. 2014;99(5):836-847.
37. Erić A, Juranić Z, Milovanović Z, et al. Effects of humoral immunity and calreticulin overexpression on postoperative course in breast cancer. *Pathol Oncol Res*. 2009;15(1):89-90.
38. Suzuki Y, Mimura K, Yoshimoto Y, et al. Immunogenic tumor cell death induced by chemoradiotherapy in patients with esophageal squamous cell carcinoma. *Cancer Res*. 2012; 72(16):3967-3976.
39. Rashidi A, Walter RB. Antigen-specific immunotherapy for acute myeloid leukemia: where are we now, and where do we go from here? *Expert Rev Hematol*. 2016;9(4): 335-350.
40. Grimwade D, Hills RK, Moorman AV, et al, National Cancer Research Institute Adult Leukaemia Working Group. Refinement of cytogenetic classification in acute myeloid leukemia: determination of prognostic significance of rare recurring chromosomal abnormalities among 5876 younger adult patients treated in the United Kingdom Medical Research Council trials. *Blood*. 2010;116(3):354-365.

2016 128: 3113-3124
doi:10.1182/blood-2016-08-731737 originally published online November 1, 2016

Calreticulin exposure by malignant blasts correlates with robust anticancer immunity and improved clinical outcome in AML patients

Jitka Fucikova, Iva Truxova, Michal Hensler, Etienne Becht, Lenka Kasikova, Irena Moserova, Sarka Vosahlikova, Jana Klouckova, Sarah E. Church, Isabelle Cremer, Oliver Kepp, Guido Kroemer, Lorenzo Galluzzi, Cyril Salek and Radek Spisek

Blood (print ISSN 0006-4971, online ISSN 1528-0020), is published weekly by the American Society of Hematology, 2021 L St, NW, Suite 900, Washington DC 20036.

5.4. Dendritické buňky připravené v médiu CellGro protokolem zkrácené diferenciace a aktivované Poly (I:C) za účelem imunoterapie nádorových onemocnění jsou porovnatelné s dendritickými buňkami připravenými standardním 5-ti denním protokolem

Dendritické buňky používané v rámci imunoterapeutických vakcín založených na DCs jsou nejčastěji diferencovány protokolem zahrnujícím kultivaci monocytů v přítomnosti IL-4 a GM-CSF po dobu 5-7 dní. Výroba těchto imunoterapeutických produktů musí probíhat za podmínek správné výrobní praxe (GMP) a řídí se protokoly schvalovanými regulačními institucemi. Tento proces zahrnuje validované čisté prostory, GMP materiál a speciálně vyškolený personál, což znamená značnou finanční a časovou náročnost. Z tohoto důvodu bylo v rámci různých studií testováno zkrácení protokolu diferenciace DCs, které by pomohlo zredukovat množství laboratorní práce, zvýšit efektivitu práce v čistých prostorech a kapacitu GMP zařízení.

V této práci jsme hodnotili použití zkrácené verze našeho standardního certifikovaného protokolu na přípravu DCs. Porovnávali jsme DCs diferencované po dobu 3 dní s DCs vyrobenými během 5 dní (standartní protokol) v GMP médiu CellGro, konkrétně jejich morfologii, životnost, schopnost fagocytovat a jejich potenciál odpovídat na aktivační stimuly (Poly (I:C) a LPS), produkovat cytokiny a indukovat antigen-specifické T lymfocyty. Výtěžek nezralých DCs, jejich životnost a schopnost pohlcovat nádorové linie inaktivované UVB byly v obou případech stejné, pouze DCs kultivované po dobu 5 dní měly větší velikost a byly více granulární. Dendritické buňky připravené standardním protokolem a aktivované Poly (I:C) exprimovaly více CD80, CD86 a HLA-DR v porovnání s DCs vyrobenými 3 denním protokolem. Nicméně standardní a 3 denní DCs aktivované LPS byly fenotypicky identické. Produkce IL-6, TNF-α, IL-12p70, IL-1β a IL-10 DCs byla obecně vyšší, pokud byl jako

aktivační signál použit LPS a nezaznamenali jsme signifikantní rozdíly mezi 5-ti denními a 3 denními DCs. Důležitým zjištěním bylo, že standardní DCs a DCs připravené zkráceným protokolem měly porovnatelnou schopnost indukovat antigen-specifické $CD8^+$ T lymfocyty a regulační T lymfocyty. Dendritické buňky diferencované z monocytů během zkráceného 3 denního protokolu jsou tedy v nejdůležitějších funkčních aspektech porovnatelné se standardními DCs. Tato preklinická data ukazují, jak mohou být GMP protokoly pro přípravu DCs pro klinické použití flexibilně a efektivně modifikovány.

Immunology Letters 160 (2014) 39–49

Contents lists available at ScienceDirect

Immunology Letters

journal homepage: www.elsevier.com/locate/immlet

Day 3 Poly (I:C)-activated dendritic cells generated in CellGro for use in cancer immunotherapy trials are fully comparable to standard Day 5 DCs

Iva Truxova[a,b], Katerina Pokorna[b], Kamila Kloudova[b], Simona Partlova[a,b], Radek Spisek[a,b], Jitka Fucikova[a,b,*]

[a] Department of Immunology, Charles University, Second Faculty of Medicine and University Hospital Motol, Prague, Czech Republic
[b] Sotio, Prague, Czech Republic

ARTICLE INFO

Article history:
Received 8 November 2013
Received in revised form 19 March 2014
Accepted 26 March 2014
Available online 12 April 2014

Keywords:
Dendritic cell
Monocyte
Fast generation
Cancer immunotherapy
Vaccine

ABSTRACT

Background: Dendritic cells (DCs) are professional antigen-presenting cells that are capable of inducing immune responses. DC-based vaccines are normally generated using a standard 5- to 7-day protocol. To shorten the DC-based vaccine production for use in cancer immunotherapy, we have developed a fast DC protocol by comparing standard DCs (Day 5 DCs) and fast DCs (Day 3 DCs).
Methods: We tested the generation of Day 5 versus Day 3 DCs using CellGro media and subsequent activation by two activation stimuli: Poly (I:C) and LPS. We evaluated DC morphology, viability, phagocyte activity, cytokine production and ability to stimulate antigen-specific T cells.
Results: Day 5 and Day 3 DCs exhibited similar phagocytic capacity. Poly (I:C)-activated Day 5 DCs expressed higher levels of the costimulatory and surface molecules CD80, CD86 and HLA-DR compared to Poly (I:C)-activated Day 3 DCs. Nevertheless, LPS-activated Day 5 and Day 3 DCs were phenotypically similar. Cytokine production was generally stronger when LPS was used as the maturation stimulus, and there were no significant differences between Day 5 and Day 3 DCs. Importantly, Day 5 and Day 3 DCs were able to generate comparable numbers of antigen-specific $CD8^+$ T cells. The number of Tregs induced by Day 5 and Day 3 DCs was also comparable.
Conclusion: We identified monocyte-derived DCs generated in CellGro for 3 days and activated using Poly (I:C) similarly potent in most functional aspects as DCs produced by the standard 5 day protocol. These results provide the rationale for the evaluation of faster protocols for DC generation in clinical trials.

1. Introduction

Dendritic cells (DCs) are the most potent antigen-presenting cells in the human immune system. Due to their unique ability to prime and stimulate both $CD8^+$ and $CD4^+$ T cells, DCs loaded with whole tumor cells and tumor lysates have been investigated in a number of clinical trials for their ability to induce anti-tumor T cell responses [1]. Encouraging immunologic and therapeutic responses have been observed in cancer patients treated with DC vaccines, leading to an increased interest in developing protocols for the clinical-scale production of DCs [2–6]. The most widely used DCs for clinical trials are the myeloid DCs that are differentiated from peripheral blood monocytes in the presence of recombinant granulocyte–macrophage colony-stimulating factor (GM-CSF) and interleukin 4 (IL-4). In most trials, 5- to 7-day protocols are used to generate fully differentiated DCs [7–11]. These DCs resemble immature DCs and exhibit a high phagocytic capacity. When they encounter proinflammatory, microbial, or T cell-derived stimuli, Day 7 DCs become activated and upregulate surface markers such as CD80, CD86, CD40, MHC and chemokine receptors, such as CCR7. Therefore, mature DCs acquire the capacity to migrate to the T cell areas of draining secondary lymphoid organs, where they encounter naive T cells and induce antigen-specific T cell responses [12,13]. It is now mandatory that DC-based vaccine manufacturing complies with the strict guidelines of regulatory agencies for use of cellular therapy products and proceeds according to Good Manufacturing Practices (GMPs). This process

Abbreviations: DC, dendritic cell; APC, antigen-presenting cell; GMP, good manufacturing practice; Poly (I:C), polyriboinosinic polyribocytidylic acid; TLR, toll-like receptor; LPS, lipopolysacharide; GM-CSF, granulocyte–macrophage colony stimulating factor.

* Corresponding author at: Institute of Immunology, Charles University, Second Faculty of Medicine, V Úvalu 84, Prague 5, Czech Republic. Tel.: +420 224 435 963.
E-mail addresses: jitka.fucikova@fnmotol.cz, fucikova@sotio.com (J. Fucikova).

http://dx.doi.org/10.1016/j.imlet.2014.03.010
0165-2478/

includes validated clean rooms, trained staff and GMP materials. These requirements make the manufacturing of DC-based products laborious and costly. Therefore, to manufacture DC-based products for cancer immunotherapy, shorter DC differentiation protocols have been investigated to reduce the amount of lab work, increase the turnover rate in clean boxes and increase the capacity of GMP facilities. Several groups have established short-term experimental protocols in which monocytes were exposed for 2–3 days to recombinant GM-CSF and IL-4 [14–16]. In this study, we evaluated a shortened version of our standard regulatory agency's-certified protocol. We compared the generation of Day 5 DCs versus Day 3 DCs using GMP compliant reagents, and evaluated their morphology, viability, endocytic capacity, activation status, ability to produce cytokines and capacity to induce antigen-specific T cells and regulatory T cells. We demonstrate that Day 3 clinical grade monocyte-derived DCs are comparable to standard DCs in all important functional aspects. Thus, this study provides important preclinical data for more flexible and cost effective modifications of GMP compliant protocols for clinical grade DC generation.

2. Materials and methods

2.1. Generation of dendritic cells

Immature monocyte-derived DCs (moDCs) were generated as previously described [17]. Briefly, peripheral blood mononuclear cells (PBMCs) were isolated from buffy coats of healthy HLA-A2$^+$ or HLA-A2$^-$ donors by Ficoll-Paque PLUS gradient centrifugation (GE Healthcare, Uppsala, Sweden) and monocytes were isolated by plastic adherence after 2 h of cell adhesion (75×10^6 PBMCs) in Nunclon 75-cm^2 culture flasks (Nunc). To generate standard immature Day 5 moDCs, adherent monocytes were subsequently cultured for 5 days in serum-free CellGro DC media (CellGenix) in the presence of GM-CSF (Gentaur) at a concentration of 500 U/ml and 20 ng/ml of IL-4 (Gentaur). After 3 days of culture, fresh CellGro and cytokines were added to the culture flasks. After 5 days, immature DCs were seeded in Nunclon 48-well plates (5×10^5 DCs in 500 μl of CellGro supplemented with cytokines per well) and activated for 24 h using Poly (I:C) (InvivoGen) at 25 μg/ml or LPS (Sigma–Aldrich) at 1 μg/ml. Alternatively, monocytes were cultured for 3 days in CellGro with GM-CSF (500 U/ml) and IL-4 (20 ng/ml) (immature Day 3 moDCs), followed by incubation with the same maturation stimulus (Poly (I:C) or LPS) for 24 h. Immature and mature DCs were used for further studies. For cocultures, a fraction of the PBMCs was cryopreserved, thawed and used for generation of DCs for restimulation. Non-adherent monocyte-depleted PBMCs were frozen and used as lymphocytes for cocultures with DCs.

2.2. Flow cytometry

Immature and mature Day 5 and Day 3 DCs were phenotyped using the following monoclonal antibodies: CD80-FITC, CD86-PE, CD83-PE-Cy5 (Beckman Coulter), CD14-PE-Dy590, CD11c-APC (Exbio) and HLA-DR-PE-Cy7 (BD Biosciences). The cells were stained for 20 min at 4 °C, washed twice in PBS and analyzed using LSRFortessa (BD Biosciences) with FlowJo software (Tree Star). DCs were gated according to their FSC and SSC properties and as CD11c positive cells. Only viable DCs (DAPI negative cells) were included in the analysis. DAPI was purchased from Invitrogen.

2.3. Cytokine measurements

Cytokines in supernatants, released from immature and mature DCs, were measured using Milliplex Human Cytokine/Chemokine kit (Millipore) according to the manufacturer's instructions and analyzed by Luminex 200 (Luminex). Six cytokines were measured including IL-12p70, IL-6, IL-1β, TNF-α, IL-10 and IFN-α.

2.4. Uptake of UVB-irradiated cancer cells by DCs

LNCap prostate adenocarcinoma cell line and OV-90 ovarian cancer cell line were cultured in RPMI 1640 (Gibco) supplemented with 10% heat-inactivated FBS (PAA), 2 mM GlutaMAX I CTS (Gibco) and 100 U/ml penicillin + 100 μg/ml streptomycin (Gibco). For flow cytometry analysis of phagocytosis, tumor cells were harvested and labeled with Vybrant DiD cell labeling solution (Invitrogen). A fraction of tumor cells were labeled with Vybrant DiI cell labeling solution (Invitrogen) and used for fluorescent microscopy analysis. To prepare UVB-irradiated cells, stained LNCap or OV-90 cells were seeded in CellGro media in Nunclon 25-cm^2 culture flasks (Nunc) at a concentration of 4×10^5 cells/ml and subjected to a 302 nm UVB-irradiation for 10 min to induce apoptosis. Cells were then incubated for 48 h at 37 °C with 5% CO_2 before use. To determine the uptake of UVB-irradiation killed tumor cells by DCs, immature Day 5 or Day 3 DCs were stained with Vybrant DiO cell labeling solution (Invitrogen) and cocultured with LNCap or OV-90 cells at a cell ratio of 5:1 in Nunclon U-bottom 96-well plates (Nunc) for 24 h at 37 °C with 5% CO_2. Parallel control cultures were set up for 24 h on ice to evaluate the passive transfer of dye or labeled tumor fragments to DCs. The phagocytic ability of DCs was evaluated by flow cytometry and fluorescent microscopy.

2.5. Fluorescent microscopy

A suspension of labeled DCs and tumor cells was incubated on cover slips for 30 min at 37 °C with 5% CO_2. Then, cells were washed in PBS, fixed with 4% paraformaldehyde for 25 min, washed twice in PBS and mounted on slides with ProLong Gold antifade reagent (Invitrogen).

2.6. Expansion of antigen-specific T-lymphocytes and intracellular IFN-γ staining

Immature DCs were activated for 4 h with Poly (I:C) (25 μg/ml) or LPS (1 μg/ml). Activated DCs were then pulsed with HLA-A2-restricted peptide from influenza MP (flu-MP) (GILGFVFTL) (Jpt peptide technologies) at 2.4 μg/ml or with CEF peptide mix (Jpt peptide technologies) at 2.5 μg/ml. We also pulsed DCs with purified protein derivative of tuberculin (PPD) from *Mycobacterium tuberculosis* at 1 μg/ml, 5 μg/ml and 10 μg/ml and tetanus toxoid at 1 μg/ml. DCs were incubated with peptides and proteins overnight. Non-adherent peripheral blood lymphocytes (PBL) (2×10^5 in RPMI-1640 + 10% AB human serum (Invitrogen)) and the mature pulsed DCs (4×10^4 in CellGro) were cocultured at a ratio of 5:1 in U-bottom 96-well plates for 7 days. A total of 20 U/ml of IL-2 (PeproTech) was added on days 3 and 5. On day 7, the lymphocytes were restimulated with fresh peptide or protein-loaded DCs, and the frequency of antigen-specific CD8$^+$ and CD4$^+$ T cells was determined using intracellular staining for IFN-γ. Brefeldin A (BioLegend) was added to block the extracellular release of IFN-γ 1.5 h after restimulation. After 3 h of incubation with Brefeldin A, the cells were washed in PBS, stained with anti-CD3-PerCP-Cy5.5 (eBioscience), CD4-PE-Cy7 (eBioscience) and CD8-PE-Dy590 antibody (Exbio), fixed using Fixation Buffer (eBioscience), permeabilized with Permeabilization Buffer (eBioscience) and stained using anti-IFN-γ-FITC antibody (BD Biosciences). Cells were acquired using the LSRFortessa (BD Biosciences) and analyzed with FlowJo software (Tree Star).

2.7. Isolation of naive CD4+ T cells and induction of Tregs by activated DCs

$CD4^+CD25^-$ T cells were isolated from non-adherent peripheral blood lymphocytes by depleting $CD25^+$ cells using the EasySep Human $CD4^+CD25^{high}$ T cell isolation kit (STEMCELL Technologies). The purity of the cell population was verified by flow cytometry. Purified $CD4^+CD25^-$ T cells (2×10^5 in RPMI-1640 + 10% AB human serum) and the mature peptide-pulsed DCs (4×10^4 in CellGro) were cocultured at a ratio of 5:1 in U-bottom 96-well plates for 7 days. A total of 20 U/ml of IL-2 (PeproTech) was added on days 3 and 5. On day 7, the cells were stained with anti-CD4-PE-Cy7 (eBioscience) and anti-CD25-PerCP-Cy5.5 antibody (BioLegend), fixed with Fixation buffer (eBioscience), permeabilized with Permeabilization Buffer (eBioscience) and stained using anti-FoxP3-Alexa Fluor 488 antibody (eBioscience) [18]. The cells were acquired using LSRFortessa (BD Biosciences) and analyzed with FlowJo software (Tree Star).

2.8. Extraction of genomic DNA and quantitative real time PCR-based methylation assay

Genomic DNA (gDNA) was isolated from a lysate of 2×10^6 autologous induced Tregs using the PureLink Genomic DNA Mini kit (Invitrogen, Carlsbad, USA). One to 2 μg of gDNA was treated with sodium bisulfite using the MethylCode Bisulfite Conversion kit (Invitrogen, Carlsbad, USA). Methylated and demethylated *FoxP3* TSDR sequences were amplified by Platinum Taq DNA polymerase (Invitrogen, Carlsbad, USA) in quantitative real-time PCR amplification assay. PCR reactions were performed using a CFX 96 cycler (BioRad, Hercules, USA) with an appropriate cycling protocol (95 °C for 3 min followed with 50 cycles at 95 °C for 15 s and 60 °C for 1 min). Methylation-specific and demethylation-specific primers and TaqMan© probes were commercially synthesized (TIB MOLBIOL, Berlin, Germany). Amounts of methylated and demethylated *FoxP3* TSDR DNA were estimated from calibration curves by crossing points linear regression using the second derivative maximum method. The proportion of cells with a demethylated *FoxP3* TSDR was calculated as the ratio of demethylated *FoxP3* TSDR DNA to the sum of methylated and demethylated *FoxP3* TSDR DNA [19,20].

2.9. Statistical analysis

The data were analyzed by One-Way ANOVA with Dunnett's multiple comparison post hoc test and Student's unpaired two-tailed *t* test using GraphPad Prism 5 (San Diego, California, USA). The results were considered statistically significant when $p < 0.05$.

3. Results

3.1. The yield, viability and morphology of immature Day 5 and Day 3 DCs

We first compared the characteristics of Day 5 and Day 3 DCs differentiated in CellGro from 75×10^6 PBMCs. There were no significant differences detected either in the yield of immature Day 5 and Day 3 DCs (Fig. 1A) or their viability (Fig. 1B). In contrast, FSC/SSC analysis showed that Day 5 DCs were larger in size and more granular than Day 3 DCs (Fig. 1C).

3.2. Immunophenotype of Day 5 and Day 3 DCs following maturation

To determine the capacity of immature Day 5 and Day 3 DCs to be activated by Toll-like receptor ligands (Poly (I:C) or LPS), we evaluated the expression of costimulatory molecules CD80 and CD86, CD83 and MHC class II after 24 h incubation with maturation stimuli. As a control, immature DCs were incubated for 24 h in the presence of IL-4 and GM-CSF. The phenotype analyses revealed that exposure of immature DCs to LPS significantly upregulated the expression of all costimulatory molecules and HLA-DR (Fig. 2). Additionally, the downregulation of CD14 expression was not statistically significant. We did not detect any significant differences between LPS-activated Day 5 and Day 3 DCs in the expression of maturation-associated molecules. Poly (I:C) induced weaker phenotypic maturation compared to LPS, and Poly (I:C)-activated Day 5 DCs expressed higher levels of CD80, CD86 and HLA-DR compared to Day 3 DCs.

3.3. Cytokine production by mature Day 5 and Day 3 DCs

We measured the production of IL-12p70, IL-6, IL-1β, TNF-α, IFN-α and IL-10 by Poly (I:C)- or LPS-activated Day 5 and Day 3 DCs. As a control, immature DCs were incubated for 24 h in the presence of IL-4 and GM-CSF. Cytokine production was stronger when LPS was used as a maturation stimulus (Fig. 3). DCs activated by LPS produced high levels of all cytokines, except for IFN-α, when compared to immature and Poly (I:C)-activated DCs (as there was a high variability in IL-12p70 secretion between individual donors, difference in IL-12p70 secretion was not statistically significant), and there were no significant differences between Day 5 and Day 3 DCs. In contrast, Poly (I:C) only induced production of IL-6 and IFN-α. TNF-α was only weakly secreted by Poly (I:C)-activated DCs and at the same levels as by immature DCs. The levels of IL-1β and IL-10 were almost undetectable. Furthermore, there was an absence of IL-12p70 in culture supernatants from Poly (I:C)-activated DCs. When we compared Day 5 and Day 3 Poly (I:C)-activated DCs, Day 5 DCs secreted relatively high amounts of IL-6 and IFN-α. However, this difference was not statistically significant.

3.4. Phagocytic ability of immature Day 5 and Day 3 DCs

To assess the uptake of killed tumor cells via phagocytosis, immature DiO labeled Day 5 and Day 3 DCs were cultured in the presence of IL-4 and GM-CSF and incubated with DiD or DiI labeled UVB-irradiation killed LNCap or OV-90 cells for 24 h at 37 °C and 5% CO_2. As a control, DCs and tumor cells were incubated for 24 h on ice. DCs that phagocytosed killed tumor cells were identified as DiO^+DiD^+ double-positive cells. We did not detect any significant differences in the uptake of UVB-irradiation killed LNCap and OV-90 cells (Fig. 4), and immature Day 5 and Day 3 DCs showed similar phagocytic capabilities. The uptake of killed tumor cells by immature DCs was confirmed to be an active process, as the passive transfer of tumor fragments onto DC surfaces on ice was minimal (<15%, data not shown). Furthermore, fluorescent microscopy revealed that killed LNCap and OV-90 cells, or their fragments, were present inside the DCs, indicating that immature Day 5 and Day 3 DCs were able to fully engulf killed tumor cells (Fig. 4C).

3.5. In vitro capacity of mature Day 5 and Day 3 DCs to induce antigen-specific T cells

We evaluated the capacity of mature DCs to expand influenza MP, CEF peptide mix, PPD and tetanus toxoid-specific T cells. Mature Day 5 and Day 3 DCs generated in CellGro media were pulsed with antigens and used for the expansion of antigen-specific T cells for 7 days. The frequency of IFN-γ-producing T cells was analyzed one week later, after restimulation with identical peptide or protein-loaded DCs. As a control, lymphocytes were cocultured with immature DCs or Poly (I:C)- or LPS-activated DCs without

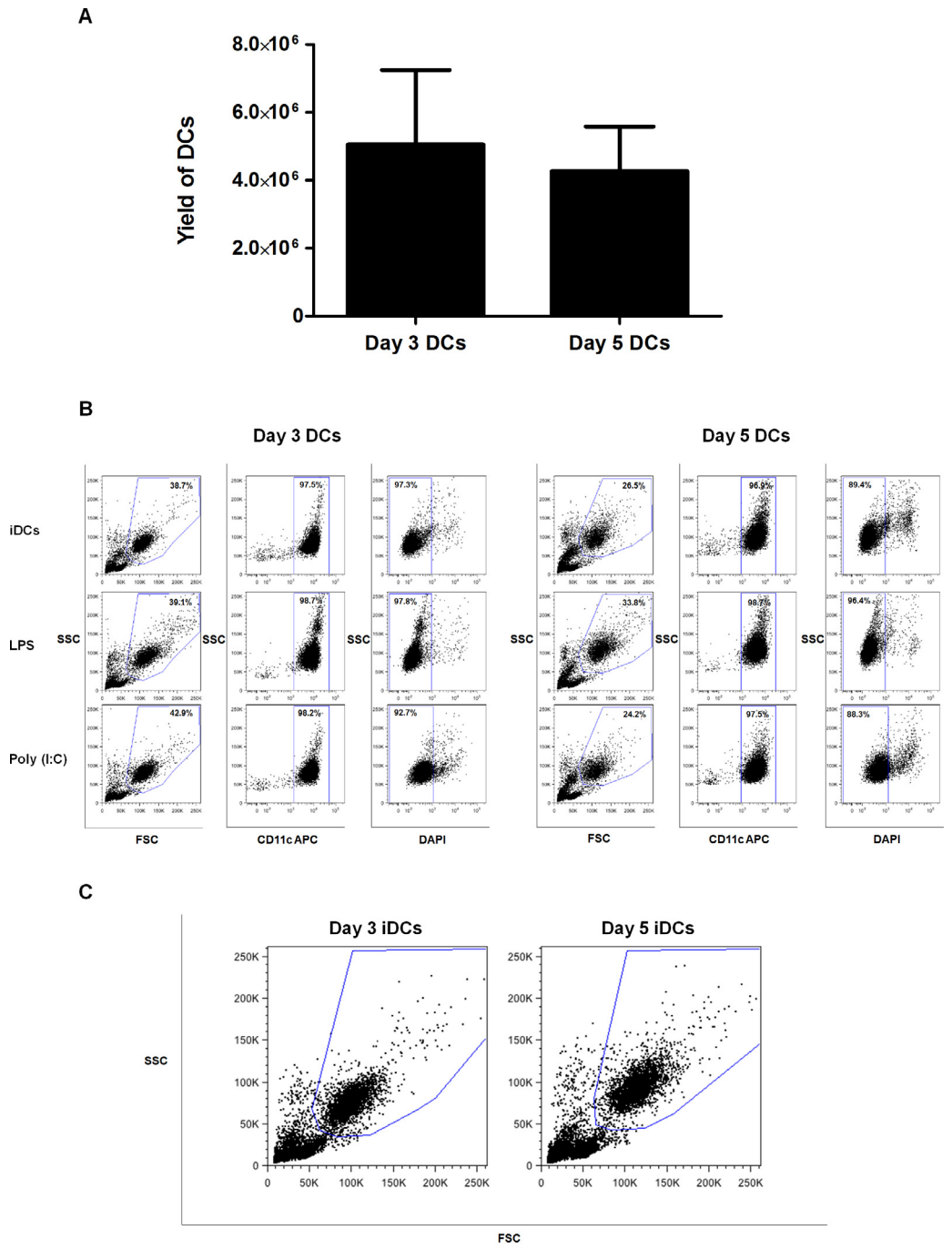

Fig. 1. Characteristics of immature Day 5 and Day 3 DCs. (A) Total number of immature Day 5 and Day 3 DCs that were generated from 75×10^6 of PBMCs in CellGro. Data are presented as the mean ± SD for 7 independent experiments. (B) Purity (percentage of $CD11c^+$ DCs) and viability (percentage of $DAPI^-$ cells) of immature and maturation stimuli-activated Day 5 and Day 3 DCs. One of seven performed experiments is presented. (C) Morphology of Day 5 and Day 3 DCs. Day 5 DCs were larger in size and were more granular compared to Day 3 DCs.

added peptides. Antigen-loaded Poly (I:C), as well as LPS-activated, Day 3 DCs were equally effective at inducing the expansion of antigen-specific $CD8^+$ T cells compared to Day 5 DCs (Fig. 5A and B). The strongest response was observed when CEF peptide mix-loaded Poly (I:C)-activated DCs were used for the stimulation of autologous T cells. The results showed that Day 3 DCs were as potent as Day 5 DCs in stimulating antigen-specific $CD8^+$ T cells. There was no difference between Day 3 and Day 5 DCs regarding to their capacity to induce expansion of influenza MP and CEF peptide mix-specific $CD4^+$ T cells. However, the number of induced peptide-specific $CD4^+$ T cells was in general low. The reason for this is a fact that peptides used for pulsation of dendritic cells are MHC class I-restricted and thus primarily $CD8^+$ T cell responses can be observed. Conversely, stimulation of T cells by protein-loaded DCs led to massive expansion of antigen-specific $CD4^+$ T cells (especially in case of PPD protein). PPD and tetanus toxoid-loaded LPS-activated Day 3 and Day 5 DCs were able to induce similar numbers of antigen-specific $CD4^+$ T cells. Poly (I:C)-activated Day 3 DCs were less potent in inducing antigen-specific $CD4^+$ T cells compared to Day 5 DCs (Fig. 5C).

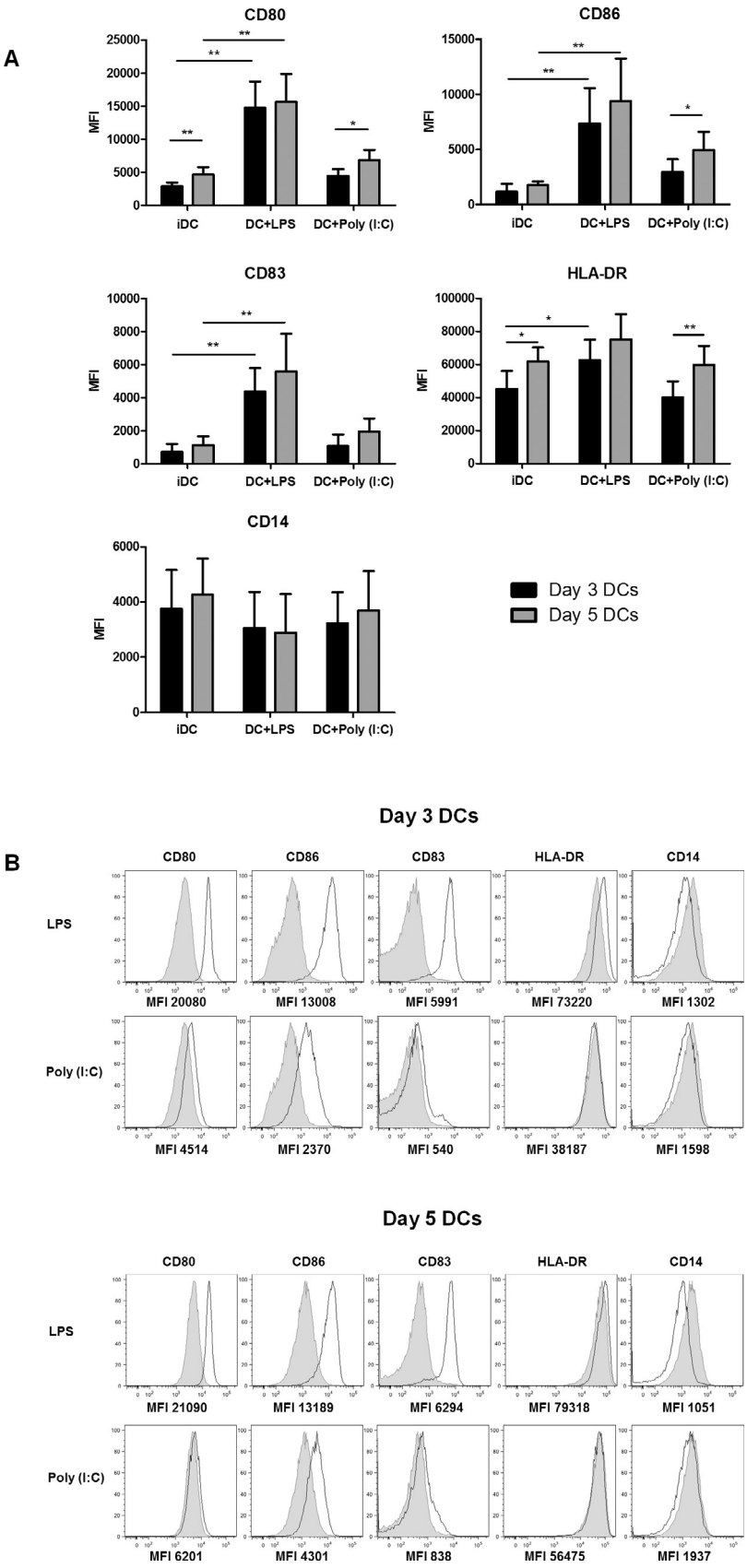

Fig. 2. The phenotype of Day 5 and Day 3 DCs activated for 24 h using LPS or Poly (I:C). The summary of six independent experiments ± SD (A) and representative histograms (B) are shown. Significant differences are shown ($^{*}P$ value ≤ 0.05, $^{**}P$ value ≤ 0.01). Gray histograms represent the expression of maturation-associated molecules on immature DCs. MFI values below the histograms represent the expression of individual markers on mature DCs (white histograms).

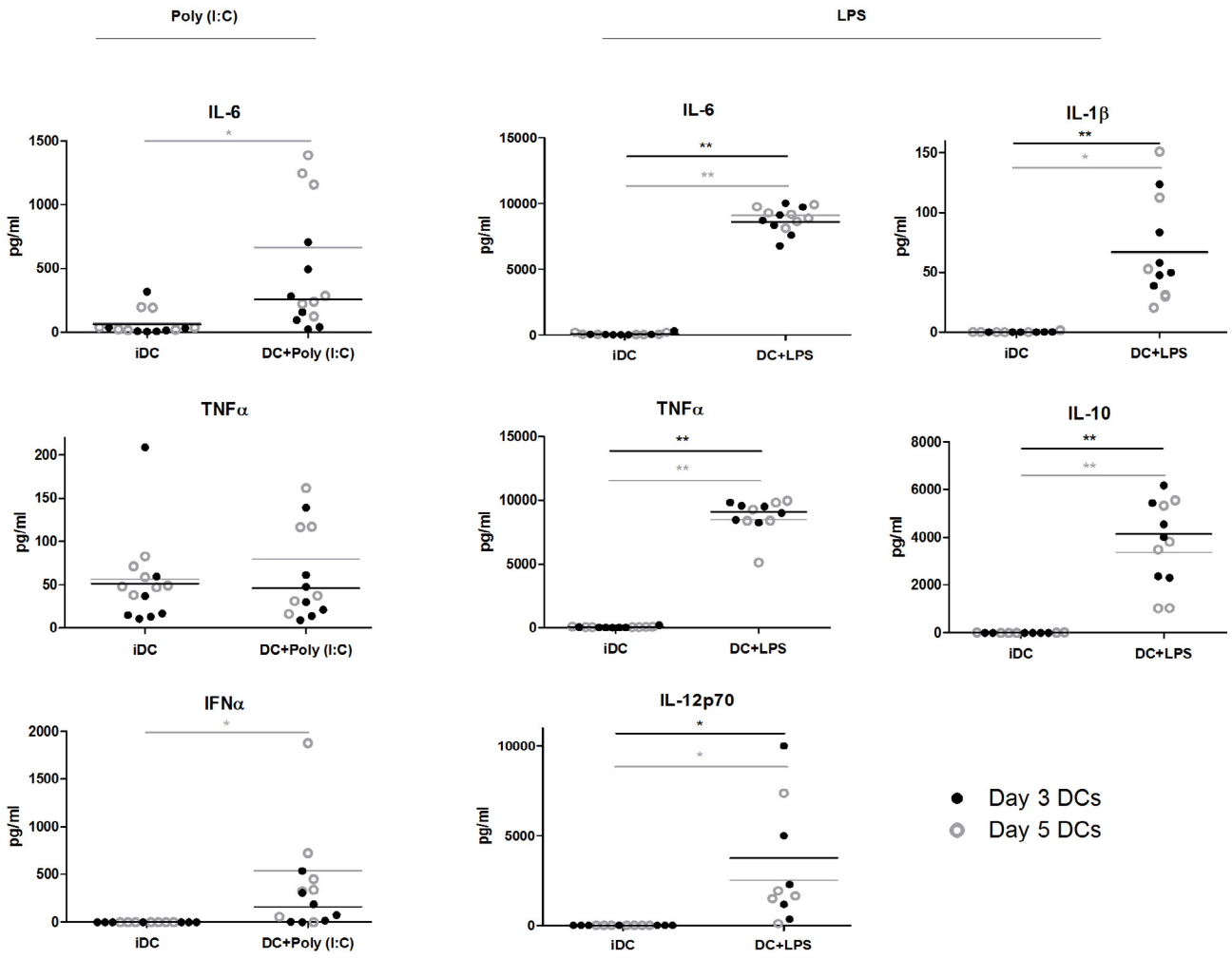

Fig. 3. Cytokine production by mature Day 5 and Day 3 DCs. Concentration of six cytokines – IL-12p70, IL-6, IL-1β, TNF-α, IL-10 and IFN-α was measured in supernatants from immature and mature Day 5 and Day 3 DCs. The data from seven independent experiments ± SD are shown. Significant differences are shown ($^{*}P$ value ≤ 0.05, $^{**}P$ value ≤ 0.01).

3.6. *Capacity of mature Day 5 and Day 3 DCs to induce regulatory T cells from CD4^{+}CD25^{-} T cells*

We tested the capacity of activated peptide-pulsed Day 5 and Day 3 DCs to induce regulatory T cells (Tregs). Tregs induced after 7 days of DC and T cell cocultures were determined to be CD4^{+}CD25^{high}FoxP3^{+} T cells. In general, immature DCs generated the highest numbers of Tregs. There was not a significant difference in the numbers of Tregs induced by DCs that were activated by either LPS or Poly (I:C). LPS or Poly (I:C)-activated Day 3 DCs generated slightly lower numbers of Tregs compared to LPS or Poly (I:C)-activated Day 5 DCs (Fig. 6A and B). This finding was further confirmed using a quantitative real-time PCR-based methylation assay, which assessed the percentage of stable Tregs that were demethylated at *FoxP3* TSDR (Fig. 6C).

4. Discussion

The production of DCs for clinical use has to comply with the European Medicines Agency guideline on advanced therapy medicinal products EC1394/2007. These guidelines include requirements of validated clean rooms, trained staff and GMP certified materials, which makes the manufacturing of DC-based products laborious, time consuming and costly. Therefore, modifications of standard protocols for DC generation are sought to reduce the amount of lab work, increase the turnover rate in clean boxes and increase the capacity of GMP facilities while still maintaining the functional characteristics of generated DCs. DCs are typically differentiated from blood monocytes for 5–7 days in the presence of GM-CSF and IL-4 and then activated by proinflammatory or microbial stimuli for another 1–3 days (standard DCs) [7–9,11,21]. We tested a shorter version of the protocol for clinical grade DC differentiation that is used in our laboratory for the production of DCs for cancer immunotherapy clinical trials. Generated DCs were tested for several criteria that reflect their function, such as upregulation of maturation markers, expression of costimulatory molecules, cytokine production, capacity to activate antigen-specific T cells and capacity to expand regulatory T cells and these criteria were compared to standard Day 5 DCs.

There have been many studies carried out by Dauer et al. [14] regarding rapid generation of DCs. To test a shorter protocol for DC generation that is compatible with clinical use, we cultured the monocyte-derived DCs in GMP-certified CellGro DC media, and DCs were activated using Poly (I:C) that is available in GMP quality. We report that DCs can be differentiated from human monocytes within 3 days of *in vitro* culture. Three day- and 5 day-cultivation of adherent monocytes in CellGro media in the presence of GM-CSF and IL-4 yielded similar numbers of viable immature DCs. Although

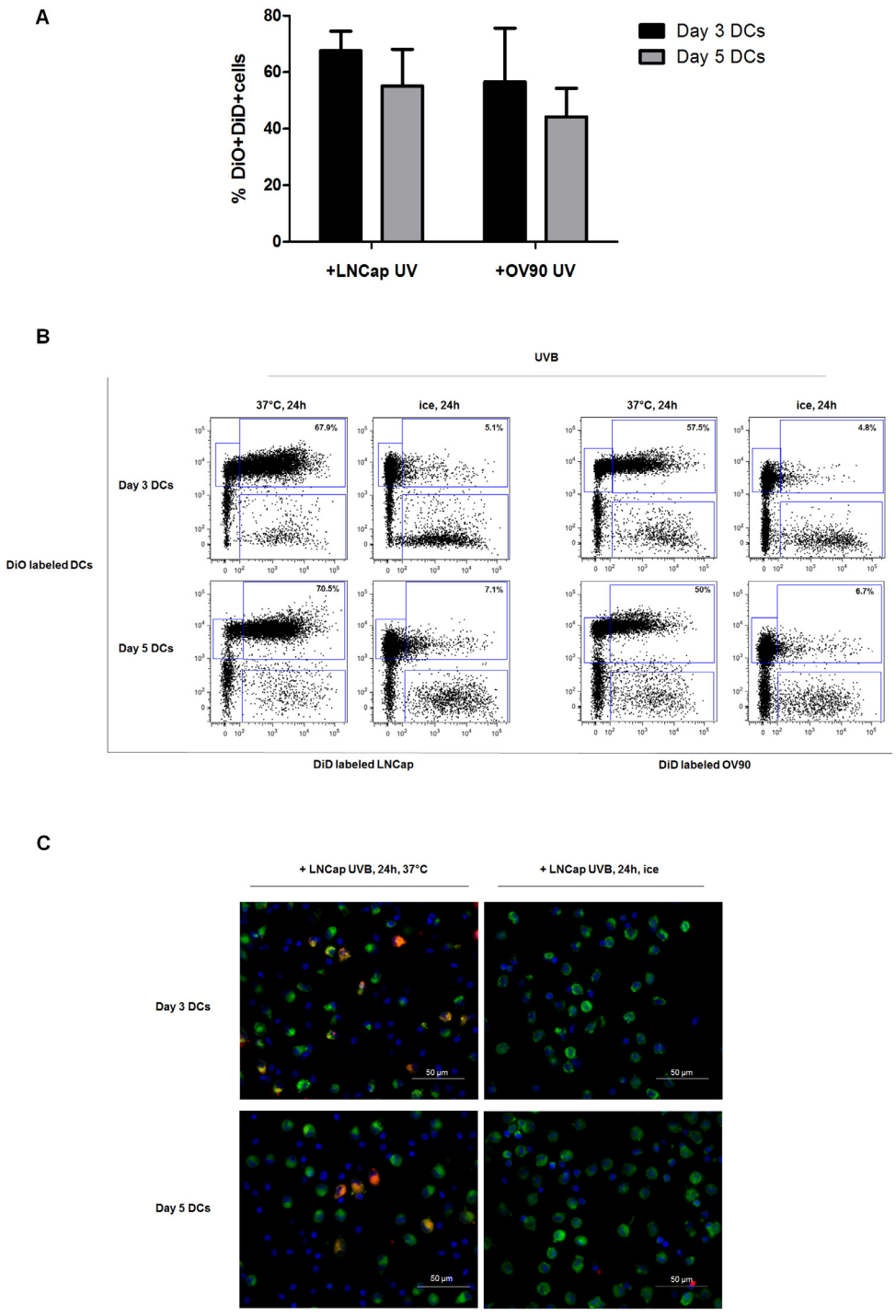

Fig. 4. Phagocytic ability of immature Day 5 and Day 3 DCs. (A) DiO-labeled immature Day 5 and Day 3 DCs were cocultured with DiD-labeled UVB-killed LNCap or OV-90 cells at 37 °C for 24 h. As a control, DCs and tumor cells were cocultured on ice for 24 h (data not shown). DCs that phagocytosed killed tumor cells were identified as DiO^+DiD^+ double-positive cells. The results shown summarize five independent experiments ± SD. (B) Representative dot plots of phagocytosed killed LNCap and OV-90 cells are shown. (C) Fluorescent microscopy analysis of the phagocytosis. DiO-labeled immature Day 5 and Day 3 DCs were cocultured with DiI-labeled UVB-killed tumor cells at 37 °C for 24 h, and the engulfment of tumor cells was verified by fluorescent microscopy. DiO-labeled DCs are green and DiI-labeled tumor cells are red. Only phagocytosis of killed LNCap cells is shown. The almost complete lack of unphagocytosed killed tumor cells on the pictures is due to their weak adhesion to the slides; thus, they were washed out during the wash steps.

FSC/SSC analysis showed that Day 5 DCs were larger in size with higher granularity, Day 3 DCs had the same phagocytic capacity as Day 5 DCs.

The maturation status of DC is crucial for adequate T cell recruitment, activation, expansion and differentiation [22,23]. Thus, we tested the capacity of Poly (I:C) and LPS to activate Day 5 and Day 3 DCs. The maturation of DCs with LPS resulted in the highest expression of maturation-associated molecules with no significant differences between Day 5 and Day 3 DCs. Poly (I:C) induced weaker phenotypic maturation than LPS, and Day 5 Poly (I:C)-activated DCs expressed higher levels of CD80, CD86 and HLA-DR compared to Day 3 DCs.

We next analyzed the production of proinflammatory cytokines IL-12p70, IL-6, IL-1β, TNF-α, IFN-α, and anti-inflammatory

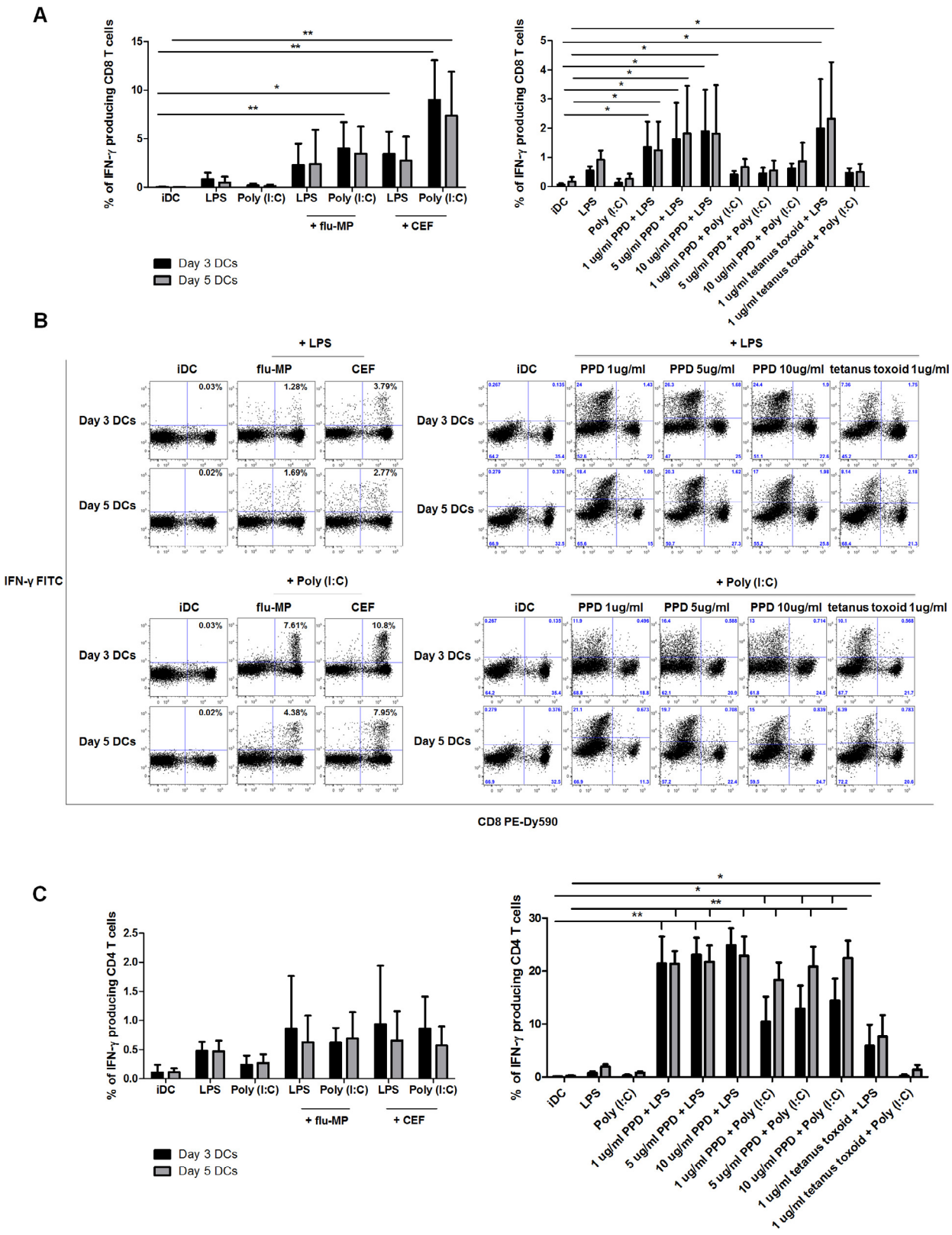

Fig. 5. The induction of antigen-specific T cells by mature Day 5 and Day 3 DCs. DCs were activated using maturation stimuli (LPS or Poly (I:C)), pulsed with antigens and subsequently used as stimulators for the induction of antigen-specific T cells. The frequency of antigen-specific T cells was analyzed by intracellular IFN-γ staining. A. Induction of influenza MP, CEF peptide mix, PPD and tetanus toxoid-specific $CD8^+$ T cells. The summary (A) and representative staining (B) of seven independent experiments are shown. C. Induction of influenza MP, CEF peptide mix, PPD and tetanus toxoid-specific $CD4^+$ T cells. The data are presented as the mean ± SD (A). Significant differences are shown ($^*P$ value ≤ 0.05, $^{**}P$ value ≤ 0.01).

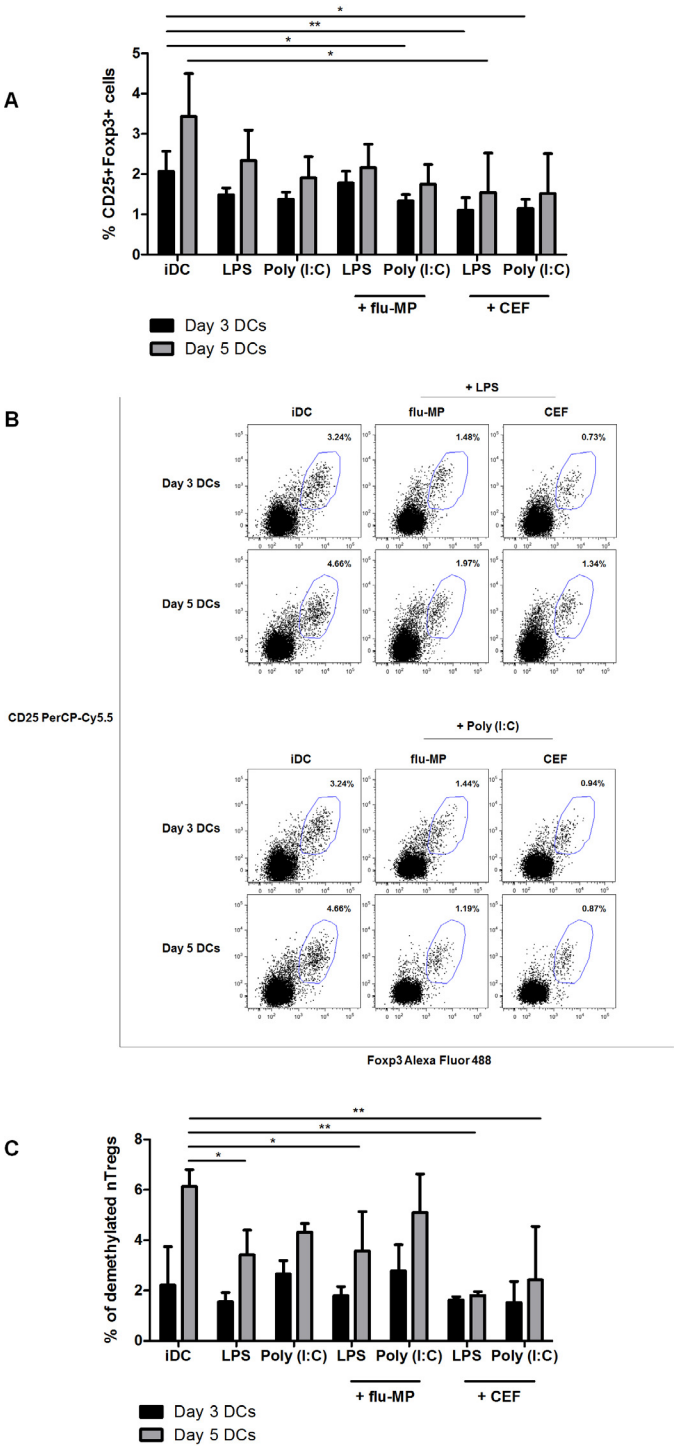

Fig. 6. The induction of regulatory T cells from $CD4^+$ $CD25^-$ T cells by mature Day 5 and Day 3 DCs. $CD4^+CD25^-$ T cells were obtained by depleting the $CD25^+$ cells with CD25 beads (STEMCELL Technologies) (data not shown) and cultured alone or with activated peptide-pulsed Day 5 and Day 3 DCs. The frequency of $CD4^+CD25^+FoxP3^+$ cells was analyzed from 7 day of cultures. $CD25^+FoxP3^+$ cells shown in graphs are expressed as the percentage of $CD4^+$ cells. The results are expressed as percentage of $CD25^+FoxP3^+$ cells after 7 days of culture – percentage of $CD25^+FoxP3^+$ cells remaining after isolation. The summary (A) and representative staining (B) of three independent experiments are shown. The data are presented as the mean ± SD (A). Significant differences are shown ($^*P$ value ≤ 0.05, $^{**}P$ value ≤ 0.01). (C) Columns represent proportions of Tregs demethylated in *FoxP3* TSDR.

cytokine IL-10, by activated DCs. LPS-induced production of all cytokines tested, except IFN-α, lacked a significant difference between Day 5 and Day 3 DCs. In contrast, Poly (I:C) was only able to induce the production of IL-6 and IFN-α. DCs activated by Poly (I:C) did not produce IL-10, an immunosuppressive cytokine, which is known to induce tolerance by directly inhibiting the production of IL-12 and thereby Th1 cell polarization [24,25]. IL-12 is a key cytokine for the generation of Th1 cells, CTL and anti-tumor responses [26–31]. Moreover, IL-12 production together with the mature state of DCs appears to correlate with therapeutic efficacy in clinical trials [9,32–35]. Therefore, for DC-based immunotherapy, in cancer as well as in chronic infectious diseases, it is crucial to generate stable mature DCs that secrete bioactive IL-12.

The fact that Poly (I:C) is not able to stimulate DC maturation to the same level as LPS and that Poly (I:C)-activated DCs do not produce any IL-12 has been described. Previously, Spisek et al. [36] described the use of Poly (I:C) combined with TNF-α for the generation of clinical grade fully mature DCs, but this group failed to obtain fully mature DCs with Poly (I:C) alone. Furthermore, Rouas et al. [37] reported a lack of IL-12p70 secretion after Poly (I:C) treatment in serum-free media. However, for DC-based immunotherapy, a major concern is whether mature DCs are capable of secreting IL-12p70 after *in vivo* administration. Rouas et al. [37] showed that *in vitro* generated Poly (I:C)-activated DCs retain their capacity to produce IL-12 after migration to the lymph nodes and upon subsequent contact with activated T cells. It has been shown that DC:T cell interaction via CD40:CD40L upregulates the expression of costimulatory and adhesion molecules on DCs and triggers DCs to secrete IL-12 [38,39]. These data suggest that ligation of CD40 on DCs may be an additional way to boost IL-12 production.

The ability to activate antigen-specific T cells is critical for the clinical effect of DC-based vaccines [40,41]. Therefore, we used a HLA-A2-restricted influenza MP and CEF peptide mix and proteins PPD and tetanus toxoid as model antigens to assess the activating potential of our generated Day 5 and Day 3 DCs. Antigen-loaded Poly (I:C), as well as LPS-activated, Day 3 DCs acquired full T cell stimulatory capacity and, thus, were equally effective at inducing the expansion of antigen-specific cytotoxic $CD8^+$ T cells compared to Day 5 DCs. $CD4^+$ T cells were massively expanded by protein-loaded DCs. While PPD and tetanus toxoid-loaded LPS-activated Day 3 and Day 5 DCs induced similar numbers of antigen-specific $CD4^+$ T cells, Poly (I:C)-activated Day 3 DCs were less potent in inducing antigen-specific $CD4^+$ T cells compared to Day 5 DCs. As Poly (I:C)-activated Day 3 DCs express lower levels of HLA-DR (and CD80/CD86), it may influence antigen presentation and can lead to induction of lower numbers of antigen-specific $CD4^+$ T cells. However, it is important that antigen-specific $CD4^+$ T cells are still induced by Poly (I:C)-activated Day 3 DCs and the percentage is not negligible (10–15%). Furthermore, presentation of antigens, even complex antigens, on MHC class I in Day 3 DCs is not impaired and Poly (I:C)-activated Day 3 DCs are able to expand antigen-specific $CD8^+$ T cells at same numbers compared to Day 5 DCs. It is very important fact because it is generally accepted that $CD8^+$ T cells play a major role in tumor control [42]. Poly (I:C)- and LPS-activated Day 3 DCs also induced slightly lower numbers of regulatory T cells compared to Day 5 DCs.

5. Conclusions

In this study, we identified monocyte-derived clinical grade DCs generated in accordance with the GMP standards during a 3 day culture process, and these cells, when activated by Poly (I:C), were comparable in most functional aspects to DCs produced by the standard 5 day protocol. These results provide the rationale for the testing of shorter protocols for DC generation in clinical trials. The generation of DCs using shorter protocols would markedly reduce the time, work load and costs associated with the GMP-compliant manufacturing of DC-based cellular therapy products, and may therefore facilitate the use of DCs in clinical trials of cellular immunotherapy.

Competing interests

The authors declare that they have no competing interests.

Acknowledgment

This project was supported by the research grant IGA NT12402-5.

References

[1] Fucikova J, Moserova I, Truxova I, Hermanova I, Vancurova I, Partlova S, et al. High hydrostatic pressure induces immunogenic cell death in human tumor cells. Int J Cancer 2014.
[2] Iwashita Y, Tahara K, Goto S, Sasaki A, Kai S, Seike M, et al. A phase I study of autologous dendritic cell-based immunotherapy for patients with unresectable primary liver cancer. Cancer Immunol Immunother 2003;52:155–61.
[3] Hernando JJ, Park TW, Kubler K, Offergeld R, Schlebusch H, Bauknecht T. Vaccination with autologous tumour antigen-pulsed dendritic cells in advanced gynaecological malignancies: clinical and immunological evaluation of a phase I trial. Cancer Immunol Immunother 2002;51:45–52.
[4] Nestle FO, Alijagic S, Gilliet M, Sun Y, Grabbe S, Dummer R, et al. Vaccination of melanoma patients with peptide- or tumor lysate-pulsed dendritic cells. Nat Med 1998;4:328–32.
[5] Pandha HS, John RJ, Hutchinson J, James N, Whelan M, Corbishley C, et al. Dendritic cell immunotherapy for urological cancers using cryopreserved allogeneic tumour lysate-pulsed cells: a phase I/II study. BJU Int 2004;94:412–8.
[6] Vacchelli E, Vitale I, Eggermont A, Fridman WH, Fucikova J, Cremer I, et al. Trial watch: dendritic cell-based interventions for cancer therapy. Oncoimmunology 2013;2:e25771.
[7] Berger TG, Strasser E, Smith R, Carste C, Schuler-Thurner B, Kaempgen E, et al. Efficient elutriation of monocytes within a closed system (Elutra) for clinical-scale generation of dendritic cells. J Immunol Methods 2005;298:61–72.
[8] Curti A, Ferri E, Pandolfi S, Isidori A, Lemoli RM. Dendritic cell differentiation. J Immunol 2004;172:3 [author reply 3–4].
[9] Dhodapkar MV, Steinman RM, Sapp M, Desai H, Fossella C, Krasovsky J, et al. Rapid generation of broad T-cell immunity in humans after a single injection of mature dendritic cells. J Clin Invest 1999;104:173–80.
[10] Rozkova D, Tiserova H, Fucikova J, Last'ovicka J, Podrazil M, Ulcova H, et al. FOCUS on FOCIS: combined chemo-immunotherapy for the treatment of hormone-refractory metastatic prostate cancer. Clin Immunol 2009;131:1–10.
[11] Thurner B, Roder C, Dieckmann D, Heuer M, Kruse M, Glaser A, et al. Generation of large numbers of fully mature and stable dendritic cells from leukapheresis products for clinical application. J Immunol Methods 1999;223:1–15.
[12] Dauer M, Schad K, Herten J, Junkmann J, Bauer C, Kiefl R, et al. FastDC derived from human monocytes within 48 h effectively prime tumor antigen-specific cytotoxic T cells. J Immunol Methods 2005;302:145–55.
[13] Ramadan G, Konings S, Kurup VP, Keever-Taylor CA. Generation of *Aspergillus*- and CMV-specific T-cell responses using autologous fast DC. Cytotherapy 2004;6:223–34.
[14] Dauer M, Obermaier B, Herten J, Haerle C, Pohl K, Rothenfusser S, et al. Mature dendritic cells derived from human monocytes within 48 h: a novel strategy for dendritic cell differentiation from blood precursors. J Immunol 2003;170:4069–76.
[15] Jarnjak-Jankovic S, Hammerstad H, Saeboe-Larssen S, Kvalheim G, Gaudernack G. A full scale comparative study of methods for generation of functional dendritic cells for use as cancer vaccines. BMC Cancer 2007;7:119.
[16] Kvistborg P, Boegh M, Pedersen AW, Claesson MH, Zocca MB. Fast generation of dendritic cells. Cell Immunol 2009;260:56–62.
[17] Galluzzi L, Kepp O, Kroemer G. Enlightening the impact of immunogenic cell death in photodynamic cancer therapy. EMBO J 2012;31:1055–7.
[18] Krysko DV, Vandenabeele P. From regulation of dying cell engulfment to development of anti-cancer therapy. Cell Death Differ 2008;15:29–38.
[19] Ozols RF, Bundy BN, Greer BE, Fowler JM, Clarke-Pearson D, Burger RA, et al. Phase III trial of carboplatin and paclitaxel compared with cisplatin and paclitaxel in patients with optimally resected stage III ovarian cancer: a Gynecologic Oncology Group study. J Clin Oncol 2003;21:3194–200.
[20] van den Broek ME, Kagi D, Ossendorp F, Toes R, Vamvakas S, Lutz WK, et al. Decreased tumor surveillance in perforin-deficient mice. J Exp Med 1996;184:1781–90.
[21] Fucikova J, Rozkova D, Ulcova H, Budinsky V, Sochorova K, Pokorna K, et al. Poly I:C-activated dendritic cells that were generated in CellGro for use in cancer immunotherapy trials. J Transl Med 2011;9:223.
[22] Sabado RL, Bhardwaj N. Directing dendritic cell immunotherapy towards successful cancer treatment. Immunotherapy 2010;2:37–56.
[23] Zhou LJ, Tedder TF. $CD14^+$ blood monocytes can differentiate into functionally mature $CD83^+$ dendritic cells. Proc Natl Acad Sci U S A 1996;93:2588–92.
[24] Bogunovic D, Manches O, Godefroy E, Yewdall A, Gallois A, Salazar AM, et al. TLR4 engagement during TLR3-induced proinflammatory signaling in dendritic cells promotes IL-10-mediated suppression of antitumor immunity. Cancer Res 2011;71:5467–76.
[25] O'Garra A, Murphy KM. From IL-10 to IL-12: how pathogens and their products stimulate APCs to induce T(H)1 development. Nat Immunol 2009;10:929–32.
[26] Gherardi MM, Ramirez JC, Esteban M. Towards a new generation of vaccines: the cytokine IL-12 as an adjuvant to enhance cellular immune responses to pathogens during prime-booster vaccination regimens. Histol Histopathol 2001;16:655–67.
[27] Grohmann U, Bianchi R, Ayroldi E, Belladonna ML, Surace D, Fioretti MC, et al. A tumor-associated and self antigen peptide presented by dendritic cells may induce T cell anergy in vivo, but IL-12 can prevent or revert the anergic state. J Immunol 1997;158:3593–602.
[28] Grufman P, Karre K. Innate and adaptive immunity to tumors: IL-12 is required for optimal responses. Eur J Immunol 2000;30:1088–93.

[29] Hilkens CM, Kalinski P, de Boer M, Kapsenberg ML. Human dendritic cells require exogenous interleukin-12-inducing factors to direct the development of naive T-helper cells toward the Th1 phenotype. Blood 1997;90:1920–6.
[30] Moser M, Murphy KM. Dendritic cell regulation of TH1–TH2 development. Nat Immunol 2000;1:199–205.
[31] Trinchieri G. Interleukin-12: a cytokine at the interface of inflammation and immunity. Adv Immunol 1998;70:83–243.
[32] Jonuleit H, Giesecke-Tuettenberg A, Tuting T, Thurner-Schuler B, Stuge TB, Paragnik L, et al. A comparison of two types of dendritic cell as adjuvants for the induction of melanoma-specific T-cell responses in humans following intranodal injection. Int J Cancer 2001;93:243–51.
[33] Morse MA, Mosca PJ, Clay TM, Lyerly HK. Dendritic cell maturation in active immunotherapy strategies. Expert Opin Biol Ther 2002;2:35–43.
[34] Schuler-Thurner B, Schultz ES, Berger TG, Weinlich G, Ebner S, Woerl P, et al. Rapid induction of tumor-specific type 1T helper cells in metastatic melanoma patients by vaccination with mature, cryopreserved, peptide-loaded monocyte-derived dendritic cells. J Exp Med 2002;195:1279–88.
[35] Thurner B, Haendle I, Roder C, Dieckmann D, Keikavoussi P, Jonuleit H, et al. Vaccination with mage-3A1 peptide-pulsed mature, monocyte-derived dendritic cells expands specific cytotoxic T cells and induces regression of some metastases in advanced stage IV melanoma. J Exp Med 1999;190:1669–78.
[36] Spisek R, Bretaudeau L, Barbieux I, Meflah K, Gregoire M. Standardized generation of fully mature p70 IL-12 secreting monocyte-derived dendritic cells for clinical use. Cancer Immunol Immunother 2001;50:417–27.
[37] Rouas R, Lewalle P, El Ouriaghli F, Nowak B, Duvillier H, Martiat P. Poly(I:C) used for human dendritic cell maturation preserves their ability to secondarily secrete bioactive IL-12. Int Immunol 2004;16:767–73.
[38] van Kooten C, Banchereau J. CD40–CD40 ligand. J Leukoc Biol 2000;67:2–17.
[39] Walzer T, Dalod M, Robbins SH, Zitvogel L, Vivier E. Natural-killer cells and dendritic cells: l'union fait la force. Blood 2005;106:2252–8.
[40] Mailliard RB, Lotze MT. Dendritic cells prolong tumor-specific T-cell survival and effector function after interaction with tumor targets. Clin Cancer Res 2001;7:980s–8s.
[41] Schuler-Thurner B, Dieckmann D, Keikavoussi P, Bender A, Maczek C, Jonuleit H, et al. Mage-3 and influenza-matrix peptide-specific cytotoxic T cells are inducible in terminal stage HLA-A2.1^{+} melanoma patients by mature monocyte-derived dendritic cells. J Immunol 2000;165:3492–6.
[42] Pedersen SR, Sorensen MR, Buus S, Christensen JP, Thomsen AR. Comparison of vaccine-induced effector CD8 T cell responses directed against self- and non-self-tumor antigens: implications for cancer immunotherapy. J Immunol 2013;191:3955–67.

5.5. Dendritické buňky pulzované nádorovými buňkami ošetřenými vysokým hydrostatickým tlakem indukují imunitní odpověď v myších TC-1 a TRAMP-C2 nádorových modelech a kombinace s chemoterapií na bázi docetaxelu vede k inhibici růstu těchto nádorů

Imunoterapie nádorových onemocnění, především pokud je kombinována s dalšími terapeutickými přístupy jako např. chemoterapií, představuje atraktivní možnost protinádorové léčby. Současné poznatky ukazují, že chemoterapie může mít kromě přímého cytotoxického efektu také imunomodulační vlastnosti. Synergické působení imunoterapie a chemoterapie bylo prokázáno v řadě preklinických a klinických studií. V případě imunoterapie založené na DCs závisí účinnost této léčby také na optimální metodě inaktivace nádorových buněk určených pro pulzaci DCs a na výběru vhodných látek indukujících jejich maturaci. Imunogenní potenciál nádorových buněk může být zvýšen některými chemoterapeutiky a fyzikálními modalitami včetně HHP, které indukují specifický typ buněčné smrti doprovázené sekrecí/uvolněním/vystavením DAMPs. Tyto molekuly mají schopnost modulovat aktivitu DCs, čehož může být využito při přípravě DC s optimálním fenotypem a funkcemi v rámci imunoterapeutických protokolů.

V tomto projektu jsme testovali použití vakcíny na bázi DCs pulzovaných nádorovými buňkami ošetřenými HHP *in vivo* na myších nádorových modelech a sledovali jsme její schopnost stimulovat imunitní odpověď a terapeutický potenciál v kombinaci s adekvátní chemoterapií. Zaměřili jsme se na imunoterapii slabě imunogenních TRAMP-C2 nádorů, myšího modelu lidského karcinomu prostaty, u kterého se kombinace imunoterapie založené na DCs a chemoterapie docetaxelem, nejčastěji používaným chemoterapeutikem v léčbě pokročilého hormon-refrakterního karcinomu prostaty, jeví jako atraktivní a potenciálně vhodná strategie. Studie byla pro porovnání doplněna o experimenty na imunogenních TC-1

nádorech, které představují myší model nádorů asociovaných s lidským papilomavirem 16 (HPV16) a jsou citlivé na terapii DCs v různém experimentálním nastavení.

Na úvod jsme dokázali, že HHP indukuje ICD TRAMP-C2 i TC-1 nádorových buněk. Dochází k translokaci HSP90 a CRT na plazmatickou membránu a uvolnění HMGB1 z umírajících buněk. Imunizace myší takto ošetřenými nádorovými liniemi vedla v obou případech ke stimulaci imunitní odpovědi a inhibici růstu TC-1, ale ne TRAMP-C2 nádorů. Buňky ošetřené HHP byly dále použity pro pulzaci DCs v rámci přípravy vakcíny. Dendritické buňky kultivované s nádorovými buňkami ošetřenými HHP a aktivované CpG exprimovaly více molekul asociovaných s maturací a produkovaly vyšší množství IL-12, IL-1β a IFN-γ v porovnání s DCs pulzovanými nádorovými buňkami ošetřenými UVB zářením. Vakcinace myší DCs pulzovanými TC-1 a TRAMP-C2 buňkami ošetřenými HHP indukovala cytotoxicitu splenocytů a produkci IFN-γ. Kombinace takto připravené DC vakcíny s chemoterapií docetaxelem signifikantně inhibovala růst jak TC-1, tak TRAMP-C2 nádorů. Tyto výsledky naznačují, že imunoterapie na bázi DCs pulzovaných nádorovými buňkami inaktivovanými HHP kombinovaná s docetaxelem může být vhodnou strategií léčby slabě imunogenních typů nádorů, alespoň v případě karcinomu prostaty.

K této práci jsem přispěla následovně: příprava nádorových linií ošetřených HHP, měření viability a detekce DAMPs (HSP70, HSP90 a CRT) na povrchu nádorových linií ošetřených HHP pomocí průtokové cytometrie.

Dendritic cells pulsed with tumor cells killed by high hydrostatic pressure induce strong immune responses and display therapeutic effects both in murine TC-1 and TRAMP-C2 tumors when combined with docetaxel chemotherapy

ROMANA MIKYŠKOVÁ[1,2*], IVAN ŠTĚPÁNEK[1,2*], MARIE INDROVÁ[1,2], JANA BIEBLOVÁ[1,2], JANA ŠÍMOVÁ[1,2], IVA TRUXOVÁ[4], IRENA MOSEROVÁ[4], JITKA FUČÍKOVÁ[3,4], JIŘINA BARTŮŇKOVÁ[3,4], RADEK ŠPÍŠEK[3,4] and MILAN REINIŠ[1,2]

[1]Department of Transgenic Models of Diseases, Institute of Molecular Genetics of the ASCR, v.v.i., Prague; [2]Czech Centre for Phenogenomics, Institute of Molecular Genetics of the ASCR, Prague; [3]Department of Immunology, Charles University, 2nd Faculty of Medicine and University Hospital Motol, Prague; [4]SOTIO a.s., Prague, Czech Republic

Received October 20, 2015; Accepted December 2, 2015

DOI: 10.3892/ijo.2015.3314

Abstract. High hydrostatic pressure (HHP) has been shown to induce immunogenic cell death of cancer cells, facilitating their uptake by dendritic cells (DC) and subsequent presentation of tumor antigens. In the present study, we demonstrated immunogenicity of the HHP-treated tumor cells in mice. HHP was able to induce immunogenic cell death of both TC-1 and TRAMP-C2 tumor cells, representing murine models for human papilloma virus-associated tumors and prostate cancer, respectively. HHP-treated cells induced stronger immune responses in mice immunized with these tumor cells, documented by higher spleen cell cytotoxicity and increased IFNγ production as compared to irradiated tumor cells, accompanied by suppression of tumor growth *in vivo* in the case of TC-1 tumors, but not TRAMP-C2 tumors. Furthermore, HHP-treated cells were used for DC-based vaccine antigen pulsing. DC co-cultured with HHP-treated tumor cells and matured by a TLR 9 agonist exhibited higher cell surface expression of maturation markers and production of IL-12 and other cytokines, as compared to the DC pulsed with irradiated tumor cells. Immunization with DC cell-based vaccines pulsed with HHP-treated tumor cells induced high immune responses, detected by increased spleen cell cytotoxicity and elevated IFNγ production. The DC-based vaccine pulsed with HHP-treated tumor cells combined with docetaxel chemotherapy significantly inhibited growth of both TC-1 and TRAMP-C2 tumors. Our results indicate that DC-based vaccines pulsed with HHP-inactivated tumor cells can be a suitable tool for chemoimmunotherapy, particularly with regard to the findings that poorly immunogenic TRAMP-C2 tumors were susceptible to this treatment modality.

Correspondence to: Dr Milan Reiniš, Czech Centre for Phenogenomics, Institute of Molecular Genetics of the Academy of Sciences of the Czech Republic, v.v.i., Vídeňská 1083, 142 20 Prague 4, Czech Republic
E-mail: milan.reinis@img.cas.cz

*Contributed equally

Key words: dendritic cells, docetaxel, high hydrostatic pressure, immunotherapy, cancer

Introduction

Cancer immunotherapy, especially when combined with other therapeutic modalities such as chemotherapy, is an attractive approach to cancer treatment. Synergistic effects of combinations of immunotherapy and chemotherapy have been demonstrated in a number of pre-clinical and clinical studies (1,2).

Dendritic cells (DCs) are key players in the immune response as they are able to capture antigens with their pattern-recognition receptors, to process and present them to naïve T-cells, inducing their activation (3), and thus building an essential bridge between innate and adaptive responses. The possibility of their generation *in vitro* enabled their use for immunotherapy of cancer (4), and a number of clinical trials have been performed in the last decade (5,6). Typically, an autologous dendritic cell-based vaccine represents *in vitro* cultured dendritic cells pulsed with tumor antigens that can be in the form of tumor cells with subsequent DC maturation. For DC pulsing, tumor cells can be inactivated by their lysis (ultrasonic treatment, repeated freeze-thaw), lethal irradiation or other methods before mixing them with DC. Selection of the optimal inactivation method can be crucial for DC vaccine optimization, together with selection of proper maturation-inducing agents.

Therefore, a significant effort has also been invested in increasing the immunogenicity of dying cancer cells used

for vaccine production. Until now several chemotherapeutic agents [anthracyclines (7), oxaliplatin, platinum complexes (8), bortezomib (9)] and physical modalities [UV-C, irradiation (10), HHP] have been identified as inducers of immunogenic cell death (ICD). ICD is characterized by the cell-surface expression and release of damage associated molecular patterns (DAMPs). DAMPs found to be crucial for ICD include surface exposed chaperone protein calreticulin (CRT) and heat shock proteins 70 (HSP70) and 90 (HSP90), actively secreted ATP and passively released high-mobility group box 1 protein (HMGB1). These signals can activate innate immunity and, importantly, interact with phagocytosis-related receptors, purinergic receptors and pattern-recognition receptors expressed by DCs and thereby stimulate presentation of tumor antigens to T cells.

High hydrostatic pressure (HHP) has been demonstrated as a convenient tool for tumor cell inactivation preserving their immunogenic capacity (11,12). Recently, induction of ICD by HHP has been shown in several human tumor cell lines. HHP-treated cells were able to induce monocyte-derived DC maturation, and DC co-cultured with HHP-treated tumor cells were able to induce T cell activation *in vitro*. These encouraging results suggest that HHP can be an important tool for tumor cell inactivation before their use for DC pulsing or as cellular vaccines (13).

Chemotherapeutic drugs affect rapidly growing cells and, as a consequence, cause collateral damage to cells of the immune system. In this regard, they are considered immunosuppressive. However, there is increasing evidence that some cancer chemotherapies may actually aid the immunotherapy by activating the immune system rather than suppressing it (14,15). Chemotherapeutic drugs such as cyclophosphamide, doxorubicin, paclitaxel or docetaxel (16) were reported to possess immunomodulatory activities and appeared to be suitable for chemoimmunotherapy (17,18).

Docetaxel is a widely used chemotherapeutic drug and represents a first-line chemotherapy for metastatic castration-resistant prostate cancer (19,20). The autologous dendritic cell-based vaccines are intensively studied as an immunotherapy for prostate cancer, and the first cellular immunotherapy based on activated peripheral blood mononuclear cells, Sipuleucel T, has been FDA-approved (21). Collectively, combination chemoimmunotherapy based on docetaxel combined with the DC treatment represents an attractive modality for advanced prostate cancer therapy.

In the present study, we investigated, using murine tumor models, the immunogenicity of the HHP-inactivated tumor cells *in vivo* and, furthermore, the possibility to use HHP-treated tumor cells for preparation of DC-based vaccines. We have demonstrated the therapeutic capacity of the HHP cells-pulsed DC vaccines in combination with docetaxel treatments to inhibit growth of the TRAMP-C2 and TC-1 murine tumors. We have focused on the immunotherapy of poorly immunogenic TRAMP-C2 tumors, an animal model of prostate cancer treatment. For comparison, the study was completed with experiments using immunogenic TC-1 tumors representing a murine model for human papilloma virus 16-associated tumors, previously shown to be sensitive to the experimental DC treatments in various settings (22-24).

Materials and methods

Mice. C57BL/6 male mice, 6-8 weeks old, were obtained from AnLab Ltd., Prague, Czech Republic. Experimental protocols were approved by the Institutional Animal Care Committee of the Institute of Molecular Genetics, Prague.

Tumor cell lines. The TC-1 tumor cell line (obtained from the ATCC collection) was developed by co-transfection of murine C57BL/6 lung cells with HPV16 E6/E7 genes and activated (G12V) Ha-ras plasmid DNA (25). TRAMP-C2 tumor cells (obtained from the ATCC collection), MHC class I-deficient, were established from a heterogeneous 32-week tumor of the transgenic adenocarcinoma mouse prostate (TRAMP) model (26). TC-1 cells were maintained in RPMI-1640 medium (Sigma-Aldrich GmbH, Steinheim, Germany) supplemented with 10% FCS (PAN Biotech GmbH, Aidenbach, Germany), 2 mM L-glutamine and antibiotics; TRAMP-C2 cells were maintained in D-MEM medium (Sigma-Aldrich) supplemented with 5% FCS, Nu-Serum IV (5%; BD Biosciences, Bedford, MA, USA), 0.005 mg/ml human insulin (Sigma-Aldrich), dehydroisoandrosterone (DHEA, 10 nM; Sigma-Aldrich) and antibiotics. Both cell lines were cultured at 37˚C in a humidified atmosphere with 5% CO_2 cells. In the *in vivo* experiments, $5x10^4$ TC-1 cells and $1x10^6$ TRAMP-C2 cells were administered for the challenge. In our hands, $5x10^4$ TC-1 cells represent 5 TID_{50} doses and $1x10^6$ TRAMP-C2 cells represent 3 TID_{50} doses.

High hydrostatic pressure and irradiation cell treatments. Tumor cells were treated by HHP (100, 150, 175 and 200 MPa) in the custom-made device (Resato International BV, Roden, the Netherlands) that is located in the GMP manufacturing facility, Sotio a.s. (Prague, Czech Republic). This device allows reliable treatment of the tumor cells by defined levels of HHP for specified periods of time (10 min in the case of 200 MPa) (13). Inactivation of tumor cells by irradiation (150 Gy) was performed as previously described (22).

Dendritic cell preparation. Dendritic cells (DC) were prepared from bone marrow precursors as described by Indrová *et al* (24) and Lutz *et al* (27) with slight modifications (28). Briefly, the bone marrow cells were cultured for 7 days in the complete RPMI-1640 medium supplemented with $2x10^{-5}$ M mercaptoethanol (Calbiochem, La Jolla, CA, USA), 10 ng/ml GM-CSF and IL-4 (R&D Systems, Minneapolis, MN, USA). On day 5, the DC were pulsed with HHP-treated or irradiated (IR-treated) tumor cells by 48-h incubation in the ratio of 2:1 (DC/tumor cells, 10^6 DC/ml). DC pulsed with the tumor cells were treated for 24 h with unmethylated CpG containing phosphorothioate-modified oligodeoxynucleotide CpG 1826 (5'-TCCATGACGTTCCTGACGTT-3') (29) at a final concentration of 5 μg/ml (Generi Biotech, Hradec Králové, Czech Republic), were sulfur-modified in their backbone (phosphorothioate) and synthesized under endotoxin-free conditions. On day 7, non-adherent cells were harvested. These cells, designated as DC, contained ~60-70% $CD11c^+$ cells. For mouse immunization experiments, DC were washed twice with PBS and injected subcutaneously (s.c.) in PBS, 300 μl/$2x10^6$ cells/mouse.

Immunization/challenge experiments with tumor cells. Mice were twice immunized with $5x10^6$ irradiated tumor cells in a three-week interval (s.c., irradiation dose was 150 Gy, HHP dose was 200 MPa) (13,30,31). For *in vivo* studies, 10 days after the second immunization, mice were challenged s.c. with corresponding tumor cells (TC-1, $5x10^4$; TRAMP-C2, $1x10^6$ cells/mouse). Mice were observed twice weekly, and the numbers of tumor-bearing mice and the size of the tumors were recorded. Two perpendicular diameters of the tumors were measured with a caliper and the tumor size was expressed as the tumor area (cm^2). For *in vitro* analyses of the immune response, three mice were sacrificed. Single-cell suspensions from the spleens were prepared by homogenization through a cell strainer (70 μm; BD Biosciences, San Jose, CA, USA). Erythrocytes were osmotically lysed using ammonium chloride-potassium lysis buffer, the cell suspension was washed three times in the RPMI-1640 medium and used for further analysis by FACS, chromium release assay, ELISA (IFNγ) and ELISPOT (IFNγ).

Immunization/challenge experiments with dendritic cells. Mice were twice immunized with $2x10^6$ cells of DC-based vaccine in a two-week interval. For *in vivo* studies, 10 days after the second immunization, mice were challenged s.c. with corresponding tumor cells (TC-1, $5x10^4$; TRAMP-C2, $1x10^6$ cells/mouse). Mice were observed twice weekly, and the numbers of tumor-bearing mice and the size of the tumors were recorded. Two perpendicular diameters of the tumors were measured with a caliper and the tumor size was expressed as the tumor area (cm^2). For *in vitro* analyses of the immune response, three mice were sacrificed. Single-cell suspensions from the spleens were prepared as mentioned above and used for further analysis by FACS, chromium release assay, ELISA (IFNγ) and ELISPOT (IFNγ).

Therapeutic experiments. The therapeutic schemes were designed for combined chemoimmunotherapy treatment of early growing tumors. TC-1 ($5x10^4$ cells) or TRAMP-C2 ($1x10^6$ cells) tumor cells were s.c. transplanted on day 0. Docetaxel, 30 mg/kg (Actavis, North Bruncwik, NJ, USA) was repeatedly administered on days 7, 21 and 35 intraperitoneally (i.p.). Dendritic cells were administered on days 14, 28 and 42 in the vicinity of the tumor cell challenge site or peritumorally when the growing tumors appeared. Mice were observed twice a week and the size of the tumors was recorded. Two perpendicular diameters of the tumors were measured with a caliper and the tumor size was expressed as the tumor area (cm^2).

Flow cytometry. Cell surface expression of CRT, HSP90, MHC class I, CD54 and CD80 on the tumor cells was analyzed by flow cytometry. Tumor cells were collected from the cell culture 24 h after the HHP or IR treatment [10^6 cells/ml/well, 12-well plate (Nunc, Roskilde, Denmark)]. Cells ($5x10^5$/sample) were washed and labeled with primary antibodies for 25 min at 4˚C, followed by wash steps and alternatively labeled by incubation with Alexa 647- or DyLight 649-conjugated secondary antibody for 30 min at 4˚C. Apoptotic cells were determined by Annexin V apoptosis detection kit (eBiosciences) according to the manufacturer's instructions. Samples were kept in the dark and 10 min before the analysis, Hoechst 33258 was added at a final concentration of 2 μg/ml. Expression of cell surface molecules on the DC or spleen cells was analyzed by flow cytometry. Cell suspensions were washed and preincubated with anti-CD16/CD32 antibody to minimize non-specific binding for 15 min at 4˚C following washing step and incubation with labeled primary antibody for 30 min at 4˚C. Relevant isotype controls of irrelevant specificity were used. FACS buffer (PBS, 1% FBS, 0.1% NaN_3) was used for all washing steps and analysis. The following antibodies were used for FACS analyses: BD: anti-MHC class I (PE anti-H-$2D^b$ clone KH95 and PE anti-H-$2K^b$ clone AF6-88.5), FITC anti-I-A^b ($A_\beta{}^b$) (AF6-120.1), PE anti-CD54 (3E2), PE anti-CD80 (16-10A1), PE anti-CD86 (GL1), PE anti-CD274 (MIH5); BioLegend, Inc. (San Diego, CA, USA): BV421 or APC anti-CD11c (HL3), APC-CD45 (30-F11), FITC anti-CD8α (LY-2), BV711 anti-CD4 (RM4-5), PE anti-CD44 (IM7), PE-Cy7 CD62L (MEL-14); R&D Systems (Basel, Switzerland): anti-HSP70 (242707); Abcam (Cambridge, UK): anti-CRT (ab2907); Enzo Life Sciences, Inc. (Farmingdale, NY, USA): anti-HSP90 (AC88). Secondary antibodies anti-mouse conjugated to DyLight 649 (Jackson ImmunoResearch Laboratories, West Grove, PA, USA) or anti-rabbit conjugated to Alexa 647 (Cell Signaling Technology, Danvers, MA, USA) were also used. FACS analysis was performed using an LSR II flow cytometer (BD Biosciences) and analyzed by FlowJo 7.6.5 software.

Confocal microscopy. HHP-treated TC-1 and TRAMP-C2 cells were collected and washed twice with PBS. The cells were then incubated for 30 min with primary anti-CRT antibody (FMC 75; Enzo Life Sciences) diluted in PBS, followed by washing and incubation with the Alexa Fluor 488 goat anti-mouse secondary antibody (Molecular Probes). Cells were washed twice with PBS and fixed in 4% paraformaldehyde for 20 min and mounted on slides. Cells were examined under a DMI 6000 inverted Leica TCS AOBS SP5 tandem scanning confocal microscope with an AR (488 nm) laser and an x63 oil immersion objective.

ELISA. For HMGB1 release, supernatants from the tumor cell culture were collected 24 h after HHP treatment (10^6 cell/ml/well, 12-well plate (Nunc) and analyzed by an ELISA kit (IBL International GmbH, Hamburg, Germany) according to the manufacturer's instructions. For IL-1β, IL-6, IFNγ and IL-12 production, supernatants from the DC culture were collected 24 h after the addition of CpG 1826 and analyzed by ELISA kits (BD Biosciences) according to the manufacturer's instructions. For IFNγ production, supernatants from the spleen single-cell suspension were collected after 48-h incubation [$2x10^6$ cell/ml/well, 12-well plate (Nunc)] and analyzed by an ELISA kit (BD Biosciences) according to the manufacturer's instructions.

ELISPOT. To determine the amount of IFNγ-secreting cells, an ELISPOT kit for detection of murine IFNγ (BD Biosciences, San Diego, CA, USA) was used. Spleen cells were cultured for 48 h and then placed into the wells of ELISPOT plates (concentration $5x10^5$, $1x10^5$ and $5x10^4$ cells/well) for 24 h. The plates were then processed according to the manufacturer's instructions (BD Biosciences). Colored spots were counted

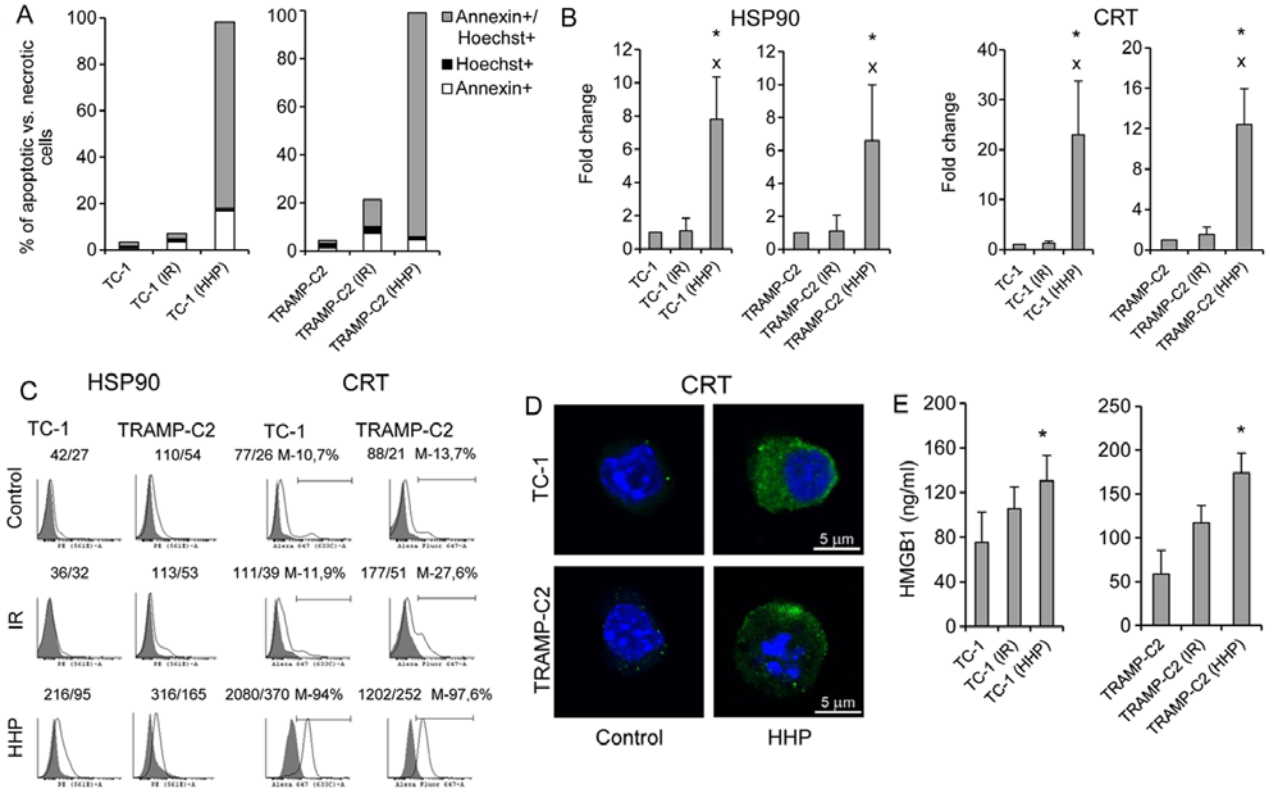

Figure 1. Phenotype of mouse TC-1 and TRAMP-C2 tumor cells 24 h after the treatment with HHP or IR. TC-1 and TRAMP-C2 tumor cells were treated with 200 MPa for 10 min and compared with irradiated (150 Gy) tumor cells. (A) Annexin V/Hoechst staining made 24 h after HHP or IR treatment. (B and C) Expression of cell surface molecules HSP90 and CRT on TC-1 or TRAMP-C2 tumor cells (presented as a fold change of mean fluorescence intensity (MFI) or histograms with MFI). (D) Fluorescence microscopy images of HHP-treated TC-1 and TRAMP-C2 tumor cells stained for CRT expression. (E) Release of HMGB1 into the tumor cell supernatants after HHP or IR-treatment. Representative results from at least three independent experiments. *P<0.05 vs. untreated control, xP<0.05 vs. IR treated group, two-sided Student's t-test.

with CTL Analyzer LLC (CTL, Cleveland, OH, USA) and analyzed using ImmunoSpot Image Analyzer software.

Chromium release microcytotoxicity assay. The cytolytic activity of effector cells was tested in 18-h ^{51}Cr release assay, as previously described (32,33). Briefly, spleen cells from control and immunized mice that served as effector cells were treated with ammonium chloride-potassium lysing buffer (1 min) to deplete erythrocytes. The mixtures of effector cells with ^{51}Cr-labeled tumor targets were incubated in selected target/effector cell ratios (1:25, 1:50, 1:100 and 1:200) in triplicate in 96-well round bottom microtiter plates (Nunc). The percentage of specific ^{51}Cr release was expressed according to the formula: [cpm experimental release - cpm control release/cpm maximum release/cpm control release] x 100.

Statistical analyses. For statistical analyses of *in vitro* experiments, Student's t-test was used. For evaluation of *in vivo* experiments, analysis of variance (ANOVA) from the NCSS, Number Cruncher Statistical System (NCSS, LLC, Kaysville, UT, USA) statistical package was utilized. Standard deviations are indicated in the figures.

Results

HHP, but not IR, induces ICD markers on both TC-1 and TRAMP-C2 tumor cells. First, we determined the ability of HHP to induce ICD in murine TC-1 or TRAMP-C2 cells, and then we compared the effect of HHP to the effect of irradiation (150 Gy) that has been standardly used for treatment of cells during preparation of DC vaccines in our previous studies (22). Fig. 1A shows that the percentage of late apoptotic/dead tumor cells (Annexin V$^+$/Hoechst$^+$) after the treatment with 200 MPa HHP was >80% within 24 h. The presence of ICD markers HSP90 and CRT on the cell surface of the tested cells was also significantly increased (Fig. 2B and C). Fluorescence microscopy images of HHP-treated tumor cells stained for CRT confirmed increased expression of CRT after HHP treatment (Fig. 1D). Release of HMGB1, late-stage ICD marker, in the supernatant was further analyzed. Fig. 1E demonstrates a significant increase of HMGB1 in the tumor cell supernatants after HHP treatment. Induction of ICD by 200 MPa HHP was similar both in TC-1 and TRAMP-C2 tumor cells. No significant upregulation of ICD markers was detected after irradiation with 150 Gy. The treatment with HHP of 200 MPa was selected as it was the most effective in inducing apoptosis and expression of ICD markers and simultaneously arresting cell proliferation, as determined by colony-forming assay in experiments, in which the effects of different doses of HHP (100, 150, 175, 200 and 250 MPa) were compared (data not shown).

Prophylactic immunization with HHP-treated tumor cells induces higher immune responses in mice when compared

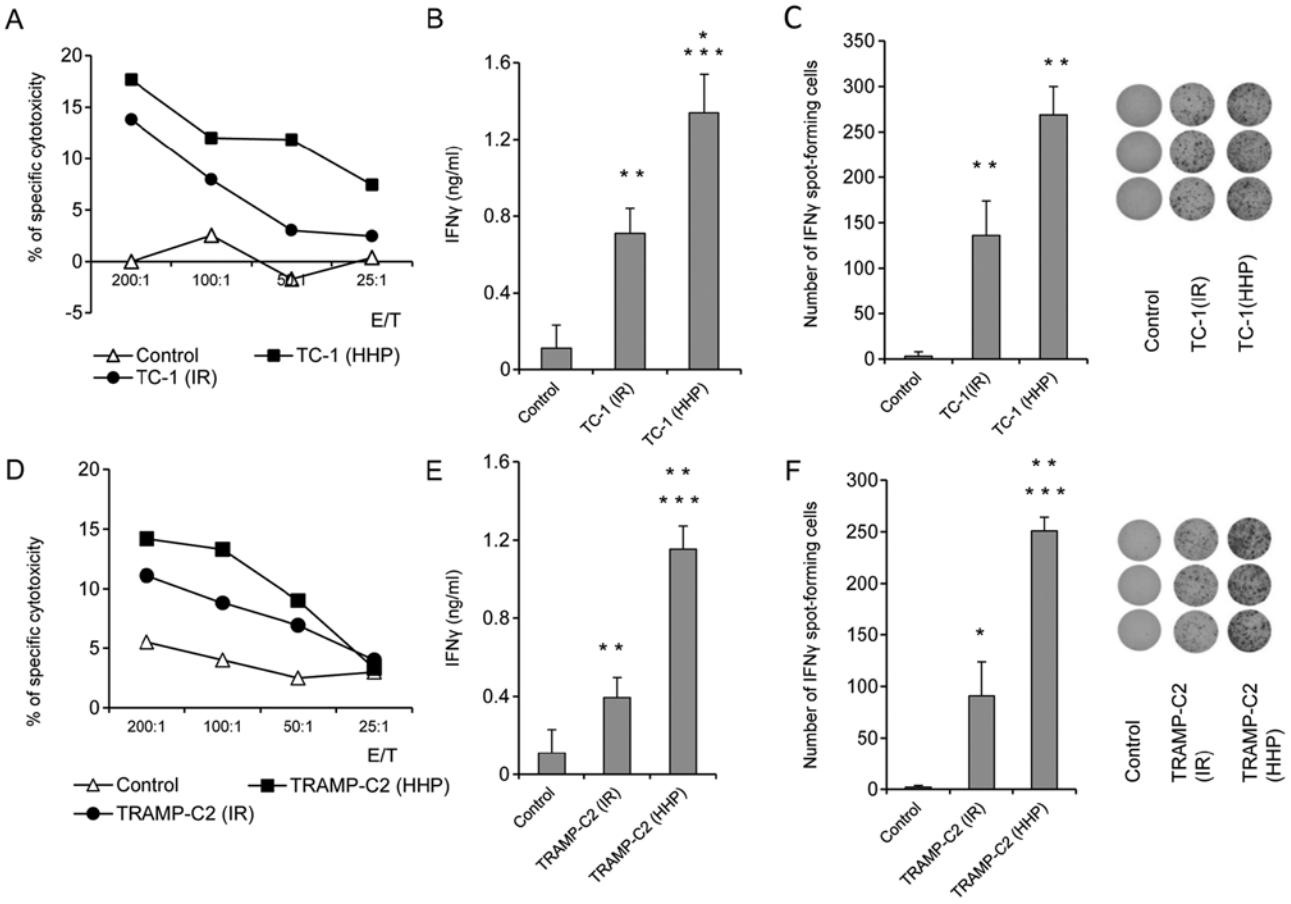

Figure 2. *In vitro* immune response after immunization with HHP-treated or IR-treated TC-1 and TRAMP-C2 tumor cells. Mice were immunized two times in a 3-week interval with $5x10^6$ HHP- or IR-treated TC-1 and TRAMP-C2 tumor cells. Ten days after the last immunization, pooled splenocytes of three mice were used for *in vitro* analysis. ^{51}Cr microcytotoxicity assay of splenocytes from mice immunized with HHP or IR-treated TC-1 (A) or TRAMP-C2 tumor cells (D). (B and E) IFNγ production by splenocytes of immunized mice (ELISA). (C and F) The number of IFNγ-producing cells (ELISPOT assay). Statistical significances were determined by Student's t-test. (B) $^{***}P<0.001$ TC-1(HHP) vs. Control; $^{**}P<0.01$ TC-1(IR) vs. Control; $^{*}P<0.05$ TC-1(HHP) vs. TC-1(IR); (C) $^{**}P<0.001$ TC-1(HHP) vs. Control; TC-1(IR) vs. Control; TC-1(HHP) vs. TC-1(IR); (E) $^{***}P<0.001$ TC-1(HHP) vs. Control; $^{**}P<0.01$ TC-1(IR) vs. Control; TC-1(HHP) vs. TC-1(IR); (F) $^{***}P<0.001$ TC-1(IR) vs. Control; $^{**}P<0.01$ TC-1(HHP) vs. TC-1(IR); $^{*}P<0.05$ TC-1(HHP) vs. Control.

with IR-treated tumor cells both in TC-1 and TRAMP-C2 tumor models. To study the ability of HHP and IR-treated tumor cells to induce immune response and their antitumor potency, mice were immunized twice at a three-week interval with $5x10^6$ HHP- or IR-treated TC-1 or TRAMP-C2 tumor cells. Ten days after the second immunization, mice were challenged with relevant tumor cells in doses of $5x10^4$ TC-1 or 10^6 TRAMP-C2. Three mice from each group were left without challenge and used for parallel *in vitro* analyses. *In vitro* analyses of the spleen effector cells prepared ten days after the second immunization with HHP-treated TC-1 or TRAMP-C2 tumor cells showed an increased cytotoxic effect of spleen effector cells on the corresponding targets. In the group of mice immunized with IR-treated tumor cells, a similar but slightly lower effect was observed (Fig. 2A and D). Despite the fact that the analysis of the spleen effector cells after immunization with HHP-treated tumor cells showed only moderately augmented cytotoxic effect when compared to immunization with IR-treated tumor cells, analysis of IFNγ production revealed significant differences. Compared to the IR-treated tumor cells, mice immunized with HHP-treated tumor cells displayed significantly increased IFNγ production by spleen cells measured by the ELISA assay (Fig. 2B and E) and significantly increased number of IFNγ-producing cells detected by the ELISPOT assay (Fig. 2C and F). These results were similar in both tumor models, immunogenic TC-1 and weakly immunogenic TRAMP-C2. However, after the challenge of immunized mice with the corresponding tumor cells, significant inhibition ($P<0.05$) of tumor growth was recorded only in the groups of mice immunized with the HHP or IR-treated TC-1 tumor cells and challenged with corresponding TC-1 cells (Fig. 3B). In contrast, mice immunized with HHP and IR-treated TRAMP-C2 cells did not exhibit any inhibition of tumor growth after the challenge with TRAMP-C2 cells (Fig. 3C).

Pulsing with HHP-treated TC-1 or TRAMP-C2 tumor cells increased expression of maturation markers on DC and stimulated production of cytokines characteristic for matured DC. Next, the HHP-treated TC-1 and TRAMP-C2 cells were used for DC pulsing, and the phenotypes of matured DC vaccines, unpulsed or pulsed with the IR-treated tumor cells or HHP-treated tumor cells, were compared (Fig. 4). We did not see any significant differences between unpulsed cells and HHP-treated tumor cells-pulsed DC. In both cases, CpG ODN1826-mediated maturation increased

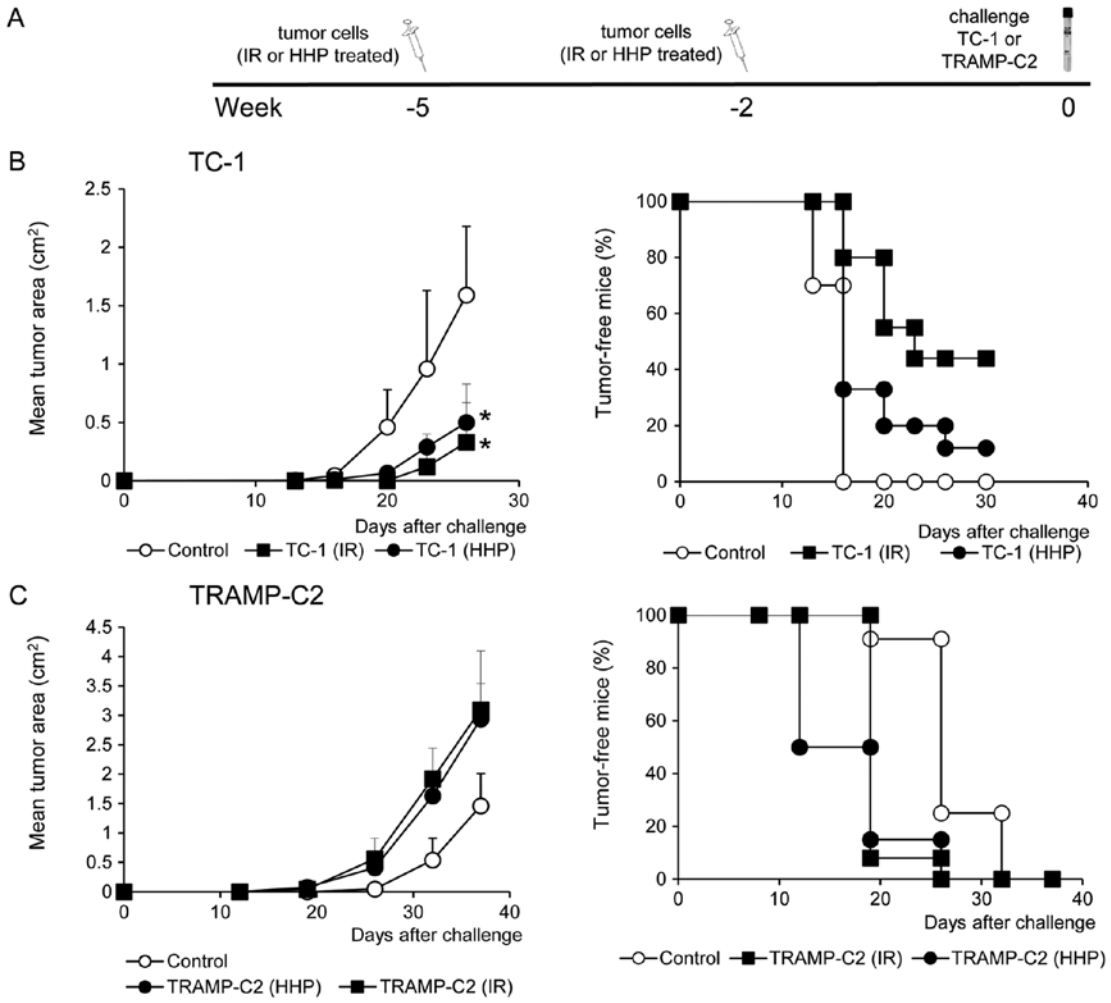

Figure 3. The effect of immunization with HHP-treated or IR-treated TC-1 and TRAMP-C2 tumor cells. Mice (10 mice per group) were two times s.c. immunized in a 3-week interval with $5x10^6$ HHP- or IR-treated TC-1 and TRAMP-C2 tumor cells (A). Ten days after the second immunization, mice were challenged with $5x10^4$ TC-1 (B) or 10^6 TRAMP-C2 (C) tumor cells. Tumor growth (left panel) and the percentage of tumor-free mice (Kaplan-Maier plot) (right panel) are shown; TC-1, $P<0.05$ (untreated vs. HHP-treated, IR-treated). TRAMP-C2, not significant (analysis of variance). The experiments were repeated twice with similar results.

the proportion of matured MHC class $II^{high}/CD86^{high}$ dendritic cells and increased CD80 and CD274 cell surface expression (Fig. 4A and B). The ratio between the CD80 and CD274 cell surface expressions (demonstrated by MFI values) was higher on matured cells compared to the immature controls (Fig. 4A). Both unpulsed cells and HHP-treated tumor cells-pulsed matured DC produced IL-12, as well as IL-1β, IL-6 and IFNγ (Fig. 4C). HHP-treated tumor cell-pulsed matured DC produced significantly higher amounts of IL-12 and IFNγ as compared to the unpulsed cells. No significant differences were observed between TRAMP-C2 and TC-1 cell co-culture. On the other hand, pulsing with the IR-treated tumor cells resulted in reduction of the proportion of matured MHC class $II^{high}/CD86^{high}$ dendritic cells in the DC populations, decreased the ratio between the CD80 and CD274 cell surface expression, and also significantly inhibited IL-12, IFNγ and IL-1β production, as compared to both unpulsed cells and HHP-treated tumor cell-pulsed matured DC (Fig. 4). These results indicate that DC co-culture with IR-treated, but not HHP-treated tumor cells, can impair DC maturation.

Prophylactic immunization with DC-based vaccine pulsed with HHP-treated TC-1 or TRAMP-C2 tumor cells induces strong immune response, but inhibits growth of TC-1 tumors only. In the next series of experiments, HHP-treated tumor cell-pulsed matured DC were investigated *in vivo*. HHP-treated tumor cell-pulsed matured DC were selected for further *in vivo* experiments as pulsing of DC with IR-treated tumor cells negatively affected DC maturation in terms of expression of costimulatory molecules and production of selected cytokines. Mice were immunized twice in a 2-week interval with $2x10^6$ HHP-treated tumor cell-pulsed matured DC. Ten days after the second immunization, mice were challenged with relevant tumor cells, in doses of $5x10^4$ TC-1 or 10^6 TRAMP-C2 tumor cells. Three mice from each group were left without challenge and used for parallel *in vitro* analyses. Both HHP-treated TRAMP-C2 and TC-1 cells pulsed DC vaccines induced strong immune responses, as determined by spleen cell analysis performed ten days after the second immunization (Fig. 5). Immunization with HHP-treated TC-1 or TRAMP-C2 pulsed DC vaccines showed a significantly increased cytotoxic effect of spleen effector cells on the

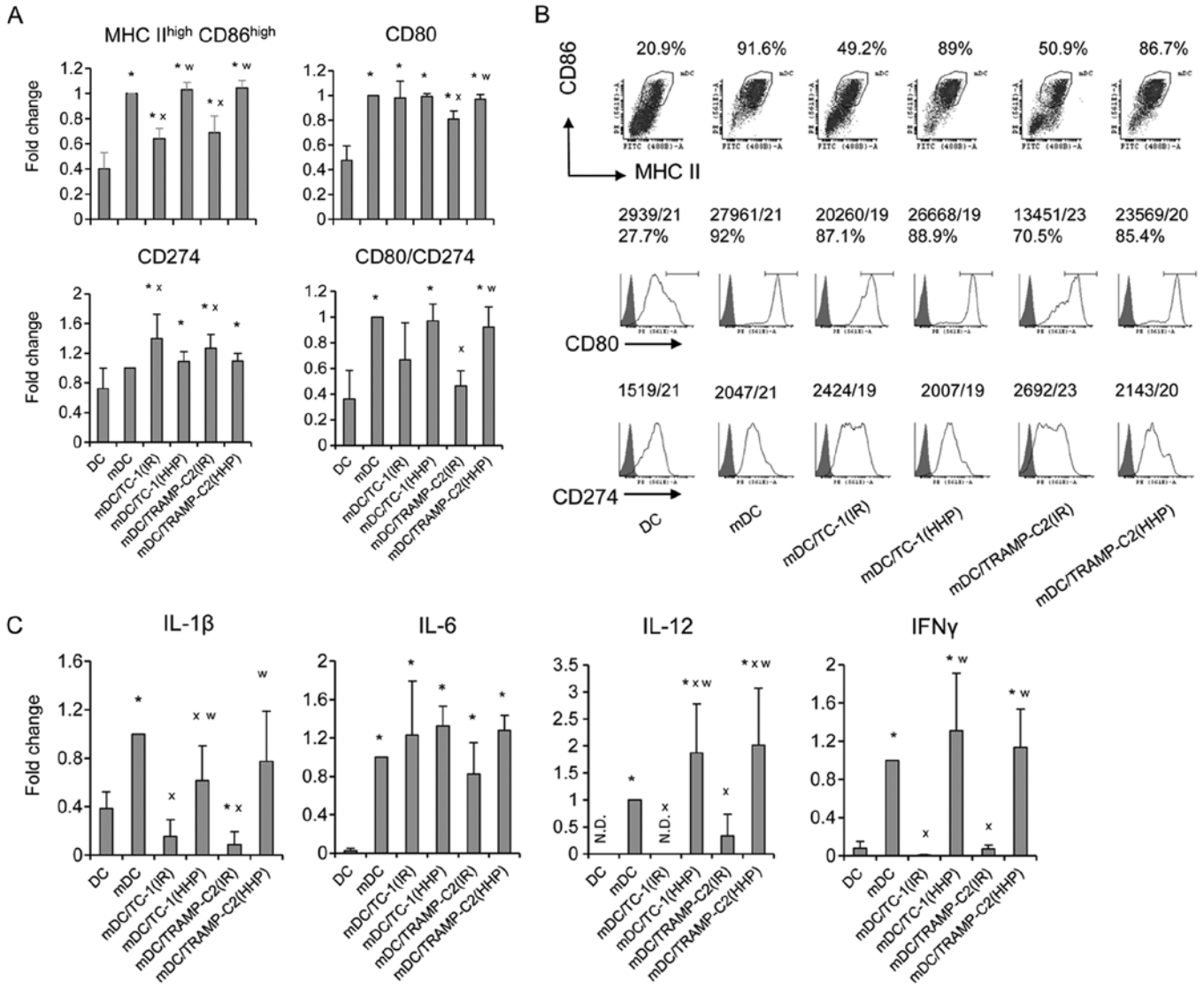

Figure 4. Phenotype of mouse DC after the interaction with HHP- or IR-treated TC-1 or TRAMP-C2 tumor cells. DC were prepared from bone marrow precursors and pulsed with HHP- or IR-treated tumor cells by 48-h incubation in the ratio of 2:1. DC pulsed with the tumor cells were then treated for 24 h with CpG 1826 and analyzed by flow cytometry. (A and B) Expression of MHC class II and costimulatory molecules (as a fold change of MFI or as a dot plot/histograms with MFI). (C) Production of cytokines by DC culture (as a fold change relative to mature DC designated as mDC). mDC produced IL-1β in the range of 233-749 pg/ml, IFNγ in the range of 299-749 pg/ml, IL-6 in the range of 18.2-49.2 ng/ml, and IL-12 in the range of 760-2235 pg/ml. Representative results from at least four independent experiments. *P<0.05 vs. DC, xP<0.05 vs. mDC, wP<0.05 vs. DC pulsed with IR-treated tumor cells, Student's t-test.

corresponding targets (Fig. 5A). As compared with control mice, mice immunized with both HHP-treated TRAMP-C2 and TC-1 cells pulsed DC vaccines displayed significantly increased numbers of IFNγ-producing cells detected by ELISPOT assay (Fig. 5B) and significantly increased IFNγ production by spleen cells measured by ELISA assay (Fig. 5C). A significant increase was also found in the percentage of $CD4^+$ and $CD8^+$ $CD44^+$ $CD62L^-$ T lymphocytes (Fig. 5D and E). These results were similar in both tumor models, immunogenic TC-1 and weakly immunogenic TRAMP-C2. Contrary to the results *in vitro*, *in vivo* analysis showed significant inhibition (P<0.05) of the tumor growth only in the group of mice immunized with the HHP-treated TC-1 tumor cell-pulsed matured DC and challenged with corresponding TC-1 cells (Fig. 6B). Mice immunized with the HHP-treated TRAMP-C2 tumor cell-pulsed matured DC did not exhibit any inhibition of tumor growth after the challenge with TRAMP-C2 cells (Fig. 6C). In both experiments, the percentage of tumor-free mice are shown in the right panel.

Combined chemoimmunotherapy of TC-1 and TRAMP-C2 tumors with docetaxel and DC-based vaccine significantly inhibits growth of subcutaneous tumors. The therapeutic efficacy of HHP-treated tumor cell-pulsed matured DC was then tested in the therapeutic setting when a combination of chemotherapy and immunotherapy with DC-based vaccine was employed. TC-1 ($5x10^4$ cells) or TRAMP-C2 (10^6 cells) tumor cells were s.c. transplanted on day 0 and treated with three doses of docetaxel chemotherapy in a 2-week interval. Dendritic cells were administered at regular intervals between the docetaxel chemotherapy. As shown in Fig. 7B, the growth of immunogenic TC-1 tumors was significantly inhibited by the treatment with DC alone or with the combination of docetaxel and DC vaccine [DC/TC-1(HHP)] (P<0.05 vs.

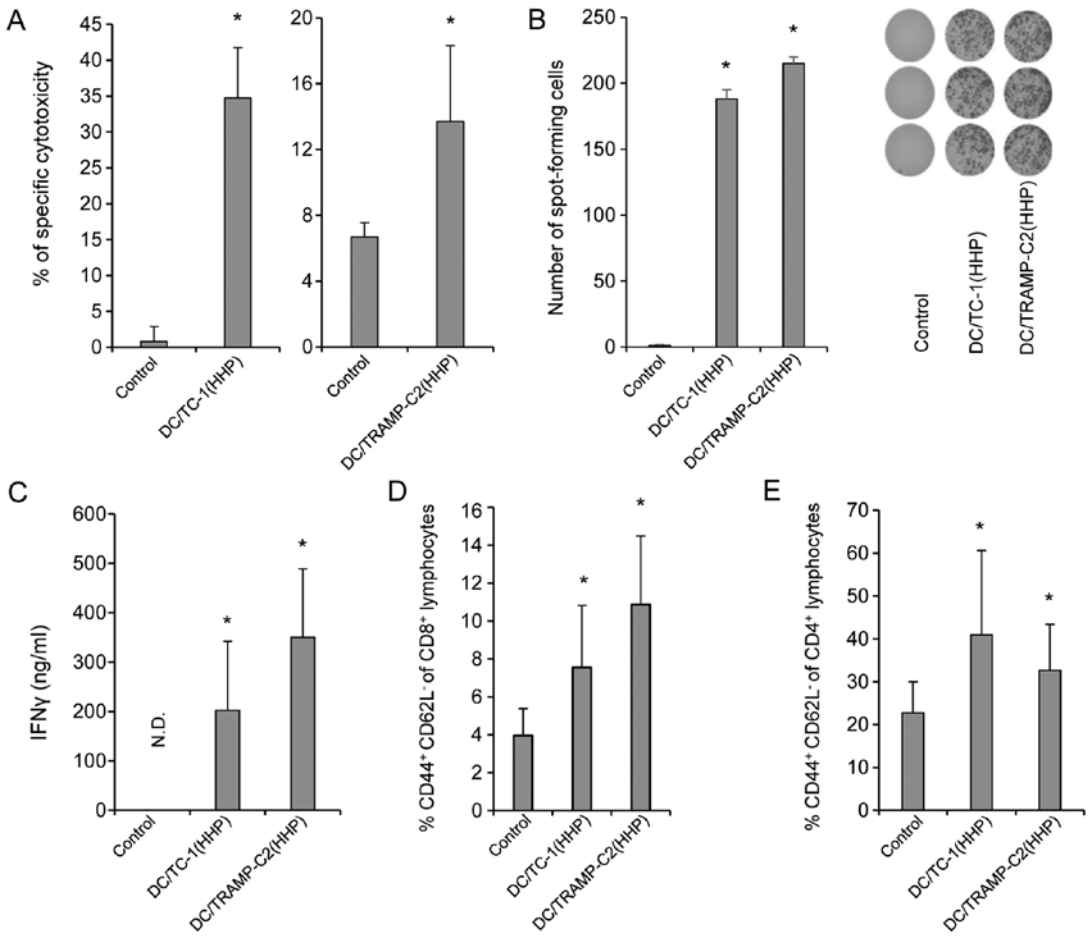

Figure 5. *In vitro* immune response after immunization with DC-based vaccines pulsed with HHP-treated TC-1 or TRAMP-C2 tumor cells. Mice were immunized two times in a 2-week interval with $2x10^6$ DC pulsed with HHP-treated TC-1 or TRAMP-C2 tumor cells. Ten days after the last immunization, pooled splenocytes of three mice were used for *in vitro* analysis. ^{51}Cr microcytotoxicity assay of splenocytes from mice immunized with HHP- and IR-treated TC-1 tumor cells or TRAMP-C2 tumor cells (A). (B) The number of IFNγ-producing cells (ELISPOT assay). (C) IFNγ production by splenocytes of immunized mice (ELISA). N.D. means that IFNγ production was under detection limit and for Student's t-test was considered as 0. (D) Percentage of $CD44^+$ $CD62L^-$ of $CD8^+$ lymphocytes. (E) Percentage of $CD44^+$ $CD62L^-$ of $CD4^+$ lymphocytes. Statistical significance was determined by Student's t-test; $^*P<0.05$ vs. control.

control). Docetaxel alone delayed the growth of tumors, but no significant difference was evident. A representative experiment of two independent ones is given in Fig. 7B. When the incidences of tumors in mice from two performed experiments were merged [Control 19/19, docetaxel 18/20, docetaxel + DC/TC-1(HHP) 14/19, DC/TC-1-HHP 6/10], the only significant difference was found between the control group and the group of combined chemoimmunotherapy (χ^2; docetaxel +DC/TC-1(HHP) vs. Control $P<0.01$). These results indicate the beneficial effect of the combination of chemotherapy with immunotherapy. The same therapeutic setting was also used for the treatment of poorly immunogenic TRAMP-C2 tumors. As shown in Fig. 7C, monotherapies with docetaxel alone or DC/TRAMP-C2(HHP) vaccine alone significantly inhibited growth of TRAMP-C2 tumors. However, when these monotherapies were combined, the therapeutic effect was even stronger. Significant inhibition of tumor growth was found between docetaxel alone or DC/TRAMP-C2(HHP) alone groups and the group treated with a combination of docetaxel and DC/TRAMP-C2(HHP) vaccine ($P<0.05$). The tumor-inhibitory effect was noted as reduction of the size of growing tumors; there was no difference between the incidences of tumors when two independent experiments were merged [Control 25/26, docetaxel 22/22, docetaxel + DC/TRAMP-C2(HHP) 22/22, DC/TRAMP-C2(HHP) 21/22].

Discussion

HHP has been previously shown to induce endoplasmic reticulum stress and consequently ICD in both murine and human cell lineages (11,13,34). This suggests that HHP, along with other modalities, such as irradiation, photodynamic therapy using hypericin, hyperthermia or treatments with selected chemotherapeutic and cytotoxic agents, can be used for preparation of tumor cells capable of inducing effective antitumor immunity (35). HHP could also be used for tumor cell inactivation before their use as cellular vaccines or as antigen donors in DC-based vaccines.

In the first part of the study, our aim was to demonstrate the capability of HHP-treated tumor cells to induce immune responses in mice, in comparison with irradiated tumor cells. Lethal irradiation represents a standard procedure used for tumor cell inactivation before their usage for immunization or for DC pulsing, and HHP treatment can serve as an attractive alternative for this procedure. Before performing the *in vivo* experiments, we optimized the HHP treatments of

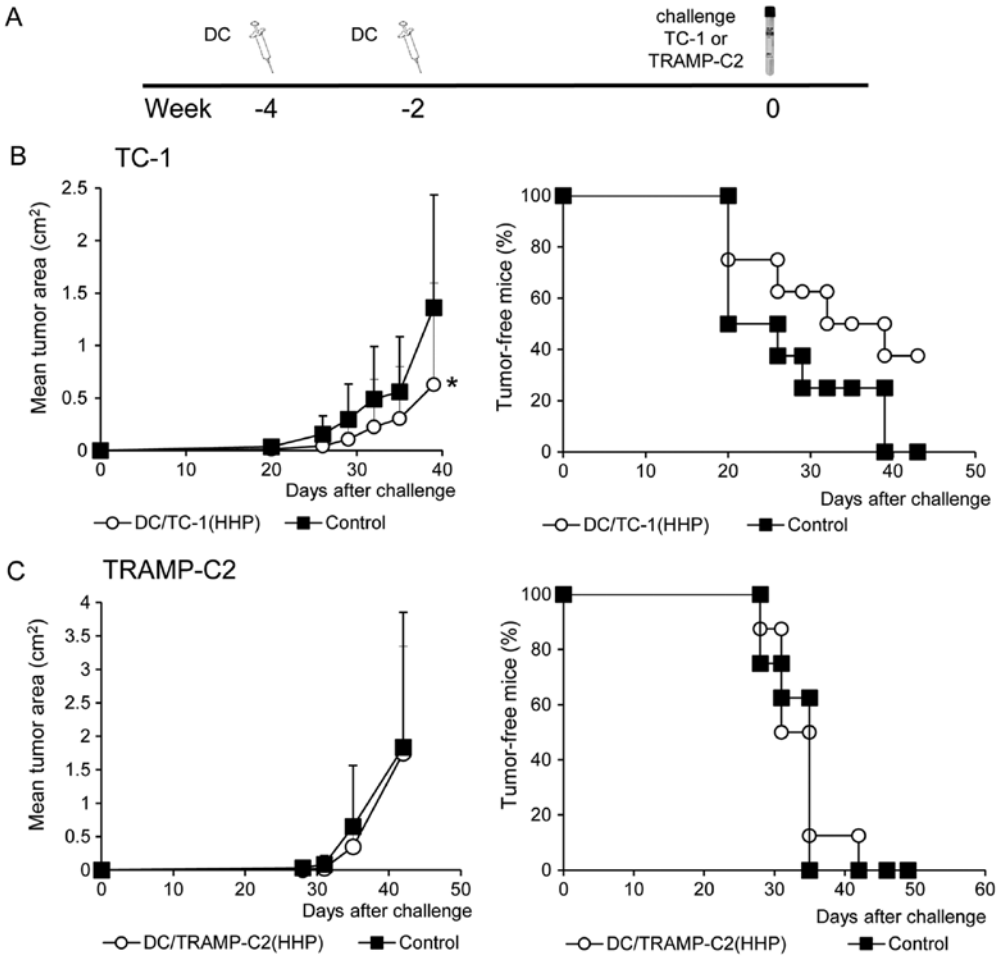

Figure 6. The effect of immunization with DC-based vaccines pulsed with HHP-treated TC-1 or TRAMP-C2 tumor cells. Mice (8 mice per group) were two times s.c. immunized in a 2-week interval with $2x10^6$ DC pulsed with HHP-treated TC-1 or TRAMP-C2 tumor cells (A). Ten days after the second immunization, mice were challenged with $5x10^4$ TC-1 (B) or $1x10^6$ TRAMP-C2 (C) tumor cells. Tumor growth (left panel) and the percentage of tumor-free mice (Kaplan-Maier plot) (right panel) are shown; *P<0.05 vs. control (analysis of variance). The experiments were repeated twice with similar results.

TC-1 and TRAMP-C2 cell lines used for the studies and we demonstrated, in comparative experiments, that HHP induced higher levels of CRT and HSP90 expression on tumor cells, as well as HMGB1 production, as compared to irradiation. The immunogenicity of irradiated and HHP-treated cells was further monitored *in vivo* and we noted higher IFNγ production by spleen cells upon immunization with the HHP-treated compared to irradiated cells. However, we did not observe significantly higher cytotoxicity of the spleen cells from the animals immunized with HHP-treated cells and this finding was in agreement with the results of immunization-challenge experiments. We did not see any significant differences between vaccination with HHP- or IR-treated tumor cells; both vaccinations inhibited TC-1 tumor growth, as expected and previously observed for the animals immunized with IR-treated cells (30,31) while the TRAMP-C2 tumor growth was not blocked by both of the vaccination protocols. It has been previously shown that TRAMP-C2 tumor cells are not immunogenic, unless their immunogenicity was increased by IFNγ treatment, inducing MHC class I cell surface expression (36). Thus, it seems that HHP treatment, which induces ICD but not MHC class I and co-stimulatory molecule cell surface expression, does not induce protective immunity effective against TRAMP-C2 cells. It is of note that in the case of TC-1 tumors, which are apparently more sensitive to immune responses, effective immunity was induced by vaccination with both irradiated and HHP-treated TC-1 cells.

Furthermore, in order to assess the suitability of HHP as a tool for tumor cell preparation in the DC-based vaccine preparation protocols, we prepared a DC-based vaccine by co-culture of immature DC with HHP-treated TC-1 or TRAMP-C2 tumor cells and subsequent DC maturation with CpG ODN 1826. CpG ODN 1826, an agonist of Toll-like receptor 9, is a potent maturation agent for murine DC (37), and the capability of DC pulsed by co-cultivation with irradiated tumor cells and matured by CpG ODN 1826 to inhibit the TC-1 tumor growth has also been demonstrated in our laboratory (38). We have compared the phenotype of matured DC vaccines, unpulsed or pulsed with the IR- or HHP-treated tumor cells. The results suggest that DC co-culture with irradiated, but not HHP-treated tumor cells, interferes with their subsequent CpG ODN-driven maturation, since the matured DC culture of the cells pulsed with IR-treated cells displayed lower proportion of matured DC (defined as MHC class $II^{high}/CD86^{high}$), and lower ratio between the expression of positive costimulatory molecule CD80 (B7.1) vs. negative

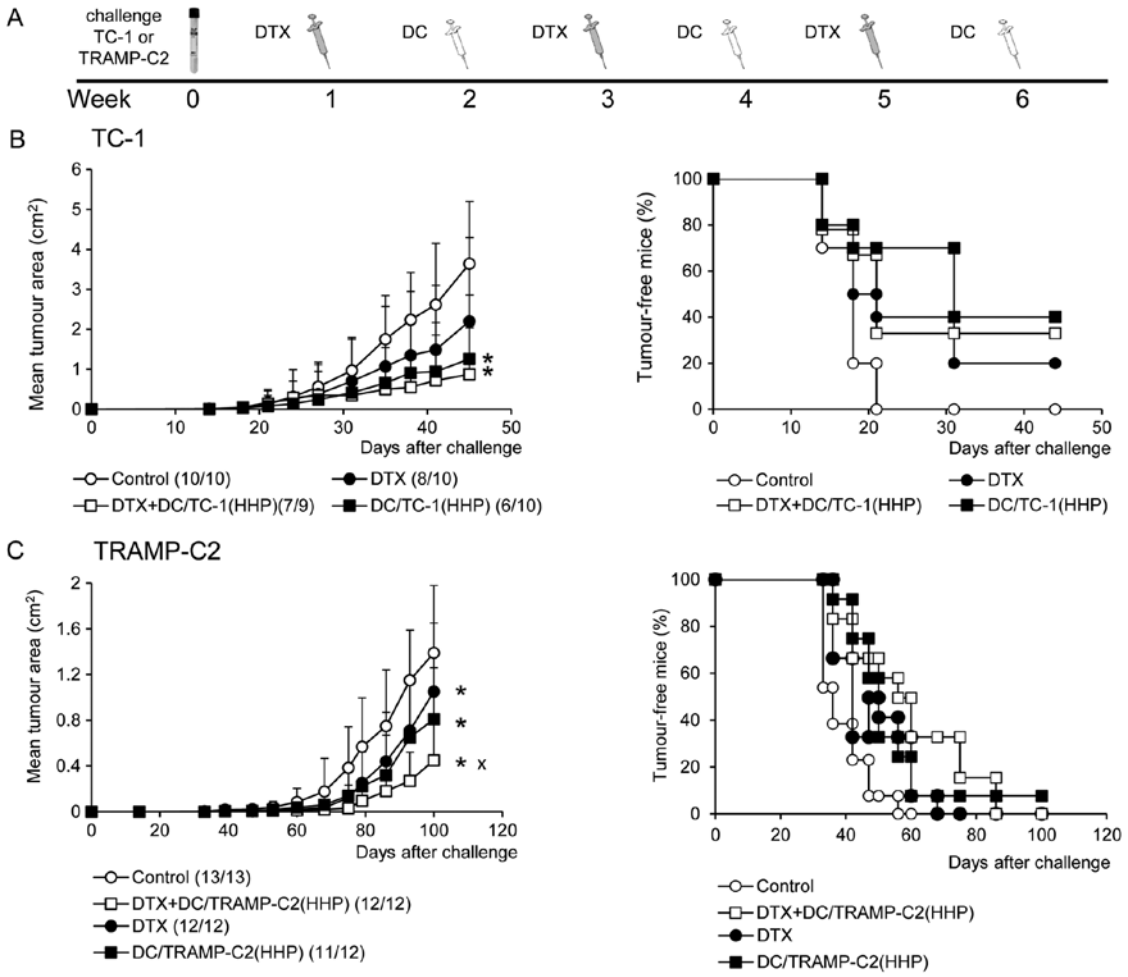

Figure 7. Combined chemoimmunotherapy of TC-1 or TRAMP-C2 tumors. (A) TC-1 ($5x10^4$ cells) or TRAMP-C2 (10^6 cells) tumor cells were s.c. transplanted on day 0. Docetaxel (DTX) was i.p. administered in a dose of 30 μg/kg, on days 7, 21 and 35. Dendritic cells ($2x10^6$ cells) were s.c. administered peritumorally on days 14, 28 and 42. (B) Tumor growth (left panel) of TC-1 tumors and the percentage of tumor-free mice (Kaplan-Maier plot) (right panel). (C) Tumor growth (left panel) of TRAMP-C2 tumors and the percentage of tumor-free mice (right panel) (Kaplan-Maier plot). Results are representative of two independent experiments. *P<0.05 vs. control, xP<0.05 vs. DC/TRAMP-C2(HHP), DTX (analysis of variance).

costimulatory molecule CD274 (B7-H1). This ratio can be considered as an important marker suggesting the DC capability to transmit positive signaling to T cells (39). Selected cytokine expression levels, including that of IL-12, were lower in DC pulsed with IR-treated tumor cells, as compared to the unpulsed controls. Notably, this was not observed when the HHP-treated tumor cells DC were compared to the unpulsed controls. These results suggest that immature DC co-culture with HHP-treated cells represents a convenient protocol for the DC-based vaccine preparation and corroborates previous findings of Fucikova *et al* (13).

The next step was therefore to perform *in vivo* experiments and to evaluate the immunogenicity of the matured DC pulsed with the HHP-treated tumor cells. As expected, DC vaccines induced much higher IFNγ production by spleen cells as compared to immunization with tumor cells. This, together with further parameters investigated in the spleens (chromium release assay, effector memory CD4 and CD8 cell proportion), suggested that DC vaccines induced strong immunity against TC-1 or TRAMP-C2 tumors, respectively. However, as determined in the immunization-challenge experiments, DC vaccination in a prophylactic setting induced protection against TC-1, but not TRAMP-C2 tumor growth. This was in agreement with IR- and HHP-treated tumor cell immunization, confirming different immunogenicity or sensitivity of the TC-1 and TRAMP-C2 tumors to the immune response induced by prophylactic immunization.

Next, we tested the vaccine efficacy in a therapeutic setting in combination with docetaxel chemotherapy, which is clinically relevant especially for prostate cancer treatment (19,20). DC-based vaccines are in general intended to be used rather for tumor immunotherapy in a multimodal setting than for immunization. In our experiments, unlike in prophylactic use, the DC treatments of both immunogenic TC-1 and poorly immunogenic/treatable TRAMP-C2 tumors resulted in significant inhibition of the tumor growth, albeit the effect on the TRAMP-C2 appeared to be weaker as compared to the TC-1 tumors. The difference was observed for the therapeutic protocol using docetaxel and DC combination. This treatment led to the highest therapeutic effect, as compared to the chemotherapy or immunotherapy only treatments, in the case of the TRAMP-C2 prostate cancer model. In this model, both chemo- and immunotherapy, when used as monotherapies, displayed only moderate antitumor effects, and additive/

synergistic effects were observed when these treatments were used in combination. On the contrary, synergistic effects of the combination therapy were not seen for the TC-1 therapy. We can speculate that TC-1 tumors are much more vulnerable to immunotherapy, as compared to the TRAMP-C2 tumors, and that it may be difficult to boost it. Moreover, DTX treatment can increase the TRAMP-C2 tumor cell sensitivity to the immune responses.

In conclusion, in the present study we demonstrated that HHP-treatment induced ICD in the cells of TRAMP-C2 and TC-1 murine tumor cell lines. Furthermore, our results show that DC-based vaccines pulsed with HHP-treated cells is an effective instrument for immunotherapy, mainly when combined with chemotherapy, as has been demonstrated in the prostate cancer TRAMP-C2 model, which is poorly immunogenic and difficult to treat.

Acknowledgements

The present study was supported by research grant provided by SOTIO a.s., and in part by MEYS (LM2011032), the Academy of Sciences of the Czech Republic (RVO 68378050), the project 'BIOCEV-Biotechnology and Biomedicine Centre of the Academy of Sciences and Charles University' (CZ.1.05/1.1.00/02.0109) from the European Regional Development Fund. The authors are grateful to Mrs. Renáta Turečková for skillful technical assistance and to Dr Šárka Takáčová for editorial help. Conflict of interest: J. Bartůňková and R. Špišek are employees and shareholders of SOTIO a.s.

References

1. Ramakrishnan R, Antonia S and Gabrilovich DI: Combined modality immunotherapy and chemotherapy: A new perspective. Cancer Immunol Immunother 57: 1523-1529, 2008.
2. Nowak AK, Lake RA and Robinson BW: Combined chemoimmunotherapy of solid tumours: Improving vaccines? Adv Drug Deliv Rev 58: 975-990, 2006.
3. Banchereau J and Steinman RM: Dendritic cells and the control of immunity. Nature 392: 245-252, 1998.
4. Palucka K and Banchereau J: Cancer immunotherapy via dendritic cells. Nat Rev Cancer 12: 265-277, 2012.
5. Galluzzi L, Senovilla L, Vacchelli E, Eggermont A, Fridman WH, Galon J, Sautès-Fridman C, Tartour E, Zitvogel L and Kroemer G: Trial watch: Dendritic cell-based interventions for cancer therapy. Oncoimmunology 1: 1111-1134, 2012.
6. Podrazil M, Horvath R, Becht E, Rozkova D, Bilkova P, Sochorova K, Hromadkova H, Kayserova J, Vavrova K, Lastovicka J, *et al*: Phase I/II clinical trial of dendritic-cell based immunotherapy (DCVAC/PCa) combined with chemotherapy in patients with metastatic, castration-resistant prostate cancer. Oncotarget 6: 18192-18205, 2015.
7. Fucikova J, Kralikova P, Fialova A, Brtnicky T, Rob L, Bartunkova J and Spísek R: Human tumor cells killed by anthracyclines induce a tumor-specific immune response. Cancer Res 71: 4821-4833, 2011.
8. Hato SV, Khong A, de Vries IJ and Lesterhuis WJ: Molecular pathways: The immunogenic effects of platinum-based chemotherapeutics. Clin Cancer Res 20: 2831-2837, 2014.
9. Spisek R, Charalambous A, Mazumder A, Vesole DH, Jagannath S and Dhodapkar MV: Bortezomib enhances dendritic cell (DC)-mediated induction of immunity to human myeloma via exposure of cell surface heat shock protein 90 on dying tumor cells: Therapeutic implications. Blood 109: 4839-4845, 2007.
10. Galluzzi L, Kepp O and Kroemer G: Immunogenic cell death in radiation therapy. Oncoimmunology 2: e26536, 2013.
11. Weiss EM, Frey B, Rödel F, Herrmann M, Schlücker E, Voll RE, Fietkau R and Gaipl US: Ex vivo- and in vivo-induced dead tumor cells as modulators of antitumor responses. Ann NY Acad Sci 1209: 109-117, 2010.
12. Frey B, Rubner Y, Kulzer L, Werthmöller N, Weiss EM, Fietkau R and Gaipl US: Antitumor immune responses induced by ionizing irradiation and further immune stimulation. Cancer Immunol Immunother 63: 29-36, 2014.
13. Fucikova J, Moserova I, Truxova I, Hermanova I, Vancurova I, Partlova S, Fialova A, Sojka L, Cartron PF, Houska M, *et al*: High hydrostatic pressure induces immunogenic cell death in human tumor cells. Int J Cancer 135: 1165-1177, 2014.
14. Emens LA: Chemoimmunotherapy. Cancer J 16: 295-303, 2010.
15. Ménard C, Martin F, Apetoh L, Bouyer F and Ghiringhelli F: Cancer chemotherapy: Not only a direct cytotoxic effect, but also an adjuvant for antitumor immunity. Cancer Immunol Immunother 57: 1579-1587, 2008.
16. van Dodewaard-de Jong JM, Verheul HM, Bloemendal HJ, de Klerk JM, Carducci MA and van den Eertwegh AJ: New treatment options for patients with metastatic prostate cancer: What is the optimal sequence? Clin Genitourin Cancer 13: 271-279, 2015.
17. Machiels JP, Reilly RT, Emens LA, Ercolini AM, Lei RY, Weintraub D, Okoye FI and Jaffee EM: Cyclophosphamide, doxorubicin, and paclitaxel enhance the antitumor immune response of granulocyte/macrophage-colony stimulating factor-secreting whole-cell vaccines in HER-2/neu tolerized mice. Cancer Res 61: 3689-3697, 2001.
18. Malvicini M, Rizzo M, Alaniz L, Piñero F, García M, Atorrasagasti C, Aquino JB, Rozados V, Scharovsky OG, Matar P, *et al*: A novel synergistic combination of cyclophosphamide and gene transfer of interleukin-12 eradicates colorectal carcinoma in mice. Clin Cancer Res 15: 7256-7265, 2009.
19. Tannock IF, de Wit R, Berry WR, Horti J, Pluzanska A, Chi KN, Oudard S, Théodore C, James ND, Turesson I, *et al*; TAX 327 Investigators: Docetaxel plus prednisone or mitoxantrone plus prednisone for advanced prostate cancer. N Engl J Med 351: 1502-1512, 2004.
20. Petrylak DP, Tangen CM, Hussain MH, Lara PN Jr, Jones JA, Taplin ME, Burch PA, Berry D, Moinpour C, Kohli M, *et al*: Docetaxel and estramustine compared with mitoxantrone and prednisone for advanced refractory prostate cancer. N Engl J Med 351: 1513-1520, 2004.
21. Kantoff PW, Higano CS, Shore ND, Berger ER, Small EJ, Penson DF, Redfern CH, Ferrari AC, Dreicer R, Sims RB, *et al*; IMPACT Study Investigators: Sipuleucel-T immunotherapy for castration-resistant prostate cancer. N Engl J Med 363: 411-422, 2010.
22. Reinis M, Indrová M, Mendoza L, Mikysková R, Bieblová J, Bubeník J and Símová J: HPV16-associated tumours: Therapy of surgical minimal residual disease with dendritic cell-based vaccines. Int J Oncol 25: 1165-1170, 2004.
23. Reinis M, Stepanek I, Simova J, Bieblova J, Pribylova H, Indrova M and Bubenik J: Induction of protective immunity against MHC class I-deficient, HPV16-associated tumours with peptide and dendritic cell-based vaccines. Int J Oncol 36: 545-551, 2010.
24. Indrová M, Reinis M, Bubeník J, Jandlová T, Bieblová J, Vonka V and Velek J: Immunogenicity of dendritic cell-based HPV16 E6/E7 peptide vaccines: CTL activation and protective effects. Folia Biol (Praha) 50: 184-193, 2004.
25. Lin KY, Guarnieri FG, Staveley-O'Carroll KF, Levitsky HI, August JT, Pardoll DM and Wu TC: Treatment of established tumors with a novel vaccine that enhances major histocompatibility class II presentation of tumor antigen. Cancer Res 56: 21-26, 1996.
26. Foster BA, Gingrich JR, Kwon ED, Madias C and Greenberg NM: Characterization of prostatic epithelial cell lines derived from transgenic adenocarcinoma of the mouse prostate (TRAMP) model. Cancer Res 57: 3325-3330, 1997.
27. Lutz MB, Kukutsch N, Ogilvie AL, Rössner S, Koch F, Romani N and Schuler G: An advanced culture method for generating large quantities of highly pure dendritic cells from mouse bone marrow. J Immunol Methods 223: 77-92, 1999.
28. Stepanek I, Indrova M, Bieblova J, Fucikova J, Spisek R, Bubenik J and Reinis M: Effects of 5-azacytidine and trichostatin A on dendritic cell maturation. J Biol Regul Homeost Agents 25: 517-529, 2011.

29. Yi AK and Krieg AM: CpG DNA rescue from anti-IgM-induced WEHI-231 B lymphoma apoptosis via modulation of I kappa B alpha and I kappa B beta and sustained activation of nuclear factor-kappa B/c-Rel. J Immunol 160: 1240-1245, 1998.
30. Reinis M, Símová J, Indrová M, Bieblová J, Pribylová H, Moravcová S, Jandlová T and Bubeník J: Immunization with MHC class I-negative but not -positive HPV16-associated tumour cells inhibits growth of MHC class I-negative tumours. Int J Oncol 30: 1011-1017, 2007.
31. Indrová M, Símová J, Bieblová J, Bubeník J and Reinis M: NK1.1$^+$ cells are important for the development of protective immunity against MHC I-deficient, HPV16-associated tumours. Oncol Rep 25: 281-288, 2011.
32. Bubenik J, Zeuthen J, Indrova M, Bubenikova D and Simova J: Kinetics and function of peritoneal-exudate cells during local IL-2 gene-therapy of cancer. Int J Oncol 4: 13-16, 1994.
33. Indrová M, Mikysková R, Jandlová T, Vonka V, Bubeník J and Bieblová J: Adjuvant cytokine treatment of minimal residual disease after surgical therapy in mice carrying HPV16-associated tumours: Cytolytic activity of spleen cells from tumour regressors. Folia Biol (Praha) 49: 217-222, 2003.
34. Frey B, Janko C, Ebel N, Meister S, Schlücker E, Meyer-Pittroff R, Fietkau R, Herrmann M and Gaipl US: Cells under pressure - treatment of eukaryotic cells with high hydrostatic pressure, from physiologic aspects to pressure induced cell death. Curr Med Chem 15: 2329-2336, 2008.
35. Adkins I, Fucikova J, Garg AD, Agostinis P and Špíšek R: Physical modalities inducing immunogenic tumor cell death for cancer immunotherapy. Oncoimmunology 3: e968434, 2014.
36. Martini M, Testi MG, Pasetto M, Picchio MC, Innamorati G, Mazzocco M, Ugel S, Cingarlini S, Bronte V, Zanovello P, *et al*: IFN-gamma-mediated upmodulation of MHC class I expression activates tumor-specific immune response in a mouse model of prostate cancer. Vaccine 28: 3548-3557, 2010.
37. Okamoto M and Sato M: Toll-like receptor signaling in anti-cancer immunity. J Med Invest 50: 9-24, 2003.
38. Reinis M, Símová J, Indrová M, Bieblová J and Bubeník J: CpG oligodeoxynucleotides are effective in therapy of minimal residual tumour disease after chemotherapy or surgery in a murine model of MHC class I-deficient, HPV16-associated tumours. Int J Oncol 30: 1247-1251, 2007.
39. Spranger S, Javorovic M, Bürdek M, Wilde S, Mosetter B, Tippmer S, Bigalke I, Geiger C, Schendel DJ and Frankenberger B: Generation of Th1-polarizing dendritic cells using the TLR7/8 agonist CL075. J Immunol 185: 738-747, 2010.

5.6. Dendritické buňky pulzované nádorovými buňkami inaktivovanými vysokým hydrostatickým tlakem inhibují růst nádoru prostaty v myších TRAMP-C2 modelech

Předcházející práce ukázala, že terapie na bázi DCs pulzovaných nádorovými buňkami inaktivovanými HHP představuje slibnou strategii v chemoimunoterapii karcinomu prostaty. Dendritické buňky (jak pulzované, tak nepulzované) vykazovaly stejnou účinnost jako docetaxel v inhibici slabě imunogenních TRAMP-C2 nádorů. I když kombinovaná chemoimunoterapie neměla žádný synergický efekt a již nevedla k dalšímu zpomalení růstu nádoru, tak snížená proliferace nádorových buněk byla detekována pouze v histologických vzorcích odebraných z TRAMP-C2 nádorů léčených DCs pulzovanými nádorovými buňkami inaktivovanými HHP v kombinaci s docetaxelem. Podobné výsledky byly také získány v případě kombinace pulzovaných DCs s dalším klinicky používaným cytostatikem, cyklofosfamidem. Myším byly DCs také aplikovány až po chirurgickém odstranění nádorů, tedy ve stavu odpovídajícím minimální reziduální nemoci. V tomto nastavení vedla aplikace vakcíny založené na DCs ke sníženému výskytu recidivy onemocnění, a to jak v případě imunogenních TC-1, tak slabě imunogenních TRAMP-C2 nádorů. Po aplikaci DCs byla také analyzována cytotoxická aktivita splenocytů ve snaze identifikovat populaci efektorových buněk. Tyto buňky byly definovány jako $CD4^+NK1.1^+$, což poukazuje spíše na nespecifický terapeutický efekt vakcíny na bázi DCs v tomto nastavení.

K této práci jsem přispěla následovně: příprava nádorových linií ošetřených HHP, měření viability a detekce DAMPs (HSP70, HSP90 a CRT) na povrchu nádorových linií ošetřených HHP pomocí průtokové cytometrie.

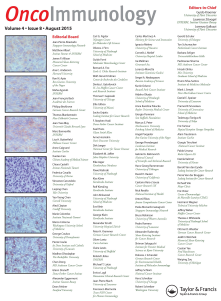

OncoImmunology

ISSN: (Print) 2162-402X (Online) Journal homepage: http://www.tandfonline.com/loi/koni20

Dendritic cells pulsed with tumor cells killed by high hydrostatic pressure inhibit prostate tumor growth in TRAMP mice

Romana Mikyskova, Marie Indrova, Ivan Stepanek, Ivan Kanchev, Jana Bieblova, Sarka Vosahlikova, Irena Moserova, Iva Truxova, Jitka Fucikova, Jirina Bartunkova, Radek Spisek, Radislav Sedlacek & Milan Reinis

To cite this article: Romana Mikyskova, Marie Indrova, Ivan Stepanek, Ivan Kanchev, Jana Bieblova, Sarka Vosahlikova, Irena Moserova, Iva Truxova, Jitka Fucikova, Jirina Bartunkova, Radek Spisek, Radislav Sedlacek & Milan Reinis (2017): Dendritic cells pulsed with tumor cells killed by high hydrostatic pressure inhibit prostate tumor growth in TRAMP mice, OncoImmunology, DOI: 10.1080/2162402X.2017.1362528

To link to this article: http://dx.doi.org/10.1080/2162402X.2017.1362528

Accepted author version posted online: 24 Aug 2017.
Published online: 24 Aug 2017.

ONCOIMMUNOLOGY
2017, VOL. 0, NO. 0, e1362528 (10 pages)
https://doi.org/10.1080/2162402X.2017.1362528

Taylor & Francis
Taylor & Francis Group

ORIGINAL RESEARCH

Dendritic cells pulsed with tumor cells killed by high hydrostatic pressure inhibit prostate tumor growth in TRAMP mice

Romana Mikyskova[a,b], Marie Indrova[a,b], Ivan Stepanek[a,b], Ivan Kanchev[a,b], Jana Bieblova[b], Sarka Vosahlikova[d], Irena Moserova[d], Iva Truxova[d], Jitka Fucikova[c,d], Jirina Bartunkova[c,d], Radek Spisek[c,d], Radislav Sedlacek[a,b], and Milan Reinis [a,b]

[a]Department of Transgenic Models of Diseases, Institute of Molecular Genetics of the AS CR, v.v.i., Prague, Czech Republic; [b]Czech Centre for Phenogenomics, Institute of Molecular Genetics of the ASCR, Prague, Czech Republic; [c]Department of Immunology, Charles University, 2nd Faculty of Medicine and University Hospital Motol, Prague, Czech Republic; [d]SOTIO, a.s., Prague, Czech Republic

ABSTRACT

Dendritic cell (DC)-based vaccines pulsed with high hydrostatic pressure (HHP)-inactivated tumor cells have recently been shown to be a promising tool for prostate cancer chemoimmunotherapy. In this study, DC-based vaccines, both pulsed and unpulsed, were as effective as docetaxel (DTX) in reducing prostate tumors in the orthotopic transgenic adenocarcinoma of the mouse prostate (TRAMP) model. However, we did not observe any additive or synergic effects of chemoimmunotherapy on the tumor growth, while only the combination of DTX and pulsed dendritic cells resulted in significantly lower proliferation detected by Ki67 staining in histological samples. The DC-based vaccine pulsed with HHP-treated tumor cells was also combined with another type of cytostatic, cyclophosphamide, with similar results. In another clinically relevant setting, minimal residual tumor disease after surgery, administration of DC-based vaccines after the surgery of poorly immunogenic transplanted TRAMP-C2, as well as in immunogenic TC-1 tumors, reduced the growth of tumor recurrences. To identify the effector cell populations after DC vaccine application, mice were twice immunized with both pulsed and unpulsed DC vaccine, and the cytotoxicity of the spleen cells populations was tested. The effector cell subpopulations were defined as $CD4^+$ and $NK1.1^+$, which suggests rather unspecific therapeutic effects of the DC-based vaccines in our settings. Taken together, our data demonstrate that DC-based vaccines represent a rational tool for the treatment of human prostate cancer.

ARTICLE HISTORY
Received 12 June 2017
Revised 27 July 2017
Accepted 28 July 2017

KEYWORDS
dendritic cells; docetaxel; high hydrostatic pressure; immunotherapy; prostate cancer

Introduction

Prostate cancer remains the most common diagnosed non-skin malignancy in elderly men and the second leading cause of cancer-related death in Western countries.[1] Up to 40% of men diagnosed with prostate cancer will eventually develop metastatic disease, and although most respond to initial medical or surgical castration, progression to castration resistance is universal.[2] Docetaxel (DTX), a widely used chemotherapeutic drug, has represented the first-line chemotherapy for metastatic castration-resistant prostate cancer since 2004.[3] DTX has also been suggested to have immune enhancing properties against tumors and was shown to antagonize myeloid-derived suppressor cells (MDSCs) by their polarization toward M1 macrophages.[4] In the past few years, cancer immunotherapy has made significant strides due to improved understanding of the underlying principles of tumor biology and immunology.[5-7] It is an attractive approach to cancer treatment, especially when combined with other therapeutic modalities such as chemotherapy. Synergic effects of combinations of immunotherapy and chemotherapy have been demonstrated in several pre-clinical and clinical studies.[8,9] Dendritic cells (DCs) are key players in the immune response as they are able to capture antigens with their pattern-recognition receptors, to process and present them to *naïve* T-cells, inducing their activation,[10] and thus building an essential bridge between innate and adaptive responses. The possibility of their generation *in vitro* enabled their use for immunotherapy of cancer,[11] and several clinical trials have been performed in the last decade.[12,13] The first cellular immunotherapy based on activated peripheral blood mononuclear cells, Sipuleucel T, has been FDA-approved.[14] Typically, an autologous dendritic cell-based vaccine represents *in vitro* cultured dendritic cells loaded with tumor antigens that can be in the form of tumor cells with subsequent DC maturation. For DC pulsing, tumor cells can be inactivated by different ways, and selection of the optimal inactivation method can be crucial for DC vaccine optimization.[15,16] High hydrostatic pressure (HHP) has been demonstrated as a method for tumor cell inactivation preserving their immunogenic capacity[17] and HHP-treated cells were able to induce monocyte-derived DC maturation, and DC co-cultured with HHP-treated tumor cells were able to induce T cell activation *in vitro*. These results showed HHP as a convenient tool for tumor cell inactivation before their use for DC pulsing.[17] In our previous work, we demonstrated, using murine tumor models, that HHP was able

CONTACT Milan Reinis milan.reinis@img.cas.cz Institute of Molecular Genetics of the Academy of Sciences of the Czech Republic, v. v. i., Vídeňská 1083, Prague 4, 142 20, Czech Republic.

to induce immunogenic cell death of both TC-1 and TRAMP-C2 tumor cells, representing murine models for human papilloma virus-associated tumors and prostate cancer, respectively. HHP-treated cells were successfully used for preparation of a DC vaccine that is based on DC pulsed with HHP-treated tumor cells inducing high immune responses. In combination with docetaxel chemotherapy, these vaccines significantly inhibited not only growth of immunogenic TC-1, but also poorly immunogenic TRAMP-C2 tumors.[18] Here, we investigated the therapeutic capacity of the HHP cell-pulsed DC vaccines using a clinically more relevant, orthotopic model for prostate cancer treatment, transgenic adenocarcinoma of the mouse prostate (TRAMP) mice, males that spontaneously develop prostate tumors following the onset of puberty.[19] We have also demonstrated the DC vaccine efficacy in a previously established therapeutic setting, minimal residual tumor disease after surgery.[20-23]

Material and methods

Mice

Female heterozygous C57BL/6/TGN TRAMP mice, line PB Tag 8247NG were purchased from The Jackson Laboratory (Bar Harbor, ME). Transgenic males for the studies were routinely obtained as [TRAMP x C57BL/6/TGN]F1 or [TRAMP x C57BL/6/TGN]F2 offspring. The genotypes of TRAMP mice were confirmed by PCR-based screening using tail biopsies. We added 0.3 ml 50 mM NaOH to the tail biopsies and incubated them for 90 minutes at 95°C, neutralized by adding 0.4 ml Tris buffer (pH 7.2, 20 mM) and centrifuged (4000 *g*, 3 min). We prepared aliquots of the master mix (Aptamer hot start master mix, Top-Bio) for each PCR reaction with primers specific for the transgene (fw GCGCTGCTGACTTTCTAAACATAAG, rev GAGCTCACGTTAAGTTTTGATGTGT), for positive control (fw CTAGGCCACAGAATTGAAAGATCT, rev GTAGG TGGAAATTCTAGCATCATCC) and finally, we added 2.5 μl of 10x diluted DNA in water. C57BL/6/TGN (B6) male mice, 6–8 weeks old, were obtained from AnLab Co., Prague, Czech Republic. Experimental protocols were approved by the Institutional Animal Care Committee of the Institute of Molecular Genetics, Prague.

Tumor cell lines

The TC-1 tumor cell line (obtained from ATCC collection) was developed by co-transfection of murine C57BL/6/TGN lung cells with HPV16 E6/E7 genes and activated (G12V) Ha-ras plasmid DNA.[24] TRAMP-C2 tumor cells (obtained from ATCC collection), MHC class I-deficient, were established from a heterogeneous 32-week tumor of the transgenic adenocarcinoma mouse prostate (TRAMP) model.[25] TC-1 cells were maintained in RPMI 1640 medium (Sigma-Aldrich GmbH) supplemented with 10% FCS (PAN Biotech GmbH), 2 mM L-glutamine and antibiotics; TRAMP-C2 cells were maintained in D-MEM medium (Sigma-Aldrich GmbH) supplemented with 5% FCS, 5%Nu-Serum IV (Corning), 0.005 mg/ml human insulin (Sigma-Aldrich GmbH), 10 nM dehydroisoandrosterone (DHEA, Sigma-Aldrich GmbH) and antibiotics. Both cell lines were cultured at 37°C in a humidified atmosphere with 5% CO_2.

High hydrostatic pressure treatment

Tumor cells were treated by 200 MPa in the custom-made device (Resato International BV, Netherlands) that is located in the GMP manufacturing facility, SOTIO, a.s., Prague. This device allows reliable treatment of tumor cells by the defined levels of HHP for specified periods of time (10 minutes in the case of 200 MPa).[17]

Dendritic cell preparation

Dendritic cells (DC) were prepared from bone marrow precursors as described by Lutz [26,27] with slight modifications.[28] Briefly, the bone marrow cells were cultured for 7 d in the complete RPMI 1640 medium supplemented with 2×10^{-5} M mercaptoethanol (Calbiochem), 10 ng/ml GM-CSF and IL-4 (R&D Systems). On day 5, the DC were pulsed with HHP-treated tumor cells by 48 h incubation in a ratio of 2:1 (DC/tumor cells, 10^6 DC/ml). Some DC were also left unpulsed. DC pulsed or unpulsed with the tumor cells were treated for 24 h with unmethylated CpG containing phosphorothioate-modified oligodeoxynucleotide CpG ODN 1826 (5'-TCCATGACGTTCCTGACGTT-3')[29] at a final concentration of 5 μg/ml (Generi Biotech), that were sulfur-modified in their backbone (phosphorothioate) and synthesized under endotoxin-free conditions. On day 7, non-adherent cells were harvested. These cells, designated as DC, pulsed or unpulsed, contained approximately 60–70% $CD11c^+$ cells. For mouse therapeutic experiments, DC were washed twice with PBS and injected subcutaneously (s.c.) in PBS, 300 μl/2×10^6 cells/mouse.

Therapeutic experiments with TRAMP mice

Approximately 8-week-old male TRAMP mice were used for the therapeutic experiments. In each experiment, 10–12 mice per experimental group were used. Docetaxel, 30 mg/kg (Actavis) was repeatedly administered on weeks 8, 10, 12 and 14 intraperitoneally (i.p.). Dendritic cells were s.c. administered on weeks 9, 11, 13 and 15. Tumor growth was followed by palpation. When the animals were 28 weeks old, the experiment was terminated. Mice underwent autopsy, their genitourinary tracts (GUT) were dissected and weighed, and fixed in 4% paraformaldehyde in PBS for 24 h, then embedded and mounted for histopathology analysis. In case of the combination experiment where CY treatment was used, CY, 200 mg/kg (Endoxan, Baxter Oncology GmbH) was administered i.p. only once, on week 8, and the vaccine on weeks 9, 11, 13 and 15. For evaluation of this part, the values of untreated group and the group treated with pulsed dendritic cells from DTX combination experiment were used, as allowed by the spontaneous tumor model.

Treatment of surgical minimal residual tumor disease

To obtain the minimal residual tumor disease after surgery, B6 mice were inoculated s.c. with TC-1 (5×10^4 cells) or TRAMP-C2 (10^6 cells). After approximately 28 days, when the

transplanted tumors reached ~5–10 mm in diameter, the tumors were excised under i.p. anesthesia, leaving no macroscopically visible tumor residuum.[30] The hypothetical microscopic tumor residua after surgery were designated as surgical minimal residual tumor disease. Mice were randomly divided into 3 experimental groups. One experimental group was left without treatment as a control group (operated-only mice). Two groups of experimental mice were s.c. treated with DC-based vaccines, one group with pulsed and one group with unpulsed cells (2×10^6 cells/mouse). Vaccines were administered on days 7 and 21 in the site of previous tumor surgery. In one experiment, mice were also pretreated with pulsed DC vaccine on day -7 in case of TC-1 surgery and -21, -7 in case of TRAMP-C2 surgery. Mice were observed twice a week and the size of the tumors was recorded. Two perpendicular diameters of the tumors were measured with a caliper and the tumor size was expressed as the tumor area (cm^2).

Histopathology analysis

Morphology of the therapeutic response

Semi-thin sections of 5 μm were obtained from 3 different regions of the dissected tumor and stained with hematoxylin and eosin in an autostainer (Ventana Symphony, entana Medical Systems). Analysis for response assessed either diminished amount tumor infiltrates in the section and/or presence of neoplastic cell degeneration, necrosis, or apoptotic bodies. Grading of the response to different therapeutic regimens was done evaluating 3 regions: the primary neoplasm in the dorsal prostate, the secondary infiltrate in the proximal part of the seminal vesicle, and the tertiary: presence of infiltrate in the distal part of the seminal vesicle. The scoring system used complete response (equals 2; includes complete neoplastic cell degeneration in the respective region), incomplete response (equals 1; partial degeneration of the tumor) and absence (equals 0; the neoplasm is not affected and represents typical morphology) of the neoplasm in any of the 3 regions evaluated, i.e. the tumor vitality score. A cumulative score of minimum 0 and maximum of 6 was calculated as a sum of individual scores in every single mouse.

Immunohistochemistry

Immunohistochemistry was performed on sections of the primary neoplasia to evaluate the Ki67 labeling index. In brief, 3 μm thick sections were submitted to automated rehydration, antigen damasking, and immune reaction in a Ventana Discovery ULTRA automated slide stainer. The variable points in the procedure are epitope retrieval for 32 min in CC1 buffer (Ventana Medical Systems Tucson AZ; pH 9.0), automatic application of anti Ki67 antibody (Clone SP6, 1:500; Thermo Scientific) at 37 °C for 32 min. The detection was done by a secondary anti-rabbit polymer system conjugated with peroxidase (Zytomed GmbH) after its manual application and incubation in the stainer at 37°C for 32 min. The reaction was developed by the amino-ethyl-carbazole ready-to-use solution (DAKO) at 37°C for 20 min. Counterstaining was performed by the autostainer using Gill's hematoxylin II. All slides were consecutively coverslipped in Ventana Symphony using its coverslipper function.

Immunohistochemistry evaluation and scoring

Scoring was done using quantitative and qualitative approach. In brief, 5 individual high power fields (40fold magnification) were analyzed for presence of Ki67-positive reaction by manual counting of 4 different intensity levels: negative (0), weakly positive (1), moderately positive (2) and strongly positive (3) as a normalizer the total count of the nuclei in every respective field was counted. At least 250 cells were counted per field. The score was calculated as a proportion of the maximum possible score per field, meaning as sum of the individual cell numbers multiplied by their group intensity (n_1 x0, for negative cells; n_2 x1 for weak positive cells; n_3 x2 for moderate positive and n_4 x3 for strong positive cells), divided by the maximum score per field:

$$Score = \frac{n1.0 + n2.1 + n3.2 + n4.3}{\Sigma(n1, 2, 3, 4).3}$$

Flow cytometry

Expression of cell surface molecules on the DC was determined by flow cytometry. The expression of CD11c, MHC class II, and CD86 was analyzed using the following antibodies: APC anti-CD11c (HL3), FITC anti-MHCII (AF6–120.1) and PE anti-CD86 (GL1) (RB6–8C5). The percentage of $CD44^+$ $CD62L^-$ of $CD8^+$ and $CD4^+$ lymphocytes in splenocytes from immunized mice was determined by flow cytometry using the following antibodies: PE anti-CD44 (IM7), APC-CY7 anti-CD62L (MEL-14), PE-CF594 anti-CD8 (53–6.7), and FITC anti-CD4 (RM4–5). Relevant unspecific isotype controls were used. All products were purchased from BD Biosciences. FACS analysis was performed using an LSR II flow cytometer (BD Biosciences) and analyzed by FlowJo 7.6.5 software.

Immunization/challenge experiments with dendritic cells

Mice, 3 animals per group, were twice immunized with 2×10^6 cells of pulsed and unpulsed DC-based vaccine in a 2-week interval. Control mice received vehiculum only. Ten day after the second immunization, mice were killed, single-cell suspensions from the spleens were prepared and the cells were used for further analysis by FACS, chromium release assay, and ELISPOT.

Chromium release microcytotoxicity assay

The cytolytic activity of effector cells was tested in 18 h ^{51}Cr release assay, as described earlier.[21,31] Briefly, spleen cells from control and immunized mice that served as effector cells were treated with ammonium chloride-potassium lysing buffer (1 min) to deplete erythrocytes. The mixtures of effector cells with relevant ^{51}Cr-labeled tumor targets were incubated in selected target/effector cell ratios (1:25, 1:50, 1:100, 1:200) in triplicate in 96-well round bottom microtiter plates (Nunc). The percentage of specific ^{51}Cr release was expressed according to the formula: [cpm experimental release – cpm control release / cpm maximum release /cpm control release] × 100.

For depletion of selected spleen cell subpopulations, 5×10 and 2.5×10^5 spleen cells/well were seeded in 96-well round bottom microtiter plates (Nunc) and incubated for 1 h at 37°C with 5 μg/ml of anti-CD8 (2.43), anti-CD4 (GK1.5) or anti-NK 1.1 (PK136) antibodies (EXBIO) with addition of the same

volume of RPMI 1640 media and Baby Rabbit Complement (Cedarlane) diluted according to the manufacturer's instruction. After the incubation, plates were washed 2 times with RPMI 1640 and used for the microcytotoxicity assay.

For positive selection of effector cells, CD8-positive, CD4-positive and NK1.1-positive cells from the spleens of immunized animals were isolated using anti mouse CD8 (Ly-2) CD4 (L3T4), or CD49b (DX5) NK1.1 antibodies conjugated to magnetic MicroBeads (Miltenyi Biotec), in accordance with the manufacturer's instructions, as described previously.[32,33] Cell separation was performed with the autoMACS system (Miltenyi Biotec). The purity of cells was verified by FACS analysis. The percentage of $CD8^+$, $CD4^+$ and $NK1.1^+$ cells achieved 86–91%. 5×10^5 and 2.5×10^5 spleen cells/well were seeded in 96-well round bottom microtiter plates (Nunc) and used for microcytotoxicity assay.

ELISPOT

To determine the amount of IFNγ-secreting cells, an ELISPOT kit for detection of murine IFNγ (BD Biosciences) was used. Spleen cells were cultured for 48 h and then placed into the wells of ELISPOT plates (concentration 1×10^5, 5×10^4, 5×10^3 cells/well) for 24 h. The plates were then processed according to the manufacturer's instructions (BD Biosciences). Colored spots were counted with CTL Analyzer LLC (CTL) and analyzed using the ImmunoSpot Image Analyzer software.

Statistical analyses

For statistical analyses of *in vitro* experiments, Student's t-test was used. For evaluation of *in vivo* experiments, Analysis of Variance (ANOVA) from the NCSS, Number Cruncher Statistical System (Kaysville, Utah, USA) statistical package was used. Standard deviations are indicated in the figures.

Results

Combined chemoimmunotherapy of TRAMP mice with docetaxel and DC-based vaccine inhibited tumor growth

The therapeutic efficacy of HHP-treated tumor cell-pulsed or unpulsed matured DC used either as monotherapy or in combination with the DTX treatment was tested in TRAMP mice. Approximately 8-week-old male TRAMP mice were repeatedly treated with DTX alone, antigen-pulsed or unpulsed DC-based vaccine, or with their combination (Fig. 1A). Tumor growth was verified by palpation and 28 weeks old mice were autopsied. The tumor development was quantified by genitourinary tract weight evaluation, as well as by scoring of the therapeutic response using histopathology analysis. As can be seen in Fig. 1B, genitourinary tract weights expressed as weight GUT per mouse body weight were significantly decreased after the treatments with DTX or both DC pulsed with HHP-treated tumor cells and unpulsed ($^*P<0.05$). Combined chemoimmunotherapy using DTX and DC vaccines also resulted in significantly decreased GUT weights. However, we did not observe any additive or synergic effects of the combined treatments. Therapeutic responses were confirmed by histopathology scoring of the neoplasms analyzed in 3 different positions of the primary site, proximal part of the seminal vesicle and distal part of the vesicular gland, as described in Material and Methods. Histopathology evaluation showed a significantly higher therapeutic response to DC-based vaccine, both pulsed and unpulsed, as well as to their combination with DTX (Fig. 2A). Figure 2B shows representative pictures of scoring. The trend toward less advanced cancer was also

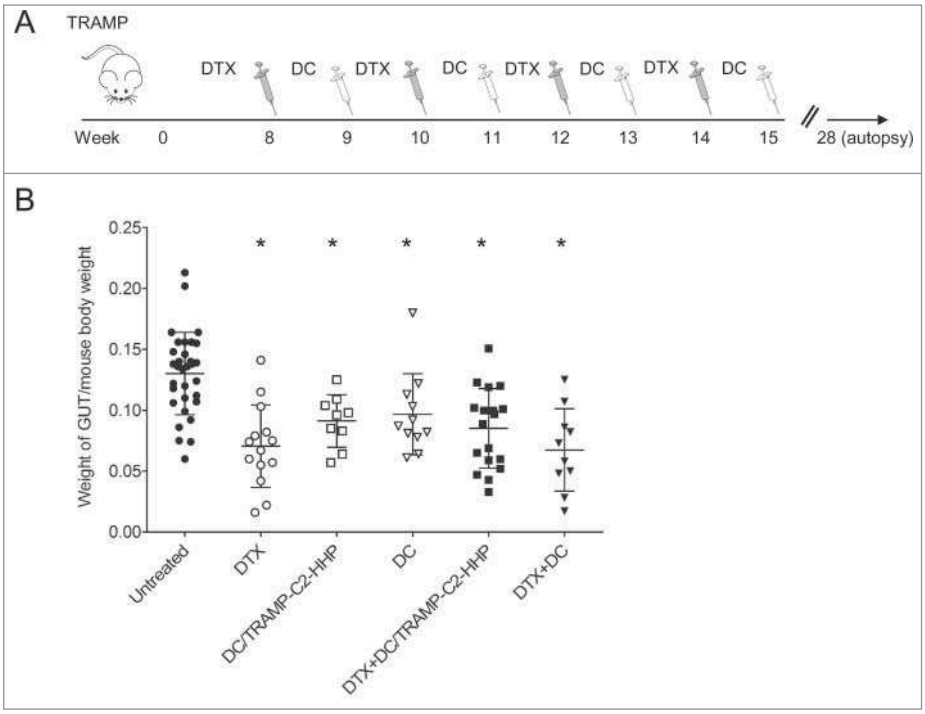

Figure 1. Combined chemoimmunotherapy of TRAMP mice with docetaxel and DC-based vaccines. (A) Approximately 8-week-old male TRAMP mice were treated with DTX alone (30 mg/kg), pulsed or unpulsed DC-based vaccines (2×10^6 cells/mouse), or with their combination. (B) Dotplots of GUT expressed as weight of genitourinary tract (GUT) per mouse body weight. $^*P<0.05$ vs. control (t-test).

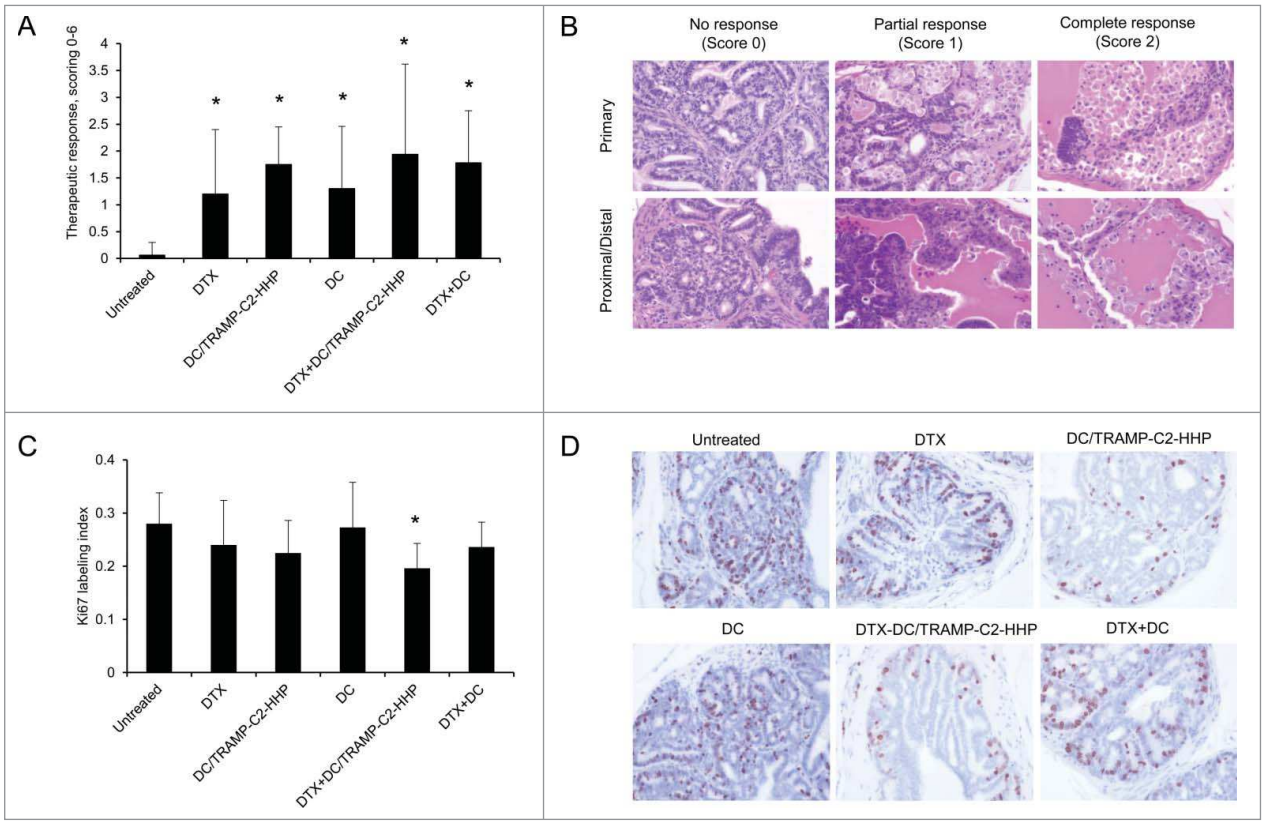

Figure 2. Histopathology analysis of TRAMP mice treated with docetaxel and DC-based vaccines. (A) Quantitative analysis of therapeutic response scoring in TRAMP mice treated with docetaxel and DC-based vaccines. (B) Representative pictures of scoring. (C) Ki67 labeling index and representative pictures of all treated groups and untreated control (D). *P<0.05 vs. control (t-test).

confirmed by immunochemistry focused on tumor cell proliferation. As shown in Fig. 2C, the Ki67 labeling index in the group treated with DTX in combination with the pulsed DC vaccine was the only significantly lower index when compared with untreated controls. Figure 2D shows representative pictures of Ki67 staining of the samples from all treated groups and untreated group.

Chemoimmunotherapy of TRAMP mice with cyclophosphamide and pulsed DC-based vaccine inhibited tumor growth

For comparison, the therapeutic efficacy of HHP-treated tumor cell-pulsed matured DC was thereafter tested in the TRAMP model using a combination with another cytostatic agent, cyclophosphamide. Approximately 8-week-old male TRAMP mice were treated either with CY alone using a previously optimized therapeutic scheme,[20] or in combination with the pulsed DC-based vaccine (Fig. 3A). As can be seen in Fig. 3B, after the treatment with CY or pulsed DC-based vaccine, or after their combination as well, genitourinary tract weights expressed as weight of genitourinary tract (GUT) per mouse body weight significantly decreased (*P<0.05). Therapeutic responses were confirmed by histopathology scoring of the neoplasms. The histopathology evaluation surprisingly showed a significantly higher therapeutic response in groups treated with monotherapy (both CY and DC), while the therapeutic response score in the combination group did not reach the statistical significance (Fig. 3C).

Immunotherapy of surgical minimal residual tumor disease of TC-1 and TRAMP-C2 tumors with DC-based vaccine inhibited growth of recurrent tumors

The therapeutic efficacy of HHP-treated tumor cell-pulsed or unpulsed matured DC was then tested in the therapeutic setting when immunotherapy with DC-based vaccine was used for the treatment of surgical minimal residual tumor disease of TC-1 and TRAMP-C2 tumors. Mice were s.c. transplanted with TC-1 or TRAMP-C2 and underwent tumor excision when the transplanted tumors reached ~5–10 mm in diameter. The DC-based vaccine was administered one and three weeks after the surgery. In selected experiments, mice were pretreated with DC 7 d before surgery (or in case of TRAMP-C2 also 21) (Fig. 4A). Figure 4B indicates that the growth of tumor recurrences of poorly immunogenic TRAMP-C2 tumors was inhibited by both unpulsed and pulsed DC-based vaccines. Similar results were obtained for the immunogenic TC-1 tumor model (*P<0.05 vs. control) (Fig. 4C). Interestingly, the therapeutic effect of the vaccine was abolished by DC vaccine pretreatment in both TRAMP-C2 and TC-1 tumor models.

Analysis of splenocytes from mice immunized with pulsed and unpulsed DC vaccines

As both pulsed and unpulsed DC-based vaccines displayed similar anti-tumor effects, we characterized the immune

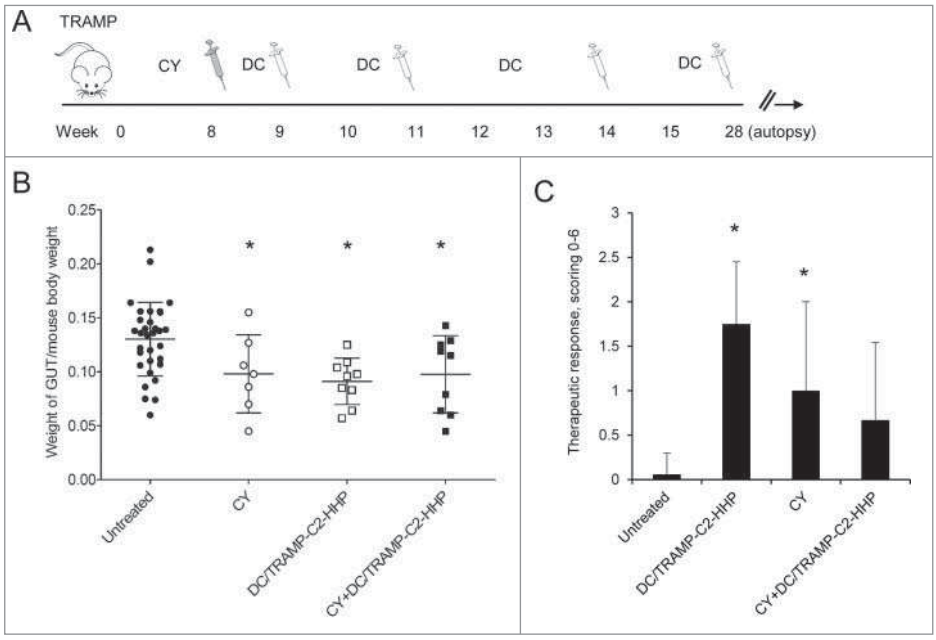

Figure 3. Combined chemoimmunotherapy of TRAMP mice with CY and DC-based vaccines. (A) Approximately 8-week-old male TRAMP mice were treated with CY alone (200 mg/kg), pulsed DC-based vaccine (2×10^6 cells/mouse), or with their combination. (B) Dotplots of GUT expressed as weight of genitourinary tract (GUT) per mouse body weight. (C) Quantitative analysis of therapeutic response scoring in TRAMP mice treated with CY and DC-based vaccines. *$P<0.05$ vs. control (t-test).

effector cell subpopulations. Mice were twice immunized with 2×10^6 cells of DC-based vaccine, both pulsed and unpulsed with HHP-treated TRAMP-C2 or TC-1 tumor cells, in a 2-week interval. Ten days after the second immunization, spleen cells were used for further analysis by FACS, chromium release assay, and ELISPOT. *In vitro* analyses of the spleen effector cells depleted with antibodies against CD8, CD4 and NK1.1 showed no difference between the groups immunized by pulsed

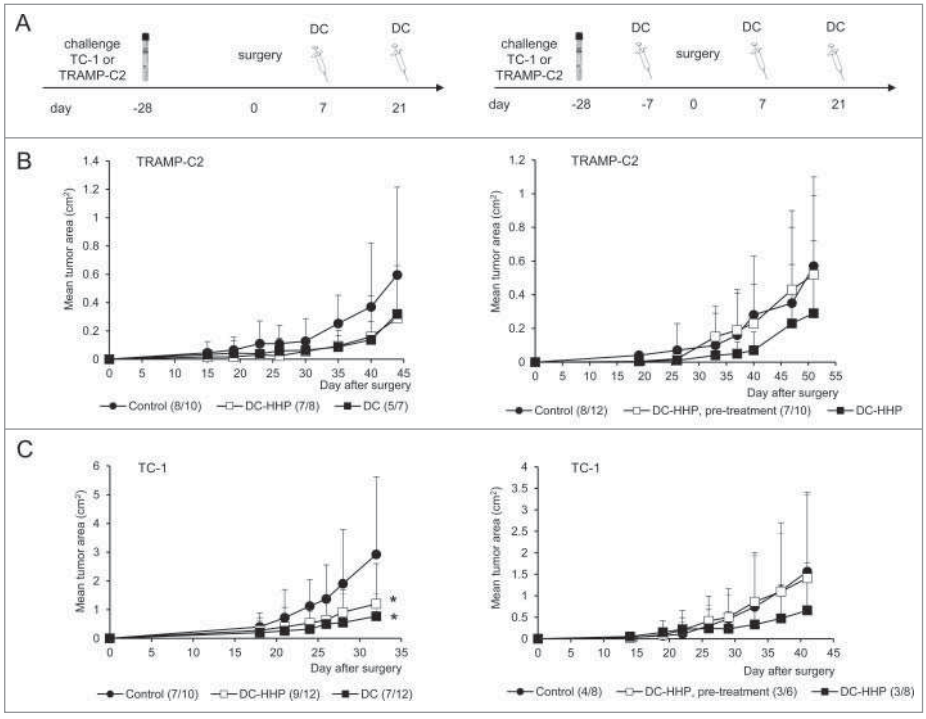

Figure 4. Immmunotherapy of surgical minimal residual tumor disease of TC-1 and TRAMP-C2 tumors with DC-based vaccine. (A) Mice were inoculated s.c. with TC-1 (5×10^4 cells) or TRAMP-C2 (10^6 cells). When the transplanted tumors reached ~5–10 mm in diameter, the tumors were excised. DC-based vaccines (2×10^6 cells/mouse) were administered on days 7 and 21 after surgery (left panel). In the case of pretreatment, DC-based vaccines (2×10^6 cells/mouse) were additionally administered on days -7 (TC-1, TRAMP-C2) and -21 (TRAMP-C2) before surgery (right panel) (B) Growth of TRAMP-C2 tumor recurrences after treatment with unpulsed and pulsed DC-based vaccine (left panel) and the growth of TRAMP-C2 tumor recurrences after pre-treatment or treatment with pulsed DC-based vaccine (right panel). (C) Growth of TC-1 tumor recurrences after treatment with unpulsed and pulsed DC-based vaccine (left panel) and the growth of TC-1 tumor recurrences after pre-treatment or treatment with pulsed DC-based vaccine (right panel). *$P<0.05$ vs. control (Analysis of Variance).

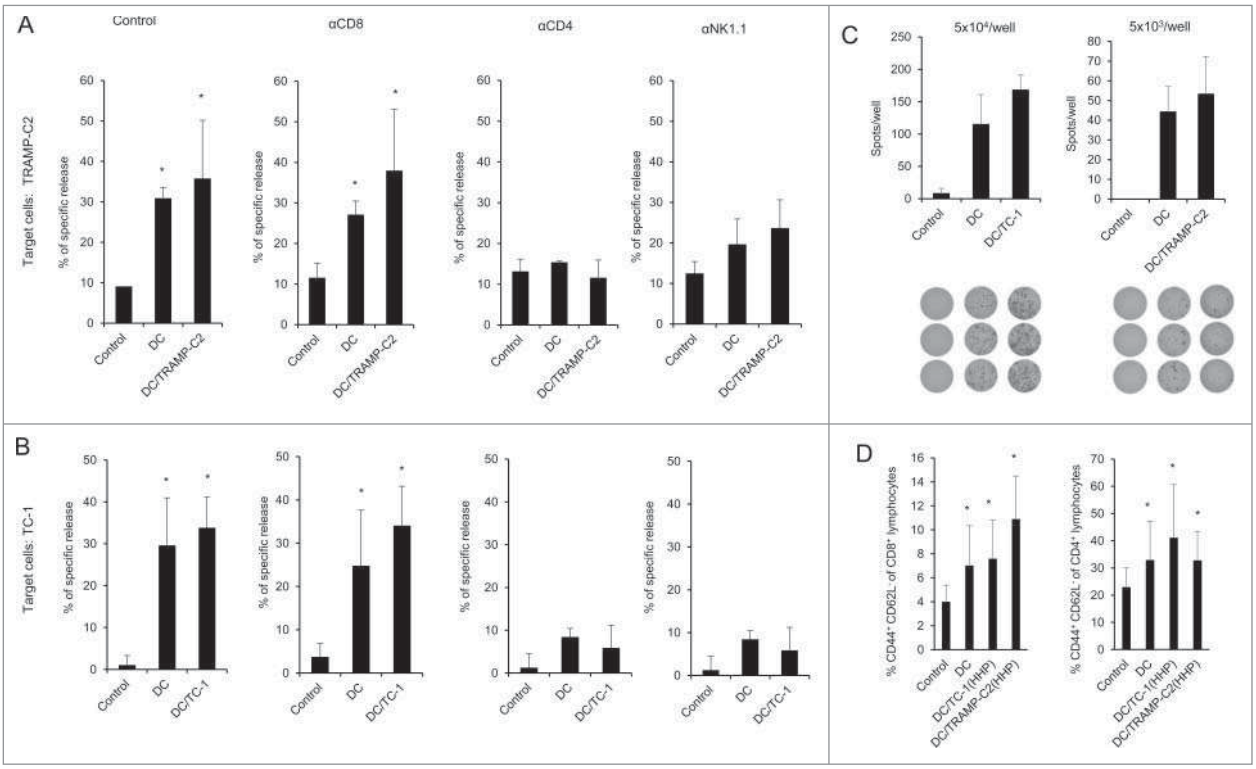

Figure 5. Analysis of splenocytes from mice immunized with pulsed and unpulsed DC-based vaccine. Mice were immunized 2 times in a 2-week interval with 2×10^6 DC pulsed with HHP-treated TC-1 or TRAMP-C2 tumor cells. Ten days after the last immunization, pooled splenocytes of 3 mice were used for *in vitro* analysis. (A) ^{51}Cr microcytotoxicity assay of depleted splenocytes (αCD8, αCD4, αNK1.1) from mice immunized with DC-based vaccines unpulsed or pulsed with HHP-treated TRAMP-C2 tumor cells or (B) TC-1 tumor cells. (C) The number of IFNγ-producing cells (ELISPOT assay). (D) Percentage of CD44$^+$ CD62L$^-$ of CD8$^+$ lymphocytes or CD4$^+$ lymphocytes in splenocytes from mice immunized with pulsed or unpulsed DC-based vaccines. $^*P<0.05$ vs. control. Statistical significances were determined by Student's t-test. Results are representative of 2 independent experiments.

or unpulsed DC, suggesting induction of unspecific immune responses. The cytotoxic effect was mediated by CD4$^+$ and NK1.1$^+$ effector cell subpopulations (Fig. 5AB). Both mice immunized with DC unpulsed and pulsed with HHP-treated tumor cells (TRAMP-C2 or TC-1) displayed significantly increased numbers of IFNγ-producing cells detected by the ELISPOT assay (Fig. 5C). On the other hand, flow cytometry analysis of the spleen cells (Fig. 5D) revealed that the percentage of effector memory T cells (CD44$^+$ CD62L$^-$ of CD8$^+$ and CD4$^+$ T lymphocytes) in the spleens from mice immunized with pulsed or unpulsed DC vaccines was significantly increased. The results obtained in immunization experiments using the TRAMP-C2 model were comparable with the results of experiments using the TC-1 tumor model. These results suggest rather unspecific therapeutic effects of the DC-based vaccines in our settings, mediated by NK1.1$^+$ and CD4$^+$ spleen cells as the effector cell population.

Discussion

We have recently demonstrated that the DC-based vaccine loaded by co-culture with stressed, HHP-treated tumor cells inhibited growth of both transplanted syngeneic tumors TRAMP-C2 and the TC-1 tumors.[18] Further, we have observed additive-synergic effects with chemotherapy in this setting. In this study, we assessed the therapeutic capacity of this cellular vaccine using a clinically more relevant TRAMP transgenic murine model, which spontaneously developed prostate tumors. Using this experimental model, the DC vaccine was able to slow down the tumor growth when used either as monotherapy or in combination with DTX chemotherapy to the same extent as DTX alone. Indeed, in all these treatment settings, immunotherapy and chemotherapy only, as well as combined chemoimmunotherapy, we observed significant tumor growth inhibition when compared with the untreated tumor-bearing animals. Similar results were obtained when the DC vaccine treatment was combined with another chemotherapeutic agent, CY. These results suggest that the DC therapeutic vaccination is effective when used as monotherapy during long-term tumor development, with an efficacy corresponding to the effects of chemotherapy. On the other hand, in this model we did not observe any additive of synergic effects when combined with immunotherapy, according to the GUT weight analysis, in contrast to the therapy of small transplanted tumors. We have to consider that the long-term development of spontaneously arisen tumors differs from the relatively fast growth of transplanted tumors. However, our cell proliferation analysis indicates that combined DTX chemotherapy with the Ag pulsed DC vaccine can be beneficial in the later stages of the tumor growth. So far, only a few studies focused on the DC-based immunotherapy have been performed in TRAMP mice. Ricupito et al. have shown that DC pulsed with the SV40 T Ag-derived immunodominant peptide $Tag_{404-411}$ restored immune competence and induced tumor shrinkage in TRAMP mice that had been previously sublethally irradiated and subjected to HSCT from

congenic females and received donor lymphocyte infusions from female donors presensitized against male antigens.[34]

Further, we compared the therapeutic effectiveness of the DC vaccines either pulsed with the HHP-treated TRAMP-C2 cells or unpulsed. We noticed no significant differences in the GUT size when these 2 different vaccines were used. As mentioned above, the only difference was seen in histological analysis focused on Ki67 positive replicating cells, in which tumors treated with the DTX and pulsed DC combination displayed significantly lower proliferation. These results suggest that the effective anti-tumor immune responses elicited by the DC-based vaccination are either unspecific, or that the specific immunity is induced by *in vivo* antigen processing and presentation after DC administration. Our analysis of the spleen cells from mice immunized with pulsed or unpulsed vaccines documents that the major effector cells belonged to the $NK1.1^+$ and $CD4^+$ populations, and cytotoxic tests revealed non-specificity of effector cells. Notably, tumor surveillance dependence on NK cells in TRAMP mice has been demonstrated,[35] and our data support the idea that engagement of activated NK cells can be crucial for DC vaccine-induced antitumor immunity.[36-38]

On the other hand, our data showing that the proliferation capacity of tumor cells was lower in tumors from animals treated with the combination of pulsed DC and chemotherapy, compared with all other treatment combinations, indicate the potential beneficial effect and specific immunity induction in the long-term perspective.

However, the therapeutic potential of the Ag-unloaded DC remains a controversial topic in tumor immunology. In our laboratory, we have previously investigated both pulsed and unpulsed bone marrow-derived DC prepared by the protocols similar to that used in this study in several settings and we found that unpulsed DC were effective in some therapeutic settings,[39] while in immunization-challenge protocols the protective effects were seen on mice treated with pulsed DC only.[40]

In a second experiment focused on DC-based immunotherapy combined with chemotherapy using TRAMP mice, we evaluated the efficacy of the DC treatments combined with CY. In these experiments, we used the setting in which CY that was administered once in a dose that displayed antitumor effects in previous experiments.[20] It is noteworthy that this treatment leads to induction of myeloid-derived suppressive cells that are potent inhibitors of T cell and NK cell proliferation.[32] This could explain the fact that the results with CY combination were not as convincing as those with DTX. Contrary to CY, DTX is a chemotherapeutic that is able to efficiently inhibit myeloid-derived suppressor cells.[4] The character of the tumor microenvironment, meaning its immunosuppressive status, might have influenced the effect of the immunotherapy used.

The effectiveness of both pulsed and unpulsed DC vaccines observed in the TRAMP model was also demonstrated using the clinically relevant model for therapy of minimal residual tumor disease after surgery. The only situation in which the vaccine did not bring any effect was the scheme in which the vaccine was also used before surgery and this administration abolished the effects of subsequent post-surgery vaccinations. It corresponds with our previous results using a murine model that the treatment before surgery with irradiated IL-2 producing tumor cells used as a cellular vaccine was without effect.[30] These facts show that proper timing of DC vaccine administration (or immunotherapy in general) and surgery can be crucial for the final therapeutic output. Notably, in humans, possible clinical benefit has been suggested for adjuvant immunotherapy using autologous DC loaded with autologous tumor lysate after revision in patients with relapsed glioblastoma multiforme. [41]

Collectively, our data indicate that DC-based immunotherapy, either using DC loaded with HHP-treated tumor cells or unpulsed DC, was effective against spontaneously developing prostate tumors, as well as in the model for therapy of minimal residual tumor disease. The fact that the unpulsed DC were also effective can be advantageous and justify the therapeutic use of dendritic cells loaded with a spectrum of antigens that might not be overlapping with the antigens expressed in growing tumors. On the other hand, our data do not exclude the possible superiority of DC loaded with HHP-treated tumor cells, and their possible long-term effect has to be particularly considered.

Disclosure of potential conflict of interest

Jirina Bartunkova and Radek Spisek are minority shareholders of SOTIO, a.s., a biotech company developing DC based immunotherapy.

Acknowledgments

This work was supported by research grant provided by SOTIO, a.s., and in part by the Ministry of Education, Youth and Sports (MEYS, LM2015040, Czech Center for Phenogenomics), Academy of Sciences of the Czech Republic (RVO 68378050), the project "BIOCEV – Biotechnology and Biomedicine Center of the Academy of Sciences and Charles University" (CZ.1.05/1.1.00/02.0109) and "Higher quality and capacity for transgenic models" (CZ.1.05/2.1.00/19.0395) by the Ministry of Education, Youth and Sports and the European Regional Development Fund and research grant No. 15–24769S from the Czech Science Foundation. The work of the Department of Immunology of Charles University is supported by Ministry of Health, Czech Republic-Conceptual Development of Research Organization (University Hospital Motol, Prague, Czech Republic, 00064203) and grant AZV ČR (agency for medical research, Czech Republic) 16–28135A.

The authors are grateful to Mrs. Renáta Turečková and Markéta Pícková for skillful technical assistance and to Dr. Šárka Takáčová for editorial help.

ORCID

Milan Reinis http://orcid.org/0000-0001-7083-2898

References

1. Siegel RL, Miller KD, Jemal A. Cancer statistics, 2017. CA Cancer J Clin. 2017;67:7-30. doi:10.3322/caac.21387. PMID:28055103
2. Beltran H, Beer TM, Carducci MA, de Bono J, Gleave M, Hussain M, Kelly WK, Saad F, Sternberg C, Tagawa ST, et al. New therapies for castration-resistant prostate cancer: Efficacy and safety. Eur Urol. 2011;60:279-90. doi:10.1016/j.eururo.2011.04.038. PMID:21592649
3. Maluf FC, Smaletz O, Herchenhorn D. Castration-resistant prostate cancer: Systemic therapy in 2012. Clinics (Sao Paulo, Brazil). 2012;67:389-94. doi:10.6061/clinics/2012(04)13. PMID:22522765
4. Kodumudi KN, Woan K, Gilvary DL, Sahakian E, Wei S, Djeu JY. A novel chemoimmunomodulating property of docetaxel: Suppression of

myeloid-derived suppressor cells in tumor bearers. Clin Cancer Res. 2010;16:4583-94. doi:10.1158/1078-0432.CCR-10-0733. PMID:20702612
5. Chen G, Emens LA. Chemoimmunotherapy: Reengineering tumor immunity. Cancer Immunol Immunother. 2013;62:203-16. doi:10.1007/s00262-012-1388-0. PMID:23389507
6. Kirkwood JM, Butterfield LH, Tarhini AA, Zarour H, Kalinski P, Ferrone S. Immunotherapy of cancer in 2012. CA Cancer J Clin. 2012;62:309-35. doi:10.3322/caac.20132. PMID:22576456
7. Emens LA. Chemoimmunotherapy. Cancer J (Sudbury, Mass). 2010;16:295-303. doi:10.1097/PPO.0b013e3181eb5066. PMID:20693839
8. Ramakrishnan R, Antonia S, Gabrilovich DI. Combined modality immunotherapy and chemotherapy: A new perspective. Cancer Immunol Immunother. 2008;57:1523-9. doi:10.1007/s00262-008-0531-4. PMID:18488219
9. Nowak AK, Lake RA, Robinson BW. Combined chemoimmunotherapy of solid tumours: Improving vaccines? Adv Drug Deliv Rev. 2006;58:975-90. doi:10.1016/j.addr.2006.04.002. PMID:17005292
10. Banchereau J, Steinman RM. Dendritic cells and the control of immunity. Nature. 1998;392:245-52. doi:10.1038/32588. PMID:9521319
11. Palucka K, Banchereau J. Cancer immunotherapy via dendritic cells. Nat Rev Cancer. 2012;12:265-77. doi:10.1038/nrc3258. PMID:22437871
12. Galluzzi L, Senovilla L, Vacchelli E, Eggermont A, Fridman WH, Galon J, Sautès-Fridman C, Tartour E, Zitvogel L, Kroemer G. Trial watch: Dendritic cell-based interventions for cancer therapy. Oncoimmunology. 2012;1:1111-34. doi:10.4161/onci.21494. PMID:23170259
13. Podrazil M, Horvath R, Becht E, Rozkova D, Bilkova P, Sochorova K, Hromadkova H, Kayserova J, Vavrova K, Lastovicka J, et al. Phase I/II clinical trial of dendritic-cell based immunotherapy (DCVAC/PCa) combined with chemotherapy in patients with metastatic, castration-resistant prostate cancer. Oncotarget 2015;6:18192-205. doi:10.18632/oncotarget.4145. PMID:26078335
14. Kantoff PW, Higano CS, Shore ND, Berger ER, Small EJ, Penson DF, Redfern CH, Ferrari AC, Dreicer R, Sims RB, et al. Sipuleucel-T immunotherapy for castration-resistant prostate cancer. N Engl J Med. 2010;363:411-22. doi:10.1056/NEJMoa1001294. PMID:20818862
15. Vandenberk L, Belmans J, Van Woensel M, Riva M, Van Gool SW. Exploiting the immunogenic potential of cancer cells for improved dendritic cell vaccines. Front Immunol. 2015;6:663. PMID:26834740
16. Adkins I, Fucikova J, Garg AD, Agostinis P, Spisek R. Physical modalities inducing immunogenic tumor cell death for cancer immunotherapy. Oncoimmunology. 2014;3:e968434. doi:10.4161/21624011.2014.968434. PMID:25964865
17. Fucikova J, Moserova I, Truxova I, Hermanova I, Vancurova I, Partlova S, Fialova A, Sojka L, Cartron PF, Houska M, et al. High hydrostatic pressure induces immunogenic cell death in human tumor cells. Int J Cancer. 2014;135:1165-77. doi:10.1002/ijc.28766. PMID:24500981
18. Mikyskova R, Stepanek I, Indrova M, Bieblova J, Simova J, Truxova I, Moserová I, Fučíková J, Bartůňková J, Špíšek R, et al. Dendritic cells pulsed with tumor cells killed by high hydrostatic pressure induce strong immune responses and display therapeutic effects both in murine TC-1 and TRAMP-C2 tumors when combined with docetaxel chemotherapy. Int J Oncol. 2016;48:953-64. PMID:26718011
19. Gingrich JR, Barrios RJ, Foster BA, Greenberg NM. Pathologic progression of autochthonous prostate cancer in the TRAMP model. Prostate Cancer Prostatic Dis. 1999;2:70-5. doi:10.1038/sj.pcan.4500296. PMID:12496841
20. Mikyskova R, Indrova M, Simova J, Jandlova T, Bieblova J, Jinoch P, Bubeník J, Vonka V. Treatment of minimal residual disease after surgery or chemotherapy in mice carrying HPV16-associated tumours: Cytokine and gene therapy with IL-2 and GM-CSF. Int J Oncol. 2004;24:161-7. PMID:14654953
21. Indrova M, Mikyskova R, Jandlova T, Vonka V, Bubenik J, Bieblova J. Adjuvant cytokine treatment of minimal residual disease after surgical therapy in mice carrying HPV16-associated tumours: Cytolytic activity of spleen cells from tumour regressors. Folia Biol (Praha). 2003;49:217-22. PMID:14748435
22. Bubenik J, Mikyskova R, Vonka V, Mendoza L, Simova J, Smahel M, Indrová M. Interleukin-2 and dendritic cells as adjuvants for surgical therapy of tumours associated with human papillomavirus type 16. Vaccine. 2003;21:891-6. doi:10.1016/S0264-410X(02)00537-6. PMID:12547599
23. Reinis M, Indrova M, Mendoza L, Mikyskova R, Bieblova J, Bubenik J, Símová J. HPV16-associated tumours: Therapy of surgical minimal residual disease with dendritic cell-based vaccines. Int J Oncol. 2004;25:1165-70. PMID:15375569
24. Lin KY, Guarnieri FG, Staveley-O'Carroll KF, Levitsky HI, August JT, Pardoll DM, Wu TC. Treatment of established tumors with a novel vaccine that enhances major histocompatibility class II presentation of tumor antigen. Cancer Res. 1996;56:21-6. PMID:8548765
25. Foster BA, Gingrich JR, Kwon ED, Madias C, Greenberg NM. Characterization of prostatic epithelial cell lines derived from transgenic adenocarcinoma of the mouse prostate (TRAMP) model. Cancer Res. 1997;57:3325-30. PMID:9269988
26. Lutz MB, Kukutsch N, Ogilvie AL, Rossner S, Koch F, Romani N, Schuler G. An advanced culture method for generating large quantities of highly pure dendritic cells from mouse bone marrow. J Immunol Methods. 1999;223:77-92. doi:10.1016/S0022-1759(98)00204-X. PMID:10037236
27. Indrova M, Reinis M, Bubenik J, Jandlova T, Bieblova J, Vonka V, Velek J. Immunogenicity of dendritic cell-based HPV16 E6/E7 peptide vaccines: CTL activation and protective effects. Folia Biol (Praha). 2004;50:184-93. PMID:15709713
28. Stepanek I, Indrova M, Bieblova J, Fucikova J, Spisek R, Bubenik J, Reinis M. Effects of 5-azacytidine and trichostatin A on dendritic cell maturation. J Biol Regul Homeost Agents. 2011;25:517-29. PMID:22217985
29. Yi AK, Krieg AM. CpG DNA rescue from anti-IgM-induced WEHI-231 B lymphoma apoptosis via modulation of I kappa B alpha and I kappa B beta and sustained activation of nuclear factor-kappa B/c-Rel. J Immunol. 1998;160:1240-5. PMID:9570540
30. Vlk V, Rossner P, Indrova M, Bubenik J, Sobota V. Interleukin-2 gene therapy of surgical minimal residual tumour disease. Int J Cancer. 1998;76:115-9. doi:10.1002/(SICI)1097-0215(19980330)76:1<115::AID-IJC18>3.0.CO;2-B. PMID:9533770
31. Bubenik J, Zeuthen J, Indrova M, Bubenikova D, Simova J. Kinetics and function of peritoneal-exudate cells during local IL-2 gene-therapy of cancer. Int J Oncol. 1994;4:13-6. PMID:21566882
32. Mikyskova R, Indrova M, Pollakova V, Bieblova J, Simova J, Reinis M. Cyclophosphamide-induced myeloid-derived suppressor cell population is immunosuppressive but not identical to myeloid-derived suppressor cells induced by growing TC-1 tumors. J Immunother. 2012;35:374-84. doi:10.1097/CJI.0b013e318255585a. PMID:22576342
33. Mikyskova R, Indrova M, Vlkova V, Bieblova J, Simova J, Parackova Z, Pajtasz-Piasecka E, Rossowska J, Reiniš M. DNA demethylating agent 5-azacytidine inhibits myeloid-derived suppressor cells induced by tumor growth and cyclophosphamide treatment. J Leukoc Biol. 2014;95:743-53. doi:10.1189/jlb.0813435. PMID:24389335
34. Ricupito A, Grioni M, Calcinotto A, Hess Michelini R, Longhi R, Mondino A, Bellone M. Booster vaccinations against cancer are critical in prophylactic but detrimental in therapeutic settings. Cancer Res. 2013;73:3545-54. doi:10.1158/0008-5472.CAN-12-2449. PMID:23539449
35. Chin AI, Miyahira AK, Covarrubias A, Teague J, Guo BC, Dempsey PW, Cheng G. Toll-like Receptor 3-mediated suppression of TRAMP prostate cancer shows the critical role of type I interferons in tumor immune surveillance. Cancer Res. 2010;70:2595-603. doi:10.1158/0008-5472.CAN-09-1162. PMID:20233880
36. Lion E, Smits ELJM, Berneman ZN, Van Tendeloo VFI. NK Cells: Key to success of DC-based cancer vaccines? Oncologist. 2012;17:1256-70. doi:10.1634/theoncologist.2011-0122. PMID:22907975
37. Shimizu K, Fujii SI. DC therapy induces long-term NK reactivity to tumors via host DC. Eur J Immunol. 2009;39:457-68. doi:10.1002/eji.200838794. PMID:19180466
38. Bonaccorsi I, Pezzino G, Morandi B, Ferlazzo G. Novel perspectives on dendritic cell-based immunotherapy of cancer. Immunol Lett. 2013;155:6-10. doi:10.1016/j.imlet.2013.09.021. PMID:24076312
39. Mendoza L, Indrova M, Hajkova R, Reinis M, Smahel M, Vonka V, Bubeník J, Jandlová T. Peritumoral administration of antigen-unstimulated bone marrow-derived dendritic cells inhibits tumour growth. Folia Biol-Prague. 2000;46:91-7.

40. Reinis M, Stepanek I, Simova J, Bieblova J, Pribylova H, Indrova M, Bubenik J. Induction of protective immunity against MHC class I-deficient, HPV16-associated tumours with peptide and dendritic cell-based vaccines. Int J Oncol. 2010;36:545-51. doi:10.3892/ijo_00000528. PMID:20126973

41. De Vleeschouwer S, Fieuws S, Rutkowski S, Van Calenbergh F, Van Loon J, Goffin J, Sciot R, Wilms G, Demaerel P, Warmuth-Metz M, et al. Postoperative adjuvant dendritic cell-based immunotherapy in patients with relapsed glioblastoma multiforme. Clin Cancer Res. 2008;14:3098-104. doi:10.1158/1078-0432.CCR-07-4875. PMID:18483377

5.7. Sumarizace literárních poznatků o významu CRT pro klinický průběh nádorových onemocnění

Buněčná smrt může být v závislosti na počátečním stimulu buď imunogenní nebo neimunogenní. Imunogenní vlastnosti umírajících buněk jsou převážně zprostředkovány tzv. DAMPs. Tyto molekuly jsou rozpoznávány různými receptory na povrchu APCs a podporují prezentaci nádorových antigenů T lymfocytům. Současné poznatky ukazují, že CRT je jednou z klíčových DAMP molekul určujících imunogenní potenciál umírajících buněk jak *in vitro*, tak *in vivo* v myších modelech. Navíc nejnovější studie identifikovaly CRT jako důležitý faktor asociovaný s aktivací protinádorové imunitní odpovědi a lepší prognózou u některých typů nádorových onemocnění. Hlavním cílem tohoto přehledového článku bylo popsat roli CRT v buněčném stresu zprostředkovaném ER a shrnout současné informace o prognostické a prediktivní roli CRT pro klinický průběh nádorových onemocnění.

K této práci jsem přispěla následovně: příprava obrázků a tabulek do manuskriptu, účast na revizi manuskriptu.

Vzhledem k tomu, že se jedná o přehled literárních poznatků, není tato publikace v dizertační práci přiložena.

5.8. Sumarizace literárních poznatků zabývajících se kombinovaným přístupem léčby nádorových onemocnění založené na spojení imunoterapie na bázi dendritických buněk s chemoterapií

Dendritické buňky hrají zásadní roli v iniciaci a regulaci protinádorové imunitní odpovědi a z tohoto důvodu byly intenzivně testovány pro použití v rámci imunoterapie nádorových onemocnění. I když některé klinické studie zaznamenaly povzbudivé výsledky, obecně nejsou tato data konzistentní. Z tohoto důvodu byly navrženy strategie vedoucí potenciálně ke zvýšení klinické účinnosti vakcín založených na DCs. Jednou ze strategií by mohla být kombinace s protinádorovými látkami, které mají synergické funkce a tedy schopnost posílit funkční kapacitu DCs. Některé cytotoxické látky mají potenciál buď přímo indukovat maturaci DCs nebo mohou DCs stimulovat nepřímo prostřednictvím ICD nádorových buněk. Navíc vybraná chemoterapeutika mohou narušit imunosupresivní nádorové mikroprostředí selektivní deplecí nebo inhibicí regulačních subpopulací imunitních buněk, jako např. MDSCs (myeloid-derived suppressor cells) a Tregs, což může vést k posílení adaptivní protinádorové imunitní odpovědi indukované DCs. Hlavním cílem bylo shrnout dosavadní poznatky týkající se schopnosti protinádorových chemoterapeutik modulovat fenotyp a funkce DCs a také poskytnout přehled probíhajících klinických studií hodnotících imunoterapii na bázi DCs v kombinaci s chemoterapií u onkologických pacientů.

Vzhledem k tomu, že se jedná o přehled literárních poznatků, není tato publikace v dizertační práci přiložena.

6. DISKUZE A ZÁVĚR

Tato dizertační práce tématicky pojednává o ICD a jejím významu pro aktivaci protinádorové imunitní reakce. Po řadu let byla klasifikace buněčné smrti z pohledu dopadu na imunitní systém velice zavádějící. Zatímco apoptóza (definovaná na základě morfologických znaků) byla považována za fyziologický, regulovaný a neimunogenní děj, na nekrózu bylo pohlíženo jako na patologickou, nekontrolovanou a imunogenní formu buněčné smrti. Tento pohled je dnes již zastaralý a je jasné, že buňky umírající regulovanou buněčnou smrtí mohou také vykazovat znaky nekrózy, existují regulované formy nekrózy účastnící se vývoje a remodelace tkání a apoptotické buňky mohou stimulovat antigen-specifickou imunitní odpověď (Galluzzi et al., 2015). Jedním z důsledků této změny konceptu je, že standardní přístup při zjišťování, zda se jedná o ICD, se již nespoléhá na morfologické a biochemické charakteristiky umírajících buněk, ale spíše spočívá v myších vakcinačních experimentech dokazujících imunostimulační účinky ICD *in vivo* (Kepp et al., 2014).

Imunogenicita nádorových buněk je jedním ze základních předpokladů efektivní protinádorové imunitní reakce. Jak již bylo opakovaně zmíněno v celém textu, během imunogenních forem buněčné smrti dochází k vystavení nejrůznějších DAMPs a dalších imunostimulačních molekul na plazmatickou membránu nádorových buněk, popřípadě k jejich sekreci nebo uvolnění do extracelulárního prostředí. Tyto molekuly mají potenciál stimulovat buňky vrozené imunity jako DCs a makrofágy, což napomáhá iniciaci terapeuticky relevantní adaptivní imunitní odpovědi (Garg et al., 2015b). V uplynulých letech byla objevena řada látek a modalit se schopností indukovat ICD. Seznam těchto induktorů je již poměrně široký a zahrnuje jak chemoterapeutika, některé látky cílené protinádorové terapie, patogeny (např. viry), tak i fyzikální modality (viz kapitola 2.2.2.).

My jsme v rámci této práce identifikovali HHP jako jednu z dalších modalit indukujících ICD. Nádorové buňky ošetřené HHP vystavují/sekretují/uvolňují klíčové imunostimulační

DAMPs (HSP70, HSP90, CRT, ATP a HMGB1), jsou rychle fagocytovány DCs a mají schopnost je aktivovat (upregulace exprese CD83, CD86 a HLA-DR a zvýšení produkce prozánětlivých cytokinů IL-6, IL-12p70 a TNF-α). Dendritické buňky pulzované nádorovými buňkami ošetřenými HHP indukují zvýšenou proliferaci a produkci IFN-γ antigen-specifickými $CD4^+$ a $CD8^+$ T lymfocyty. Tento koncept byl ověřen také *in vivo* pomocí experimentálních myších modelů. Protektivní imunizace myší pomocí nádorových buněk ošetřených HHP vede k aktivaci $CD4^+$ a $CD8^+$ T lymfocytární odpovědi, která vede ke zpomalení růstu nádoru a delšímu přežívání myší (Fucikova et al., 2014, Moserova et al., 2017). Podobné *in vitro* a *in vivo* imunostimulační efekty byly také pozorovány v případě nádorových buněk ošetřených dalšími induktory ICD jako např. antracykliny, mitoxantronem (Panaretakis et al., 2009) a hyp-PDT (Garg et al., 2012b). Výhodou HHP je, že může být použit pro standardizovanou přípravu velkého množství imunogenních nádorových buněk v GMP podmínkách. Tato modalita je součástí výrobního protokolu vakcíny založené na DCs pro imunoterapii karcinomu prostaty, ovárií a plic, která je testována v rámci několika probíhajících klinických studií fáze II a III (Podrazil et al., 2015).

Zatímco mechanismy vedoucí k emisi DAMPs indukované např. antracykliny a hyp-PDT zahrnují především rozvoj intenzivního buněčného stresu závislého na produkci ROS a stresu ER (Garg et al., 2012b, Obeid et al., 2007b), signalizace nezbytná pro tento proces je v případě HHP kompletně neznámá. Naším dalším cílem proto bylo identifikovat signalizační dráhy vedoucí k translokaci CRT, jedné z klíčových DAMP molekul asociované s ICD, na povrch nádorových buněk v důsledku ošetření HHP. Zjistili jsme, že tento proces je, podobně jako u antracyklinů, závislý na nadprodukci ROS, indukci stresu ER spojeného s aktivací PERK kinázy a fosforylací eIF2α a aktivaci kaspázy 8. Novým zjištěním bylo, že vystavení CRT na buněčný povrch indukované HHP závisí také na aktivaci kaspázy 2 (Moserova et al., 2017). Předchozí studie ukázaly, že štěpení kaspázy 2 může být v závislosti na kontextu

indukováno v důsledku produkce ROS nebo stresem ER (Prasad et al., 2006, Upton et al., 2008). V tuto chvíli není jasné, jak kaspáza 2 reguluje translokaci CRT na plazmatickou membránu, ale lokalizace této kaspázy v ER a Golgiho aparátu napovídá, že by se mohla účastnit mechanismů buněčného transportu.

I když existuje shoda, že transport CRT na buněčný povrch je závislý především na proteinech účastnících se stresu ER, přesné molekulární mechanismy se mohou mezi jednotlivými induktory ICD lišit. To samé platí také pro další fáze tohoto procesu, jako je aktivace proapoptotických proteinů a anterográdního transportu. Proto mohou být jednotlivé molekulární determinanty ICD rozděleny na ty, které jsou společné pro všechny ICD induktory a ty, které jsou specifické pouze pro určitý konkrétní ICD induktor (Garg et al., 2015b). Například PERK kináza je považována za nepostradatelnou signalizační komponentu pro všechny stimuly vyvolávající ICD. Naopak některé komponenty, které jsou nezbytné pro ICD indukovanou některými látkami (např. fosforylace eIF2α, zvýšení cytoplazmatické koncentrace Ca^{2+} nebo aktivace kaspázy 8 pro antracykliny), nemusí hrát roli v indukci jinými látkami (Garg et al., 2012b, Obeid et al., 2007b). Tyto poznatky ukazují, že translokace CRT na plazmatickou membránu je důsledkem sítě heterogenních signalizačních drah, z nichž některé jsou společné pro různé induktory ICD, jiné závisí na kontextu a typu vyvolávajícího stimulu.

Experimentální data charakterizující ICD a popisující její dopad na buňky imunitního systému byla převážně získána *in vitro* na lidských a myších nádorových buňkách a *in vivo* na myších modelech. I když je většina z dosud popsaných induktorů ICD používána v klinické praxi, důkazy o schopnosti těchto látek navodit ICD *in vivo* u lidí jsou stále omezené. Výsledky nejnovějších preklinických studií ukazují, že některé DAMPs a parametry asociované se signalizací vedoucí k jejich sekreci/uvolnění/vystavení (např. fosforylace eIF2α, sestřih mRNA kódující XBP1, vysoká hladina GRP78, atd.) mohou mít u onkologických pacientů

prognostický nebo prediktivní význam (Fucikova et al., 2015). Vysoká exprese celkového CRT v maligních buňkách například koreluje s lepší prognózou pacientů s neuroblastomem, glioblastomem, karcinomem plic a kolorektálním karcinomem (Fucikova et al., 2016a, Hsu et al., 2005, Muth et al., 2016, Peng et al., 2010). Podstatně méně studií se zabývalo vlivem DAMPs transportovaných na buněčnou membránu v důsledku procesů asociovaných s ICD. Hlavním cílem další práce proto bylo zjistit, zda u pacientů s AML léčených imunogenní terapií na bázi antracyklinů dochází k translokaci DAMPs, konkrétně CRT, HSP70 a HSP90, na povrch maligních blastů a zda přítomnost těchto molekul koreluje s imunitní odpovědí a prognózou těchto pacientů. Ukázali jsme, že maligní blasty vystavují na plazmatické membráně CRT, HSP70 a HSP90 nezávisle na chemoterapii. To je pravděpodobně dáno obecně vysokou mírou ER stresu v blastech, protože množství CRT na blastech AML pacientů je asociováno se signifikantně vyšší expresí ATF4, HSPA5, DDIT3, genů kódujících proteiny zúčastněné v tomto procesu (Fucikova et al., 2016c). Podobně bylo ukázáno, že translokace CRT na povrch AML blastů koreluje s mírou fosforylace eIF2α (Wemeau et al., 2010) a je také důsledkem aktivace mechanismů ER stresu závislých na aktivaci transkripčního faktoru ATF6 (Schardt et al., 2009). Zásadním zjištěním vyplývajícím z naší studie bylo, že vyšší množství povrchového CRT pozitivně koreluje s množstvím cirkulujících T lymfocytů specifických pro antigeny asociované s leukémií, což naznačuje, že povrchový CRT napomáhá iniciaci protinádorové imunitní odpovědi u AML pacientů. Přítomnost CRT na maligních blastech je navíc asociována s delší dobou přežití těchto pacientů (Fucikova et al., 2016c). V budoucnosti by bylo zajímavé zjistit, jestli může mít zvýšený imunogenní potenciál blastů nesoucích vyšší množství CRT na povrchu také vliv na schopnost AML pacientů lépe odpovídat na imunoterapii. Je potřeba zmínit, že výsledky studií hodnotících prognostickou a prediktivní roli CRT nejsou jednoznačné. Z řady studií totiž vyplývá, že přítomnost CRT je spíše spojena s horší prognózou onemocnění (Fucikova et

al., 2018). U pacientů s karcinomem žaludku a pankreatu koreluje exprese CRT například se zvýšenou angiogenezí, invazivitou a proliferací nádorových buněk (Chen et al., 2009, Matsukuma et al., 2016). Podobně u pacientů s karcinomem močového měchýře a lymfomem plášťových buněk je přítomnost CRT asociována s horší prognózou onemocnění (Chao et al., 2010). Tyto výsledky odráží intracelulární funkce CRT, které jsou důležité zejména pro udržení zrychleného anabolického metabolismu nádorových buněk (Galluzzi et al., 2013) a dále také fakt, že translokace CRT na plazmatickou membránu je obecně asociována se zvýšenou expresí CD47, klíčové molekuly inhibující fagocytózu (Chao et al., 2010). Nejednoznačnost dat platí také pro další DAMPs (HSPs, HMGB1, ATP, IFN I. typu, atd.) a parametry asociované se signalizací vedoucí k jejich sekreci/uvolnění/vystavení (Fucikova et al., 2015). Tento fakt závisí na řadě faktorů, z nichž stojí za zmínku především typ nádorového onemocnění, stádium, léčba a složení nádorového mikroprostředí (buněčné složení, imunitní infiltrát, přítomnost imunosupresivních populací imunitních buněk, cytokinové složení, přítomnost zdrojů energie a růstových faktorů, hypoxie, rozdílná reakce nádorů na stres ER, atd.). V neposlední řadě také záleží na způsobu detekce jednotlivých DAMPs (PCR, western blot, imunohistochemie, ELISA, průtoková cytometrie, atd.) a na tom, zda byla hodnocena celková exprese (na úrovni mRNA nebo proteinu) DAMPs v nádorových buňkách, přítomnost solubilních forem v séru nebo pouze frakce vystavená na plazmatické membráně v důsledku procesů asociovaných s ICD (Fucikova et al., 2015). Intracelulární funkce proteinů zařazených do kategorie DAMPs se totiž mohou od jejich extracelulárních funkcí značně lišit. Jako příklad můžeme uvést intracelulární HSPs, které se vyznačují spíše cytoprotektivními vlastnostmi a schopností inhibovat apoptózu. Naopak extracelulární nebo membránově vázané HSPs působí na nádor supresivně díky silným imunostimulačním vlastnostem (Tesniere et al., 2008). Nicméně tato data naznačují, že racionální přístup v monitorování těchto parametrů by v budoucnu mohl napomoci stratifikovat pacienty do

rizikových skupin a v ideálním případě predikovat průběh onemocnění a odpověď na dostupnou léčbu.

Poznatky týkající se DAMPs, jejich dopadu na buňky vrozené imunity a potenciálního významu *in vivo* u pacientů s nádorovým onemocněním by také mohly být využity pro design imunoterapeutických protokolů, včetně imunoterapie na bázi DCs. Dendritické buňky se od svého objevu staly slibným nástrojem v imunoterapii nádorových onemocnění. Na rozdíl od chemoterapie nebo terapie monoklonálními protilátkami a cytokiny, monoterapie dendritickými buňkami většinou nevyvolává závažné toxické vedlejší účinky a je pacienty dobře snášena. Pro zvýšení klinické účinnosti DC vakcín je proces výroby DCs neustále optimalizován a standardizován. Velice důležitým aspektem ovlivňujícím kvalitu DCs je výběr vhodného zdroje antigenu, který je použit pro pulzaci DCs v rámci výrobního protokolu. Jedním takovým zdrojem jsou inaktivované celé nádorové buňky, jejichž imunogenicita hraje významnou roli v aktivaci DCs. V řadě preklinických nádorových modelů bylo ukázáno, že metoda inaktivace nádorových buněk může zásadně ovlivňovat schopnost imunoterapie založené na DCs stimulovat protinádorovou imunitní odpověď *in vivo* (Vandenberk et al., 2015). Vzhledem k finanční a časové náročnosti výrobního procesu imunoterapeutického přípravku založeného na DC jsme se v další studii zaměřili na optimalizaci zkráceného výrobního protokolu DCs. Porovnávali jsme fenotyp a funkce DCs diferencovaných po dobu 3 dní s DCs vyrobenými certifikovaným protokolem během 5 dní (standardní DCs) v GMP médiu CellGro. Dendritické buňky měly v obou případech stejnou schopnost pohlcovat nádorové buňky ošetřené UVB. I když výsledky ukázaly, že DCs kultivované 3 dny a aktivované Poly (I:C) jsou fenotypicky méně zralé (nižší exprese CD80, CD86 a HLA-DR) než DCs připravené standardním protokolem, měly oba typy DCs porovnatelnou kapacitu indukovat antigen-specifické $CD8^+$ T lymfocyty a regulační T lymfocyty (Truxova et al., 2014). Dendritické buňky připravené zkrácenou diferenciací

mohou být pulzovány nádorovými buňkami ošetřenými HHP, popřípadě jinou alternativou indukující ICD, maturovány a testovány pro klinické použití u vybraných typů nádorových onemocnění.

I když některé klinické studie hodnotící účinnost imunoterapie na bázi DCs u pacientů s nádorovým onemocněním zaznamenaly pozitivní výsledky a u většiny pacientů byla pozorována protinádorová T lymfocytární odpověď, klinický úspěch této léčby je stále považován za suboptimální. To může být dáno tím, že imunoterapie na bázi DCs byla testována především u pacientů se značně pokročilým onemocněním a špatnou prognózou. V této fázi existuje v nádoru již vysoce imunosupresivní prostředí, které může indukovat dysfunkci DCs, což může mít za následek ztrátu jejich schopnosti zprostředkovat nezbytné aktivační signály T lymfocytům (Carr-Brendel et al., 1999). Současné terapeutické přístupy se proto zaměřují na vývoj vhodných strategií kombinujících imunoterapii založenou na DCs např. s chemoterapií nebo radioterapií, které představují standard léčebné péče. Bylo prokázáno, že některá chemoterapeutika (cyklofosfamid, doxorubicin, paklitaxel, docetaxel, atd.) mají imunomodulační vlastnosti a mohly by tedy být vhodnými kandidáty pro chemoimunoterapii (Machiels et al., 2001). Aplikace chemoterapeutických látek může stimulovat imunitní systém přímo 1. přechodnou deplecí některých subpopulací imunitních buněk (Finn, 2012), 2. narušením imunosupresivních mechanismů indukovaných nádorovým mikroprostředím selektivní inhibicí supresivních imunitních populací jako např. MDSCs a Tregs (Ghiringhelli et al., 2007, Vincent et al., 2010) nebo 3. přímou stimulací imunitních efektorových buněk (Zitvogel et al., 2013). V rámci dvou studií, jejichž výsledky jsou součástí této práce, jsme testovali tento kombinovaný terapeutický přístup u slabě imunogenních nádorů, u kterých samotná monoterapie DCs není schopná zvrátit klinický průběh onemocnění. Kombinace imunoterapie na bázi DCs pulzovaných nádorovými buňkami ošetřenými HHP s chemoterapií docetaxelem signifikantně inhibovala růst slabě

imunogenních TRAMP-C2 nádorů, myšího modelu lidského karcinomu prostaty (Mikyskova et al., 2017, Mikyskova et al., 2016). Tyto výsledky naznačují, že chemoimunoterapie je možnou strategií léčby u nádorů, jejichž nádorové mikroprostředí snižuje účinnost imunoterapie.

Tato data souhrnně definují ICD a procesy asociované s ICD jako důležité parametry pro aktivaci protinádorové imunitní reakce a ukazují, jaké procesy stojí za vystavením/sekrecí/uvolněním DAMPs a jak tyto molekuly ovlivňují imunitní odpověď založenou především na DCs. Tyto aspekty mohou mít potenciálně dopad na využití DCs v protinádorové terapii a do budoucna mohou představovat slibný nástroj v predikci průběhu nádorových onemocnění.

7. SEZNAM LITERATURY

ADKINS, I., HRADILOVA, N., PALATA, O., SADILKOVA, L., PALOVA-JELINKOVA, L. & SPISEK, R. 2018. High hydrostatic pressure in cancer immunotherapy and biomedicine. *Biotechnol Adv*.

ANDERSSON, U. & TRACEY, K. J. 2011. HMGB1 is a therapeutic target for sterile inflammation and infection. *Annu Rev Immunol,* 29**,** 139-62.

APETOH, L., GHIRINGHELLI, F., TESNIERE, A., CRIOLLO, A., ORTIZ, C., LIDEREAU, R., MARIETTE, C., CHAPUT, N., MIRA, J. P., DELALOGE, S., ANDRE, F., TURSZ, T., KROEMER, G. & ZITVOGEL, L. 2007a. The interaction between HMGB1 and TLR4 dictates the outcome of anticancer chemotherapy and radiotherapy. *Immunol Rev,* 220**,** 47-59.

APETOH, L., GHIRINGHELLI, F., TESNIERE, A., OBEID, M., ORTIZ, C., CRIOLLO, A., MIGNOT, G., MAIURI, M. C., ULLRICH, E., SAULNIER, P., YANG, H., AMIGORENA, S., RYFFEL, B., BARRAT, F. J., SAFTIG, P., LEVI, F., LIDEREAU, R., NOGUES, C., MIRA, J. P., CHOMPRET, A., JOULIN, V., CLAVEL-CHAPELON, F., BOURHIS, J., ANDRE, F., DELALOGE, S., TURSZ, T., KROEMER, G. & ZITVOGEL, L. 2007b. Toll-like receptor 4-dependent contribution of the immune system to anticancer chemotherapy and radiotherapy. *Nat Med,* 13**,** 1050-9.

ASEA, A., KRAEFT, S. K., KURT-JONES, E. A., STEVENSON, M. A., CHEN, L. B., FINBERG, R. W., KOO, G. C. & CALDERWOOD, S. K. 2000. HSP70 stimulates cytokine production through a CD14-dependant pathway, demonstrating its dual role as a chaperone and cytokine. *Nat Med,* 6**,** 435-42.

ASEA, A., REHLI, M., KABINGU, E., BOCH, J. A., BARE, O., AURON, P. E., STEVENSON, M. A. & CALDERWOOD, S. K. 2002. Novel signal transduction pathway utilized by extracellular HSP70: role of toll-like receptor (TLR) 2 and TLR4. *J Biol Chem,* 277**,** 15028-34.

ASHKENAZI, A. & SALVESEN, G. 2014. Regulated cell death: signaling and mechanisms. *Annu Rev Cell Dev Biol,* 30**,** 337-56.

AURELIAN, L. 2016. Oncolytic viruses as immunotherapy: progress and remaining challenges. *Onco Targets Ther,* 9**,** 2627-37.

AYNA, G., KRYSKO, D. V., KACZMAREK, A., PETROVSKI, G., VANDENABEELE, P. & FESUS, L. 2012. ATP release from dying autophagic cells and their phagocytosis are crucial for inflammasome activation in macrophages. *PLoS One,* 7**,** e40069.

BACHER, N., RAKER, V., HOFMANN, C., GRAULICH, E., SCHWENK, M., BAUMGRASS, R., BOPP, T., ZECHNER, U., MERTEN, L., BECKER, C. & STEINBRINK, K. 2013. Interferon-alpha suppresses cAMP to disarm human regulatory T cells. *Cancer Res,* 73**,** 5647-56.

BEAVIS, P. A., STAGG, J., DARCY, P. K. & SMYTH, M. J. 2012. CD73: a potent suppressor of antitumor immune responses. *Trends Immunol,* 33**,** 231-7.

BEGOVIC, M., HERBERMAN, R. B. & GORELIK, E. 1991. Ultraviolet light-induced increase in tumor cell susceptibility to TNF-dependent and TNF-independent natural cell-mediated cytotoxicity. *Cell Immunol,* 138**,** 349-59.

BELL, C. W., JIANG, W., REICH, C. F., 3RD & PISETSKY, D. S. 2006. The extracellular release of HMGB1 during apoptotic cell death. *Am J Physiol Cell Physiol,* 291**,** C1318-25.

BEZU, L., GOMES-DE-SILVA, L. C., DEWITTE, H., BRECKPOT, K., FUCIKOVA, J., SPISEK, R., GALLUZZI, L., KEPP, O. & KROEMER, G. 2015. Combinatorial strategies for the induction of immunogenic cell death. *Front Immunol,* 6**,** 187.

BINDER, R. J. & SRIVASTAVA, P. K. 2005. Peptides chaperoned by heat-shock proteins are a necessary and sufficient source of antigen in the cross-priming of CD8+ T cells. *Nat Immunol,* 6**,** 593-9.

BIRKINSHAW, R. W. & CZABOTAR, P. E. 2017. The BCL-2 family of proteins and mitochondrial outer membrane permeabilisation. *Semin Cell Dev Biol,* 72**,** 152-162.

BLOY, N., POL, J., ARANDA, F., EGGERMONT, A., CREMER, I., FRIDMAN, W. H., FUCIKOVA, J., GALON, J., TARTOUR, E., SPISEK, R., DHODAPKAR, M. V., ZITVOGEL, L., KROEMER, G. & GALLUZZI, L. 2014. Trial watch: Dendritic cell-based anticancer therapy. *Oncoimmunology,* 3**,** e963424.

BUGAUT, H., BRUCHARD, M., BERGER, H., DERANGERE, V., ODOUL, L., EUVRARD, R., LADOIRE, S., CHALMIN, F., VEGRAN, F., REBE, C., APETOH, L., GHIRINGHELLI, F. & MIGNOT, G. 2013. Bleomycin exerts ambivalent antitumor immune effect by triggering both immunogenic cell death and proliferation of regulatory T cells. *PLoS One,* 8**,** e65181.

BURNSTOCK, G. 2007. Physiology and pathophysiology of purinergic neurotransmission. *Physiol Rev,* 87**,** 659-797.

CALDERWOOD, S. K., MAMBULA, S. S. & GRAY, P. J., JR. 2007. Extracellular heat shock proteins in cell signaling and immunity. *Ann N Y Acad Sci,* 1113**,** 28-39.

CARR-BRENDEL, V., MARKOVIC, D., SMITH, M., TAYLOR-PAPADIMITRIOU, J. & COHEN, E. P. 1999. Immunity to breast cancer in mice immunized with X-irradiated breast cancer cells modified to secrete IL-12. *J Immunother,* 22**,** 415-22.

CROUSE, J., BEDENIKOVIC, G., WIESEL, M., IBBERSON, M., XENARIOS, I., VON LAER, D., KALINKE, U., VIVIER, E., JONJIC, S. & OXENIUS, A. 2014. Type I interferons protect T cells against NK cell attack mediated by the activating receptor NCR1. *Immunity,* 40**,** 961-73.

CURTI, A., FERRI, E., PANDOLFI, S., ISIDORI, A. & LEMOLI, R. M. 2004. Dendritic cell differentiation. *J Immunol,* 172**,** 3; author reply 3-4.

CZERNIECKI, B. J., KOSKI, G. K., KOLDOVSKY, U., XU, S., COHEN, P. A., MICK, R., NISENBAUM, H., PASHA, T., XU, M., FOX, K. R., WEINSTEIN, S., OREL, S. G., VONDERHEIDE, R., COUKOS, G., DEMICHELE, A., ARAUJO, L., SPITZ, F. R., ROSEN, M., LEVINE, B. L., JUNE, C. & ZHANG, P. J. 2007. Targeting HER-2/neu in early breast cancer development using dendritic cells with staged interleukin-12 burst secretion. *Cancer Res,* 67**,** 1842-52.

DANG, V. T., TANABE, K., TANAKA, Y., TOKUMOTO, N., MISUMI, T., SAEKI, Y., FUJIKUNI, N. & OHDAN, H. 2014. Fasting enhances TRAIL-mediated liver natural killer cell activity via HSP70 upregulation. *PLoS One,* 9**,** e110748.

DELAMARRE, L., HOLCOMBE, H. & MELLMAN, I. 2003. Presentation of exogenous antigens on major histocompatibility complex (MHC) class I and MHC class II molecules is differentially regulated during dendritic cell maturation. *J Exp Med,* 198**,** 111-22.

DELGADO, M. A., ELMAOUED, R. A., DAVIS, A. S., KYEI, G. & DERETIC, V. 2008. Toll-like receptors control autophagy. *EMBO J,* 27**,** 1110-21.

DEMARIA, S., SANTORI, F. R., NG, B., LIEBES, L., FORMENTI, S. C. & VUKMANOVIC, S. 2005. Select forms of tumor cell apoptosis induce dendritic cell maturation. *J Leukoc Biol,* 77**,** 361-8.

DIACONU, I., CERULLO, V., HIRVINEN, M. L., ESCUTENAIRE, S., UGOLINI, M., PESONEN, S. K., BRAMANTE, S., PARVIAINEN, S., KANERVA, A., LOSKOG, A. S., ELIOPOULOS, A. G., PESONEN, S. & HEMMINKI, A. 2012. Immune response is an important aspect of the antitumor effect produced by a CD40L-encoding oncolytic adenovirus. *Cancer Res,* 72**,** 2327-38.

DICKENS, L. S., POWLEY, I. R., HUGHES, M. A. & MACFARLANE, M. 2012. The 'complexities' of life and death: death receptor signalling platforms. *Exp Cell Res,* 318**,** 1269-77.

DONNELLY, O. G., ERRINGTON-MAIS, F., STEELE, L., HADAC, E., JENNINGS, V., SCOTT, K., PEACH, H., PHILLIPS, R. M., BOND, J., PANDHA, H., HARRINGTON, K., VILE, R., RUSSELL, S., SELBY, P. & MELCHER, A. A. 2013. Measles virus causes immunogenic cell death in human melanoma. *Gene Ther,* 20**,** 7-15.

DOODY, A. D., KOVALCHIN, J. T., MIHALYO, M. A., HAGYMASI, A. T., DRAKE, C. G. & ADLER, A. J. 2004. Glycoprotein 96 can chaperone both MHC class I- and class II-restricted epitopes for in vivo presentation, but selectively primes CD8+ T cell effector function. *J Immunol,* 172**,** 6087-92.

ECKELMAN, B. P., SALVESEN, G. S. & SCOTT, F. L. 2006. Human inhibitor of apoptosis proteins: why XIAP is the black sheep of the family. *EMBO Rep,* 7**,** 988-94.

ELLIOTT, M. R., CHEKENI, F. B., TRAMPONT, P. C., LAZAROWSKI, E. R., KADL, A., WALK, S. F., PARK, D., WOODSON, R. I., OSTANKOVICH, M., SHARMA, P., LYSIAK, J. J., HARDEN, T. K., LEITINGER, N. & RAVICHANDRAN, K. S. 2009. Nucleotides released by apoptotic cells act as a find-me signal to promote phagocytic clearance. *Nature,* 461**,** 282-6.

ELSNER, L., MUPPALA, V., GEHRMANN, M., LOZANO, J., MALZAHN, D., BICKEBOLLER, H., BRUNNER, E., ZIENTKOWSKA, M., HERRMANN, T., WALTER, L., ALVES, F., MULTHOFF, G. & DRESSEL, R.

2007. The heat shock protein HSP70 promotes mouse NK cell activity against tumors that express inducible NKG2D ligands. *J Immunol,* 179**,** 5523-33.

FINN, O. J. 2012. Immuno-oncology: understanding the function and dysfunction of the immune system in cancer. *Ann Oncol,* 23 Suppl 8**,** viii6-9.

FREY, B., FRANZ, S., SHERIFF, A., KORN, A., BLUEMELHUBER, G., GAIPL, U. S., VOLL, R. E., MEYER-PITTROFF, R. & HERRMANN, M. 2004. Hydrostatic pressure induced death of mammalian cells engages pathways related to apoptosis or necrosis. *Cell Mol Biol (Noisy-le-grand),* 50**,** 459-67.

FUCIKOVA, J., BECHT, E., IRIBARREN, K., GOC, J., REMARK, R., DAMOTTE, D., ALIFANO, M., DEVI, P., BITON, J., GERMAIN, C., LUPO, A., FRIDMAN, W. H., DIEU-NOSJEAN, M. C., KROEMER, G., SAUTES-FRIDMAN, C. & CREMER, I. 2016a. Calreticulin Expression in Human Non-Small Cell Lung Cancers Correlates with Increased Accumulation of Antitumor Immune Cells and Favorable Prognosis. *Cancer Res*.

FUCIKOVA, J., BECHT, E., IRIBARREN, K., GOC, J., REMARK, R., DAMOTTE, D., ALIFANO, M., DEVI, P., BITON, J., GERMAIN, C., LUPO, A., FRIDMAN, W. H., DIEU-NOSJEAN, M. C., KROEMER, G., SAUTES-FRIDMAN, C. & CREMER, I. 2016b. Calreticulin Expression in Human Non-Small Cell Lung Cancers Correlates with Increased Accumulation of Antitumor Immune Cells and Favorable Prognosis. *Cancer Res,* 76**,** 1746-56.

FUCIKOVA, J., KASIKOVA, L., TRUXOVA, I., LACO, J., SKAPA, P., RYSKA, A. & SPISEK, R. 2018. Relevance of the chaperone-like protein calreticulin for the biological behavior and clinical outcome of cancer. *Immunol Lett,* 193**,** 25-34.

FUCIKOVA, J., KRALIKOVA, P., FIALOVA, A., BRTNICKY, T., ROB, L., BARTUNKOVA, J. & SPISEK, R. 2011a. Human tumor cells killed by anthracyclines induce a tumor-specific immune response. *Cancer Res,* 71**,** 4821-33.

FUCIKOVA, J., MOSEROVA, I., TRUXOVA, I., HERMANOVA, I., VANCUROVA, I., PARTLOVA, S., FIALOVA, A., SOJKA, L., CARTRON, P. F., HOUSKA, M., ROB, L., BARTUNKOVA, J. & SPISEK, R. 2014. High hydrostatic pressure induces immunogenic cell death in human tumor cells. *Int J Cancer,* 135**,** 1165-77.

FUCIKOVA, J., MOSEROVA, I., URBANOVA, L., BEZU, L., KEPP, O., CREMER, I., SALEK, C., STRNAD, P., KROEMER, G., GALLUZZI, L. & SPISEK, R. 2015. Prognostic and Predictive Value of DAMPs and DAMP-Associated Processes in Cancer. *Front Immunol,* 6**,** 402.

FUCIKOVA, J., ROZKOVA, D., ULCOVA, H., BUDINSKY, V., SOCHOROVA, K., POKORNA, K., BARTUNKOVA, J. & SPISEK, R. 2011b. Poly I: C-activated dendritic cells that were generated in CellGro for use in cancer immunotherapy trials. *J Transl Med,* 9**,** 223.

FUCIKOVA, J., TRUXOVA, I., HENSLER, M., BECHT, E., KASIKOVA, L., MOSEROVA, I., VOSAHLIKOVA, S., KLOUCKOVA, J., CHURCH, S. E., CREMER, I., KEPP, O., KROEMER, G., GALLUZZI, L., SALEK, C. & SPISEK, R. 2016c. Calreticulin exposure by malignant blasts correlates with robust anticancer immunity and improved clinical outcome in AML patients. *Blood,* 128**,** 3113-3124.

GALLUZZI, L., BRAVO-SAN PEDRO, J. M., VITALE, I., AARONSON, S. A., ABRAMS, J. M., ADAM, D., ALNEMRI, E. S., ALTUCCI, L., ANDREWS, D., ANNICCHIARICO-PETRUZZELLI, M., BAEHRECKE, E. H., BAZAN, N. G., BERTRAND, M. J., BIANCHI, K., BLAGOSKLONNY, M. V., BLOMGREN, K., BORNER, C., BREDESEN, D. E., BRENNER, C., CAMPANELLA, M., CANDI, E., CECCONI, F., CHAN, F. K., CHANDEL, N. S., CHENG, E. H., CHIPUK, J. E., CIDLOWSKI, J. A., CIECHANOVER, A., DAWSON, T. M., DAWSON, V. L., DE LAURENZI, V., DE MARIA, R., DEBATIN, K. M., DI DANIELE, N., DIXIT, V. M., DYNLACHT, B. D., EL-DEIRY, W. S., FIMIA, G. M., FLAVELL, R. A., FULDA, S., GARRIDO, C., GOUGEON, M. L., GREEN, D. R., GRONEMEYER, H., HAJNOCZKY, G., HARDWICK, J. M., HENGARTNER, M. O., ICHIJO, H., JOSEPH, B., JOST, P. J., KAUFMANN, T., KEPP, O., KLIONSKY, D. J., KNIGHT, R. A., KUMAR, S., LEMASTERS, J. J., LEVINE, B., LINKERMANN, A., LIPTON, S. A., LOCKSHIN, R. A., LOPEZ-OTIN, C., LUGLI, E., MADEO, F., MALORNI, W., MARINE, J. C., MARTIN, S. J., MARTINOU, J. C., MEDEMA, J. P., MEIER, P., MELINO, S., MIZUSHIMA, N., MOLL, U., MUNOZ-PINEDO, C., NUNEZ, G., OBERST, A., PANARETAKIS, T., PENNINGER, J. M., PETER, M. E., PIACENTINI, M., PINTON, P., PREHN, J. H., PUTHALAKATH, H., RABINOVICH, G.

A., RAVICHANDRAN, K. S., RIZZUTO, R., RODRIGUES, C. M., RUBINSZTEIN, D. C., RUDEL, T., SHI, Y., SIMON, H. U., STOCKWELL, B. R., SZABADKAI, G., TAIT, S. W., TANG, H. L., TAVERNARAKIS, N., TSUJIMOTO, Y., VANDEN BERGHE, T., VANDENABEELE, P., VILLUNGER, A., WAGNER, E. F., et al. 2015. Essential versus accessory aspects of cell death: recommendations of the NCCD 2015. *Cell Death Differ,* 22**,** 58-73.

GALLUZZI, L., KEPP, O., VANDER HEIDEN, M. G. & KROEMER, G. 2013. Metabolic targets for cancer therapy. *Nat Rev Drug Discov,* 12**,** 829-46.

GALLUZZI, L., VACCHELLI, E., BRAVO-SAN PEDRO, J. M., BUQUE, A., SENOVILLA, L., BARACCO, E. E., BLOY, N., CASTOLDI, F., ABASTADO, J. P., AGOSTINIS, P., APTE, R. N., ARANDA, F., AYYOUB, M., BECKHOVE, P., BLAY, J. Y., BRACCI, L., CAIGNARD, A., CASTELLI, C., CAVALLO, F., CELIS, E., CERUNDOLO, V., CLAYTON, A., COLOMBO, M. P., COUSSENS, L., DHODAPKAR, M. V., EGGERMONT, A. M., FEARON, D. T., FRIDMAN, W. H., FUCIKOVA, J., GABRILOVICH, D. I., GALON, J., GARG, A., GHIRINGHELLI, F., GIACCONE, G., GILBOA, E., GNJATIC, S., HOOS, A., HOSMALIN, A., JAGER, D., KALINSKI, P., KARRE, K., KEPP, O., KIESSLING, R., KIRKWOOD, J. M., KLEIN, E., KNUTH, A., LEWIS, C. E., LIBLAU, R., LOTZE, M. T., LUGLI, E., MACH, J. P., MATTEI, F., MAVILIO, D., MELERO, I., MELIEF, C. J., MITTENDORF, E. A., MORETTA, L., ODUNSI, A., OKADA, H., PALUCKA, A. K., PETER, M. E., PIENTA, K. J., PORGADOR, A., PRENDERGAST, G. C., RABINOVICH, G. A., RESTIFO, N. P., RIZVI, N., SAUTES-FRIDMAN, C., SCHREIBER, H., SELIGER, B., SHIKU, H., SILVA-SANTOS, B., SMYTH, M. J., SPEISER, D. E., SPISEK, R., SRIVASTAVA, P. K., TALMADGE, J. E., TARTOUR, E., VAN DER BURG, S. H., VAN DEN EYNDE, B. J., VILE, R., WAGNER, H., WEBER, J. S., WHITESIDE, T. L., WOLCHOK, J. D., ZITVOGEL, L., ZOU, W. & KROEMER, G. 2014. Classification of current anticancer immunotherapies. *Oncotarget,* 5**,** 12472-508.

GARDAI, S. J., MCPHILLIPS, K. A., FRASCH, S. C., JANSSEN, W. J., STAREFELDT, A., MURPHY-ULLRICH, J. E., BRATTON, D. L., OLDENBORG, P. A., MICHALAK, M. & HENSON, P. M. 2005. Cell-surface calreticulin initiates clearance of viable or apoptotic cells through trans-activation of LRP on the phagocyte. *Cell,* 123**,** 321-34.

GARG, A. D., ELSEN, S., KRYSKO, D. V., VANDENABEELE, P., DE WITTE, P. & AGOSTINIS, P. 2015a. Resistance to anticancer vaccination effect is controlled by a cancer cell-autonomous phenotype that disrupts immunogenic phagocytic removal. *Oncotarget,* 6**,** 26841-60.

GARG, A. D., GALLUZZI, L., APETOH, L., BAERT, T., BIRGE, R. B., BRAVO-SAN PEDRO, J. M., BRECKPOT, K., BROUGH, D., CHAURIO, R., CIRONE, M., COOSEMANS, A., COULIE, P. G., DE RUYSSCHER, D., DINI, L., DE WITTE, P., DUDEK-PERIC, A. M., FAGGIONI, A., FUCIKOVA, J., GAIPL, U. S., GOLAB, J., GOUGEON, M. L., HAMBLIN, M. R., HEMMINKI, A., HERRMANN, M., HODGE, J. W., KEPP, O., KROEMER, G., KRYSKO, D. V., LAND, W. G., MADEO, F., MANFREDI, A. A., MATTAROLLO, S. R., MAUERODER, C., MERENDINO, N., MULTHOFF, G., PABST, T., RICCI, J. E., RIGANTI, C., ROMANO, E., RUFO, N., SMYTH, M. J., SONNEMANN, J., SPISEK, R., STAGG, J., VACCHELLI, E., VANDENABEELE, P., VANDENBERK, L., VAN DEN EYNDE, B. J., VAN GOOL, S., VELOTTI, F., ZITVOGEL, L. & AGOSTINIS, P. 2015b. Molecular and Translational Classifications of DAMPs in Immunogenic Cell Death. *Front Immunol,* 6**,** 588.

GARG, A. D., KRYSKO, D. V., VANDENABEELE, P. & AGOSTINIS, P. 2012a. Hypericin-based photodynamic therapy induces surface exposure of damage-associated molecular patterns like HSP70 and calreticulin. *Cancer Immunol Immunother,* 61**,** 215-21.

GARG, A. D., KRYSKO, D. V., VERFAILLIE, T., KACZMAREK, A., FERREIRA, G. B., MARYSAEL, T., RUBIO, N., FIRCZUK, M., MATHIEU, C., ROEBROEK, A. J., ANNAERT, W., GOLAB, J., DE WITTE, P., VANDENABEELE, P. & AGOSTINIS, P. 2012b. A novel pathway combining calreticulin exposure and ATP secretion in immunogenic cancer cell death. *EMBO J,* 31**,** 1062-79.

GARG, A. D., NOWIS, D., GOLAB, J., VANDENABEELE, P., KRYSKO, D. V. & AGOSTINIS, P. 2010. Immunogenic cell death, DAMPs and anticancer therapeutics: an emerging amalgamation. *Biochim Biophys Acta,* 1805**,** 53-71.

GARG, N. K., DWIVEDI, P., PRABHA, P. & TYAGI, R. K. 2013. RNA pulsed dendritic cells: an approach for cancer immunotherapy. *Vaccine,* 31**,** 1141-56.

GARRIDO, C. & KROEMER, G. 2004. Life's smile, death's grin: vital functions of apoptosis-executing proteins. *Curr Opin Cell Biol,* 16**,** 639-46.

GASTPAR, R., GEHRMANN, M., BAUSERO, M. A., ASEA, A., GROSS, C., SCHROEDER, J. A. & MULTHOFF, G. 2005. Heat shock protein 70 surface-positive tumor exosomes stimulate migratory and cytolytic activity of natural killer cells. *Cancer Res,* 65**,** 5238-47.

GASTPAR, R., GROSS, C., ROSSBACHER, L., ELLWART, J., RIEGGER, J. & MULTHOFF, G. 2004. The cell surface-localized heat shock protein 70 epitope TKD induces migration and cytolytic activity selectively in human NK cells. *J Immunol,* 172**,** 972-80.

GHIRINGHELLI, F., APETOH, L., TESNIERE, A., AYMERIC, L., MA, Y., ORTIZ, C., VERMAELEN, K., PANARETAKIS, T., MIGNOT, G., ULLRICH, E., PERFETTINI, J. L., SCHLEMMER, F., TASDEMIR, E., UHL, M., GENIN, P., CIVAS, A., RYFFEL, B., KANELLOPOULOS, J., TSCHOPP, J., ANDRE, F., LIDEREAU, R., MCLAUGHLIN, N. M., HAYNES, N. M., SMYTH, M. J., KROEMER, G. & ZITVOGEL, L. 2009. Activation of the NLRP3 inflammasome in dendritic cells induces IL-1beta-dependent adaptive immunity against tumors. *Nat Med,* 15**,** 1170-8.

GHIRINGHELLI, F., MENARD, C., PUIG, P. E., LADOIRE, S., ROUX, S., MARTIN, F., SOLARY, E., LE CESNE, A., ZITVOGEL, L. & CHAUFFERT, B. 2007. Metronomic cyclophosphamide regimen selectively depletes CD4+CD25+ regulatory T cells and restores T and NK effector functions in end stage cancer patients. *Cancer Immunol Immunother,* 56**,** 641-8.

GREEN, D. R. & LLAMBI, F. 2015. Cell Death Signaling. *Cold Spring Harb Perspect Biol,* 7.

GREEN, D. R. & REED, J. C. 1998. Mitochondria and apoptosis. *Science,* 281**,** 1309-12.

GROSS, C., HANSCH, D., GASTPAR, R. & MULTHOFF, G. 2003. Interaction of heat shock protein 70 peptide with NK cells involves the NK receptor CD94. *Biol Chem,* 384**,** 267-79.

GUILLOT, B., PORTALES, P., THANH, A. D., MERLET, S., DEREURE, O., CLOT, J. & CORBEAU, P. 2005. The expression of cytotoxic mediators is altered in mononuclear cells of patients with melanoma and increased by interferon-alpha treatment. *Br J Dermatol,* 152**,** 690-6.

GUO, Z. S., LIU, Z. & BARTLETT, D. L. 2014. Oncolytic Immunotherapy: Dying the Right Way is a Key to Eliciting Potent Antitumor Immunity. *Front Oncol,* 4**,** 74.

HANADA, T., NODA, N. N., SATOMI, Y., ICHIMURA, Y., FUJIOKA, Y., TAKAO, T., INAGAKI, F. & OHSUMI, Y. 2007. The Atg12-Atg5 conjugate has a novel E3-like activity for protein lipidation in autophagy. *J Biol Chem,* 282**,** 37298-302.

HARDING, H. P., ZHANG, Y., BERTOLOTTI, A., ZENG, H. & RON, D. 2000. Perk is essential for translational regulation and cell survival during the unfolded protein response. *Mol Cell,* 5**,** 897-904.

HARGADON, K. M. 2013. Tumor-altered dendritic cell function: implications for anti-tumor immunity. *Front Immunol,* 4**,** 192.

HE, C. & LEVINE, B. 2010. The Beclin 1 interactome. *Curr Opin Cell Biol,* 22**,** 140-9.

HE, S., WANG, L., MIAO, L., WANG, T., DU, F., ZHAO, L. & WANG, X. 2009. Receptor interacting protein kinase-3 determines cellular necrotic response to TNF-alpha. *Cell,* 137**,** 1100-11.

HE, Y., CORREA, A. M., RASO, M. G., HOFSTETTER, W. L., FANG, B., BEHRENS, C., ROTH, J. A., ZHOU, Y., YU, L., WISTUBA, II, SWISHER, S. G. & PATAER, A. 2011. The role of PKR/eIF2alpha signaling pathway in prognosis of non-small cell lung cancer. *PLoS One,* 6**,** e24855.

HELMSTEIN, K. 1972. Treatment of bladder carcinoma by a hydrostatic pressure technique. Report on 43 cases. *Br J Urol,* 44**,** 434-50.

HONG, C., QIU, X., LI, Y., HUANG, Q., ZHONG, Z., ZHANG, Y., LIU, X., SUN, L., LV, P. & GAO, X. M. 2010. Functional analysis of recombinant calreticulin fragment 39-272: implications for immunobiological activities of calreticulin in health and disease. *J Immunol,* 185**,** 4561-9.

HRADILOVA, N., SADILKOVA, L., PALATA, O., MYSIKOVA, D., MRAZKOVA, H., LISCHKE, R., SPISEK, R. & ADKINS, I. 2017. Generation of dendritic cell-based vaccine using high hydrostatic pressure for non-small cell lung cancer immunotherapy. *PLoS One,* 12**,** e0171539.

HSU, W. M., HSIEH, F. J., JENG, Y. M., KUO, M. L., CHEN, C. N., LAI, D. M., HSIEH, L. J., WANG, B. T., TSAO, P. N., LEE, H., LIN, M. T., LAI, H. S. & CHEN, W. J. 2005. Calreticulin expression in neuroblastoma--a novel independent prognostic factor. *Ann Oncol,* 16**,** 314-21.

HUYAN, T., LI, Q., DONG, D. D., YANG, H., ZHANG, J., HUANG, Q. S., YIN, D. C. & SHANG, P. 2016. Heat shock protein 90 inhibitors induce functional inhibition of human natural killer cells in a dose-dependent manner. *Immunopharmacol Immunotoxicol,* 38**,** 77-86.

CHAO, M. P., JAISWAL, S., WEISSMAN-TSUKAMOTO, R., ALIZADEH, A. A., GENTLES, A. J., VOLKMER, J., WEISKOPF, K., WILLINGHAM, S. B., RAVEH, T., PARK, C. Y., MAJETI, R. & WEISSMAN, I. L. 2010. Calreticulin is the dominant pro-phagocytic signal on multiple human cancers and is counterbalanced by CD47. *Sci Transl Med,* 2**,** 63ra94.

CHEKENI, F. B., ELLIOTT, M. R., SANDILOS, J. K., WALK, S. F., KINCHEN, J. M., LAZAROWSKI, E. R., ARMSTRONG, A. J., PENUELA, S., LAIRD, D. W., SALVESEN, G. S., ISAKSON, B. E., BAYLISS, D. A. & RAVICHANDRAN, K. S. 2010. Pannexin 1 channels mediate 'find-me' signal release and membrane permeability during apoptosis. *Nature,* 467**,** 863-7.

CHEN, C. N., CHANG, C. C., SU, T. E., HSU, W. M., JENG, Y. M., HO, M. C., HSIEH, F. J., LEE, P. H., KUO, M. L., LEE, H. & CHANG, K. J. 2009. Identification of calreticulin as a prognosis marker and angiogenic regulator in human gastric cancer. *Ann Surg Oncol,* 16**,** 524-33.

CHEN, D., FREZZA, M., SCHMITT, S., KANWAR, J. & DOU, Q. P. 2011. Bortezomib as the first proteasome inhibitor anticancer drug: current status and future perspectives. *Curr Cancer Drug Targets,* 11**,** 239-53.

CHEN, G., WARD, M. F., SAMA, A. E. & WANG, H. 2004. Extracellular HMGB1 as a proinflammatory cytokine. *J Interferon Cytokine Res,* 24**,** 329-33.

CHEN, Z., MOYANA, T., SAXENA, A., WARRINGTON, R., JIA, Z. & XIANG, J. 2001. Efficient antitumor immunity derived from maturation of dendritic cells that had phagocytosed apoptotic/necrotic tumor cells. *Int J Cancer,* 93**,** 539-48.

JANELLE, V., LANGLOIS, M. P., LAPIERRE, P., CHARPENTIER, T., POLIQUIN, L. & LAMARRE, A. 2014. The strength of the T cell response against a surrogate tumor antigen induced by oncolytic VSV therapy does not correlate with tumor control. *Mol Ther,* 22**,** 1198-210.

JARNJAK-JANKOVIC, S., HAMMERSTAD, H., SAEBOE-LARSSEN, S., KVALHEIM, G. & GAUDERNACK, G. 2007. A full scale comparative study of methods for generation of functional Dendritic cells for use as cancer vaccines. *BMC Cancer,* 7**,** 119.

JONULEIT, H., KUHN, U., MULLER, G., STEINBRINK, K., PARAGNIK, L., SCHMITT, E., KNOP, J. & ENK, A. H. 1997. Pro-inflammatory cytokines and prostaglandins induce maturation of potent immunostimulatory dendritic cells under fetal calf serum-free conditions. *Eur J Immunol,* 27**,** 3135-42.

KALINSKI, P., VIEIRA, P. L., SCHUITEMAKER, J. H., DE JONG, E. C. & KAPSENBERG, M. L. 2001. Prostaglandin E(2) is a selective inducer of interleukin-12 p40 (IL-12p40) production and an inhibitor of bioactive IL-12p70 heterodimer. *Blood,* 97**,** 3466-9.

KANDALAFT, L. E., POWELL, D. J., JR., CHIANG, C. L., TANYI, J., KIM, S., BOSCH, M., MONTONE, K., MICK, R., LEVINE, B. L., TORIGIAN, D. A., JUNE, C. H. & COUKOS, G. 2013. Autologous lysate-pulsed dendritic cell vaccination followed by adoptive transfer of vaccine-primed ex vivo co-stimulated T cells in recurrent ovarian cancer. *Oncoimmunology,* 2**,** e22664.

KAWAI, T. & AKIRA, S. 2010. The role of pattern-recognition receptors in innate immunity: update on Toll-like receptors. *Nat Immunol,* 11**,** 373-84.

KEPP, O., GALLUZZI, L., GIORDANETTO, F., TESNIERE, A., VITALE, I., MARTINS, I., SCHLEMMER, F., ADJEMIAN, S., ZITVOGEL, L. & KROEMER, G. 2009. Disruption of the PP1/GADD34 complex induces calreticulin exposure. *Cell Cycle,* 8**,** 3971-7.

KEPP, O., MENGER, L., VACCHELLI, E., LOCHER, C., ADJEMIAN, S., YAMAZAKI, T., MARTINS, I., SUKKURWALA, A. Q., MICHAUD, M., SENOVILLA, L., GALLUZZI, L., KROEMER, G. & ZITVOGEL, L. 2013. Crosstalk between ER stress and immunogenic cell death. *Cytokine Growth Factor Rev,* 24**,** 311-8.

KEPP, O., SENOVILLA, L., VITALE, I., VACCHELLI, E., ADJEMIAN, S., AGOSTINIS, P., APETOH, L., ARANDA, F., BARNABA, V., BLOY, N., BRACCI, L., BRECKPOT, K., BROUGH, D., BUQUE, A., CASTRO, M. G., CIRONE, M., COLOMBO, M. I., CREMER, I., DEMARIA, S., DINI, L., ELIOPOULOS, A. G., FAGGIONI, A., FORMENTI, S. C., FUCIKOVA, J., GABRIELE, L., GAIPL, U. S.,

GALON, J., GARG, A., GHIRINGHELLI, F., GIESE, N. A., GUO, Z. S., HEMMINKI, A., HERRMANN, M., HODGE, J. W., HOLDENRIEDER, S., HONEYCHURCH, J., HU, H. M., HUANG, X., ILLIDGE, T. M., KONO, K., KORBELIK, M., KRYSKO, D. V., LOI, S., LOWENSTEIN, P. R., LUGLI, E., MA, Y., MADEO, F., MANFREDI, A. A., MARTINS, I., MAVILIO, D., MENGER, L., MERENDINO, N., MICHAUD, M., MIGNOT, G., MOSSMAN, K. L., MULTHOFF, G., OEHLER, R., PALOMBO, F., PANARETAKIS, T., POL, J., PROIETTI, E., RICCI, J. E., RIGANTI, C., ROVERE-QUERINI, P., RUBARTELLI, A., SISTIGU, A., SMYTH, M. J., SONNEMANN, J., SPISEK, R., STAGG, J., SUKKURWALA, A. Q., TARTOUR, E., THORBURN, A., THORNE, S. H., VANDENABEELE, P., VELOTTI, F., WORKENHE, S. T., YANG, H., ZONG, W. X., ZITVOGEL, L., KROEMER, G. & GALLUZZI, L. 2014. Consensus guidelines for the detection of immunogenic cell death. *Oncoimmunology,* 3**,** e955691.

KIM, H. E., DU, F., FANG, M. & WANG, X. 2005. Formation of apoptosome is initiated by cytochrome c-induced dATP hydrolysis and subsequent nucleotide exchange on Apaf-1. *Proc Natl Acad Sci U S A,* 102**,** 17545-50.

KLECHEVSKY, E., FLAMAR, A. L., CAO, Y., BLANCK, J. P., LIU, M., O'BAR, A., AGOUNA-DECIAT, O., KLUCAR, P., THOMPSON-SNIPES, L., ZURAWSKI, S., REITER, Y., PALUCKA, A. K., ZURAWSKI, G. & BANCHEREAU, J. 2010. Cross-priming CD8+ T cells by targeting antigens to human dendritic cells through DCIR. *Blood,* 116**,** 1685-97.

KOIDO, S., HOMMA, S., OKAMOTO, M., NAMIKI, Y., TAKAKURA, K., UCHIYAMA, K., KAJIHARA, M., ARIHIRO, S., IMAZU, H., ARAKAWA, H., KAN, S., KOMITA, H., ITO, M., OHKUSA, T., GONG, J. & TAJIRI, H. 2013. Fusions between dendritic cells and whole tumor cells as anticancer vaccines. *Oncoimmunology,* 2**,** e24437.

KOKS, C. A., GARG, A. D., EHRHARDT, M., RIVA, M., VANDENBERK, L., BOON, L., DE VLEESCHOUWER, S., AGOSTINIS, P., GRAF, N. & VAN GOOL, S. W. 2015. Newcastle disease virotherapy induces long-term survival and tumor-specific immune memory in orthotopic glioma through the induction of immunogenic cell death. *Int J Cancer,* 136**,** E313-25.

KORN, A., FREY, B., SHERIFF, A., GAIPL, U. S., FRANZ, S., MEYER-PITTROFF, R., BLUEMELHUBERH, G. & HERRMANN, M. 2004. High hydrostatic pressure inactivated human tumour cells preserve their immunogenicity. *Cell Mol Biol (Noisy-le-grand),* 50**,** 469-77.

KROEMER, G., GALLUZZI, L., KEPP, O. & ZITVOGEL, L. 2013. Immunogenic cell death in cancer therapy. *Annu Rev Immunol,* 31**,** 51-72.

KRYSKO, D. V., D'HERDE, K. & VANDENABEELE, P. 2006. Clearance of apoptotic and necrotic cells and its immunological consequences. *Apoptosis,* 11**,** 1709-26.

KRYSKO, D. V., GARG, A. D., KACZMAREK, A., KRYSKO, O., AGOSTINIS, P. & VANDENABEELE, P. 2012. Immunogenic cell death and DAMPs in cancer therapy. *Nat Rev Cancer,* 12**,** 860-75.

LANNEAU, D., BRUNET, M., FRISAN, E., SOLARY, E., FONTENAY, M. & GARRIDO, C. 2008. Heat shock proteins: essential proteins for apoptosis regulation. *J Cell Mol Med,* 12**,** 743-61.

LAZAROWSKI, E. R., SESMA, J. I., SEMINARIO-VIDAL, L. & KREDA, S. M. 2011. Molecular mechanisms of purine and pyrimidine nucleotide release. *Adv Pharmacol,* 61**,** 221-61.

LEE, J., BOCZKOWSKI, D. & NAIR, S. 2013. Programming human dendritic cells with mRNA. *Methods Mol Biol,* 969**,** 111-25.

LEHNER, M., MORHART, P., STILPER, A., PETERMANN, D., WELLER, P., STACHEL, D. & HOLTER, W. 2007. Efficient chemokine-dependent migration and primary and secondary IL-12 secretion by human dendritic cells stimulated through Toll-like receptors. *J Immunother,* 30**,** 312-22.

LENNON-DUMENIL, A. M., BAKKER, A. H., WOLF-BRYANT, P., PLOEGH, H. L. & LAGAUDRIERE-GESBERT, C. 2002. A closer look at proteolysis and MHC-class-II-restricted antigen presentation. *Curr Opin Immunol,* 14**,** 15-21.

LEVINE, B. & KROEMER, G. 2008. Autophagy in the pathogenesis of disease. *Cell,* 132**,** 27-42.

LIU, W. M., FOWLER, D. W., SMITH, P. & DALGLEISH, A. G. 2010. Pre-treatment with chemotherapy can enhance the antigenicity and immunogenicity of tumours by promoting adaptive immune responses. *Br J Cancer,* 102**,** 115-23.

LOCKSLEY, R. M., KILLEEN, N. & LENARDO, M. J. 2001. The TNF and TNF receptor superfamilies: integrating mammalian biology. *Cell,* 104**,** 487-501.

MA, Y., ADJEMIAN, S., MATTAROLLO, S. R., YAMAZAKI, T., AYMERIC, L., YANG, H., PORTELA CATANI, J. P., HANNANI, D., DURET, H., STEEGH, K., MARTINS, I., SCHLEMMER, F., MICHAUD, M., KEPP, O., SUKKURWALA, A. Q., MENGER, L., VACCHELLI, E., DROIN, N., GALLUZZI, L., KRZYSIEK, R., GORDON, S., TAYLOR, P. R., VAN ENDERT, P., SOLARY, E., SMYTH, M. J., ZITVOGEL, L. & KROEMER, G. 2013. Anticancer chemotherapy-induced intratumoral recruitment and differentiation of antigen-presenting cells. *Immunity,* 38**,** 729-41.

MA, Y., BREWER, J. W., DIEHL, J. A. & HENDERSHOT, L. M. 2002. Two distinct stress signaling pathways converge upon the CHOP promoter during the mammalian unfolded protein response. *J Mol Biol,* 318**,** 1351-65.

MA, Y. & HENDERSHOT, L. M. 2002. The mammalian endoplasmic reticulum as a sensor for cellular stress. *Cell Stress Chaperones,* 7**,** 222-9.

MA, Y., MATTAROLLO, S. R., ADJEMIAN, S., YANG, H., AYMERIC, L., HANNANI, D., PORTELA CATANI, J. P., DURET, H., TENG, M. W., KEPP, O., WANG, Y., SISTIGU, A., SCHULTZE, J. L., STOLL, G., GALLUZZI, L., ZITVOGEL, L., SMYTH, M. J. & KROEMER, G. 2014. CCL2/CCR2-dependent recruitment of functional antigen-presenting cells into tumors upon chemotherapy. *Cancer Res,* 74**,** 436-45.

MACHIELS, J. P., REILLY, R. T., EMENS, L. A., ERCOLINI, A. M., LEI, R. Y., WEINTRAUB, D., OKOYE, F. I. & JAFFEE, E. M. 2001. Cyclophosphamide, doxorubicin, and paclitaxel enhance the antitumor immune response of granulocyte/macrophage-colony stimulating factor-secreting whole-cell vaccines in HER-2/neu tolerized mice. *Cancer Res,* 61**,** 3689-97.

MALHOTRA, J. D. & KAUFMAN, R. J. 2011. ER stress and its functional link to mitochondria: role in cell survival and death. *Cold Spring Harb Perspect Biol,* 3**,** a004424.

MARTIN, K., SCHREINER, J. & ZIPPELIUS, A. 2015. Modulation of APC Function and Anti-Tumor Immunity by Anti-Cancer Drugs. *Front Immunol,* 6**,** 501.

MARTINON, F., PETRILLI, V., MAYOR, A., TARDIVEL, A. & TSCHOPP, J. 2006. Gout-associated uric acid crystals activate the NALP3 inflammasome. *Nature,* 440**,** 237-41.

MARTINS, I., TESNIERE, A., KEPP, O., MICHAUD, M., SCHLEMMER, F., SENOVILLA, L., SEROR, C., METIVIER, D., PERFETTINI, J. L., ZITVOGEL, L. & KROEMER, G. 2009. Chemotherapy induces ATP release from tumor cells. *Cell Cycle,* 8**,** 3723-8.

MARTINS, I., WANG, Y., MICHAUD, M., MA, Y., SUKKURWALA, A. Q., SHEN, S., KEPP, O., METIVIER, D., GALLUZZI, L., PERFETTINI, J. L., ZITVOGEL, L. & KROEMER, G. 2014. Molecular mechanisms of ATP secretion during immunogenic cell death. *Cell Death Differ,* 21**,** 79-91.

MATSUKUMA, S., YOSHIMURA, K., UENO, T., OGA, A., INOUE, M., WATANABE, Y., KURAMASU, A., FUSE, M., TSUNEDOMI, R., NAGAOKA, S., EGUCHI, H., MATSUI, H., SHINDO, Y., MAEDA, N., TOKUHISA, Y., KAWANO, R., FURUYA-KONDO, T., ITOH, H., YOSHINO, S., HAZAMA, S., OKA, M. & NAGANO, H. 2016. Calreticulin is highly expressed in pancreatic cancer stem-like cells. *Cancer Sci,* 107**,** 1599-1609.

MATZINGER, P. 1994. Tolerance, danger, and the extended family. *Annu Rev Immunol,* 12**,** 991-1045.

MAYORDOMO, J. I., ZORINA, T., STORKUS, W. J., ZITVOGEL, L., GARCIA-PRATS, M. D., DELEO, A. B. & LOTZE, M. T. 1997. Bone marrow-derived dendritic cells serve as potent adjuvants for peptide-based antitumor vaccines. *Stem Cells,* 15**,** 94-103.

MENARD, C., MARTIN, F., APETOH, L., BOUYER, F. & GHIRINGHELLI, F. 2008. Cancer chemotherapy: not only a direct cytotoxic effect, but also an adjuvant for antitumor immunity. *Cancer Immunol Immunother,* 57**,** 1579-87.

MESAELI, N. & PHILLIPSON, C. 2004. Impaired p53 expression, function, and nuclear localization in calreticulin-deficient cells. *Mol Biol Cell,* 15**,** 1862-70.

MICHAUD, M., MARTINS, I., SUKKURWALA, A. Q., ADJEMIAN, S., MA, Y., PELLEGATTI, P., SHEN, S., KEPP, O., SCOAZEC, M., MIGNOT, G., RELLO-VARONA, S., TAILLER, M., MENGER, L., VACCHELLI, E., GALLUZZI, L., GHIRINGHELLI, F., DI VIRGILIO, F., ZITVOGEL, L. & KROEMER, G.

2011. Autophagy-dependent anticancer immune responses induced by chemotherapeutic agents in mice. *Science,* 334**,** 1573-7.

MIKYSKOVA, R., INDROVA, M., STEPANEK, I., KANCHEV, I., BIEBLOVA, J., VOSAHLIKOVA, S., MOSEROVA, I., TRUXOVA, I., FUCIKOVA, J., BARTUNKOVA, J., SPISEK, R., SEDLACEK, R. & REINIS, M. 2017. Dendritic cells pulsed with tumor cells killed by high hydrostatic pressure inhibit prostate tumor growth in TRAMP mice. *Oncoimmunology,* 6**,** e1362528.

MIKYSKOVA, R., STEPANEK, I., INDROVA, M., BIEBLOVA, J., SIMOVA, J., TRUXOVA, I., MOSEROVA, I., FUCIKOVA, J., BARTUNKOVA, J., SPISEK, R. & REINIS, M. 2016. Dendritic cells pulsed with tumor cells killed by high hydrostatic pressure induce strong immune responses and display therapeutic effects both in murine TC-1 and TRAMP-C2 tumors when combined with docetaxel chemotherapy. *Int J Oncol,* 48**,** 953-64.

MIYAMOTO, S., INOUE, H., NAKAMURA, T., YAMADA, M., SAKAMOTO, C., URATA, Y., OKAZAKI, T., MARUMOTO, T., TAKAHASHI, A., TAKAYAMA, K., NAKANISHI, Y., SHIMIZU, H. & TANI, K. 2012. Coxsackievirus B3 is an oncolytic virus with immunostimulatory properties that is active against lung adenocarcinoma. *Cancer Res,* 72**,** 2609-21.

MOEHLER, M., ZEIDLER, M., SCHEDE, J., ROMMELAERE, J., GALLE, P. R., CORNELIS, J. J. & HEIKE, M. 2003. Oncolytic parvovirus H1 induces release of heat-shock protein HSP72 in susceptible human tumor cells but may not affect primary immune cells. *Cancer Gene Ther,* 10**,** 477-80.

MOSEROVA, I., TRUXOVA, I., GARG, A. D., TOMALA, J., AGOSTINIS, P., CARTRON, P. F., VOSAHLIKOVA, S., KOVAR, M., SPISEK, R. & FUCIKOVA, J. 2017. Caspase-2 and oxidative stress underlie the immunogenic potential of high hydrostatic pressure-induced cancer cell death. *Oncoimmunology,* 6**,** e1258505.

MULTHOFF, G., BOTZLER, C., JENNEN, L., SCHMIDT, J., ELLWART, J. & ISSELS, R. 1997. Heat shock protein 72 on tumor cells: a recognition structure for natural killer cells. *J Immunol,* 158**,** 4341-50.

MURSHID, A., GONG, J. & CALDERWOOD, S. K. 2014. Hsp90-peptide complexes stimulate antigen presentation through the class II pathway after binding scavenger receptor SREC-I. *Immunobiology,* 219**,** 924-31.

MUTH, C., RUBNER, Y., SEMRAU, S., RUHLE, P. F., FREY, B., STRNAD, A., BUSLEI, R., FIETKAU, R. & GAIPL, U. S. 2016. Primary glioblastoma multiforme tumors and recurrence : Comparative analysis of the danger signals HMGB1, HSP70, and calreticulin. *Strahlenther Onkol,* 192**,** 146-55.

NAPOLITANI, G., RINALDI, A., BERTONI, F., SALLUSTO, F. & LANZAVECCHIA, A. 2005. Selected Toll-like receptor agonist combinations synergistically trigger a T helper type 1-polarizing program in dendritic cells. *Nat Immunol,* 6**,** 769-76.

NESTLE, F. O., ALIJAGIC, S., GILLIET, M., SUN, Y., GRABBE, S., DUMMER, R., BURG, G. & SCHADENDORF, D. 1998. Vaccination of melanoma patients with peptide- or tumor lysate-pulsed dendritic cells. *Nat Med,* 4**,** 328-32.

NIIYA, M., NIIYA, K., KIGUCHI, T., SHIBAKURA, M., ASAUMI, N., SHINAGAWA, K., ISHIMARU, F., KIURA, K., IKEDA, K., UEOKA, H. & TANIMOTO, M. 2003. Induction of TNF-alpha, uPA, IL-8 and MCP-1 by doxorubicin in human lung carcinoma cells. *Cancer Chemother Pharmacol,* 52**,** 391-8.

NOVIKOV, A., CARDONE, M., THOMPSON, R., SHENDEROV, K., KIRSCHMAN, K. D., MAYER-BARBER, K. D., MYERS, T. G., RABIN, R. L., TRINCHIERI, G., SHER, A. & FENG, C. G. 2011. Mycobacterium tuberculosis triggers host type I IFN signaling to regulate IL-1beta production in human macrophages. *J Immunol,* 187**,** 2540-7.

OBEID, M., PANARETAKIS, T., JOZA, N., TUFI, R., TESNIERE, A., VAN ENDERT, P., ZITVOGEL, L. & KROEMER, G. 2007a. Calreticulin exposure is required for the immunogenicity of gamma-irradiation and UVC light-induced apoptosis. *Cell Death Differ,* 14**,** 1848-50.

OBEID, M., TESNIERE, A., GHIRINGHELLI, F., FIMIA, G. M., APETOH, L., PERFETTINI, J. L., CASTEDO, M., MIGNOT, G., PANARETAKIS, T., CASARES, N., METIVIER, D., LAROCHETTE, N., VAN ENDERT, P., CICCOSANTI, F., PIACENTINI, M., ZITVOGEL, L. & KROEMER, G. 2007b. Calreticulin exposure dictates the immunogenicity of cancer cell death. *Nat Med,* 13**,** 54-61.

PALUMBO, R., SAMPAOLESI, M., DE MARCHIS, F., TONLORENZI, R., COLOMBETTI, S., MONDINO, A., COSSU, G. & BIANCHI, M. E. 2004. Extracellular HMGB1, a signal of tissue damage, induces mesoangioblast migration and proliferation. *J Cell Biol,* 164**,** 441-9.

PANARETAKIS, T., JOZA, N., MODJTAHEDI, N., TESNIERE, A., VITALE, I., DURCHSCHLAG, M., FIMIA, G. M., KEPP, O., PIACENTINI, M., FROEHLICH, K. U., VAN ENDERT, P., ZITVOGEL, L., MADEO, F. & KROEMER, G. 2008. The co-translocation of ERp57 and calreticulin determines the immunogenicity of cell death. *Cell Death Differ,* 15**,** 1499-509.

PANARETAKIS, T., KEPP, O., BROCKMEIER, U., TESNIERE, A., BJORKLUND, A. C., CHAPMAN, D. C., DURCHSCHLAG, M., JOZA, N., PIERRON, G., VAN ENDERT, P., YUAN, J., ZITVOGEL, L., MADEO, F., WILLIAMS, D. B. & KROEMER, G. 2009. Mechanisms of pre-apoptotic calreticulin exposure in immunogenic cell death. *EMBO J,* 28**,** 578-90.

PAPEWALIS, C., JACOBS, B., WUTTKE, M., ULLRICH, E., BAEHRING, T., FENK, R., WILLENBERG, H. S., SCHINNER, S., COHNEN, M., SEISSLER, J., ZACHAROWSKI, K., SCHERBAUM, W. A. & SCHOTT, M. 2008. IFN-alpha skews monocytes into CD56+-expressing dendritic cells with potent functional activities in vitro and in vivo. *J Immunol,* 180**,** 1462-70.

PAWARIA, S. & BINDER, R. J. 2011. CD91-dependent programming of T-helper cell responses following heat shock protein immunization. *Nat Commun,* 2**,** 521.

PENG, R. Q., CHEN, Y. B., DING, Y., ZHANG, R., ZHANG, X., YU, X. J., ZHOU, Z. W., ZENG, Y. X. & ZHANG, X. S. 2010. Expression of calreticulin is associated with infiltration of T-cells in stage IIIB colon cancer. *World J Gastroenterol,* 16**,** 2428-34.

PETER, C., WESSELBORG, S. & LAUBER, K. 2010. Molecular suicide notes: last call from apoptosing cells. *J Mol Cell Biol,* 2**,** 78-80.

PODRAZIL, M., HORVATH, R., BECHT, E., ROZKOVA, D., BILKOVA, P., SOCHOROVA, K., HROMADKOVA, H., KAYSEROVA, J., VAVROVA, K., LASTOVICKA, J., VRABCOVA, P., KUBACKOVA, K., GASOVA, Z., JAROLIM, L., BABJUK, M., SPISEK, R., BARTUNKOVA, J. & FUCIKOVA, J. 2015. Phase I/II clinical trial of dendritic-cell based immunotherapy (DCVAC/PCa) combined with chemotherapy in patients with metastatic, castration-resistant prostate cancer. *Oncotarget,* 6**,** 18192-205.

POL, J., BUQUE, A., ARANDA, F., BLOY, N., CREMER, I., EGGERMONT, A., ERBS, P., FUCIKOVA, J., GALON, J., LIMACHER, J. M., PREVILLE, X., SAUTES-FRIDMAN, C., SPISEK, R., ZITVOGEL, L., KROEMER, G. & GALLUZZI, L. 2016a. Trial Watch-Oncolytic viruses and cancer therapy. *Oncoimmunology,* 5**,** e1117740.

POL, J., KROEMER, G. & GALLUZZI, L. 2016b. First oncolytic virus approved for melanoma immunotherapy. *Oncoimmunology,* 5**,** e1115641.

PRASAD, V., CHANDELE, A., JAGTAP, J. C., SUDHEER KUMAR, P. & SHASTRY, P. 2006. ROS-triggered caspase 2 activation and feedback amplification loop in beta-carotene-induced apoptosis. *Free Radic Biol Med,* 41**,** 431-42.

PRESTWICH, R. J., ERRINGTON, F., ILETT, E. J., MORGAN, R. S., SCOTT, K. J., KOTTKE, T., THOMPSON, J., MORRISON, E. E., HARRINGTON, K. J., PANDHA, H. S., SELBY, P. J., VILE, R. G. & MELCHER, A. A. 2008. Tumor infection by oncolytic reovirus primes adaptive antitumor immunity. *Clin Cancer Res,* 14**,** 7358-66.

RABBANI, A., FINN, R. M. & AUSIO, J. 2005. The anthracycline antibiotics: antitumor drugs that alter chromatin structure. *Bioessays,* 27**,** 50-6.

ROBSON, S. C., SEVIGNY, J. & ZIMMERMANN, H. 2006. The E-NTPDase family of ectonucleotidases: Structure function relationships and pathophysiological significance. *Purinergic Signal,* 2**,** 409-30.

SCAFFIDI, P., MISTELI, T. & BIANCHI, M. E. 2002. Release of chromatin protein HMGB1 by necrotic cells triggers inflammation. *Nature,* 418**,** 191-5.

SCARLETT, U. K., RUTKOWSKI, M. R., RAUWERDINK, A. M., FIELDS, J., ESCOVAR-FADUL, X., BAIRD, J., CUBILLOS-RUIZ, J. R., JACOBS, A. C., GONZALEZ, J. L., WEAVER, J., FIERING, S. & CONEJO-GARCIA, J. R. 2012. Ovarian cancer progression is controlled by phenotypic changes in dendritic cells. *J Exp Med,* 209**,** 495-506.

SENOVILLA, L., VITALE, I., MARTINS, I., TAILLER, M., PAILLERET, C., MICHAUD, M., GALLUZZI, L., ADJEMIAN, S., KEPP, O., NISO-SANTANO, M., SHEN, S., MARINO, G., CRIOLLO, A., BOILEVE, A., JOB, B., LADOIRE, S., GHIRINGHELLI, F., SISTIGU, A., YAMAZAKI, T., RELLO-VARONA, S., LOCHER, C., POIRIER-COLAME, V., TALBOT, M., VALENT, A., BERARDINELLI, F., ANTOCCIA, A., CICCOSANTI, F., FIMIA, G. M., PIACENTINI, M., FUEYO, A., MESSINA, N. L., LI, M., CHAN, C. J., SIGL, V., POURCHER, G., RUCKENSTUHL, C., CARMONA-GUTIERREZ, D., LAZAR, V., PENNINGER, J. M., MADEO, F., LOPEZ-OTIN, C., SMYTH, M. J., ZITVOGEL, L., CASTEDO, M. & KROEMER, G. 2012. An immunosurveillance mechanism controls cancer cell ploidy. *Science,* 337**,** 1678-84.

SCHARDT, J. A., WEBER, D., EYHOLZER, M., MUELLER, B. U. & PABST, T. 2009. Activation of the unfolded protein response is associated with favorable prognosis in acute myeloid leukemia. *Clin Cancer Res,* 15**,** 3834-41.

SCHAUE, D., RATIKAN, J. A., IWAMOTO, K. S. & MCBRIDE, W. H. 2012. Maximizing tumor immunity with fractionated radiation. *Int J Radiat Oncol Biol Phys,* 83**,** 1306-10.

SCHIAVONI, G., SISTIGU, A., VALENTINI, M., MATTEI, F., SESTILI, P., SPADARO, F., SANCHEZ, M., LORENZI, S., D'URSO, M. T., BELARDELLI, F., GABRIELE, L., PROIETTI, E. & BRACCI, L. 2011. Cyclophosphamide synergizes with type I interferons through systemic dendritic cell reactivation and induction of immunogenic tumor apoptosis. *Cancer Res,* 71**,** 768-78.

SCHUMACHER, L. Y., VO, D. D., GARBAN, H. J., COMIN-ANDUIX, B., OWENS, S. K., DISSETTE, V. B., GLASPY, J. A., MCBRIDE, W. H., BONAVIDA, B., ECONOMOU, J. S. & RIBAS, A. 2006. Immunosensitization of tumor cells to dendritic cell-activated immune responses with the proteasome inhibitor bortezomib (PS-341, Velcade). *J Immunol,* 176**,** 4757-65.

SINGH-JASUJA, H., TOES, R. E., SPEE, P., MUNZ, C., HILF, N., SCHOENBERGER, S. P., RICCIARDI-CASTAGNOLI, P., NEEFJES, J., RAMMENSEE, H. G., ARNOLD-SCHILD, D. & SCHILD, H. 2000. Cross-presentation of glycoprotein 96-associated antigens on major histocompatibility complex class I molecules requires receptor-mediated endocytosis. *J Exp Med,* 191**,** 1965-74.

SISTIGU, A., VIAUD, S., CHAPUT, N., BRACCI, L., PROIETTI, E. & ZITVOGEL, L. 2011. Immunomodulatory effects of cyclophosphamide and implementations for vaccine design. *Semin Immunopathol,* 33**,** 369-83.

SISTIGU, A., YAMAZAKI, T., VACCHELLI, E., CHABA, K., ENOT, D. P., ADAM, J., VITALE, I., GOUBAR, A., BARACCO, E. E., REMEDIOS, C., FEND, L., HANNANI, D., AYMERIC, L., MA, Y., NISO-SANTANO, M., KEPP, O., SCHULTZE, J. L., TUTING, T., BELARDELLI, F., BRACCI, L., LA SORSA, V., ZICCHEDDU, G., SESTILI, P., URBANI, F., DELORENZI, M., LACROIX-TRIKI, M., QUIDVILLE, V., CONFORTI, R., SPANO, J. P., PUSZTAI, L., POIRIER-COLAME, V., DELALOGE, S., PENAULT-LLORCA, F., LADOIRE, S., ARNOULD, L., CYRTA, J., DESSOLIERS, M. C., EGGERMONT, A., BIANCHI, M. E., PITTET, M., ENGBLOM, C., PFIRSCHKE, C., PREVILLE, X., UZE, G., SCHREIBER, R. D., CHOW, M. T., SMYTH, M. J., PROIETTI, E., ANDRE, F., KROEMER, G. & ZITVOGEL, L. 2014. Cancer cell-autonomous contribution of type I interferon signaling to the efficacy of chemotherapy. *Nat Med,* 20**,** 1301-9.

SIURALA, M., BRAMANTE, S., VASSILEV, L., HIRVINEN, M., PARVIAINEN, S., TAHTINEN, S., GUSE, K., CERULLO, V., KANERVA, A., KIPAR, A., VAHA-KOSKELA, M. & HEMMINKI, A. 2015. Oncolytic adenovirus and doxorubicin-based chemotherapy results in synergistic antitumor activity against soft-tissue sarcoma. *Int J Cancer,* 136**,** 945-54.

SPISEK, R. & DHODAPKAR, M. V. 2007. Towards a better way to die with chemotherapy: role of heat shock protein exposure on dying tumor cells. *Cell Cycle,* 6**,** 1962-5.

SPISEK, R., CHARALAMBOUS, A., MAZUMDER, A., VESOLE, D. H., JAGANNATH, S. & DHODAPKAR, M. V. 2007. Bortezomib enhances dendritic cell (DC)-mediated induction of immunity to human myeloma via exposure of cell surface heat shock protein 90 on dying tumor cells: therapeutic implications. *Blood,* 109**,** 4839-45.

STOJANOVSKA, V., SAKKAL, S. & NURGALI, K. 2015. Platinum-based chemotherapy: gastrointestinal immunomodulation and enteric nervous system toxicity. *Am J Physiol Gastrointest Liver Physiol,* 308**,** G223-32.

SUN, L., WANG, H., WANG, Z., HE, S., CHEN, S., LIAO, D., WANG, L., YAN, J., LIU, W., LEI, X. & WANG, X. 2012. Mixed lineage kinase domain-like protein mediates necrosis signaling downstream of RIP3 kinase. *Cell,* 148**,** 213-27.

SZEGEZDI, E., FITZGERALD, U. & SAMALI, A. 2003. Caspase-12 and ER-stress-mediated apoptosis: the story so far. *Ann N Y Acad Sci,* 1010**,** 186-94.

TAKASU, A., MASUI, A., HAMADA, M., IMAI, T., IWAI, S. & YURA, Y. 2016. Immunogenic cell death by oncolytic herpes simplex virus type 1 in squamous cell carcinoma cells. *Cancer Gene Ther,* 23**,** 107-13.

TANG, D., KANG, R., ZEH, H. J., 3RD & LOTZE, M. T. 2010. High-mobility group box 1 and cancer. *Biochim Biophys Acta,* 1799**,** 131-40.

TESNIERE, A., PANARETAKIS, T., KEPP, O., APETOH, L., GHIRINGHELLI, F., ZITVOGEL, L. & KROEMER, G. 2008. Molecular characteristics of immunogenic cancer cell death. *Cell Death Differ,* 15**,** 3-12.

TESNIERE, A., SCHLEMMER, F., BOIGE, V., KEPP, O., MARTINS, I., GHIRINGHELLI, F., AYMERIC, L., MICHAUD, M., APETOH, L., BARAULT, L., MENDIBOURE, J., PIGNON, J. P., JOOSTE, V., VAN ENDERT, P., DUCREUX, M., ZITVOGEL, L., PIARD, F. & KROEMER, G. 2010. Immunogenic death of colon cancer cells treated with oxaliplatin. *Oncogene,* 29**,** 482-91.

THORBURN, J., HORITA, H., REDZIC, J., HANSEN, K., FRANKEL, A. E. & THORBURN, A. 2009. Autophagy regulates selective HMGB1 release in tumor cells that are destined to die. *Cell Death Differ,* 16**,** 175-83.

TOMIHARA, K., GUO, M., SHIN, T., SUN, X., LUDWIG, S. M., BRUMLIK, M. J., ZHANG, B., CURIEL, T. J. & SHIN, T. 2010. Antigen-specific immunity and cross-priming by epithelial ovarian carcinoma-induced CD11b(+)Gr-1(+) cells. *J Immunol,* 184**,** 6151-60.

TRUXOVA, I., HENSLER, M., SKAPA, P., HALASKA, M. J., LACO, J., RYSKA, A., SPISEK, R. & FUCIKOVA, J. 2017. Rationale for the Combination of Dendritic Cell-Based Vaccination Approaches With Chemotherapy Agents. *Int Rev Cell Mol Biol,* 330**,** 115-156.

TRUXOVA, I., POKORNA, K., KLOUDOVA, K., PARTLOVA, S., SPISEK, R. & FUCIKOVA, J. 2014. Day 3 Poly (I:C)-activated dendritic cells generated in CellGro for use in cancer immunotherapy trials are fully comparable to standard Day 5 DCs. *Immunol Lett,* 160**,** 39-49.

UDONO, H. & SRIVASTAVA, P. K. 1994. Comparison of tumor-specific immunogenicities of stress-induced proteins gp96, hsp90, and hsp70. *J Immunol,* 152**,** 5398-403.

UPTON, J. P., AUSTGEN, K., NISHINO, M., COAKLEY, K. M., HAGEN, A., HAN, D., PAPA, F. R. & OAKES, S. A. 2008. Caspase-2 cleavage of BID is a critical apoptotic signal downstream of endoplasmic reticulum stress. *Mol Cell Biol,* 28**,** 3943-51.

URANO, F., WANG, X., BERTOLOTTI, A., ZHANG, Y., CHUNG, P., HARDING, H. P. & RON, D. 2000. Coupling of stress in the ER to activation of JNK protein kinases by transmembrane protein kinase IRE1. *Science,* 287**,** 664-6.

VACCHELLI, E., MA, Y., BARACCO, E. E., SISTIGU, A., ENOT, D. P., PIETROCOLA, F., YANG, H., ADJEMIAN, S., CHABA, K., SEMERARO, M., SIGNORE, M., DE NINNO, A., LUCARINI, V., PESCHIAROLI, F., BUSINARO, L., GERARDINO, A., MANIC, G., ULAS, T., GUNTHER, P., SCHULTZE, J. L., KEPP, O., STOLL, G., LEFEBVRE, C., MULOT, C., CASTOLDI, F., RUSAKIEWICZ, S., LADOIRE, S., APETOH, L., BRAVO-SAN PEDRO, J. M., LUCATTELLI, M., DELARASSE, C., BOIGE, V., DUCREUX, M., DELALOGE, S., BORG, C., ANDRE, F., SCHIAVONI, G., VITALE, I., LAURENT-PUIG, P., MATTEI, F., ZITVOGEL, L. & KROEMER, G. 2015. Chemotherapy-induced antitumor immunity requires formyl peptide receptor 1. *Science,* 350**,** 972-8.

VACCHELLI, E., MA, Y., BARACCO, E. E., ZITVOGEL, L. & KROEMER, G. 2016. Yet another pattern recognition receptor involved in the chemotherapy-induced anticancer immune response: Formyl peptide receptor-1. *Oncoimmunology,* 5**,** e1118600.

VAN EDEN, W., SPIERING, R., BROERE, F. & VAN DER ZEE, R. 2012. A case of mistaken identity: HSPs are no DAMPs but DAMPERs. *Cell Stress Chaperones,* 17**,** 281-92.

VANDEN BERGHE, T., VANLANGENAKKER, N., PARTHOENS, E., DECKERS, W., DEVOS, M., FESTJENS, N., GUERIN, C. J., BRUNK, U. T., DECLERCQ, W. & VANDENABEELE, P. 2010. Necroptosis, necrosis

and secondary necrosis converge on similar cellular disintegration features. *Cell Death Differ,* 17**,** 922-30.

VANDENBERK, L., BELMANS, J., VAN WOENSEL, M., RIVA, M. & VAN GOOL, S. W. 2015. Exploiting the Immunogenic Potential of Cancer Cells for Improved Dendritic Cell Vaccines. *Front Immunol,* 6**,** 663.

VANLANGENAKKER, N., VANDEN BERGHE, T. & VANDENABEELE, P. 2012. Many stimuli pull the necrotic trigger, an overview. *Cell Death Differ,* 19**,** 75-86.

VENEREAU, E., CASALGRANDI, M., SCHIRALDI, M., ANTOINE, D. J., CATTANEO, A., DE MARCHIS, F., LIU, J., ANTONELLI, A., PRETI, A., RAELI, L., SHAMS, S. S., YANG, H., VARANI, L., ANDERSSON, U., TRACEY, K. J., BACHI, A., UGUCCIONI, M. & BIANCHI, M. E. 2012. Mutually exclusive redox forms of HMGB1 promote cell recruitment or proinflammatory cytokine release. *J Exp Med,* 209**,** 1519-28.

VIAUD, S., THERY, C., PLOIX, S., TURSZ, T., LAPIERRE, V., LANTZ, O., ZITVOGEL, L. & CHAPUT, N. 2010. Dendritic cell-derived exosomes for cancer immunotherapy: what's next? *Cancer Res,* 70**,** 1281-5.

VINCENT, J., MIGNOT, G., CHALMIN, F., LADOIRE, S., BRUCHARD, M., CHEVRIAUX, A., MARTIN, F., APETOH, L., REBE, C. & GHIRINGHELLI, F. 2010. 5-Fluorouracil selectively kills tumor-associated myeloid-derived suppressor cells resulting in enhanced T cell-dependent antitumor immunity. *Cancer Res,* 70**,** 3052-61.

WANG, Y., MA, X., SU, C., PENG, B., DU, J., JIA, H., LUO, M., FANG, C. & WEI, Y. 2015. Uric acid enhances the antitumor immunity of dendritic cell-based vaccine. *Sci Rep,* 5**,** 16427.

WEISS, E. M., MEISTER, S., JANKO, C., EBEL, N., SCHLUCKER, E., MEYER-PITTROFF, R., FIETKAU, R., HERRMANN, M., GAIPL, U. S. & FREY, B. 2010. High hydrostatic pressure treatment generates inactivated mammalian tumor cells with immunogeneic features. *J Immunotoxicol,* 7**,** 194-204.

WEMEAU, M., KEPP, O., TESNIERE, A., PANARETAKIS, T., FLAMENT, C., DE BOTTON, S., ZITVOGEL, L., KROEMER, G. & CHAPUT, N. 2010. Calreticulin exposure on malignant blasts predicts a cellular anticancer immune response in patients with acute myeloid leukemia. *Cell Death Dis,* 1**,** e104.

WILLINGHAM, S. B., ALLEN, I. C., BERGSTRALH, D. T., BRICKEY, W. J., HUANG, M. T., TAXMAN, D. J., DUNCAN, J. A. & TING, J. P. 2009. NLRP3 (NALP3, Cryopyrin) facilitates in vivo caspase-1 activation, necrosis, and HMGB1 release via inflammasome-dependent and -independent pathways. *J Immunol,* 183**,** 2008-15.

WORKENHE, S. T., POL, J. G., LICHTY, B. D., CUMMINGS, D. T. & MOSSMAN, K. L. 2013. Combining oncolytic HSV-1 with immunogenic cell death-inducing drug mitoxantrone breaks cancer immune tolerance and improves therapeutic efficacy. *Cancer Immunol Res,* 1**,** 309-19.

YANG, H., LUNDBACK, P., OTTOSSON, L., ERLANDSSON-HARRIS, H., VENEREAU, E., BIANCHI, M. E., AL-ABED, Y., ANDERSSON, U., TRACEY, K. J. & ANTOINE, D. J. 2012. Redox modification of cysteine residues regulates the cytokine activity of high mobility group box-1 (HMGB1). *Mol Med,* 18**,** 250-9.

ZITVOGEL, L., GALLUZZI, L., KEPP, O., SMYTH, M. J. & KROEMER, G. 2015. Type I interferons in anticancer immunity. *Nat Rev Immunol,* 15**,** 405-14.

ZITVOGEL, L., GALLUZZI, L., SMYTH, M. J. & KROEMER, G. 2013. Mechanism of action of conventional and targeted anticancer therapies: reinstating immunosurveillance. *Immunity,* 39**,** 74-88.

ZITVOGEL, L., KEPP, O. & KROEMER, G. 2010a. Decoding cell death signals in inflammation and immunity. *Cell,* 140**,** 798-804.

ZITVOGEL, L., KEPP, O., SENOVILLA, L., MENGER, L., CHAPUT, N. & KROEMER, G. 2010b. Immunogenic tumor cell death for optimal anticancer therapy: the calreticulin exposure pathway. *Clin Cancer Res,* 16**,** 3100-4.

ZOBYWALSKI, A., JAVOROVIC, M., FRANKENBERGER, B., POHLA, H., KREMMER, E., BIGALKE, I. & SCHENDEL, D. J. 2007. Generation of clinical grade dendritic cells with capacity to produce biologically active IL-12p70. *J Transl Med,* 5**,** 18.